TESTING AND DEVELOPMENT OF THE CANADIAN LAND SURFACE SCHEME (CLASS) FOR FORESTS, AGRICULTURAL CROPS AND BARE SOILS

by

AISHENG WU

B. Sc. (Atmospheric Science), University of Science and Technology of China, Hefei, 1983
M. Sc. (Satellite Meteorology), Institute of Plateau Atmospheric Physics, Chinese Academy of Science, Lanzhou, 1990

A THESIS SUBMITTED IN PARTIAL FULFILLMENT OF THE REQUIREMENTS FOR

THE DEGREE OF DOCTOR OF PHILOSOPHY

in

THE FACULTY OF GRADUATE STUDIES

Department of Soil Science

We accept this thesis as conforming to

the required standard

THE UNIVERSITY OF BRITISH COLUMBIA

May 1999

Department of Soil Science

The University of British Columbia
Vancouver, Canada

Date May 18, 1999

ABSTRACT

CLASS (Canadian Land Surface Scheme) is the land surface model currently used in the Canadian general circulation model. It features a single vegetation layer, three soil layers (and a snow layer when necessary) and physically-based calculations of the energy and water exchange between the atmosphere and land surface. This research focused on the validation of CLASS and the improvement of relevant parameterizations. CLASS was tested using continuous half-hourly energy balance and soil water content (θ) data collected during much of 1994 and from spring 1996 to the end of 1998 from a boreal aspen forest and during short summer periods over past 20 years from six west coast Douglas-fir forests, two agricultural crops and two bare soils. Tests identified the following deficiencies in CLASS: (1) evaporation from the soil surface was significantly overestimated, (2) transpiration from the aspen forest was underestimated under conditions of high solar irradiance, (3) winter albedo was too high, and (4) surface runoff after snowmelt was excessive.

Two semi-empirical soil evaporation relationships (the α and β methods) were compared with Philip's relationship using measurements of evaporation from a bare loam/silt-loam soil. The latter, although physically-based, performed poorly when used with a thick surface soil layer as in CLASS. The β method performed significantly better than the α method. Parameterizations of canopy conductance (g_c) based on the Jarvis-Stewart (JS) (also used in CLASS), the Ball-Woodrow-Berry (BWB) and a modified form of the BWB parameterization (MBWB) were evaluated for the aspen forest and a Douglas-fir forest. A new JS parameterization gave the best estimates of g_c, while the

MBWB parameterization performed better than the BWB parameterization. The new JS and MBWB parameterizations worked well for five Douglas-fir forests of similar age with different leaf area indices under conditions of high θ but worked poorly for conditions of low θ because the response of Douglas-fir g_c to soil water stress differed considerably from site to site. Adjusting the winter albedo for the aspen forest from 0.5 to the more realistic value of 0.25 significantly improved the calculation of winter net radiation, predicted the occurrence of snowmelt only 5-10 days later than observations and significantly reduced the overestimation of surface runoff following snowmelt.

The near-field effect on flux calculations was examined using two approaches: (1) the near-field resistance was places in series with the aerodynamic resistance in CLASS, and (2) the performance of a Lagrangian two-layer canopy model was compared with a *K*-theory two-layer canopy model and a *K*-theory single-layer canopy model. The first approach was tested using data from a Douglas-fir forest, the aspen forest and an agricultural crop. The second approach was tested using data from the aspen forest because it had a thick understory canopy. Results from both approaches confirmed that the difference between simulations from *K*-theory and the Lagrangian evaporation models was small due to the strong control by stomatal conductance. Furthermore, the two-layer canopy models were inferior to the single-layer canopy model in the calculation of the sensible and latent heat fluxes above the forest.

TABLE OF CONTENTS

LIST OF SYMBOLS AND ACRONYMS

A_0	Rate of net CO_2 assimilation by the canopy	μmol m^{-2} s^{-1}
$A_1, A_2, \ldots_5$	Functions describing the effects of Q_p, T_0, e_0, ψ, and c_0 on A_0	dimensionless
A_s	Rate of net CO_2 assimilation by the leaf	μmol m^{-2} s^{-1}
A_∞	A_0 at saturating Q_p	μmol m^{-2} s^{-1}
B	Bowen ratio	dimensionless
B^{-1}	Stanton number	dimensionless
C_D	Drag coefficient	dimensionless
$C(z)$	Total profile of a scalar concentration	-
C_1, C_2	Scalar concentration in canopy layers 1 and 2	-
C_a	Scalar concentration at the reference height	-
C_c	Effective canopy heat capacity	J m^{-3} K^{-1}
$C_f(z)$	Far-field profile of a scalar concentration	-
C_i	Volumetric heat capacity of soil layer i (i =1, 2 or 3)	J m^{-3} K^{-1}
$C_n(z)$	Near-field profile of a scalar concentration	-
E_c	Evaporation from the canopy	kg m^{-2} s^{-1}
E_i	Evaporation from ponded water on the surface	kg m^{-2} s^{-1}
$E_{i,c}$	Evaporation from ponded water on the canopy	kg m^{-2} s^{-1}
$F(z_i, t)$	Liquid water flow rate as a function of z_i and t	kg m^{-2} s^{-1}
F_m	A_0 at Q_p = 1800 μmol m^{-2} s^{-1}	μmol m^{-2} s^{-1}
$G(z_i, t)$	Heat flux as a function of z_i and t	W m^{-2}

G_0	Heat flux at the soil surface	W m^{-2}
I	Infiltration rate	kg m^{-2} s^{-1}
J_1, J_2	Flux variable $Q_{H,1} - (\gamma/s)Q_{E,1}$ and $Q_{H,1} - (\gamma/s)Q_{E,1}$	W m^{-2}
$K(z)$	Eddy diffusivity at height z	m^2 s^{-1}
$K_\downarrow$	Global solar radiation	W m^{-2}
$K^\uparrow$	Reflected solar radiation	W m^{-2}
L_v	Latent heat of vaporization of water	J kg^{-1}
$L^\uparrow$	Upward longwave radiation	W m^{-2}
P	Precipitation	mm
$Q_{E,1}$, $Q_{E,2}$	Latent heat fluxes from canopy layers 1 and 2	W m^{-2}
$Q_{E,c}$, $Q_{E,g}$	Latent heat fluxes from the canopy and soil surface	W m^{-2}
$Q_{E,g/s}$	Evaporation from the ground surface under the canopy	W m^{-2}
$Q_{H,1}$, $Q_{H,2}$	Sensible heat fluxes from canopy layers 1 and 2	W m^{-2}
Q_H, Q_E	Sensible and latent heat fluxes above the canopy	W m^{-2}
$Q_{H,g}$	Sensible heat flux from the soil surface	W m^{-2}
Q	Available energy for the canopy	W m^{-2}
Q_p	Incident photosynthetic photon flux density	μmol m^{-2} s^{-1}
Q_1 and Q_2	Available energy for the canopy layers 1 and 2	W m^{-2}
Q^*	Net radiation above the canopy	W m^{-2}
Q^*_c	Net radiation absorbed by the canopy	W m^{-2}
Q^*_g	Net radiation above soil surface	W m^{-2}
R	Dark respiration rate	μmol m^{-2} s^{-1}
R_v	Gas constant for water vapour	J $K^{-1}kg^{-1}$

S	Canopy heat storage per unit ground area	W m^{-2}
S_c	Profile of a scalar source	-
$S_{c,1}$, $S_{c,2}$	Scalar source of canopy layers 1 and 2	-
S_h	Heat for freezing or thawing of moisture stored on the canopy	W m^{-2}
S_i	Correction term for freezing or thawing in the calculation of $T_{i,g}$ in soil layer i (i =1, 2 or 3)	°C
T_0	Canopy temperature (a proper mean of the temperature of all the individual leaves)	°C
$T_{a,1}$, $T_{a,2}$	Air temperatures of the air stream within canopy layers 1 and 2	°C
T_L	Lagrangian integral time scale	s
T_a	Air temperature at the reference height	°C
$T_{a,c}$	Air temperature measured at the height $z = d + z_0$	°C
$T_{i,g}$	Average soil surface temperature of layer i (i = 1, 2 or 3)	°C
T_p	A properly chosen temperature for evaluating s	°C
T_s	Soil surface temperature	°C
$T'_{a,0}$	Virtual temperature of the air within the canopy	°C
T'_s	Virtual temperature of the soil surface	°C
V_{max0}	Maximum photosynthesis capacity	μmol m^{-2} s^{-1}
W	Interception water/snow store on the soil surface	kg m^{-2} s^{-1}
W_c	Interception water/snow store on the canopy	kg m^{-2} s^{-1}
c_0	CO_2 mole fraction at the 'big-leaf' surface	mol mol^{-1}
c_a	CO_2 mole fraction at the reference height	mol mol^{-1}

c_i	Foliage internal CO_2 concentration	mol mol^{-1}
c_p	Specific heat of air at constant pressure	J kg^{-1} $^oK^{-1}$
c_s	CO_2 mole fraction at the leaf surface	mol mol^{-1}
d	Zero plane displacement height	m
e_0	Vapour pressure at the "big-leaf' surface	kPa
e_a	Vapour pressure at the reference height	kPa
$e_{a,1}$, $e_{a,2}$	Vapour pressure of the air stream within canopy layers 1 and 2	kPa
e^*	Saturation vapour pressure	kPa
g	Acceleration due to gravity	m s^{-2}
$g_1, g_2, \ldots_5$	Functions describing the effects of Λ, Q_p, Δe_0, ψ, and T_0 on g_c	dimensionless
g_a	Canopy aerodynamic conductance	m s^{-1}
g_c, g_s	Canopy and leaf stomatal conductance	m s^{-1}
$g_{c,1}, g_{c,2}$	Canopy conductance of layers 1 and 2	m s^{-1}
$g_{c,\,max}$	Maximum value of canopy conductance	m s^{-1}
h	Canopy height	m
h_0	Relative humidity at the "big-leaf" surface	dimensionless
h_a	Relative humidity of the air outside the leaf boundary layer	dimensionless
h_c	Effective canopy source height	m
h_s	Relative humidity at the leaf surface	dimensionless
h'	Canopy understory height	m
k	von Karman constant	

$k(z)$	Hydraulic conductivity at depth z	kg m^{-2} s^{-1}
k_{sat}	Saturated hydraulic conductivity	kg m^{-2} s^{-1}
l_1, l_2	Leaf dimension of canopy layers 1 and 2	m
q_a	Specific humidity of the air	kg kg^{-1}
q_s	Specific humidity of the air at the soil surface	kg kg^{-1}
q_{sat}	Saturation specific humidity of the air	kg kg^{-1}
r	Precipitation	kg m^{-2} s^{-1}
r_a	Canopy aerodynamic resistance	s m^{-1}
$r_{a,1}$, $r_{a,2}$	Aerodynamic resistances between canopy layer 1 and the reference height and between canopy layers 2 and 1	s m^{-1}
r_b	Leaf-boundary layer resistance	s m^{-1}
$r_{b,1}$, $r_{b,2}$	Leaf-boundary layer resistances of layers 1 and 2	s m^{-1}
r_c	Canopy resistance	s m^{-1}
$r_{c,1}$, $r_{c,2}$	Canopy resistances of layers 1 and 2	s m^{-1}
$r_{c,\min}$	Minimum canopy resistance	s m^{-1}
r_{f1}	Far-field resistance to heat transfer between the effective canopy source height and the reference height	s m^{-1}
r_{f2}	Far-field resistance to heat transfer between the ground surface and the effective canopy source height	s m^{-1}
r_n	Near-field resistance	s m^{-1}
r_{soil}	Soil surface resistance	s m^{-1}
s	Rate of change of saturated vapour pressure with temperature	kPa K^{-1}
t	Time	s

u	Wind speed at the reference height	$m\ s^{-1}$
u_*	Friction velocity	$m\ s^{-1}$
z	Height or depth	m
z_0	Roughness length	m
z_i	Depth of soil layer i (i = 1, 2 or 3)	m
z_r	Reference height	m
Δe	Saturation deficit	kPa
Δe_1, Δe_2	Saturation deficit of the air stream within canopy layers 1 and 2	kPa
Δe_a	Saturation deficit of the air at the reference height	kPa
Δe_0	Saturation deficit of the air at the 'big leaf' surface	kPa
Δt	Time step	s
Δz_i	Soil layer depth of layer i (i = 1, 2 or 3)	m
Λ	Projected leaf area per unit ground area	$m^2\ m^{-2}$
Λ_{max}	Maximum value of Λ	$m^2\ m^{-2}$
Ω	The "McNaughton-Jarvis" omega factor	dimensionless
α	Relative humidity at the soil surface	dimensionless
$\hat{\alpha}_c$	Canopy albedo	dimensionless
β	Reciprocal of the sum of the soil and aerodynamic resistance ($\beta = r_a/(r_a + r_{soil})$)	dimensionless
$\hat{\chi}$	Canopy sky view factor	dimensionless
$\phi(\zeta)$	Dimensionless source distribution at height ζ	dimensionless
γ	Psychrometric "constant"	$kPa\ K^{-1}$

θ	Soil water content	$m^3\ m^{-3}$
θ_a	Air potential temperature	°C
θ_c	critical value of θ	$m^3\ m^{-3}$
θ_i	Average soil water content of layer i (i = 1, 2 or 3)	$m^3\ m^{-3}$
θ_p	Pore volume fraction	$m^3\ m^{-3}$
θ_s, θ_{sat}	Soil water content at the soil surface and saturated soil water content	$m^3\ m^{-3}$
ϱ_a	Density of air	$kg\ m^{-3}$
σ_w (z)	Standard deviation of vertical velocity	$m\ s^{-1}$
ζ	dimensionless height (z/h)	dimensionless
ψ	Soil matric potential	m
ψ_s	ψ at the soil surface	m
ψ_{sat}	Value of ψ when soil is saturated	m
BATS	Biosphere-Atmospheric Transfer Scheme	
BEST	Bare Essentials of Surface Transfer	
BERMS	Boreal Ecosystems Research and Monitoring Sites	
BWB	Ball-Woodrow-Berry model	
BOREAS	Boreal Ecosystem-Atmosphere Study	
C_3	Species fixing CO_2 mainly into 4-carbon malic and aspartic acids	
CLASS	Canadian Land Surface Scheme	
CST	Central Standard Time	
ECMWF	European Centre for Medium-Range Weather Forecasts land surface scheme	

EST	Eastern Standard Time
JS	Jarvis-Stewart model
LAI	Projected leaf area per unit ground area
LNF	Lagrangian near field
MBWB	Modified Ball-Berry model
PM	Penman-Monteith equation
SiB	Simple Biosphere Model
SiB2	Revised Simple Biosphere Model

LIST OF TABLES

LIST OF FIGURES

Acknowledgments

I would like to thank my supervisor, Dr. Andy Black, for passing to me his knowledge and experience at all stages of this research. His judgment, suggestions and criticism significantly contributed to the completion of this work. I also appreciate his patience, help, friendship and continuous support in all aspects over the past four years.

My supervisory committee, Drs. Bill Bailey, Mike Novak and Hans Schreier gave valuable comments and suggestions, and corrected many grammatical and typographical errors in the thesis. Dr. Novak helped me with the soil physics and provided me with invaluable data at the Agassiz sites. Dr. Bailey gave me completely free access to his energy balance data collected at the soybean site. Dr. Diana Verseghy gave helpful comments, suggestions and corrections to Chapters 2 and 3. Dr. Ken King, University of Guelph, generously provided energy balance data at the Elora site. All this help and cooperation is sincerely appreciated.

Zoran Nesic and Rick Ketler assisted in solving many technical problems associated with the computer network and data transfer. A pleasant working environment in Annex 3 was provided by Peter Blanken, Wenjun Chen, Paul Yang, Zoran Nesic, Rick Ketler, Bill Chen, Jon Warland, Uwe Gramann, Elyn Humphreys, Gordon Drewitt, Eva Jork, Robert Swanson, Alberto Orchansky and Altaf Arain. I also like to thank our department for providing me with a great place for my study and research. Special thanks go to Alison Block for her friendly assistance in the departmental office.

This research was part of the land surface processes node of the Canadian Climate Research Network funded by Environment Canada. Data from the Old Aspen site (PANP) were obtained during the Boreal Ecosystem-Atmosphere Study (BOREAS) and the Boreal Ecosystems Research and Monitoring Sites (BERMS) follow-on initiative. The former was funded by a Natural Sciences and Engineering Research Council (NSERC) Collaborative Special Project Grant, and grants from the AES (Atmospheric Environment Service)/NSERC Joint Science Subvention Program and the Canadian Forest Service Research at the Old Aspen site was done collaboratively with the AES (Air Quality Research Branch (AQRB) and Climate Research Branch) and the University of Guelph (Land Resource Science Department). NSERC Operating Grants (TAB) and BC Ministry of Forest contracts funded the energy balance research at the Douglas-fir sites in BC. Data from the Agassiz site were obtained from an energy balance study supported by grants from Agriculture Canada and the British Columbia Ministry of Agriculture.

Financial support to myself from 1994 to 1999 was generously provided by Environment Canada through the land surface processes node of the Canadian Climate Research Network.

Finally I would like to thank my wife, Julie, for her long-time support in pursuit of my goals. The sacrifices she has made to support the family are truly appreciated. A happy and harmonious family life provided by Julie and my son, Jesse, made this work possible and enjoyable.

CHAPTER 1

INTRODUCTION

Land surface models are designed for use in general circulation models (GCMs) to compute the fluxes of radiation, heat, water vapour, and momentum across the land-atmosphere interface. Over the last 20 years, three generations of models have evolved from simple, unrealistic schemes to sophisticated modern systems based on physical and biophysical principles which are capable of modelling not only energy and water vapour fluxes but also trace gas (e.g. CO_2) flux fluxes (Sellers et al. 1997).

The first generation of land surface models, developed in the late 1960's and 1970's, was based on simple aerodynamic bulk transfer formulas. Vegetation was not modelled as separate from the soil and its only effect was to change the surface roughness and albedo. The second generation of models developed in the early 1980's was characterized by more soil thermal and moisture layers and often had a separate layer for the vegetation canopy. Two commonly-known land surface models of this type that were developed were the Biosphere-Atmosphere Transfer Scheme "BATS" (Dickinson et al. 1986) and the Simple Biosphere Scheme "SiB" (Sellers et al. 1986). Other schemes rapidly followed, including the Bare Essentials of Surface Transfer "BEST" (Pitman et al. 1991), the Canadian Land Surface Scheme "CLASS" (Verseghy 1991; Verseghy et al. 1993), and the European Centre for Medium-range Weather Forecasts "ECMWF" land surface scheme (Viterbo and Beljaars 1995). The third generation of surface models, which is in development, relates photosynthesis to plant and soil water conditions to

provide a consistent description of the exchanges of energy, water and carbon by plants (Bonan 1995; Sellers et al. 1996; Wang and Leuning 1998; Baldocchi and Meyers 1998).

Any physical parameterization scheme designed for use in GCMs should be validated using observed data to demonstrate that the simulations it generates are physically realistic and consistent. When coupled with the Canadian GCM, the implementation of CLASS has led to simulated global surface temperatures and precipitation rates which agree more closely with large-scale observations than when the old CLASS scheme was used (Verseghy et al. 1993; Verseghy 1996). When run uncoupled from the host atmospheric model and forced with standard and measured meteorological datasets, i.e. the "stand alone" mode, CLASS has also been tested in PILPS, the Project for Intercomparison of Land-surface Parameterization Schemes (Henderson-Sellers et al., 1993). A number of problems associated with CLASS were identified (Verseghy 1999): a) evaporation from bare soil was too large, b) transpiration rates were underestimated under conditions of high solar radiation, and c) generated runoff was too low. Although some of the PILPS tests point to probable weaknesses in the formulation of some of the CLASS algorithms, it was not clear what improvements were really necessary. Consequently, there is a need to assess model performance in the stand-alone mode using a variety of comprehensive, high-quality micrometeorological datasets collected over a range of surface types and furthermore, to improve the physical formulations based on the information obtained from these tests.

Energy and water vapour fluxes are usually calculated using the gradient-diffusion relationship, i.e. K-theory, in current land surface schemes. In recent years, the applicability of K-theory within and just above plant canopies has been challenged by

observations of countergradient flux (e.g. Denmead and Bradley 1985, Thurtell 1989). New theories appeared to account for some of the features of turbulent transfer processes within canopies more accurately than *K*-theory (e.g. Meyers and Baldocchi 1988, Wilson 1989, Raupach 1989). One promising approach is Raupach's (1989) Lagrangian-based 'localized near-field' (LNF) theory (e.g. Katul et al. 1997). However, the occurrence of counter-gradient flows and intermittent turbulence within the plant canopies are often neglected in most land surface schemes.

This study was part of a research project within the Canadian Climate Research Network, set up in 1993 to encourage and financially support research aimed at reducing the uncertainties about the magnitude, timing and extent of the effects of climate change in Canada. The land surfaces under investigation within this project are alpine, Arctic tundra, agricultural crops, bare soil, grassland, forests (Douglas-fir, boreal aspen, subarctic open woodland and young Jack pine) and a variety of swamps and wetlands. This thesis has the following objectives: (1) to evaluate CLASS (current version 2.6) using continuously half-hourly energy balance and soil water content data collected from a boreal aspen forest during much of 1994 and from spring 1996 to the end of 1998 and six west coast Douglas-fir forests, two agricultural crops and two bare soils during short summer periods over past twenty years, (2) to determine the feasibility of using in CLASS semi-empirical parameterizations of evaporation from the soil surface obtained in a re-analysis of data collected in an earlier intensive study of soil evaporation, (3) to evaluate and compare empirical canopy conductance relationships obtained in several Douglas-fir forests and an aspen forest, and to determine the potential of using an approach that links canopy conductance to carbon assimilation rate, i.e. a more

physiologically-based approach, (4) to examine how well K-theory and LNF theory canopy evaporation models perform for the aspen forest, a Douglas-fir forest and an agricultural crop and (5) to compare the performance of single-layer canopy models with two-layer canopy models in calculating evaporation from the aspen forest which has a thick distinct understory.

This dissertation consists of five papers. The first paper (Chapter 2) demonstrates the need for an improved bare soil evaporation algorithm and tests its effectiveness when applied to bare soils and to soil surfaces beneath two vegetation canopies. The second paper (Chapter 3) concentrates on testing parameterizations of the canopy conductance for one of the Douglas-fir forests and the aspen forest. The third paper (Chapter 4) tests the effectiveness of the parameterizations derived in Chapters 2 and 3 using a multiyear dataset collected from the aspen forest. The fourth paper (Chapter 5) shows the effectiveness of the Lagrangian near-field resistance derived using Raupach's (1989) LNF theory in the calculation of sensible heat fluxes over the Douglas-fir and aspen forests using the flux-gradient relationship. By incorporating the near-field resistance into CLASS, its effect on the calculation of sensible and latent heat fluxes both above and below three different vegetated surfaces is also examined. The fifth paper (Chapter 6) compares the performance of two two-layer canopy models applied to the aspen forest: the first model was based on the LNF theory and the other on K-theory. Though this chapter does not deal with any physical formulations in CLASS, the results obtained here have a significant implications for the future development of land surface schemes. The conclusions of the dissertation are presented in Chapter 7. Supplementary documents and results can be found in the Appendices.

Both terms "conductance" and "resistance" are used in the thesis since both have their advantages in analysis and discussion. The units follow the Système International; however, to avoid superfluous zeros resulting from either the metre or the millimetre as a unit of length, the centimetre is retained, as suggested in 'Principles of Environmental Physics' by Monteith and Unsworth (1990).

References

Bonan, G. B. 1995. Land-atmosphere CO_2 exchange simulated by a land surface process model coupled to an atmospheric general circulation model. *J. Geophys. Res.*, 100(D2): 2817-2831.

Baldocchi, D. D. and T. P. Meyers. 1998. On using eco-physiological, micrometeorological and biogeochemical theory to evaluate carbon dioxide, water vapour and trace gas fluxes over vegetation: a perspective. *Agric. For. Meteorol.*, 90: 1-25.

Denmead, O. T. and E. F. Bradley. 1985. Flux-gradient relationships in a forest canopy. In: B.A. Hutchison and B.B. Hicks (Editors), *The Forest-Atmosphere Interaction*, Reidel, Dordrecht, 421-442.

Dickinson, R. E., Henderson-Sellers, A., P. J. Kennedy and M. F. Wilson. 1986. Biosphere-Atmosphere Transfer Scheme (BATS) for the NCAR Community Climate Model. National Centre for Atmospheric Research, Boulder, Colorado, *NCAR/TN-275+STR*, 69 pp.

Henderson-Sellers, A., Z.-L. Yang and R. E. Dickinson. 1993. The Project for Intercomparison of Land-Surface Parameterization Schemes. *Bull. Amer. Meteorol. Soc.*, 74: 1335-1349.

Katul, G, R. Oren, D. Ellsworth, C. I. Hsieh and N. Phillips. 1997. A Lagrangian dispersion model for predicting CO_2 sources, sinks, and fluxes in a uniform loblolly pine (*Pinus taeda L.*) stand. *J. Geophys. Res.*, 102(D8): 9309-9321.

Meyers, T. P. and D. D. Baldocchi. 1988. A comparison of models for deriving dry deposition fluxes of O_3 and SO_2 to a forest canopy, *Tellus*, 40B, 270-284.

Monteith, J. L. and M. H. Unsworth. 1990. *Principles of Environmental Physics,* 2nd Edition, Edward Arnold, London, 291 pp.

Pitman, A. J., Z.-L. Yang, J. G. Cogley and A. Henderson-Sellers. 1991. Description of bare essentials of surface transfer for the Bureau of Meteorology Research Centre AGCM. *Res. Rep.*, 32, Bur. of Meteorol. Res. Cent., Melbourne, Victoria, Australia.

Raupach, M. R. 1989. A practical Lagrangian method for relating scalar concentration to source distributions in vegetation canopies. *Q. J. R. Meteorol.*, 115: 609-632.

Sellers, P. J, Y. Mintz, Y. C. Sud and A. Dalcher. 1986. A simple biosphere model (SiB) for use within general circulation models. *J. Atmos. Sci.*, 43: 505-531.

Sellers, P. J., D. A. Randall, G. J. Collatz, J. A. Berry, C. B. Field, D. A. Dazlich, C. Zhang, G. D. Collelo and L. Bounoua. 1996. A revised land surface parameterization (SiB2) for atmospheric GCMs. Part I: Model Formulation. *J. of Climate*, 9: 676-705.

Sellers, P. J., R. E. Dickinson, D. A. Randall, A. K. Betts, F. G. Hall, J. A. Berry, G. J. Collatz, A. S. Denning, H. A. Mooney, C. A. Nobre, N. Sato, C. B. Field and A. Henderson-Sellers. 1997. Modeling the exchanges of energy, water, and carbon between continents and the atmosphere. *Science*, 75: 502-509.

Thurtell, G. W. 1989. Comments on using *K*-theory within and above the plant canopy to model diffusion processes. In: *Estimation of Areal Evapotranspiration*, edited by T. A. Black, D. L. Spittlehouse, M. D. Novak and D. T. Price, IAHS Publ., 177: 81-85.

Verseghy, D. L. 1991. CLASS - A Canadian land surface scheme for GCMs, I. Soil model. *Int. J. Climat.*, **11:** 111-133.

Verseghy, D. L., N. A. McFarlane and M. Lazare. 1993. CLASS - A Canadian land surface scheme for GCMs, II. Vegetation model and coupled runs. *Int. J. Climat.*, **13:** 347-370.

Verseghy, D. L. 1996. Local climates simulated by two generations of Canadian GCM land surface schemes. *Atmosphere-Ocean*, **34:** 435-456.

Verseghy, D. L. 1999. The Canadian Land Surface Scheme (CLASS): 1987-1997. *Atmosphere-Ocean*, in press.

Viterbo, P. and A. C. M. Beljaars. 1995. An improved land surface parameterization scheme in the ECMWF model and its validation. *J. Climate*, 8: 2716-2748.

Wang, Y.-P. and R. Leuning. 1998. A two-leaf model for canopy conductance, photosynthesis and partitioning of available energy I: Model description and comparison with a multi-layered model. *Agric. For. Meteorol.* 91: 89-111.

Wilson, J. D. 1989. Turbulent transport within the plant canopy. In: *Estimation of Areal Evapotranspiration*, IAHS Publ., 177, 43-80.

CHAPTER 2

TESTING THE α AND β METHODS OF ESTIMATING EVAPORATION FROM BARE SOILS AND THE SOIL SURFACE BENEATH PLANT CANOPIES IN THE CANADIAN LAND SURFACE SCHEME

2.1. Introduction

Evaporation from the soil surface accounts for a significant part of the latent heat exchange between land surfaces and the atmosphere. This process is controlled by atmospheric conditions, surface soil wetness and moisture transport below the soil surface. For many land surface models used in general circulation models (GCMs) that have a thick surface soil layer, it is particularly difficult to obtain an accurate estimate of the evaporation rate because of the marked nonlinearity of the hydraulic properties of soils close to the air-soil interface (e.g. Mahrt and Pan 1984). Consequently, simple parameterizations have been proposed relating evaporation from the soil surface to the near-surface soil water content, θ (m^3 m^{-3}). However, inaccurate parameterizations can result in significant errors in the prediction of sensible and latent heat fluxes at the soil surface (e.g. Mihailović et al. 1995a).

Three methods for the estimation of evaporation have been used in many land surface models: the α, β and threshold methods. In the α method, the relative humidity at the soil surface (α) is parameterized (Philip 1957; Noilhan and Planton 1989; Jacquemin and Noilhan 1990; Mihailović et al. 1993; Alvenas and Jansson 1997) and evaporation from the soil surface is calculated using

$$Q_E = L_v \varrho_a (\alpha q_{sat}[T_s] - q_a) / r_a \quad (2.1)$$

where Q_E is the latent heat flux (W m^{-2}), L_v is the latent heat of vaporization (J kg^{-1}), ϱ_a is the density of air (kg m^{-3}), q_a is the specific humidity of the air at a reference height, q_{sat} is the saturation value of specific humidity at the soil surface temperature T_s (°C), and r_a is the aerodynamic resistance between the soil surface and the reference height (s m^{-1}). The product of α and q_{sat} represents the specific humidity at the soil surface. In the β method, water vapour is assumed to diffuse through an isothermal thin surface layer of dry soil (with a resistance, r_{soil} (s m^{-1})) beneath which the soil is very close to saturation, i.e. specific humidity is approximately equal to q_{sat} (Barton 1979; Deardoff 1978; Passerat de Silans 1986; Kondo et al. 1990; Lee and Pielke 1992). The value of β, a dimensionless reciprocal of the sum of the soil and aerodynamic resistances ($\beta = r_a/(r_a + r_{soil})$, is parameterized and evaporation is calculated using

$$Q_E = L_v \varrho_a \beta (q_{sat}[T_s] - q_a) / r_a \quad (2.2)$$

Fuchs and Tanner (1967), however, working on a sandy soil, concluded that the concept of a surface resistance was not valid because there was not a clearly defined sharp boundary between the dry and saturated soil layers. On the other hand, Novak and Black (1985) working on a silt/loam soil (same soil as in the present study) found that r_{soil} was relatively well defined. Others have used a combination of the α and β methods (Camillo and Gurney 1986; Dorman and Sellers 1989; Ye and Pielke 1993). In the third method, evaporation occurs at the potential rate until the soil is no longer able to meet this demand and then becomes limited by supply (Mahrt and Pan 1984; Dickinson 1984; Wetzel and Chang 1987; Abramopoulos et al. 1988; Avissar and Mahrer 1988). Of the α and β

methods, it is not clear which of the two is generally superior; however, from a practical point of view, the β method appears to be easier to use (Kondo el at. 1990; Lee and Pielke 1992). The threshold method requires exact information on the hydraulic properties of the thin surface soil layer and usually tends to underestimate surface evaporation (Mahfouf and Noilhan 1991).

In CLASS (Canadian Land Surface Scheme) (Verseghy 1991; Verseghy et al. 1993) and several surface models (e.g. McCumber and Pielke 1981; Camillo et al. 1983; Chung and Horton 1987), α is determined using Philip's (1957) thermodynamic relationship

$$\alpha = \exp[g\psi_s / R_v T_s] \tag{2.3}$$

where g is the acceleration due to gravity (m s^{-2}), R_v (J kg^{-1} K^{-1}) is the gas constant for water vapour at surface temperature of T_s, and ψ_s is the soil water matric potential at the soil surface (m). In CLASS, ψ_s is calculated using the soil water retention relationship $\psi(\theta_s)$ with the surface volumetric soil water content (θ_s) extrapolated from the values of θ of the top two soil layers. This relationship can be used when a local equilibrium exists between the liquid and vapour phases. Milly (1982) indicates that vapour in the soil is generally in equilibrium with the liquid except for high infiltration rates into coarse soils and the relationship is therefore valid in most conditions. In models with fine depth resolution (i.e. a few mm), Philip's relationship appears to work well (e.g Witono and Bruckler (1989) and Passerat de Silans et al. (1989)). However, in numerical weather-climate models with a coarse resolution near the surface (i.e. 5 - 10 cm), the validity of using Philip's relationship has been questioned by Kondo et al. (1990) and Lee and Pielke (1992) because α obtained using Philip's relationship does not represent the surface

relative humidity during the latter part of a drying period when there is a large vertical gradient in soil water content near the surface. As a result, Philip's relationship in these models likely overestimates evaporation during the drying period because α is significantly overestimated (Lee and Pielke 1992, Mihailović et al. 1995a, b). A recent test of the performance of nine different α and β formulations by Dekić et al. (1995) for a bare chernozem soil with a 10-cm thick surface layer showed that Philip's relationship gave the largest errors in dry conditions.

Since many of the relationships to determine α and β have been developed based on measurements of the average θ in a 1 to 2-cm thick soil surface layer, `they were not intended to be used in soil evaporation models that have a thick surface soil layer, as in CLASS (which has a 10-cm thick surface layer) and some other land surface models such as ISBA (Noihan and Planton 1989) and the ECMWF land surface scheme (Viterbo and Beljaars 1995). Consequently, the aims of this study are (i) to examine the empirical relationship of α and β determined from measurements of evaporation to θ for different averaging depths from 0.5 to 10 cm in a bare loam/silt-loam soil and (ii) to test the effectiveness of these relationships in the calculation of evaporation by CLASS using data collected from two bare soils, one agricultural crop and two forests.

2.2. Relationships of α and β to θ

Data used to assess the α and β methods were obtained as part of an energy and water balance experiment carried out in a 145 by 175 m level field at the Agriculture Canada Research Station, Agassiz, BC, in the late spring and summer of 1978 (Novak 1981, Novak and Black 1983). The soil was a Monroe series loam/silt-loam (Eluviated

Eutric Brunisol). Profiles showed little textural variability to depths ranging from 50 to 100 cm, below which coarser textured layers were often encountered. The water table was located between 1 and 2 m below the soil surface. The field was separated into two parts, referred to as sites 1 and 2. Site 1 was disc-harrowed, then firmly packed with a culti-packer, while site 2 was disc-harrowed (to a depth of 10 cm). Net radiation flux density, Q^* (W m^{-2}), at each site was measured with a Swissteco S-1 net radiometer mounted 65 cm above the soil surface. Soil surface heat flux density, G_0 (W m^{-2}), was calculated from measured profiles of soil temperature and volumetric heat capacity using the null-alignment method of Kimball and Jackson (1975). It was found to be in good agreement with those measured with heat flux plates (Novak 1981). The sensible heat flux, Q_H (W m^{-2}), and Q_E were measured using the Bowen ratio/energy balance (BREB) method. This method uses the equations: $Q_E = (Q^* - G_0)/(1 + B)$ and $Q_H = Q_E B$, where B is the Bowen ratio (Q_H / Q_E) which is calculated from $B = \gamma \Delta T/\Delta e$, where ΔT and Δe are the measured vertical differences in temperature and vapour pressure (kPa) respectively, and γ is the psychrometric constant (kPa K^{-1}). The Bowen ratios were measured with a reversing psychrometric unit with lower and upper sensor heights of 20 and 120 cm (Black and McNaughton 1971). Soil temperatures were measured by a bank of 30 copper-constantan thermocouples installed in a single profile from 0.2 cm below the surface to a depth of 105 cm. Soil surface temperature was determined from the cubic spline polynomials that were fitted to the measured soil temperature profiles and confirmed by occasional measurements using a hand-held infrared thermometer (model PRT-10-L, Barnes Engineering) (Novak and Black 1985). Soil moisture content was measured gravimetrically in 18 layers from the surface to a depth of 80 cm. Bulk density was

measured at 5 cm intervals to a depth of 50 cm and at 10 cm intervals below 50 cm. Values of the porosity of the surface 5-cm layer were 0.63 and 0.67 for sites 1 and 2, respectively. Windspeed was measured with a sensitive anemometer (Cassella Ltd., London) located at a height of 95 cm at site 1. Precipitation and other standard meteorological variables were measured routinely by the research station staff at a climate station adjacent to the study area.

Values of α and β were determined from Eqs. (2.1) and (2.2) with measured values of Q_E, q_a and T_s. The aerodynamic resistance r_a was determined using $r_a = \varrho_a c_p [T_s - T_a] / Q_H$, where c_p is the specific heat of air (J kg^{-1} K^{-1}) and T_a is the air temperature measured at the reference height of 1.5 m (°C). The relationships of α and β to average θ for surface layer thicknesses ranging from 0.5 to 10 cm at the two sites are shown in Figs. 2.1 and 2.2. There was very little difference between the α and β relationships, which indicates that q_a was usually much less than $q_{sat}(T_s)$ because bare soil surface temperature was generally high during the experiment. With an increase in thickness, the scatter in the plots tended to decrease; however, the values of θ for low α and β and the sensitivity of α and β to θ (e.g. dα/dθ and dβ/dθ) increased. These results confirm Mahrt and Pan's (1984) findings that the relationship between evaporation and average θ is strongly dependent on thickness of the surface soil layer. Some of the scatter in the plots can be attributed to variation in wind speed (Kondo et al. 1990); however, it was found to be very small. Figs. 2.1 and 2.2 also show the effect of surface soil

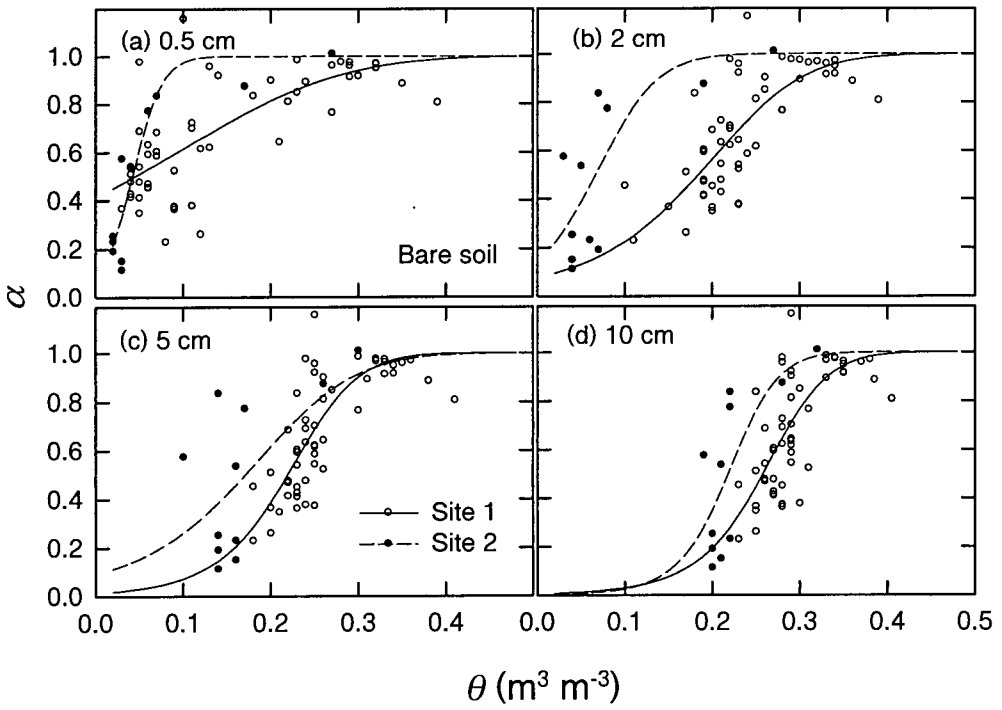

Fig. 2.1. Relationship between α and average soil water content (θ) in a soil surface layer extending to depths of 0.5, 2, 5 and 10 cm at sites 1 and 2 at Agassiz, BC. Circles are measured values and lines are the best fitting obtained using Eq. (2.4).

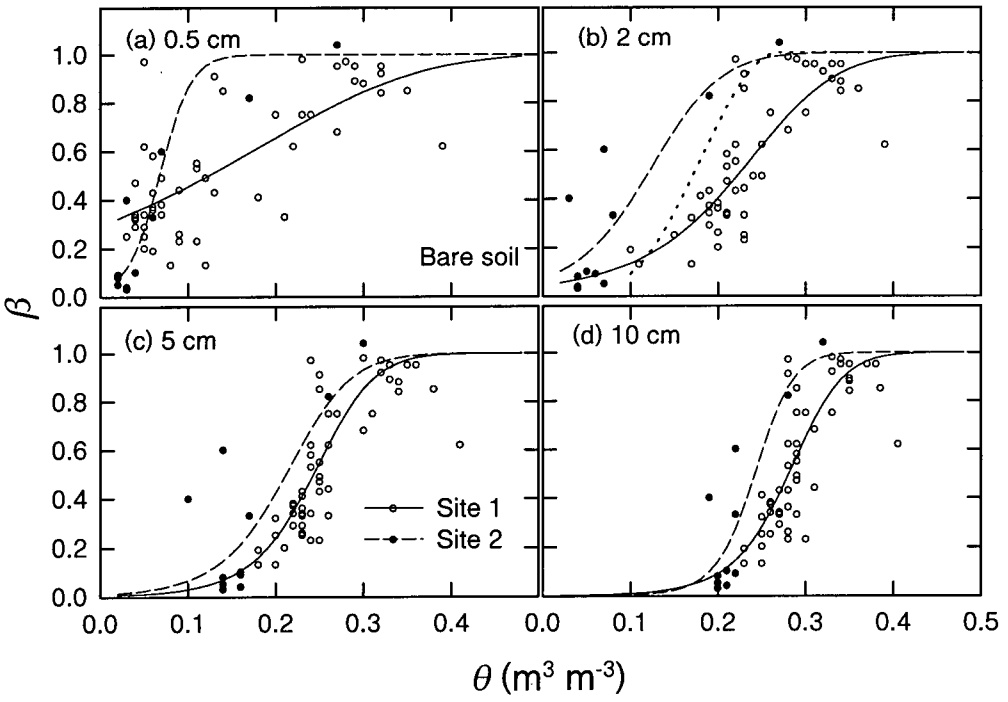

Fig. 2.2. Same as Fig. 2.1. but for β. Also shown are values (dotted line) obtained using Lee and Pielke's (1992) β formula.

conditions (i.e. the disc-harrowed and culti-packed) on these relationships. For a given value of θ, values of α and β for site 2 were larger than those for site 1. This is likely because the resistance to water vapour diffusion through the surface layer at site 2 was less than that at site 1 for same θ since the surface layer at site 2 contained a higher proportion of macropores than at site 1 (Novak, 1981).

The functional forms of α and β, shown as curves in Figs. 2.1 and 2.2, were obtained using non-linear least squares analysis based on the relationship derived by Kondo et al. (1990) (except that we assumed no effect of wind speed, following Lee and Pielke (1992))

$$\alpha = 1/[1+a_1(\theta_{sat}-\theta)^{a_2}]$$
$$\beta = 1/[1+b_1(\theta_{sat}-\theta)^{b_2}] \qquad (2.4)$$

where θ_{sat} is the saturation soil water content or porosity and a_1, a_2, b_1 and b_2 are empirical coefficients determined using the measured values of α, β and θ. Values of the coefficients for the different thicknesses at sites 1 and 2 are shown in Table 2.1. Although θ_{sat} has been used in some α and β relationships (e.g. Sellers et al. 1996), field capacity (θ_{fc}) has been more often used (e.g. Lee and Pielke (1992), Noilhan and Planton 1989)). Values of β computed using Lee and Pielke's (1992) empirical formula for a 2-cm thick loamy soil ($\beta = 1/4(1-\cos(\theta\pi/\theta_{fc}))^2$ for $\theta \leq \theta_{fc}$ and $\beta = 1$ for $\theta > \theta_{fc}$, are plotted in Fig. 2.2b. Their values lie between those for sites 1 and 2. This is likely because the soil they used was neither firmly packed nor loosened.

Table 2.1. Coefficients used in the α and β relationships for sites 1 and 2 at Agassiz, BC.

Surface layer thickness (cm)	α relationship				β relationship			
	Site 1		Site 2		Site 1		Site 2	
	a_1	a_2	a_1	a_2	b_1	b_2	b_1	b_2
0.5	1.30×10	4.79	3.30×10^7	37.2	1.50×10	3.96	2.22×10^7	33.4
2.0	3.30×10^2	7.18	5.39×10^3	17.0	5.60×10^2	7.02	2.46×10^3	13.1
5.0	7.78×10^3	10.1	2.34×10^2	7.85	3.47×10^4	11.0	1.31×10^4	12.1
10.0	1.75×10^4	9.88	2.63×10^5	15.7	1.19×10^5	11.1	1.43×10^7	19.4

2.3. Validation of the α and β relationships in CLASS

CLASS contains three soil layers (0-10 cm, 10-35 cm and 35-375 cm), an explicitly modelled snow layer and a thermally separate vegetation canopy layer. Heat and moisture transfers between layers are calculated using flux-gradient relationships, and the surface infiltration rate depends on the rainfall rate, the presence of water detained on the surface and the soil moisture profile. Canopy evapotranspiration rates depend on the presence of intercepted water on the canopy, and on the bulk stomatal resistance which varies with soil moisture, incoming solar radiation, atmospheric vapour pressure deficit, canopy temperature and leaf area index. Details of CLASS have been described by Verseghy (1991) and Verseghy et al. (1993).

The effectiveness of Philip's and the α and β relationships was examined by comparing CLASS simulated energy balance components using each of the three relationships with measured values. Since the depth of the first soil layer in CLASS is 10 cm, both the α and β relationships for the corresponding depth were used. A test was conducted with the initial conditions of soil moisture and temperature set equal to measured values. A further test, in which the soil moisture contents of the three soil layers were set equal to measured values during the entire test period, was conducted to examine the effects of modelled soil water movement below the soil surface on the calculation of evaporation from the soil. The purpose of this test was to ensure that errors in the calculation of evaporation were not due to errors in the calculation of soil water movement between soil layers.

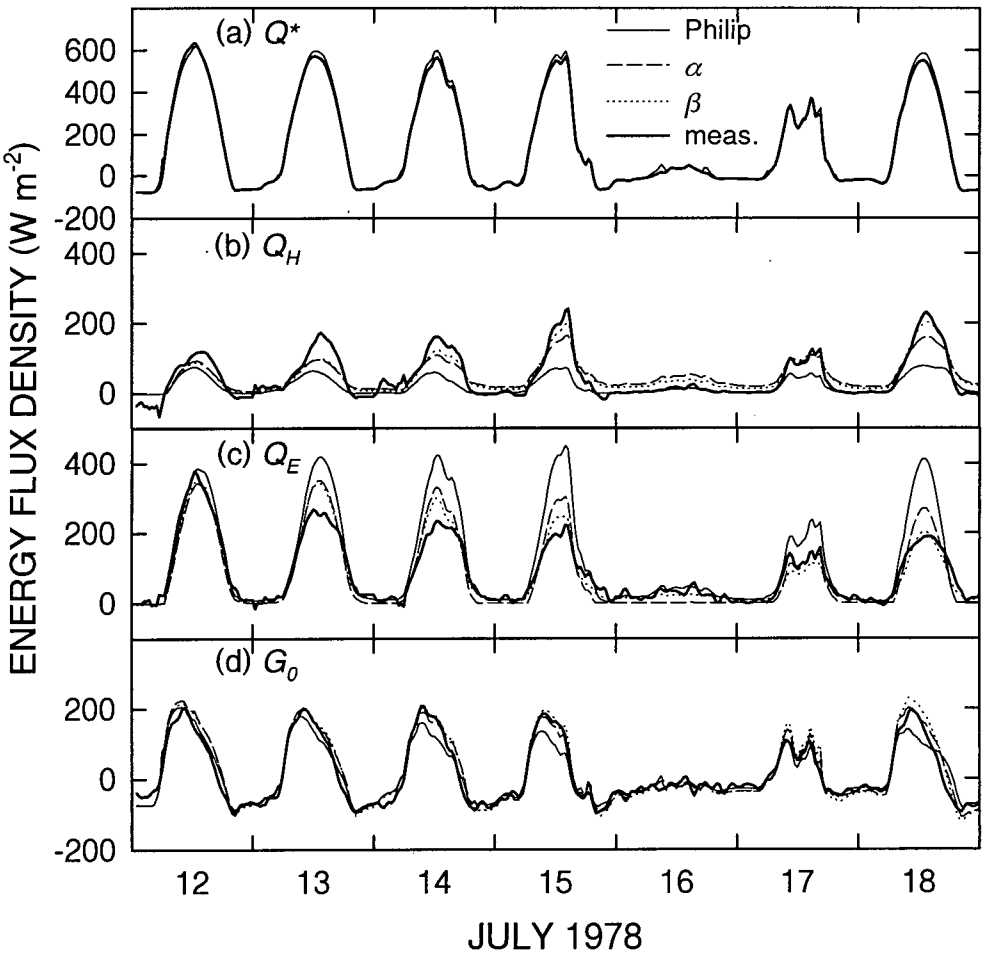

Fig. 2.3. Comparison of diurnal Q^*, Q_H, Q_E and G_0 calculated by CLASS using Philip's, α and β relationships with measured values during a 7-day drying period for site 1 at Agassiz.

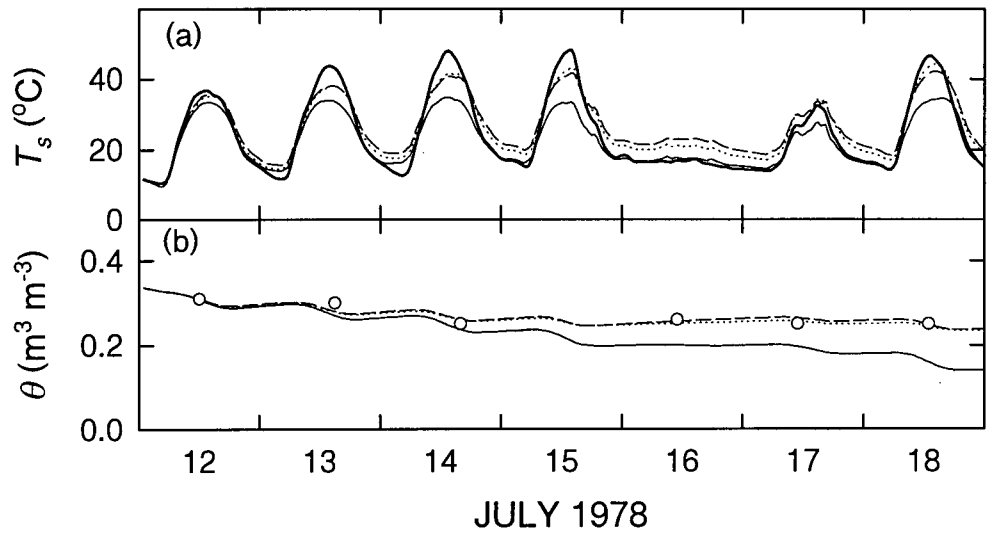

Fig. 2.4. Same as Fig. 2.3. but for T_s and average θ of the 10-cm surface layer. Also shown are measured average θ of the 10-cm surface layer (circles).

For the first test, a 7-day drying period after a rainfall event between July 9 and 11 (15 mm) at the Agassiz site 1 (packed soil) was selected (Figs. 2.3 and 2.4). The second test was not conducted for this period because there was no significant difference between modelled and measured θ. CLASS was initialized to the soil moisture and temperature measured at 00:00 PST 12 July 1978. Modelled Q^* was very close to the measured values, since calculated net longwave radiation (computed from measured values of Q^*, incoming solar radiation and albedo) was used as an input variable because there were no measurements of incoming longwave radiation. The α and β relationships gave much better estimates of Q_E than Philip's relationship. The 7-day evaporation totals computed

using the α and β relationships underestimated measured evaporation by only 5% and 2%, respectively, compared with a 41% overestimation using Philip's relationship (Fig. 2.3). However, evaporation was significantly suppressed by the α relationship during nighttime and on July 16. This was because $\alpha q_{sat}(T_s)$ was probably less than q_a when the air humidity was high, as both the α and β relationships were developed using measurements made during the daytime. This suggests that the β relationship is more useful than the α relationship. Values of T_s were underestimated during the daytime by CLASS with Philip's relationship because it generated excessive evaporation rates (Fig. 2.4). Using both the α and β relationships significantly improved daytime T_s; however, nighttime T_s was overestimated. The reason for this is unclear and is probably related to the calculation of soil heat capacity and thermal conductivity as they differed greatly from dry to wet periods according to their measured profiles on June 2 (θ_s = 0.20) and July 21 (θ_s = 0.04) (Novak, 1981). Comparison of modelled and measured soil heat fluxes at the 10-cm depth showed that there was an overestimation of the nighttime upward soil heat flux. However, whether or not this is the reason for the overestimation of nighttime T_s depends on how well the soil heat capacity is computed by CLASS.

Both tests were conducted for a 16-day drying period. This period included the 7-day period discussed above. The results of the tests in terms of the effects on the calculation of cumulative evaporation are shown in Fig. 2.5. In the first test (Fig. 2.5a), both Philip's and the β relationships gave reasonably good estimates of evaporation. The ratios of modelled to measured cumulative totals for both relationships were 1.23 and 1.07 for site 1 and 0.96 and 1.08 for site 2, respectively. In the second test (Fig. 2.5b), the

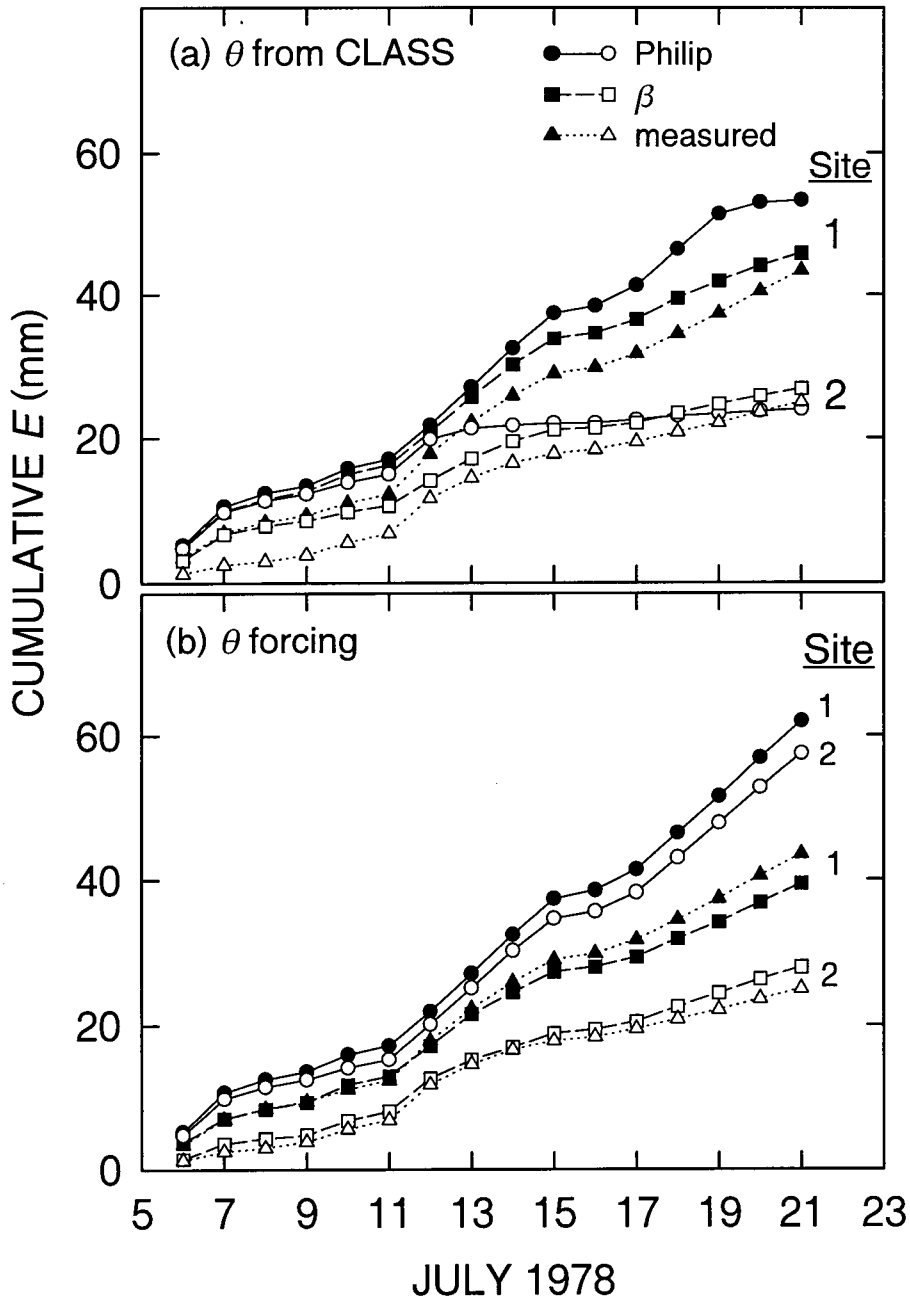

Fig. 2. 5. Comparison of modelled cumulative evaporation calculated by CLASS using Philip's and the β relationships with measured values during a 16-day period for sites 1 and 2. (a) Soil moisture was initialized and then determined by CLASS, and (b) CLASS was forced to use measured soil moisture throughout the test period.

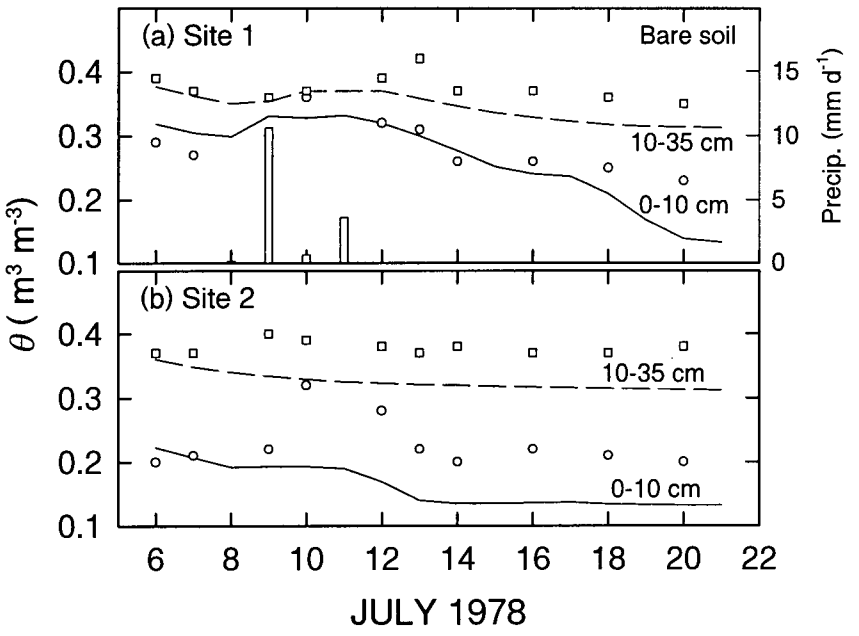

Fig. 2.6. Comparison of modelled average θ in the first (0-10 cm, solid line) and second (10-35 cm, dashed line) soil layer for site 1 (a) and site 2 (b) by CLASS using Philip's relationship with measured values (squares).

β relationship gave much better estimates (the ratios were 0.91 for site 1 and 1.12 for site 2) than Philip's relationship (the ratios were 1.43 for site 1 and 2.30 for site 2). A recent study by Desborough et al. (1996) also showed that CLASS predicted excessive evaporation rates when it was forced to use prescribed soil moisture and temperature. The reason that Philip's relationship gave reasonably good estimates of evaporation in the first test was because the drainage from the surface layer was overestimated which caused the modelled θ of the first and second layers to drop faster than the actual θ during the drying period (Fig. 2.6). This largely compensated for the effect of the overestimation of α by Philip's relationship during the 16-day period.

The two tests were repeated to examine how well the daily average Q_E was calculated in long-term simulations (65 days) for site 1. In the first test (results not shown), evaporation was significantly underestimated during dry periods due to the drainage problem with this dataset (which may be related to the calculation of the soil hydraulic conductivity). In the second test, modelled Q_E obtained using Philip's relationship was significantly overestimated, as in Fig. 2.5b, which caused Q_H to be underestimated, while those obtained using the β relationship agreed remarkably well with the measured values (Fig. 2.7). The results demonstrate the importance of correct estimates of soil surface wetness and movement of water between soil layers in the calculation of evaporation.

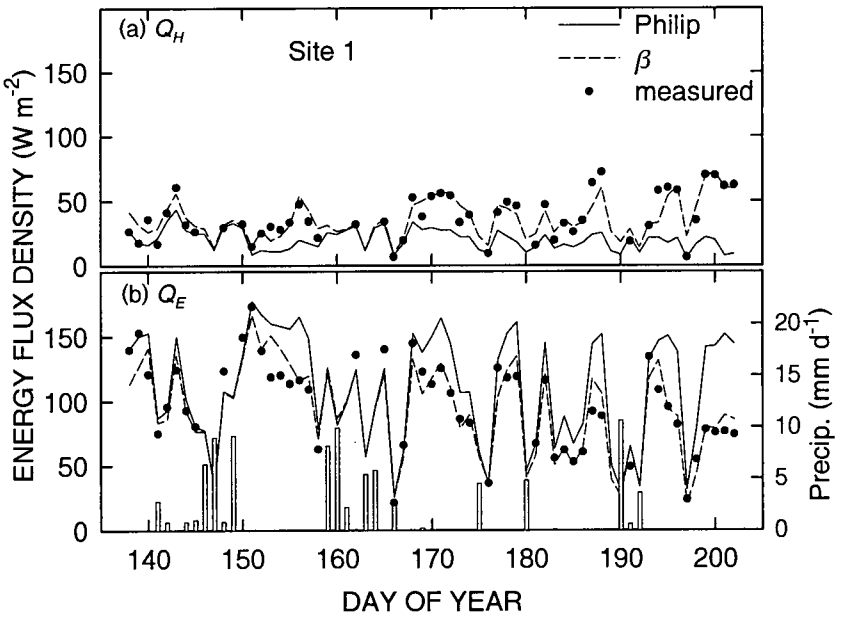

Fig. 2.7. Comparison of daily average Q_H and Q_E calculated by CLASS (forced with measured soil moisture) using Philip's and the β relationships with measured values for site 1. Also shown is the daily precipitation (vertical lines).

2.4. Testing the β relationship for other land surfaces

The β relationship (Eq. (2.4)) obtained from measurements made from site 1 was applied to another bare soil, a crop and two forests because each site has a distinctly different soil type. Actual θ_{sat} or porosity of these soils was used in Eq. (2.4) (Lee and Pielke 1992). To obtain reasonably good estimates of canopy transpiration for the three selected vegetated surfaces, the original parameterization of canopy conductance, g_c (m s^{-1}), in CLASS was either replaced by site-specific parameterizations or adjusted to agree with measured g_c. It was found that modelled Q^* agreed well with measured values and replacing Philip's relationship with the β relationship in CLASS had little effect on the calculation of Q^*.

2.4.1. Bare soil

Data were collected from July to October, 1992, on a silt loam soil at Elora Research Station, Elora, Ont. (K. King, 1995, personal communication). The soil water content of the soil layer between the surface and about the 2-cm depth was measured gravimetrically. There was much precipitation throughout the observational period, so the soil remained relatively wet. The interval DOY (day of year) 226 to 247 was selected because it contained the longest drying cycle (DOY 230 to 240) during the whole observational period to examine how well evaporation was calculated in the second test. The soil porosity was assumed to be the same as that for site 1 at Agassiz. Since soil moisture was measured in a shallow surface layer, the β relationship for the 2-cm depth

was used. This was equivalent to the change in the thickness of the surface soil layer from 10 to 2 cm. The comparison between modelled and measured daily average Q_E shows that the β relationship gave better estimates than Philip's relationship (Fig. 2.8). It is not surprising that modelled Q_E obtained using Philip's relationship agreed well with measured values except during the drying period when it overestimated by 20-25%. This overestimation was much smaller than the 40-50% overestimation shown in Fig. 2.7b, probably because in the latter case the thickness of the surface soil layer was much larger.

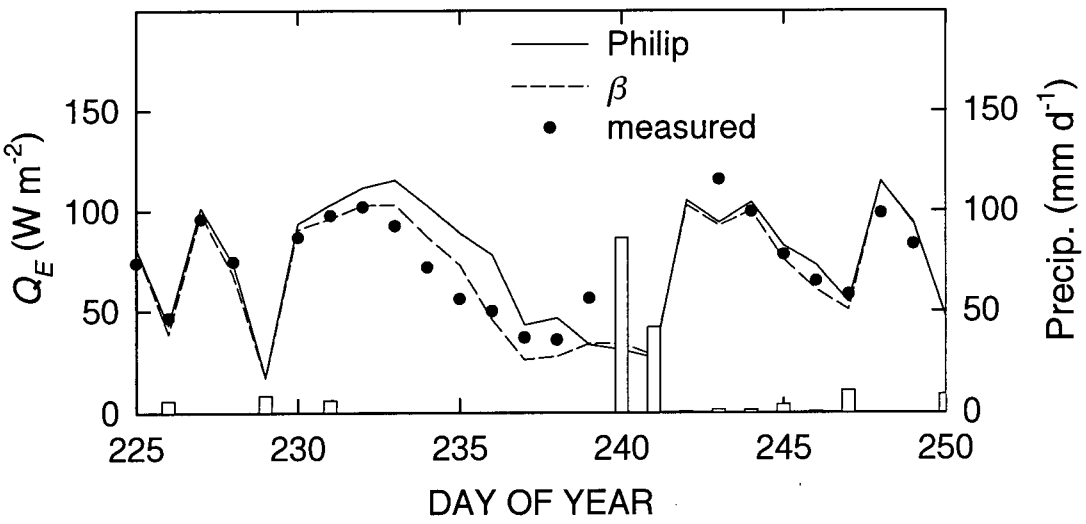

Fig. 2.8. Comparison of daily average Q_E calculated by CLASS (forced with measured soil moisture) using Philip's and β relationships with measured values for the bare soil at Elora, Ontario. Also shown is the daily precipitation.

2.4.2 Vegetated surfaces

For vegetated surfaces, g_c is one of the main factors controlling Q_E from the canopy. Since evaporation comes from the canopy and soil, carefully obtained parameterizations of g_c and evaporation from the soil surface are required to give reasonably good estimates of total Q_E. The validation of the β relationship was done for the three selected vegetated surfaces during periods when drainage was either small or simulated reasonably well by CLASS.

The first vegetation type studied was agricultural cropland. The data were collected over the growing season in 1974 at the Ontario Ministry of Agriculture and Food Horticultural Experiment Station located near Simcoe, Ontario. The site was a flat, 2.6 hectare rectangular field of soybeans (*Glycine max* (L.) Harosoy 63) and the soil had a coarse, sandy character. The crop was planted on June 6 (DOY 157) and the LAI reached unity on July 13 (DOY 194). Maximum LAI (2.93) was reached on August 20 (DOY 232), after which it decreased. The fluxes of Q_H and Q_E were measured using the BREB method during the daytime. Details of the instrumentation and measurement program have been described elsewhere (Bailey and Davies, 1981a).

For soybeans, the relationships between g_c and environmental factors such as the incoming solar radiation, $K_{\downarrow}$ (W m^{-2}), Δe and average root zone θ have been studied (Bailey and Davies 1981a, Bailey 1983). If we assume these effects to be multiplicative (Jarvis 1976), a parameterization of soybean g_c during the full-leaf period can be expressed as (Bailey and Davies 1981a, Bailey 1983)

$$g_c = 0.083 \exp\left(\frac{-89.0}{K_{\downarrow}}\right) \exp\left(\frac{-0.088}{\theta}\right) \exp(-1.0\Delta e) \qquad (2.5)$$

Four days (August 4 to 7) during the middle of a 10-day drying period when the crop was mature were selected (Fig. 2.9). The vegetation fraction for this site was assumed to be 100% covered by crops. The value of the soil porosity was estimated to be 0.50. The β relationship improved the calculation of the total evaporation, especially on August 6 and 7. It was expected that the effect of the β relationship would be small, since evaporation from the soil was considerably lower than that from the canopy because of its high g_c. Some discrepancies are probably related to errors in parameterizing the soybean g_c. Bailey and Davies (1981b) showed that Q_E from the soybean crop was strongly controlled by the canopy resistance, while the effect of the aerodynamic resistance was less important.

The second vegetation type selected was deciduous forest. The data were collected in 1994 from an extensive boreal aspen forest (*Populus tremuloides* Michx.) in the southern part of Prince Albert National Park about 50 km northwest of Prince Albert, Saskatchewan, as part of the Boreal Ecosystem-Atmosphere Study (BOREAS, 1993-1996), BOREAS was a large-scale short-term investigation of carbon, water and energy exchange between the atmosphere and the boreal forest (Sellers et al. 1995). The trees were 21 m tall and the understory was dominated by a uniform cover of hazelnut (*Corylus cornuta* Marsh) with a mean height of 2 m. The soil was an Orthic Luvisol with an 8-10-cm deep surface organic layer (bulk density and porosity were about 160 kg m^{-3} and 0.88, respectively). The mineral soil had a silty-clay texture and a bulk density $\approx$ 1300 kg m^{-3}. The site was moderately well drained due to the elevated topography, coarse-grained

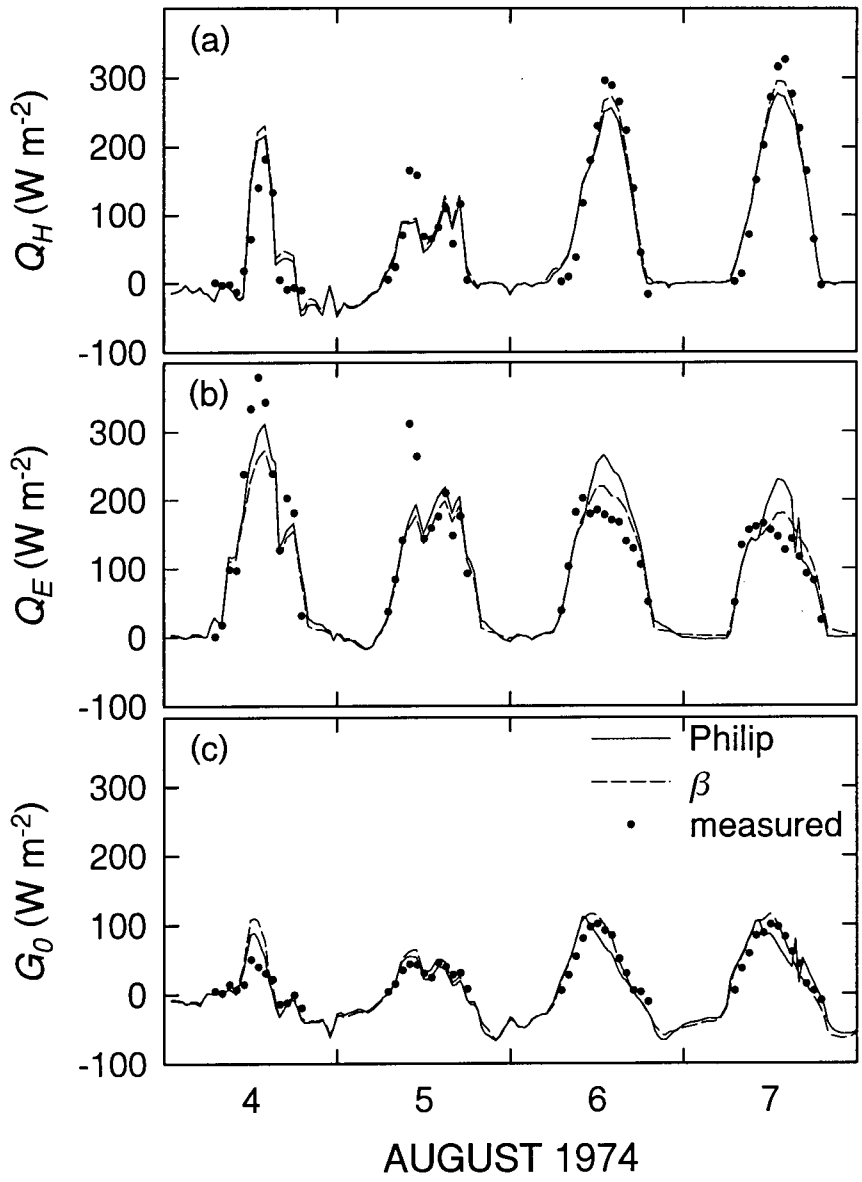

Fig. 2.9. Comparison of diurnal Q_H, Q_E and G_0 calculated by CLASS (with the soybean g_c parameterization) using Philip's and the β relationships with measured values for the soybean crop at Simcoe, ON.

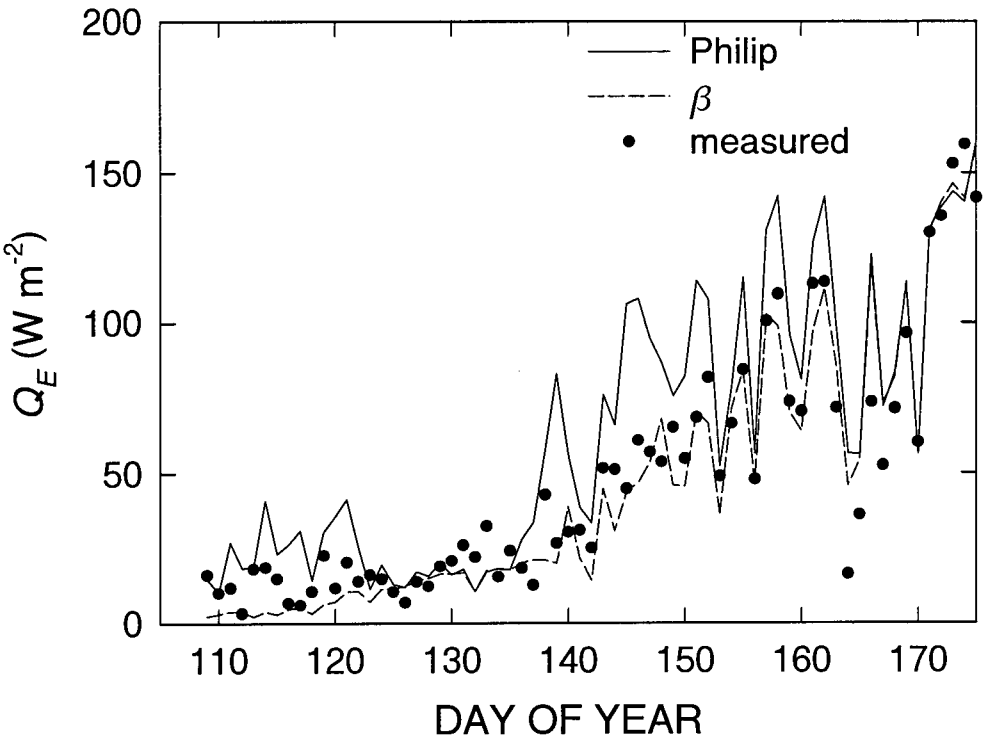

Fig. 2.10. Comparison of daily average Q_E calculated by CLASS using Philip's and β relationships with measured daily means for the aspen forest in Prince Albert National Park, Saskatchewan, before and during the leaf emergence period.

glacial deposits, and the frequent occurrence of intertill and surficial aquifers. The turbulent fluxes (Q_H and Q_E) were measured using the eddy-covariance technique (Black et al. 1996).

At this site, there is usually a 4-6 week period between snowmelt and significant leaf development during which evaporation from the soil surface accounts for most of evaporation from the forest. For this reason, the period before and during the leaf emergence (19 April (DOY 109) to 24 June (DOY 175), 1994) was selected. The

vegetation fraction for the aspen site was assumed to be 100% covered by deciduous forest. The CLASS g_c parameterization was used to compute aspen forest g_c as it gave reasonably good estimates during the leaf emergence period when the measured driving variables of LAI, $K\downarrow$, soil water potential and Δe were used (Wu et al. 1998). Fig. 2.10 compares daily average Q_E calculated by CLASS using Philip's and the β relationships with measured daily values. Although average θ of the surface organic layer measured using time-domain reflectometry (TDR) was high during this period (about 0.40 m^3 m^{-3} on average), measured Q_E was considerably lower than measured Q_H (the Bowen ratio (Q_H/Q_E) was about 7.0) due to the absence of leaves and existence of the leaf litter layer at the soil surface acting as a very effective mulch (Blanken et al. 1997). Philip's relationship overestimated evaporation from the bare forest floor. After DOY 165 when LAI was high (the sum of aspen and hazelnut LAI was about 5.0), using either Philip's or the β relationship made no significant difference to the calculation of Q_E, as evaporation from the soil surface was small. The evaporation total during this period i.e. 109 - 175 (Fig. 2.10) was overestimated by 30% with Philip's relationship, compared with an underestimation of 6% with the β relationship.

The third vegetation type was coniferous forest. The data were collected in 1983 from a 3-ha stand of young (planted in 1971) Douglas-fir (*Pseudotsuga menziesii* (Mirb.) Franco) at Dunsmuir Creek, BC (Price and Black 1990 and 1991). The height of trees was about 3 m and the stand density was low (about 200 stems ha^{-1}). There was considerable understory, mainly consisting of salal (*Gaultheria shallon* Pursh). Values of the LAI for the trees and understory were 0.2 and 1.0, respectively. The soil was classified as a Humic ferric Podzol. The surface organic layer was thin (2 - 4 cm) and the mineral soil was

classified as a gravelly sandy loam (Osberg 1986). Turbulent fluxes were measured using the BREB method.

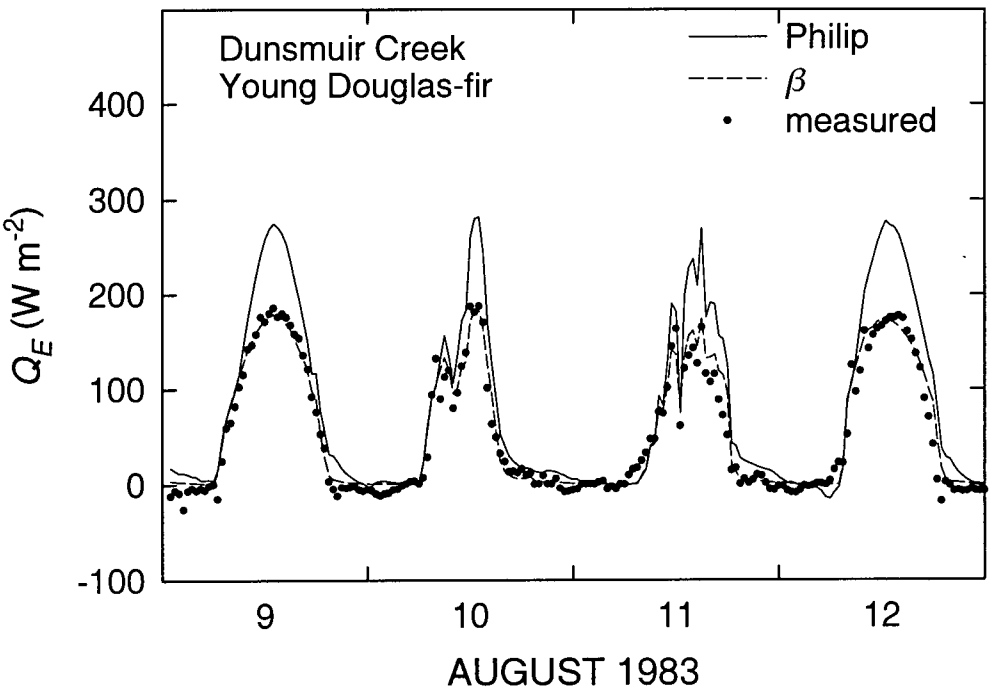

Fig. 2.11 Comparison of diurnal Q_E calculated by CLASS (with the adjusted g_c parameterization) using Philip's and the β relationships with measured values for the young Douglas-fir stand at Dunsmuir Creek, BC

During the observational period, there was no soil water stress in terms of its effect on canopy conductance; however, daytime average g_c was only 5 mm s^{-1} (to avoid a very small value with a unit of m s^{-1}, a unit of mm s^{-1} is used), compared with a value of 11 mm s^{-1} for a near-by old Douglas-fir stand under conditions of no water stress (Price and Black 1991). Thus, an approximation of the parameterization of g_c at this site was simply obtained using the CLASS parameterization with an adjustment of the value of the

maximum g_c. A value of 10 mm s^{-1} was used, compared with values of 20 and 22 mm s^{-1} for natural vegetation in CLASS (Verseghy et al. 1993) and the old Douglas-fir stand (Price and Black 1989), respectively.

Four days were selected to compare modelled diurnal Q_E by CLASS, using Philip's and the β relationships, with measured values (Fig. 2.11). The value of soil porosity was estimated to be 0.70. The grid cell for this site was assumed to be 85% covered by shrubs and 15% covered by coniferous forest. In this particular case, where both g_c and LAI were low, the β relationship significantly improved the calculation of evaporation from the forest floor. The 4-day forest evaporation total agreed with the measured value within 6%, compared with an overestimation by 60% with Philip's relationship.

2.5. Summary and Conclusions

Evaporation from the soil surface accounts for a significant proportion of the latent heat exchange between land surfaces and the overlying atmosphere. This process is largely controlled by the surface soil wetness which is particularly difficult to parameterize in land surface models used in GCMs that have a thick surface soil layer. To obtain a reliable estimate and yet maintain computational efficiency, various parameterizations have been developed to compute the relative humidity at the soil surface α (the α method) or the resistance to water vapour diffusion β (the β method).

Values of α and β were determined from measurements made from a loam/silt-loam soil. The relationships of α and β to θ were sensitive to the θ averaging depth from 0.5 to 10 cm and soil physical treatment (packed or loosened). Although the relationships

became better defined with increasing averaging depth, $d\alpha/d\theta$ (or $d\beta/d\theta$) significantly increased during the drying period. The effectiveness of both the α and β relationships were tested in the calculation of evaporation using CLASS during a 7-day drying period. Philip's relationship, which determines α thermodynamically, significantly overestimated α and generated excessive evaporation rates with the modelled 10-cm surface soil layer used in CLASS. Our proposed α and β relationships gave much better estimates than Philip's. However, under conditions of high air humidity (e.g. during the nighttime), evaporation was significantly suppressed by the α relationship. In long-term simulations, the modelling of the drainage became significantly important. When forced to use measured soil moisture, CLASS gave excellent estimates of evaporation with the β relationship, compared with a significant overestimation during the drying periods with Philip's relationship.

Using the actual values of the soil porosity, the β relationship was applied to another bare soil, a crop and two forests. It gave still better estimates of evaporation from the bare soil during the drying period than Philip's relationship, although the thickness of the surface soil layer had been decreased from 10 to 2 cm. In the case of the vegetated surfaces with low to moderate leaf area index, it significantly improved the calculation of total evaporation if the parameterization of canopy conductance in CLASS (which currently does not vary with vegetation type) was substituted or adjusted with those obtained based on canopy conductance measurements made at these sites.

In conclusion, although the proposed β relationship was derived using data from specific sites, it has been applied successfully to other soil texture classes. It thus suggests

that this relationship can be used in general, as discussed by Lee and Pielke (1992) for their empirical formula. The uniqueness of this study is that the relationship was derived for different surface layer thicknesses (0.5 to 10 cm) for soil water content and different soil treatments (culti-packed or disc-harrowed), while most existing formulas were developed for a 1- to 2-cm thick soil surface layer, for example, Lee and Pielke's formula (2 cm). In terms of the CLASS simulation, the relationship was found to be less sensitive to errors in modelled drainage than Philip's relationship. The β relationship is therefore recommended as a replacement to Philip's relationship because of the difficulty of estimating θ at the soil surface.

2.6. References

Abramopoulos, F., C. Rosenzweig and B. Choudhury. 1988. Improved ground hydrology calculations for global climate models (GCMs): Soil water movement and evapotranspiration. *J. Climate*, 1: 921-941.

Alvenäs, G. and P .-E. Jansson. 1997. Model for evaporation, moisture and temperature of bare soil: calibration and sensitivity analysis. *Agric. For. Meteorol.*, 88: 47-56.

Avissar, R. and Y. Mahrer. 1988. Mapping forest-sensitive areas with a three-dimensional local-scale numerical model. Part I: Physical and numerical aspects. *J. Appl. Meteorol.*, 27: 400-413.

Bailey, W. G. and J. A. Davies. 1981a. Evaporation from soybeans. *Boundary-Layer Meteorol.*, 20: 417-428.

Bailey, W. G. and J. A. Davies. 1981b. The effect of uncertainty in aerodynamic resistance on evaporation estimates from the combination model. *Boundary-Layer Meteorol.*, 20: 187-199.

Bailey, W. G. 1983. Modelling hourly and daily evaporation from cropped surfaces, Fifth Conference on Hydrometeorology. Tulsa, Okla. Published by the American Meteorological Society, Boston, Mass., 229-235.

Barton, I. J. 1979. A parameterization of the evaporation from non-saturated surfaces. *J. Appl. Meteorol.*, 18: 43-47.

Black, T. A., G. den Hartog, H. H. Neumann, P. D. Blanken, P. C. Yang, C. Russell, Z. Nesic, X. Lee, S. C. Chen, R. Staebler and M. D. Novak. 1996. Annual cycles of water vapour and carbon dioxide fluxes in and above a boreal aspen forest. *Global Change Biology*, 2: 219-229.

Black, T. A. and K. G. McNaughton. 1971. Psychrometric apparatus for Bowen ratio determination over forests. *Boundary-Layer Meteorol.*, 2: 246-254.

Blanken, P. D., T. A. Black, P.C. Yang, H. H. Neumann, Z. Nesic, R. Staebler, G. den Hartog, M. D. Novak and X. Lee. 1997. Energy balance and canopy conductance of a boreal aspen forest: partitioning overstory and understory components. *J. Geophys. Res.*, 102 D24, 28915-28927.

Camillo, P. J., R. J. Gurney and T. J. Schmugge. 1983. A soil and atmospheric boundary layer model for evapotranspiration and soil moisture studies. *Water Resour. Res.*, 19: 371-380.

Camillo, P. J. and R. J. Gurney. 1986. A resistance parameter for bare soil evaporation models. *Soil Science*, 141: 97-106.

Chung, S.-O. and R. Horton. 1987. Soil heat and water flow with a partial surface mulch. *Water Resour. Res.*, 12: 2175-2186.

Deardorff, J. W. 1978. Efficient prediction of ground temperature and moisture with inclusion of a layer of vegetation. *J. Geophys. Res.*, 83: 1889-1903.

Dekić, L. J., D. T. Mihailović and B. Rajković. 1995. A study of the sensitivity of bare soil evaporation schemes to soil surface wetness, using the coupled soil moisture and surface temperature prediction model, BARESOIL. *Meteorol. Atmo. Phys.*, 55: 101-112.

Desborough, C. E., A. J. Pitman and P. Irannejad. 1996. Analysis of the relationship between bare soil evaporation and soil moisture simulated by 13 land surface schemes for a simple non-vegetated site. *Global and Planetary Change*, 13: 47-56.

Dickinson, R. E. 1984. Modelling evaporation from three-dimensional global climate models. *Climate Processes and Climate Sensitivity*, Amer. Geophys. Union, Geophys. Monogr., 58-72.

Dorman, J. L. and P. J. Sellers. 1989. A global climatology for albedo, roughness length, and stomatal resistance for atmospheric generation models as represented by the Simple Biosphere model (SiB). *J. Appl. Meteorol.*, 28: 833-855.

Fuchs, M. and C. B. Tanner. 1967. Evaporation from a drying soil. *J. Appl. Meteorol.*, 6: 852-857.

Jacquemin, B. and J. Noilhan. 1990. Sensitivity study and validation of a land surface parameterization using the HAPEX-MOBILHY dataset. *Boundary-Layer Meteorol.*, 52: 93-134.

Jarvis, P. G. 1976. The interpretation of the variation in leaf water potential and stomatal conductance found in canopies in the field. *Phil. Trans. R. Soc.*, Lond. B. 273: 593-610.

Kimball, B. A. and R. D. Jackson. 1975. Soil heat flux determination: A null-alignment method. *Agric. Meteorol.*, 15: 1-9.

Kondo, J., N. Saigusa and T. Sato. 1990. A parameterization of evaporation from bare soil surface. *J. Appl. Meteorol.*, 29: 385-389.

Lee, J. and R. A. Pielke. 1992. Estimating the soil surface specific humidity. *J. Appl. Meteorol.*, 31: 480-484.

Mahfouf, J. F. and J. Noilhan. 1991. Comparative study of various formulations of evaporation from bare soil using in-situ data. *J. Appl. Meteorol.*, 30: 1354-1368.

Mahrt, L. and H. Pan. 1984. A two-layer model of soil hydrology. *Boundary-Layer Meteorol.*, 29: 1-20.

McCumber, M. C. and R. A. Pielke. 1981. Simulation of the effects of surface fluxes of heat and moisture in a Mesoscale numerical model. *J. Geophys. Res.*, 86: 9929-9938.

Milly, P. C. D. 1982. Moisture and heat transport in hysteretic, inhomogeneous porous media: a matric head-based formulation and numerical model. *Water Resour. Res.*, 18(3): 489-498.

Mihailović, D. T., R. A. Pielke, B. Rajković, T. J. Lee and M. Jeftić. 1993. A resistance representation of schemes for evaporation from bare and partly-covered surfaces for use in atmospheric models. *J. Appl. Meteorol.*, 32: 1038-1054.

Mihailović, D. T., B. Rajković, B. Lalic and L. J. Dekic. 1995a. Schemes for parameterizing evaporation from a non-plant-covered surface and their impact on partitioning the surface energy in land-air exchange parameterization. *J. Appl. Meteorol.*, 34: 2462-2475.

Mihailović, D. T., B. Rajković, B. Lalic and L. J. Dekic. 1995b. A resistance representation of schemes for evaporation from bare and partly-covered surfaces for use in atmospheric models. *J. Appl. Meteorol.*, 32: 1038-1054.

Novak, M. D. 1981. The moisture and thermal regime of a bare soil in the lower Fraser Valley during spring. Ph.D. Thesis, Univ. of British Columbia, Vancouver, BC., 153 pp.

Novak, M. D. and T. A. Black. 1983. The surface heat flux density of a bare soil. *Atmosphere-Ocean*, 21: 431-443.

Novak, M. D. and T. A. Black. 1985. Theoretical determination of the surface energy balance and thermal regimes of bare soils. *Boundary-Layer Meteorol.*, 33: 313-333.

Noilhan, J. and S. Panton. 1989. A simple parameterization of land surface processes for meteorological models. *Mon. Weather. Rev.*, 117: 536-549.

Osberg, P. M. 1986. Lysimeter measurements of salal understory evapotranspiration and forest soil evaporation after salal removal in a Douglas-fir plantation. M.Sc. Thesis, University of British Columbia, Department of Soil Science, Vancouver, BC.

Passerat de Silans, A. 1986. Transfert de masse et de chaleur dans un sol stratifé soumis à une excitation atmosphérique naturelle. Comparison: Modéles-expérience. Thesis, Institut National Polytechnique de Grenoble, 205 pp.

Passerat de Silans, A., L. Bruckler, J. L. Thony, and M. Vauclin. 1989. Numerical modelling of coupled heat and water flows during drying in a stratified bare soil, Comparison with field observations. *J. Hydrol.*, 105: 109-138.

Philip, J. R. 1957. Evaporation and moisture and heat fields in the soil. *J. Meteorol.*, 14: 354-366.

Price, D. T. and T. A. Black. 1989. Estimation of forest transpiration and CO_2 uptake using the Penman-Monteith equation and a physiological photosynthesis model. In: *Estimation of Areal Evapotranspiration, IAHS Publ.*, 177: 213-228.

Price, D. T. and T. A. Black. 1990. Effects of short-term variation in weather on diurnal canopy CO_2 flux and evapotranspiration of a juvenile Douglas-fir stand. *Agric. For. Meteorol.*, 50: 139-158.

Price, D. T. and T. A. Black. 1991. Effects of summertime changes in weather and root-zone soil water storage on canopy CO_2 flux and evapotranspiration of two juvenile Douglas-fir stands. *Agric. For. Meteorol.*, 53: 303-323.

Sellers, P., F. Hall, H. Margolis, R. Kelly, D. D. Baldocchi, G. den Hartog, J. Cihlar, M. G. Ryan, B. Goodison, P. Crill, K. J. Ranson, D. Lettermaier, and E. Wickland. 1995. The boreal ecosystem-atmosphere study (BOREAS): An overview and early results from 1994 field year. *Bull. of the Amer. Meteorol. Soc.*, 76: 1549-1577.

Sellers, P. J., D. A. Randall, G. J. Collatz, J. A. Berry, C. B. Field, D. A. Dazlich, C. Zhang, G. D. Collelo and L. Bounoua. 1996. A revised land surface parameterization (SiB2) for atmospheric GCMs. Part I: Model Formulation. *Journal of Climate*, 9: 676-705.

Verseghy, D. L. 1991. CLASS - A Canadian land surface scheme for GCMs, I. Soil model. *Int. J. Climatol.*, 11: 111-133.

Verseghy, D. L., N. A. McFarlane and M. Lazare. 1993. CLASS - a Canadian land surface scheme for GCMs, II. Vegetation model and coupled runs. *Int. J. Climatol.* 13: 347-370.

Viterbo, P. and A. C. M. Beljaars. 1995. An improved land surface parameterization scheme in the ECMWF model and its validation. *J. Climate*, 8: 2716-2748.

Wetzel, P. J. and J. T. Chang. 1987. Concerning the relationship between evaporation and soil moisture. *J. Climate Appl. Meteorol.*, 26:18-27.

Witono, H. and L. Bruckler. 1989. Use of remotely sensed soil moisture content as boundary conditions in soil-atmosphere water transport modelling, 1. Field validation of water flow model. *Water Resour. Res.*, 25(12): 2423-2435.

Wu, A., T. A. Black, D. L. Verseghy, P. D. Blanken, M. D. Novak, W. Chen, and P.C. Yang. 1998. A comparison of parameterizations of canopy conductance of aspen and Douglas-fir Forests for CLASS. *Atmosphere-Ocean* (accepted).

Ye, Z. and R. A. Pielke. 1993. Atmospheric parameterization of evaporation from non-plant-covered surfaces. *J. Appl. Meteorol.*, 32: 1248-1258.

CHAPTER 3

A COMPARISON OF PARAMETERIZATIONS OF CANOPY CONDUCTANCE OF ASPEN AND DOUGLAS-FIR FORESTS FOR THE CANADIAN LAND SURFACE SCHEME

3.1. Introduction

The second generation land surface model, CLASS (Canadian Land Surface Scheme), was recently developed for use within the Canadian General Circulation Model (GCM) (Verseghy 1991, Verseghy et al. 1993). It can be considered as belonging to the broad category of so-called "second generation" land surface models, which includes the two more widely-known GCM land surface schemes: BATS (Biosphere-Atmosphere Transfer Scheme; Dickinson et al. 1986) and SiB (Simple Biosphere model; Sellers et al. 1986, Sellers et al. 1996).

The correct simulation of the surface energy balance is of primary concern in numerical models of the atmosphere and particularly in GCMs. An important component of the overall research effort in this area is the careful and critical evaluation of the physical parameterizations of land-surface processes required in a land surface model, which includes the effects of the presence of vegetation, topographic features and surface heterogeneity on the exchanges of radiative energy, sensible heat and water vapour between land surfaces and the lower atmosphere.

For forests, stomata exert a major control over the latent heat flux because the stomatal conductance is generally much smaller than the leaf boundary-layer conductance (Jarvis and McNaughton 1986). Stomatal conductance (or canopy conductance at the

canopy level), which represents the restriction on water vapour flow through the stomata of the leaves, is the most difficult to quantify. This is because stomatal conductance depends on the physiological behaviour of the plants, rather than their physical characteristics.

Due to the complexity of the stomatal mechanism, empirical models of stomatal conductance have been developed to describe the stomatal response to the various environmental variables (Jarvis 1976, Kaufmann 1982, Schulze and Hall 1982), and extended to the canopy level, i.e. a top-down approach (Stewart 1988, Gash et al. 1989, Jarvis 1993). One approach, the Jarvis-Stewart model, has been widely used in various land surface models (Sellers et al. 1986, Verseghy et al. 1993). More recently, the Ball-Woodrow-Berry model has related stomatal control to leaf photosynthesis, relative humidity and CO_2 concentration at the leaf surface (Ball et al. 1987, Collatz et al. 1991), and has been applied at the canopy level in SiB2 (Sellers et al. 1996). Others have used a modified version of the Ball-Woodrow-Berry model, in which the relative humidity has been replaced by the reciprocal of air vapour pressure deficit (e.g. Lloyd 1991; Leuning 1995).

This chapter compares the application of the Jarvis-Stewart, Ball-Woodrow-Berry and modified Ball-Woodrow-Berry models to an old boreal aspen forest and several west coast Douglas-fir forests. Data from the aspen forest throughout a growing season and during a four-day period two years later, and from five Douglas-fir forests during short summer periods with dry and wet soil moisture conditions are used to test CLASS performance (Table 3.1). The purpose of these tests are to examine how well a conductance parameterization obtained using measurements made during one growing

season applies to a subsequent growing season and obtained at one site applies to other sites with similar species composition.

Table 3.1. Site description and measurements used in testing CLASS.

Site	Stand description	Dates	Reference
"Old stand", Dunsmuir Creek, 40 km SW of Nanaimo, BC	Douglas-fir, 8 m height, 20 years old, unthinned, salal understory, ~ 3500 stems ha^{-1}	44 days Aug 20 - 31, 1983 Jul 18 - Aug 25, 1984	Price and Black (1990), Price and Black (1991)
Browns River, 12 km NW of Courtenay, BC	Douglas-fir, 17 m height, 28 years old, thinned & pruned, no understory, 575 stems ha^{-1}	9 days Jul - Aug, 1990	Lee and Black (1993)
Iron River site 1, 40 km NW of Courtenay, BC	Douglas-fir, 9 m height, 21 years old, unthinned, no understory, 1840 stems ha^{-1}	4 days Jun - Jul, 1974	Curtis (1975), Black (1979)
Iron River site 2, 1.5 km E of site 1, BC	Douglas-fir, 8 m height, 22 years old, thinned, salal understory, 840 stems ha^{-1}	10 days Jun - Jul, 1975	Tan and Black (1976), Black (1979)
UBC Research Forest, Haney, 50 km E of Vancouver, BC	Douglas-fir, 8 m height, 11 years old, unthinned, no understory	6 days July, 1970	McNaughton and Black (1973)
Prince Albert National Park (PANP), 50 km NW of Prince Albert, SK	Old boreal aspen, 21 m height, 70 years old, hazelnut understory, 830 stems ha^{-1}	154 days Apr 19- Sep 19, 1994 27 days Jul 12 - Aug 9, 1996	Black et al. (1996)

3.2. Data

Most data used in this study have been published as shown in Table 3.1. The Douglas-fir sites, which were located in southwest B.C., were used in studies of forest energy balance, evaporation, tree water relations and growth (e.g., Lee and Black 1993). The old aspen site, located in the southern part of Prince Albert National Park (PANP) about 50 km north-west of Prince Albert, Saskatchewan, was one of ten tower flux sites used in the Boreal Ecosystem-Atmosphere Study (BOREAS), a large-scale short-term investigation of carbon, water and energy exchange between the atmosphere and the boreal forest (Sellers et al. 1995). Sensible (Q_H) and latent (Q_E) heat fluxes (W m^{-2}) at the

Haney, Iron River and Dunsmuir Creek sites were measured using the Bowen ratio/energy balance (BREB) method (Black and McNaughton, 1971, Spittlehouse and Black 1979, Price and Black 1990). The BREB method in all cases was based on reversing aspirated psychrometers separated by 1 or 3 m. At the PANP and Browns River sites, these fluxes were measured using the eddy covariance method with 3-dimensional sonic anemometers, fine wire thermocouples, an open-path krypton hygrometer (Browns River, Lee and Black 1993) and a closed-path infrared gas analyzer (IRGA) (PANP, Black et al. 1996). CO_2 fluxes were measured using a modified BREB method at the Dunsmuir Creek site (Price and Black 1990) and the eddy covariance method with a closed-path IRGA at the PANP site (Black et al. 1996). Incident solar radiation and net radiation Q^* (W m^{-2}) were measured at all sites, while incoming longwave radiation was measured only at the PANP site. The soil surface heat flux G_0 (W m^{-2}) was calculated by adding the heat flux at the 3- or 5-cm depth measured using heat flux plates and the rate of heat storage in the layer of soil above the plates. Sensible and latent heat storage S (W m^{-2}) between the ground and the height of Bowen ratio or eddy covariance equipment was estimated using air temperature profiles, vapour pressure profiles and thermocouples inserted into tree boles and twigs (e.g. Blanken et al. 1997). At all sites, volumetric soil water content θ (m^3 m^{-3}) near the surface was measured gravimetrically. At all Douglas-fir sites except Browns River, θ from the 0.15 m depth to the 1 m depth was measured using a neutron soil moisture probe. At the PANP site, θ was measured from the surface down to a depth of 1.2 m using time domain reflectometry (TDR) (Blanken et al. 1997). Rainfall was measured at all sites using a tipping bucket rain gauge supplemented by a back-up storage gauge.

Estimation of the accuracy of measurements is required in model evaluation. In this case, the main sources of measurement error are in the radiative fluxes (incident solar and longwave radiation, and Q^*), convective fluxes (i.e., Q_H, Q_E and CO_2 flux) and rainfall. Smith et al. (1997) suggest that the accuracy of polyethylene-dome net radiometers is 5 to 10%; however, there are often additional errors due to the influence of the supporting structure and the spatial representativeness of the measurement location. When using the BREB method with reversing psychrometers separated by 3 m above the forest canopy, the errors in both Q_H and Q_E are generally less than 15% if the temperature and vapour-pressure gradients are large, but the error in the latent heat flux can be up to 50% if the gradients are small (Spittlehouse and Black 1979). Examining closure of the energy balance is a very useful check on the overall accuracy of Q_H and Q_E measured above the forest using the eddy covariance method. Lee and Black (1993) found that during the daytime $Q_H + Q_E$ was 83% of the available energy ($Q^* - G_0 - S$) on a half-hourly basis at the Browns River site. Blanken et al. (1997) showed that eddy covariance measurements of $Q_H + Q_E$ underestimated the available energy by 13% on a half-hourly basis but agreed well with the available energy on a 24-hourly basis at the PANP site. Blanken et al. (1997) partitioned the missing energy into sensible and latent heat flux using the measured ratio of Q_H / Q_E. In this study, this procedure was used to correct the eddy covariance fluxes measured at the Browns River site. The term $G_0 + S$ is less usually than 5% of Q^* for forests except for periods around sunrise and sunset so that even a 50% error in $G_0 + S$ results in a minor error in the calculation of the available energy. Finally, tower flux measurements must be representative of the forest being modelled. This requires that there is a satisfactory 'footprint' size or fetch in the upwind

direction from the tower (Schuepp et al. 1990, Baldocchi 1997). The PANP and Iron River sites were in extensive forests with fetches exceeding 2 km in all directions. At the Haney and Dunsmuir Creek sites, the fetch is generally between 200 and 400 m for the prevailing wind directions, while at the Browns River site, the fetch during the daytime, when the flux measurements were made, was about 300 m.

3.3. Measurements of canopy conductance

The measured canopy conductance, g_c (m s^{-1}), is defined as the ratio of the measured water vapour flux from the forest canopy ($Q_{E,c} = Q_E - Q_{E,g}$, where $Q_{E,g}$ is the latent heat flux from the soil surface) to the difference between the vapour pressure in the stomatal cavities (i.e. the saturated vapour pressure at the leaf temperature $e^*(T_0)$ (kPa) and the vapour pressure at the surface of the canopy leaves e_0 (kPa), i.e. $g_c = (\gamma / \varrho_a c_p) Q_{E,c} / (e^*(T_0) - e_0)$, where γ is the psychrometric constant (kPa K^{-1}), ϱ_a is the air density (kg m^{-3}), c_p is the specific heat of the air (J kg^{-1} K^{-1}), and T_0 is the canopy leaf temperature (°C). The vapour pressure difference is accounted for implicitly in the Penman-Monteith (PM) equation, which describes the 'big leaf' model of evaporation from a plant canopy with dry leaves (Monteith 1981). Therefore, the following rearranged form of the PM equation was used to obtain the measured values of g_c

$$\frac{1}{g_c} = \frac{\varrho_a c_p}{\gamma} \frac{\Delta e_a}{Q_{E,c}} + \left[\left(\frac{s}{\gamma}\right) B - 1\right]\left(\frac{1}{g_a}\right) \qquad (3.1)$$

where B is the Bowen ratio (Q_H/Q_E), Δe_a is the saturation deficit of the air at the flux measurement height (kPa), s is the slope of the saturation vapour pressure-temperature curve (kPa K^{-1}), and g_a is the aerodynamic conductance of the air layer between the

canopy and the flux measurement height (m s^{-1}). For the PANP and Browns River sites, g_a was calculated using $1/(u/u_*^2 + B^{-1}/u_*)$, where u is the measured wind speed (m s^{-1}), u_* is the measured friction velocity (m s^{-1}), and B^{-1} is the dimensionless sublayer Stanton number (Owen and Thompson 1963, Verma 1989), which was set equal to 2.5 for the aspen forest (Blanken et al. 1997) and 2.0 for the Douglas-fir forest. For the other Douglas-fir forests, it was estimated from the measured wind speed corrected for the Monin-Obukhov stability function using an iterative procedure (Price and Black 1989).

The error in g_c obtained using Eq. (3.1) depends largely on errors in $Q_{E,c}$ and Δe when $g_a > 0.1$ m s^{-1} (Stewart 1989), which is common for forests. For example, the values of g_a were between 0.13 and 0.18 m s^{-1} for the Douglas-fir forest at Haney (McNaughton and Black 1973) and between 0.08 and 0.11 m s^{-1} for the aspen forest.

In order to demonstrate that the calculated forest g_c from the PM equation is a reliable measure of the average canopy conductance, values of g_c were compared with stomatal conductance measurements made during the 3-week BOREAS-96 Summer Intensive Field Campaign. Fig. 3.1a shows that the stomatal conductance of the aspen leaves decreased with increasing vapour pressure deficit. The scatter in the plot is probably associated with the effects of temperature and soil moisture since conditions of high temperature and low soil moisture that occurred during the campaign period would likely reduce stomatal conductance. There were also some sampling errors as a result of measuring stomatal conductance using a hand-held porometer (model 1600, LI-COR, Inc., Lincoln, NE). These measurements were made 5 to 6 times per half-hour mainly near midday. Furthermore, whether individual leaves were in the shade or sunlight caused a difference of about 25% on average. The stomatal conductance of the leaves of

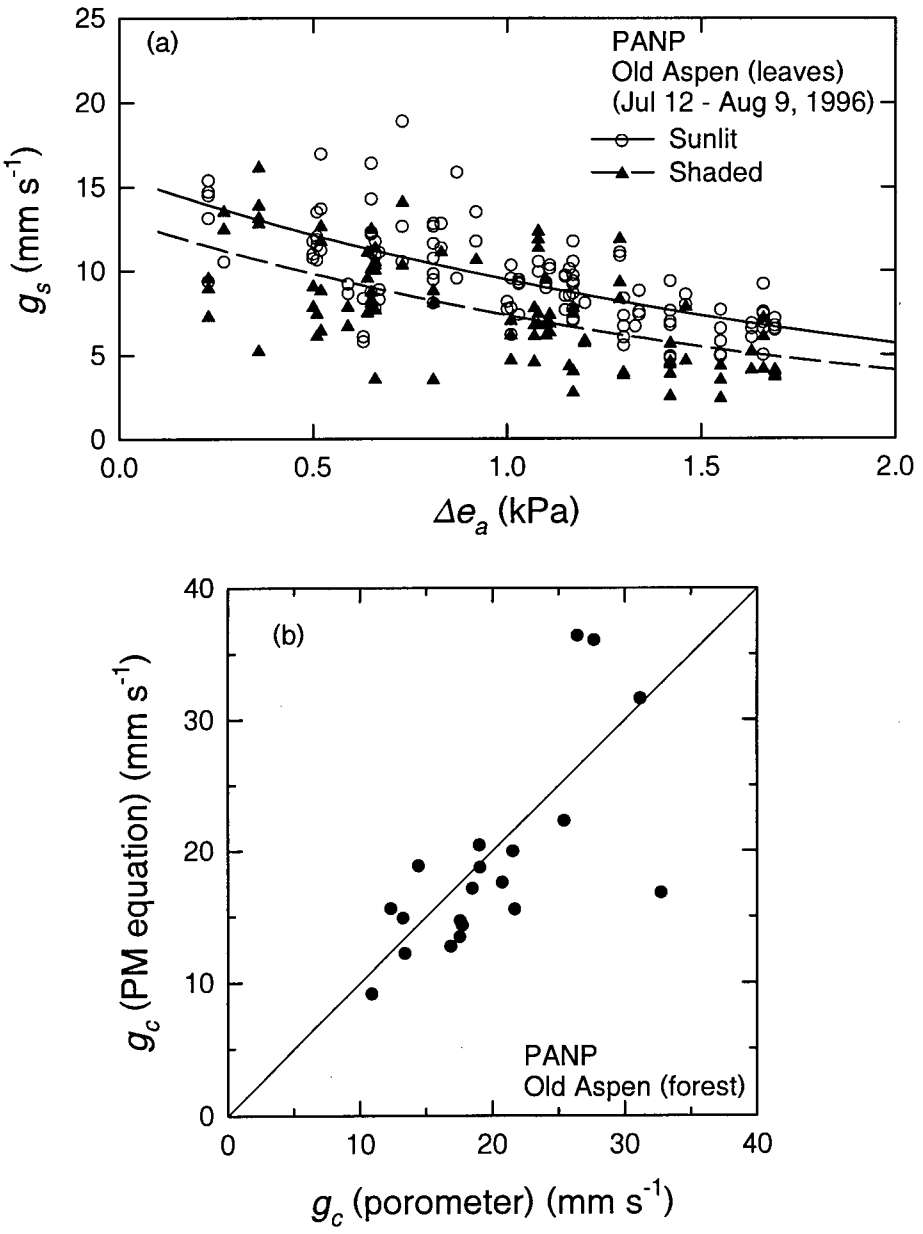

Fig. 3.1. Aspen stomatal conductance (g_s) measured by porometer at the 18-m height versus ambient vapour pressure deficit (Δe_a) on most days from 12 July to 9 August 1996 (a) and comparison of aspen g_c values computed from the PM equation and computed using leaf area index (Λ) and porometer measurements (b). Lines of best fit are shown.

the hazelnut understory was also measured, and was approximately half that of the aspen overstory leaves. A leaf area weighting method was used to scale up from leaf stomatal conductance to canopy conductance, in which the proportions of sunlit and shaded leaves were assumed to be 30% and 70%, respectively, and the effective leaf area index (LAI) of the forest was calculated by multiplying the aspen overstory LAI (2.1 m^2 m^{-2}) over this period (Chen et al. 1997) by 1.25 to account for the contribution of the hazelnut understory to forest evaporation (Black et al. 1996). Fig. 3.1b compares values of g_c computed using the 'scaling up' method with those computed using the PM equation. There was generally good agreement between the two methods. Tan and Black (1976) working in the Douglas-fir forest at the Iron River site 2 also found that values of g_c calculated from the stomatal conductance and LAI measurements agreed well with those calculated using the PM equation with BREB measurements of evaporation.

3.4. Parameterizations of the canopy conductance

The Jarvis and Stewart (JS) parameterization of g_c is the product of functions of individual plant and environmental variables as follows:

$$g_c = g_{c,\max} g_1(\Lambda) g_2(Q_p) g_3(\Delta e_0) g_4(\psi) g_5(T_0) \tag{3.2}$$

where $g_{c,\,max}$ is the maximum value of the canopy conductance, g_1, g_2, g_3, g_4, and g_5 are the functions accounting for the effects of leaf area index Λ (m^2 m^{-2}), incident photosynthetic photon flux density Q_p (μmol m^{-2} s^{-1}), saturation deficit at the leaf surface Δe_0, soil water potential ψ (m) and T_0, respectively. These functions are assumed to act independently, are obtained by optimization using non-linear least squares analysis, and have values between zero and unity.

The Ball-Woodrow-Berry (BWB) parameterization of leaf stomatal conductance g_s (mol m^{-2} s^{-1}) is expressed as (Collatz et al. 1991)

$$g_s = m_1 \frac{A_s}{c_s} h_s + b_1 \tag{3.3}$$

where A_s is the rate of net CO_2 assimilation (μmol m^{-2} s^{-1}), h_s and c_s are the relative humidity (unitless ratio) and CO_2 mole fraction of the air (μmol mol^{-1}) at the leaf surface, respectively, and m_1 (unitless) and b_1 (mol m^{-2} s^{-1}) are the slope and intercept, respectively, obtained from the linear regression analysis. This equation was applied at the canopy scale following Sellers et al. (1996)

$$g_c = m_2 \frac{A_0}{c_0} h_0 + b_2 \tag{3.4}$$

where each variable and coefficient are defined at the canopy level and subscript '0' refers to the 'big leaf' surface. A modified version of the Ball-Woodrow-Berry (MBWB) model (e.g. Lloyd 1991) where h_0 is replaced by the reciprocal of Δe_0, is written as

$$g_c = m_3 \frac{A_0}{\Delta e_0 c_0} + b_3. \tag{3.5}$$

3.5. Application of the parameterizations

3.5.1. The JS model

The form of each function in Eq. (3.2) was determined by finding the response of g_c to the function's variable. For the aspen forest, g_c increased linearly with Λ (Fig. 3.2a). The effect of Λ on g_c was simply represented by $g_1 = \Lambda/\Lambda_{max}$. The response of g_c to Δe_0 (g_3) was well represented using an exponential function at high, medium and low light levels (McCaughey and Iacobelli 1994, Blanken et at. 1997) (Fig. 3.2b), where Δe_0 was

calculated as $\Delta e_0 = (\gamma/\varrho_a c_p) Q_{E,c}/g_c$ (Blanken et at. 1997). The relationship between g_c and Q_p was well approximated by a hyperbolic function (Jarvis 1976). The influence of soil moisture stress was not included because root zone soil water was plentiful during 1994 (Blanken et al. 1997). Examination of the response of g_c / g_3 to T_0 showed that the effect of temperature was negligible. This is likely due to the strong correlation between Δe_0 and T_0. Non-linear least squares analysis was applied to determine the empirical coefficients in g_2 and g_3 by examining the relationship between g_c/g_1 and Q_p and Δe_0 during the full-leaf period. Finally, the following relationships were obtained for the aspen forest

$$
\begin{aligned}
& g_{c,\max} = 32.6\,\mathrm{mm\,s^{-1}} \\
& g_1(\Lambda) = \Lambda / \Lambda_{\max} \\
& g_2(Q_p) = \frac{Q_p}{Q_p + 430} \\
& g_3(\Delta e_0) = \exp(-0.645 \Delta e_0) \\
& g_4(\psi) = g_5(T_0) = 1.0
\end{aligned}
\qquad (3.6)
$$

where $\Lambda_{\max}$ is 2.3 $m^2\ m^{-2}$, Q_p is in μmol $m^{-2}\ s^{-1}$ and Δe_0 is in kPa. Eq. (3.6) explained only 31% (r^2 = 0.31) of the variance of the half-hourly measured values of g_c but 85% (r^2 = 0.85) of the variance in the means of the binned measured values of g_c which were calculated at binned 0.25 kPa intervals of Δe_0 and each light level (Fig. 3.2b) (Table 3.2). This increase in r^2 is because binning filters out the effects of other variables and eliminates the effects of the uneven distribution of g_c values with respect to the independent variables. Inspection of the differences between binned means of g_c showed that at the 5% significance level, differences were significant except under low light conditions with Δe_0 > 1.5 kPa. The CLASS g_c parameterization, $f_2(\Delta e)$ (Eq. (36b), Verseghy et al. 1993), shown in Fig. 3.2b gives g_c values significantly lower than

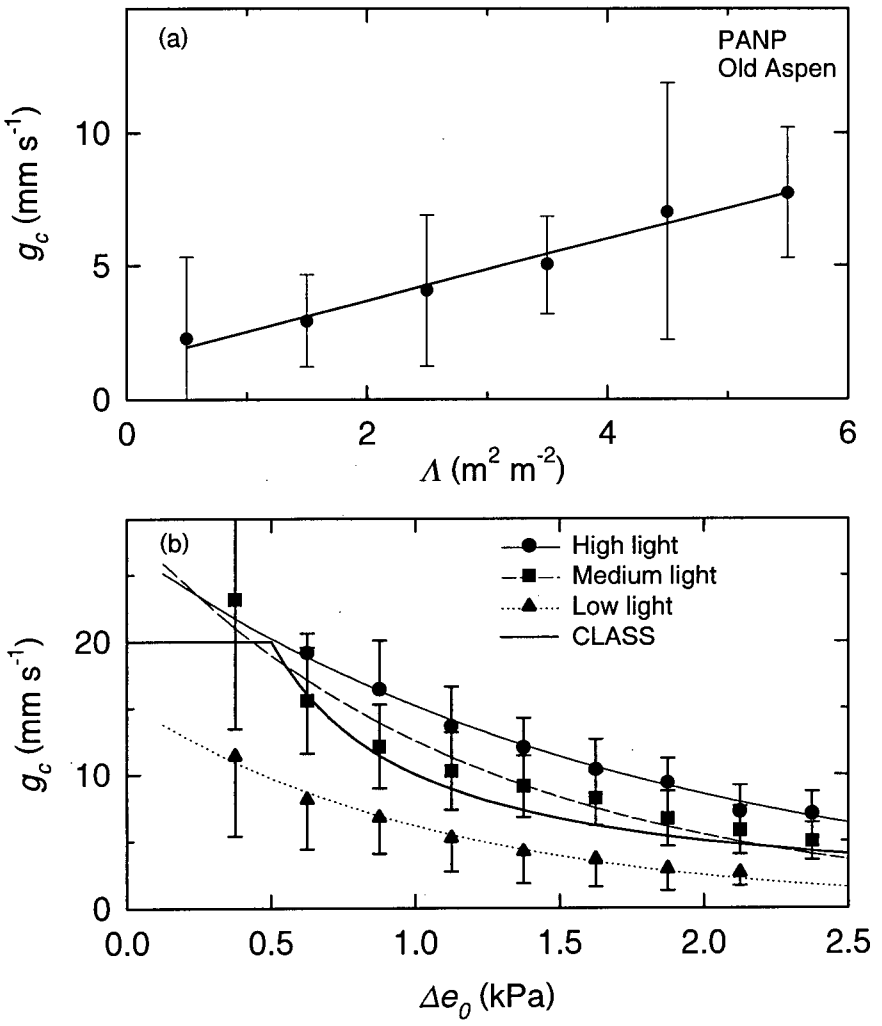

Fig. 3.2. Relationship between g_c and leaf area index (Λ) (a) and between g_c and vapour pressure deficit at the 'big leaf' surface (Δe_0) stratified by high (Q_p > 1400 μmol m^{-2}s^{-1}; solid line), medium (800 < Q_p < 1400 μmol m^{-2}s^{-1}; dashed line) and low Q_p (200 < Q_p < 800 μmol m^{-2}s^{-1}; dotted line) photosynthetic photon flux density (Q_p) (b) for the aspen forest. Vertical lines represent ± one standard deviation. Lines of best fit are shown. The corresponding relationship from CLASS under conditions of no light and soil moisture limitations is also shown.

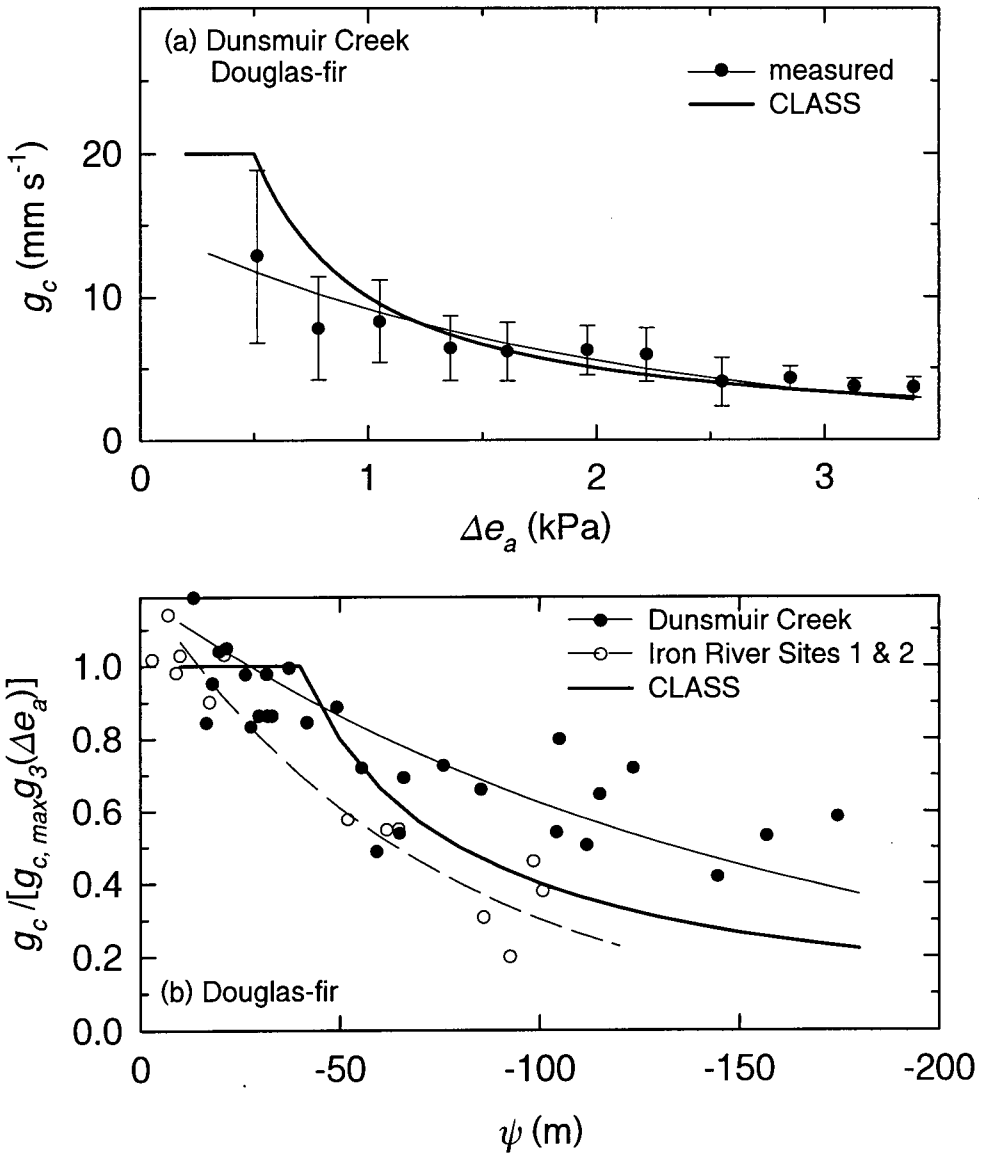

Fig. 3.3. (a) Relationship between g_c and Δe_a under conditions of high soil water potential (ψ) for the Douglas-fir forest at Dunsmuir Creek. The thin line is $g_{c,max}g_3(\Delta e_a)$ (see Eq. (3.7)) and the heavy line is the original CLASS parameterization ($20/f_2(\Delta e)$). Vertical lines are ± one standard deviation. (b) Relationship between $g_c/$ ($g_{c,max}g_3(\Delta e_a)$) (to remove the effect of Δe_a) and ψ for the Dunsmuir Creek and Iron River forests. The thin solid line is $g_4(\psi)$ (see Eq. (3.7)) and the thin dashed line is the best fit to the Iron River data. Also shown is the original CLASS parameterization $1/f_3(\psi)$.

measured values when light should not limit g_c (i.e. high light conditions). Examination of the response of g_c to light indicates that the CLASS parameterization, $f_1(K_\downarrow)$ (Eq. (36a), Verseghy et al. 1993), underestimates g_c by 10 to 20 % for $Q_p > 800$ μmol m^{-2} s^{-1}.

For the Douglas-fir forest at the Dunsmuir Creek site, an exponential relationship between g_c and Δe_a was also found (Fig. 3.3a). Inspection of the differences between binned means of g_c showed that at the 5% significance level, differences were significant except when $\Delta e_a > 2.5$ kPa. Δe_0 was not used because it was very closely approximated by the ambient value (Δe_a) due to the close coupling resulting from the high aerodynamic and laminar boundary layer conductances in this conifer forest. The relationship between g_c and ψ was obtained by plotting $g_c/(g_{c,max}\, g_3(\Delta e_a))$ against ψ (Fig. 3.3b). The effect of light was not considered because the stomata of Douglas-fir were fully open at solar irradiances greater than 100 W m^{-2} (Black and Kelliher 1989). Price and Black (1989) found that direct effects of T_0 appeared insignificant after considering Δe_a as a factor affecting g_c, and similar results were reported by Tan et al. (1977). Therefore, we assume that all effects of T_0 on g_c were expressed through Δe_a. The following simple relationships were obtained:

$$\begin{aligned} &g_{c,\max} = 19.0\,\mathrm{mm\,s^{-1}} \\ &g_3(\Delta e_a) = \exp(-0.65\Delta e_a) \\ &g_4(\psi) = \exp(0.0065\psi) \\ &g_1(\Lambda) = g_2(Q_p) = g_5(T_0) = 1.0 \end{aligned} \qquad (3.7)$$

where ψ is in m of water. The values of r^2 for the half-hourly and binned values of measured g_c were 0.37 and 0.88, respectively (Table 3.2), which were slightly higher than

for the old aspen. Even under high soil moisture conditions, values of Douglas-fir g_c were lower than old aspen values. The values of Douglas-fir g_c normalized by $g_3(\Delta e_a)$ were larger than the CLASS parameterization, $f_3(\psi)$ (Eq. (36c), Verseghy et al. 1993) for ψ < -50 m (Fig. 3.3b). By comparison, the relationship obtained using Iron River data ($g_4(\psi) = \exp(0.014\psi)$) shown in Fig. 3.3b, were lower than those calculated using both the Dunsmuir Creek and CLASS parameterizations.

Table 3.2. Values of the root mean square error (RMSE) (mm s^{-1}) and the coefficient of determination (r^2) between measured and parameterized g_c.

	JS			BWB			MBWB			Number of
	half-hourly mean		binned mean	half-hourly mean		binned mean	half-hourly mean		binned mean	half-hours
	RMSE	r^2	r^2	RMSE	r^2	r^2	RMSE	r^2	r^2	
Aspen	3.88	0.33	0.85	4.93	0.14	0.87	4.56	0.31	0.91	2681
Douglas-fir	3.37	0.37	0.88	4.04	0.27	0.40	3.70	0.35	0.52	532

3.5.2. The BWB and MBWB models

For the aspen forest, the value of A_0 required in the BWB and MBWB indices (A_0h_0/c_0 and $A_0/(\Delta e_0 c_0)$, respectively) was calculated by subtracting the measured eddy covariance CO_2 flux at the 39-m height from that at the 4-m height. While the subtraction eliminated the effects of the soil and hazelnut respiration on the calculation of the aspen A_0, it did not eliminate the effect of the aspen stem respiration. This caused an underestimation of the aspen A_0 by about 10% based on chamber measurements of stem respiration (M. G. Ryan 1997, personal communication) and eddy-covariance measurements of CO_2 flux at the two levels in 1994 (Chen et al. 1998, Yang 1998). The fluxes were corrected for the effects of changing air density due to humidity fluctuations

(Webb et al. 1980), and the difference between the fluxes was corrected for the rate of change in the CO_2 storage between the two levels (Black et al. 1996). Values of h_0 and c_0 were calculated using 1 - $\Delta e_0/e^*(T_0)$ and c_a - A_0/g_a, respectively (Blanken 1997), where c_a is the CO_2 mole fraction measured in the ambient air at the 39-m height. The linear regression of g_c on the BWB index gave a slope of 7.7 and an intercept of 133.8 mmol m^{-2} s^{-1} (note that 41 mmol m^{-2} s^{-1} $\approx$ 1 mm s^{-1}). The corresponding values for the MBWB index were 0.037 and 143.0 mmol m^{-2} s^{-1} (Fig. 3.4a). The latter index explained significantly more of the half-hourly variance ($r^2 = 0.31$) in g_c than the former ($r^2 = 0.14$) (Table 3.2).

The value of A_0 at the Dunsmuir Creek site was calculated by subtracting the measured BREB CO_2 flux above the forest corrected following Webb et al. (1980) from the measured soil respiration using the soda-lime chamber technique (Price and Black 1990). The Douglas-fir stem respiration was neglected in the above calculation. Values of h_0 and c_0 were approximated by the ambient values (h_a and c_a) measured in the air at the reference height. The relationship was not sensitive to changes in soil moisture. This is because an increase in soil moisture stress was correctly accounted for by the corresponding decrease in A_0 (Collatz et al. 1991). The slope and intercept of the BWB model were 8.8 and 205.7 mmol m^{-2} s^{-1}, respectively. The corresponding values for the MBWB index were 0.057 and 197.7 mmol m^{-2} s^{-1} (Fig. 3.4b). The latter index explained more of the binned variance ($r^2 = 0.52$) in g_c than the former ($r^2 = 0.40$).

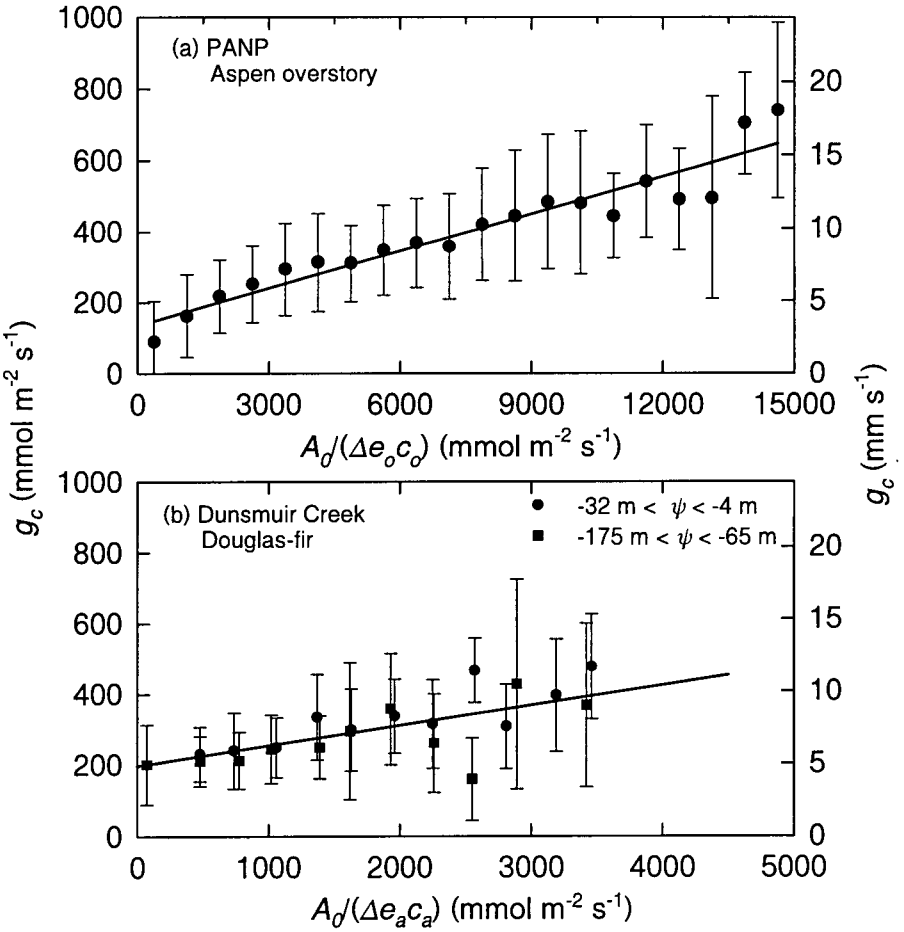

Fig. 3.4. Empirical relationship between g_c and a modified form of the Ball-Berry index ($A_0/(\Delta e_0 c_0)$ (symbols defined in text) for the aspen overstory (a) and the Douglas-fir forest (b). c_a is the CO_2 mole fraction of the air at the reference height. A mean g_c was calculated for binned modified BWB index values at 3 (aspen) and 2 (Douglas-fir) mmol m^{-2}s^{-1} intervals. The solid lines represent the linear regressions: g_c (aspen) = 0.038 BWB index + 142.9 mmol m^{-2}s^{-1}and g_c (Douglas-fir) = 0.057 BWB index + 197.7 mmol m^{-2}s^{-1}. Vertical lines represent ± one standard deviation.

The slopes of the BWB model for the PANP and Dunsmuir Creek sites were close to the value given for C_3 species (9.0) by Collatz et al. (1991). It is not possible, however,

to compare the intercepts obtained here with those of Collatz et al. because they represent the integrated effect of all the leaves in the canopy.

The fact that the JS model gave the smallest values of the root mean square error (RMSE) among the three models for the two forests (Table 3.2) indicates that the other two models made little improvement on the JS model. This is surprising considering the well known correlation between stomatal conductance and leaf net assimilation rate (Collatz et al. 1991). This may be a problem in applying these models at canopy level rather than at leaf level (Baldocchi 1993). The surprisingly low values of the binned r^2 for the Douglas-fir forest in the BWB and MBWB models may be due to the inaccuracy of the soda-lime chamber measurements of the soil CO_2 efflux.

3.6. Model of canopy net assimilation rate

In order to use the BWB and MBWB models, it is necessary to have a relationship for estimating A_0. A canopy-level equation governing photosynthesis can be written as (Sellers et al. 1997)

$$A_0 = V_{max0} A_1 A_2 \ldots A_5 \tag{3.8}$$

where V_{max0} is the maximum photosynthetic capacity (μmol m^{-2} s^{-1}), the parameter A_1 through A_5 describe the effects of Q_p, T_0, Δe_0, ψ and c_0, respectively (unitless). Ruimy et al. (1996) compared many simple relationships between canopy photosynthesis and Q_p over closed plant canopies with adequate soil moisture for a range of vegetation types. They found the most reliable relationship to be a rectangular hyperbola:

$$A_0 = \frac{aQ_p A_\infty}{aQ_p + A_\infty} - R \tag{3.9}$$

where A_∞ is A_0 at saturating Q_p, a is quantum yield (i.e. dA_0/dQ_p at $Q_p = 0$), and R is the dark respiration rate (μmol m^{-2} s^{-1}). Eq. (3.9) was used to approximate $V_{max0}A_1$. The advantage of this top-down approach is that it by-passes the complex processes of photosynthesis and respiration which depend on many environmental variables. In models that account for the dependence of A_0 on the internal CO_2 concentration of the foliage (c_i), the regulating effect of g_c on CO_2 uptake must also be included. Since Eq. (3.9) does not account for the effect of the seasonal variation of Λ, the effect of Λ on the relationship between A_0 and Q_p for the aspen forest are investigated. Fig. 3.5a shows that Λ has a marked effect on A_0, which is not surprising since Λ largely controls the number of photons absorbed by the canopy foliage. The phenology of growth also affects canopy photosynthesis independently of Λ, but it is difficult to separate its effect from that of Λ. The dependence of a, A_∞ and R on Λ for the aspen forest was examined. A_∞ was found to be linearly related to Λ, i.e. $A_\infty = K\Lambda$, where K is an additional empirical coefficient. Chen et al. (1998) found that Eq. (3.8) using only A_1 (absorbed Q_p), A_2 and A_3 explained about 70% of the variance for the aspen forest. Furthermore, in the case of the aspen overstory, Yang (1998) found that this equation explained 76% of the variance of which A_1 accounted for about 69%, A_2 about 5% and A_3 only 1.6%. Little or no effect of soil moisture on photosynthesis was found over the growing season for this forest because of relatively high rainfall during the growing season (Chen et al 1998). As their effects were small, A_2, A_3 and A_4 were not included in the model. For the Douglas-fir forest at Dunsmuir Creek, Λ was not changed because it appeared to be very similar in the 1983

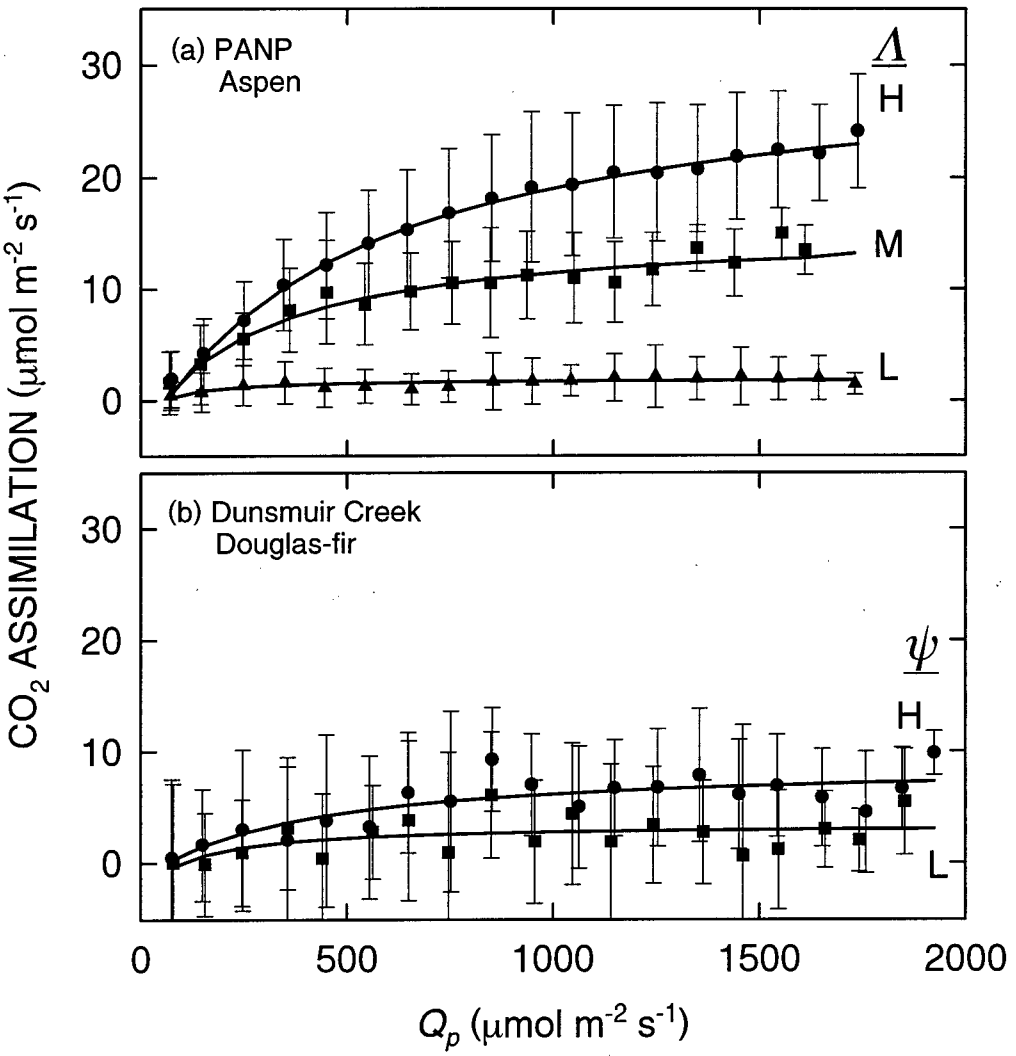

Fig. 3.5. Relationship between canopy net assimilation rate (A_0) and Q_p for the aspen forest stratified by high, H (Λ >3.9), medium, M (2.4 < Λ < 3.9) and low, L (2.4 > Λ) leaf area index (Λ) (a) and for the Douglas-fir forest stratified by high, H (-32 m (of water) < ψ < -4 m) and low, L (-175 m < ψ < -65 m) soil water potential (ψ) (b). Vertical lines represent ± one standard deviation. Lines of best fit are shown.

and 1984 periods. The effect of ψ on Douglas-fir photosynthesis (A_4) was expressed using a simple linear relationship

$$A_4 = 1 + 4.0 \times 10^{-3} \psi \tag{3.10}$$

As a consequence of the conservative response of the Douglas-fir forest A_0 to soil moisture stress (Price and Black 1991), only the difference in A_0 between high and low ranges of ψ appeared significant (Fig. 3.5b). Although observations at the Douglas-fir site showed some evidence that temperature had a major influence on A_0, no simple relationship between temperature and A_0 was observed and it was not clear whether A_0 was limited directly by effects of temperature or humidity and other factors (Price and Black 1990). Thus, the model of A_0 for the Douglas-fir forest does not include A_2 and A_3.

Table 3.3 gives the values of the parameters in Eq. (3.8) for both the aspen and Douglas-fir forests. The photosynthetic capacity of the Douglas-fir forest (7.2 μmol m^{-2} s^{-1}) at high ψ was much lower than that of the of the aspen forest (24.4 μmol m^{-2} s^{-1}), and also lower than the value of 18.5 μmol m^{-2} s^{-1} reported by Ruimy et al. (1996) as a mean value for several conifer forests. The low observed value was likely owing to the fact that the forest suffered from a nitrogen deficiency (Price and Black 1989).

Table 3.3. Parameters in the relationship (Eq. (3.9)) between canopy net assimilation rate (A_0) and photosynthetic photon flux density (Q_p)

Description	a	K	Λ	R (μmol m^{-2} s^{-1})	F_m (μmol m^{-2} s^{-1})
Aspen	0.0605	6.379	5.6	2.536	24.36
Douglas-fir (high soil moisture)	0.0284	2.114	5.0	1.557	7.202
Douglas-fir (low soil moisture)	0.0543	1.264	5.0	2.923	3.013

Photosynthetic capacity (F_m) defined as A_0 at Q_p = 1800 μmol m^{-2} s^{-1}.

3.7. Performance of the parameterizations

Half-hourly values of g_c were calculated using the JS, BWB and MBWB models with the measurements of the relevant environmental variables made at the PANP and Dunsmuir Creek sites. The value of A_0 in the latter two models was calculated using Eq. (3.8). Fig. 3.6 compares the calculated ensemble-averaged diurnal g_c of the aspen forest with the measured values for each month from May to September, 1994. In May, values of g_c calculated using the three empirical models were less than the measured values. The underestimation of g_c by the three models during May is probably because the parameterizations were done using the data from the full-leaf period (June 7 - September 10) and the stomatal conductance of the young leaves in May was likely higher than later in the growing season. During the full leaf period (June to August), values of g_c obtained using the JS and MBWB models agreed with the measured values better than those obtained using the BWB model. Values obtained using the JS model are larger than those obtained using the BWB and MBWB models. This is because the latter two models caused a depression in g_c during midday hours. Collatz et al. (1991) also found that simulations using the BWB model at the leaf level resulted in a pronounced midday depression of stomatal conductance. Although midday stomatal closure has been observed in some tree species (e.g. Tan and Black 1976, Blanken and Rouse 1996), it was not observed in 1994 (Blanken's (1997) canopy conductance analysis) or in 1996 (the stomatal conductance measurements mentioned earlier). Blanken (1997) attributed the absence of midday stomatal closure in 1994 to the lack of soil water stress and the high

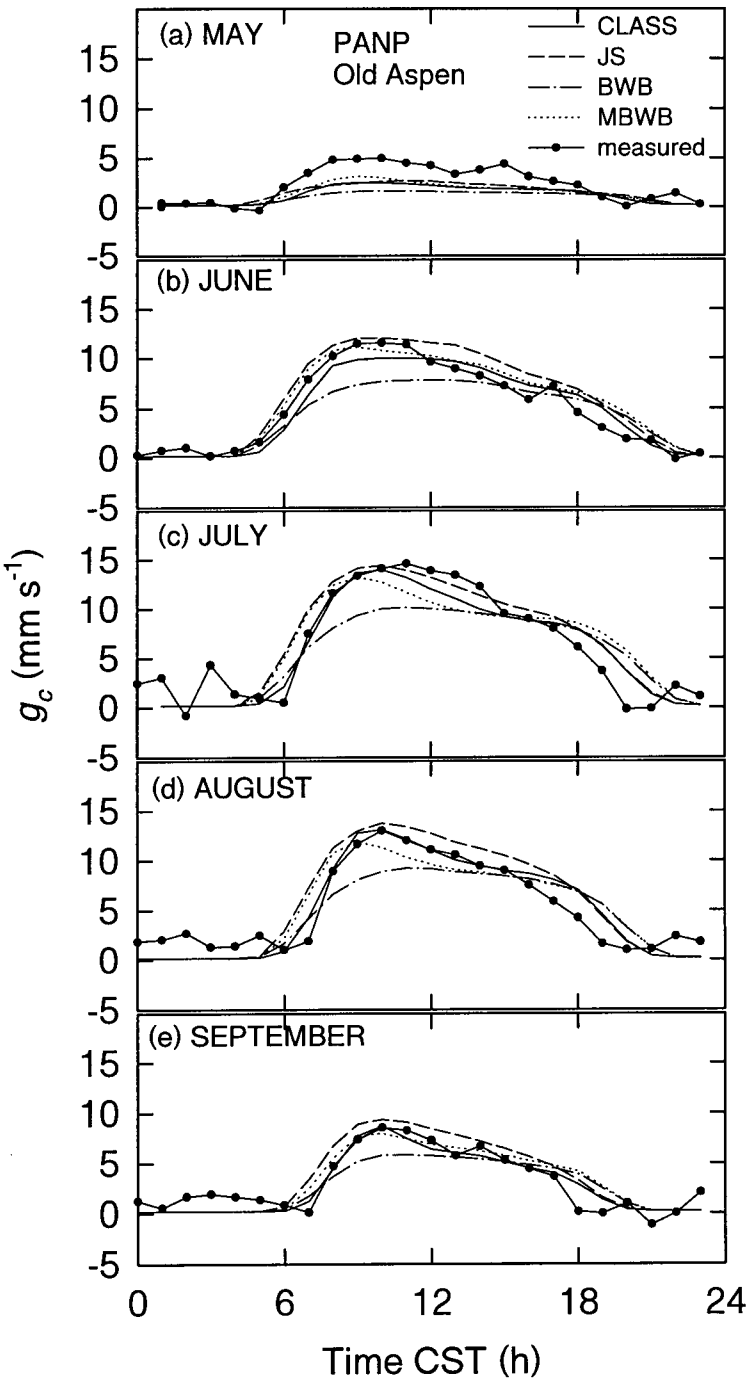

Fig. 3.6. Comparison of ensemble monthly averages (May to September) of half-hourly g_c of the aspen forest for 1994 obtained using CLASS, JS, BWB and MBWB parameterizations with those obtained using the PM equation.

drought tolerance of aspen. No midday stomatal closure was produced by the JS model because of the simple empirical basis of the model. In September, the overestimate of g_c by the JS model is probably due to not accounting for the effect of leaf senescence (Fig. 3.6c). An additional independent function of leaf age in the JS model appears to be necessary and has been used successfully by Avissar and Pielke (1991). Fig. 3.6 indicates that the CLASS parameterization performed as well as the JS and MBWB models in all months; however, it underestimated g_c under high light conditions (see Fig. 3.2b). The BWB model underestimated g_c during the morning in all months (Fig. 3.6). This shortcoming of the BWB model has been remedied to a large extend by the replacement of h_0 by $1/\Delta e_0$ in the MBWB model (Lloyd, 1991, Blanken, 1997). Monteith (1995) argues that a $g_c(1/\Delta e_0)$ relationship suggests that the stomata respond to transpiration rather than humidity as found by Mott and Parkhurst (1991).

Fig. 3.7 compares modelled and measured g_c at the Dunsmuir Creek site for high and low soil moisture conditions. The three models significantly underestimate g_c during the morning, particularly between 08:00 and 10:00 PST. The BWB model performs worst since it fails to predict any variation in g_c during most the daytime. The performance of the JS model is worse than expected considering the relative high r^2 for the binned mean values of g_c. It is possible that some nighttime dew fall was evaporating from the canopy during the early morning causing an overestimation of the measured g_c (Price 1987).

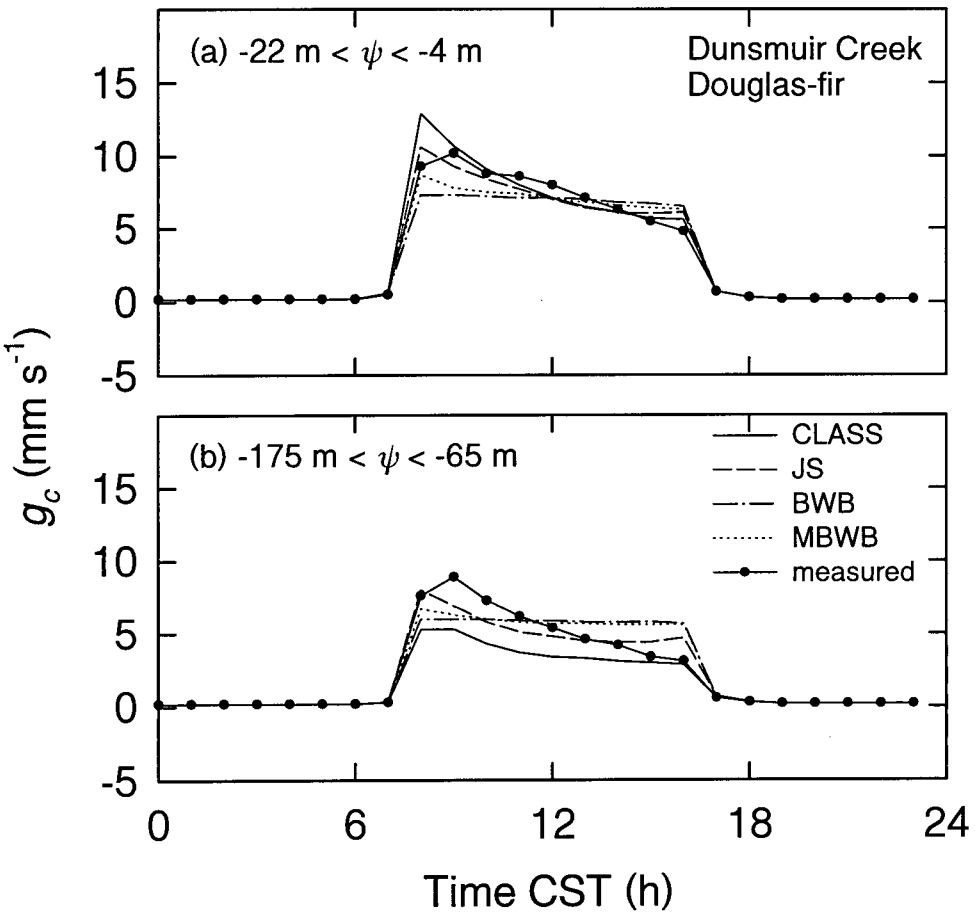

Fig. 3.7. Comparison of ensemble averages of half-hourly g_c of the Douglas-fir forest obtained from CLASS, JS, BWB and MBWB parameterizations, and those obtained from the PM equation. (a) high ψ (Aug 20 - 31, 1983); (b) low ψ (Aug 13 - 25, 1984).

3.8. Testing CLASS using the parameterizations

The JS and MBWB parameterizations developed here were incorporated into CLASS to further test its performance. To avoid the effects of possible errors in the input variables generated by CLASS on the comparison between the two new and the original

CLASS parameterizations, measured variables of Λ, Q_p, Δe_0 (or Δe_a) and ψ were used in the three parameterizations. The BWB parameterization was not tested in CLASS because, as shown above, it was inferior to the MBWB parameterization. Since Q^* modelled by CLASS generally agreed to within 25 W m^{-2} of values measured at both the PANP and Dunsmuir Creek sites, comparison was done for modelled and measured values of Q_E to assess the two canopy conductance models.

3.8.1. Diurnal simulations

Five consecutive days (August 13 to 17, 1994) at the PANP site were selected to represent a wide range of weather conditions. The first three days were cloud-free with a wide range of Δe, and August 16 and 17 were overcast and partly cloudy, respectively (Fig. 3.8a). Values of θ at the 8, 15-30, 30-61, 61-92 and 92-123-cm depths were approximately 0.11, 0.22, 0.26, 0.33 and 0.45 m^3 m^{-3}, respectively (the estimated maximum rooting depth was 60 cm), indicating that there was virtually no soil water stress. CLASS was initialized at 0:00 CST on August 13 using the measured soil moisture and temperature values. Fig. 3.8b compares the diurnal courses of modelled and measured Q_E. Over the five days, the JS parameterization estimated Q_E better than the MBWB and original CLASS parameterizations. The cumulative evaporation totals obtained for this period using the JS, MBWB and CLASS parameterizations were 8%, 21% and 20% less, respectively, than the measured values. During the three clear days, the average daytime values of Q_E obtained using the JS, MBWB and CLASS parameterizations were 8%, 21% and 24% smaller than the measured values. Furthermore, the original CLASS parameterization fails to predict the steady increase in Q_E over the three days. The

underestimation of Q_E by the MBWB parameterization is mainly because, as discussed earlier, it causes a depression in g_c during midday. On August 16, the overcast day, modelled Q_E obtained using the original CLASS parameterization was higher than the measured values. This is because of the lack of the response of g_c to light at low to medium values of incoming solar radiation ($200 < K_{\downarrow} < 500$ W m^{-2}) in the CLASS parameterization, $f_1(K_{\downarrow})$ (Eq. (36a)) (Verseghy et al. 1993). On August 17, the partly cloudy day, all three parameterizations provided good estimates of Q_E.

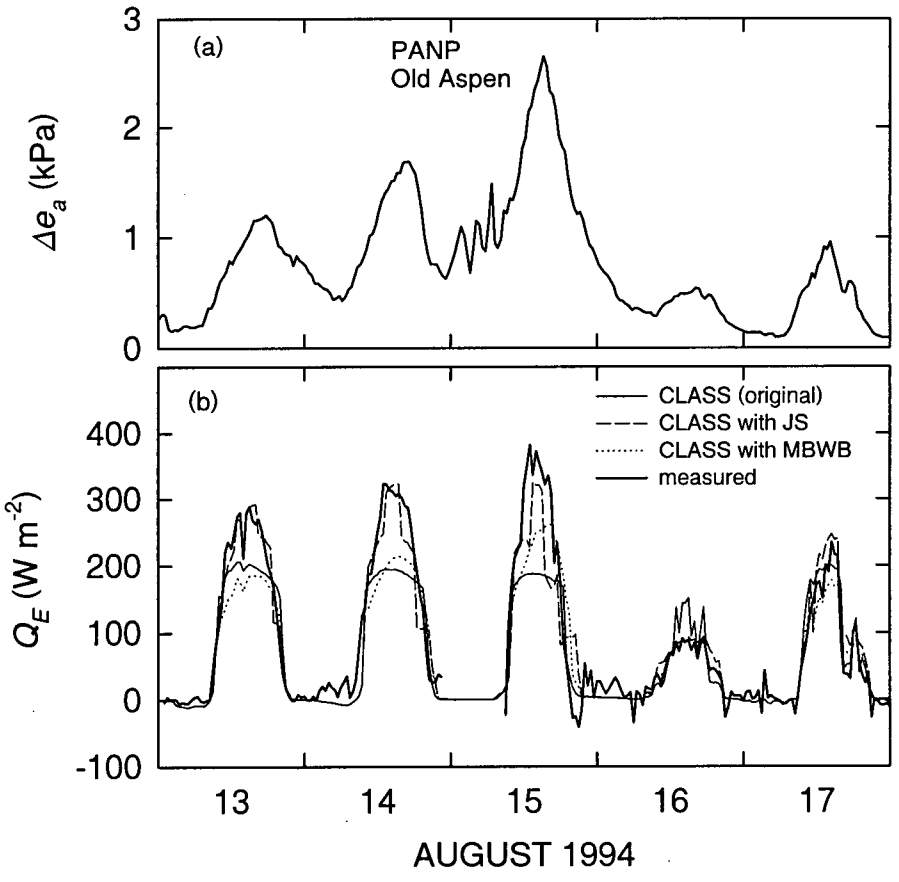

Fig. 3.8. Variation of Δe_a (a) and comparison of the half-hourly Q_E calculated by CLASS using CLASS, JS and MBWB parameterizations with the measured values (b) for the aspen forest on five consecutive days in 1994. Aug 13-15 were cloudless, Aug 16 was overcast and Aug 17 was partly cloudy.

To determine how well a canopy conductance parameterization obtained using one year's data would perform during a different year, the PANP parameterizations obtained using 1994 data were applied to a short period (August 6-9) in 1996. August 6 was a cloudy day, whereas August 7 - 9 were clear days with a steady increase in Δe until it reached a maximum value on August 9, a pattern similar to that of the three clear days in Fig. 3.8. Since the root-zone soil moisture was relatively high in both years, no data were available to test the performance of the parameterizations under low soil moisture conditions. However, it was still possible to assess the effectiveness of the parameterizations for similar high soil moisture conditions. Fig. 3.9 compares the diurnal courses of modelled and measured Q_E. The JS parameterization performed better than the MBWB and original CLASS parameterizations. The diurnal performance of the JS and

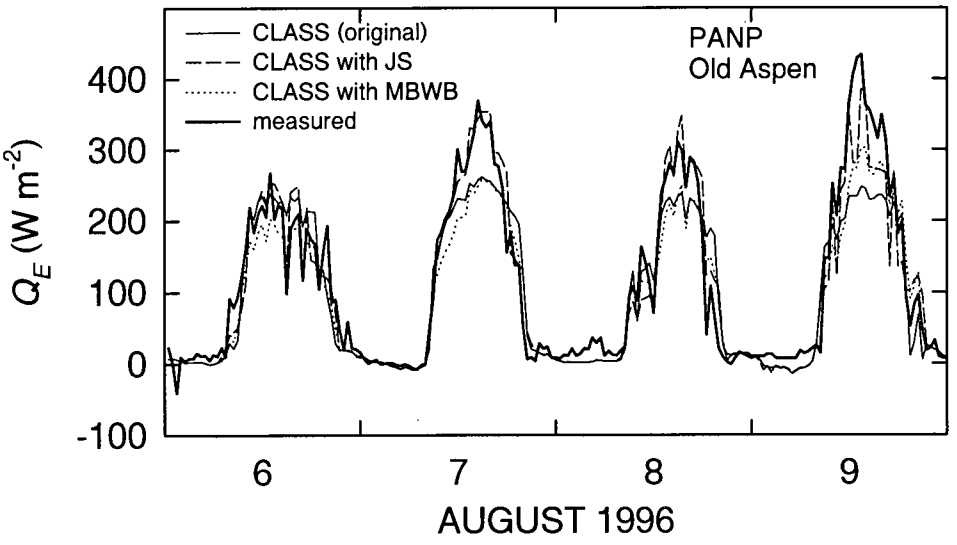

Fig. 3.9. Comparison of the half-hourly Q_E calculated by CLASS using CLASS, JS and MBWB parameterizations with the measured values for the aspen forest on four consecutive days in 1996. Aug 6 was partly cloudy and Aug 7-9 were mainly clear.

MBWB parameterizations in 1996 was very similar to that in 1994. During the three cloudless days, the average daytime values of Q_E obtained using the JS, MBWB and CLASS parameterizations were 4%, 16% and 14% less than the measured values. Although the MBWB parameterization underestimated Q_E more than the original CLASS parameterization during the three cloudless days, the error in 1996 (16%) was less than in 1994 (21%).

The diurnal comparison of modelled and measured Q_E for the Douglas-fir forest is shown in Fig. 3.10. Three consecutive high soil water potential days in 1983 were selected to represent a range of weather conditions (overcast, partly cloudy and sunny), and three relatively sunny days during a drying period in 1984 to represent a range of soil water potentials. CLASS was initialized with the measured soil moisture and temperature at the beginning of Aug 29, 1983 and at the beginning of each of the three days in 1984. The relative errors in the average latent heat flux for the entire 3-day period in 1983 obtained using the JS, MBWB and original CLASS parameterizations were only 3%, -7%, and 4%, respectively. However, on August 31, the sunny day, all three methods had a relative error of about -20%. Early in the drying period (July 21) in 1984, when the soil water potential was relatively high, modelled Q_E using all three parameterizations agreed quite well with the measured Q_E. As ψ dropped below -50 m during the drying period, the original CLASS parameterization increasingly underestimated Q_E due to the increasing underestimation of g_c with the decrease of ψ (see Fig. 3.3b). Not surprisingly, the other two parameterizations gave reasonably good estimates of Q_E later in the drying period. The relatively small decrease in Q_E during the drying period supports Robert's

(1983) conclusion that forest transpiration often responds conservatively to changes in soil water deficit.

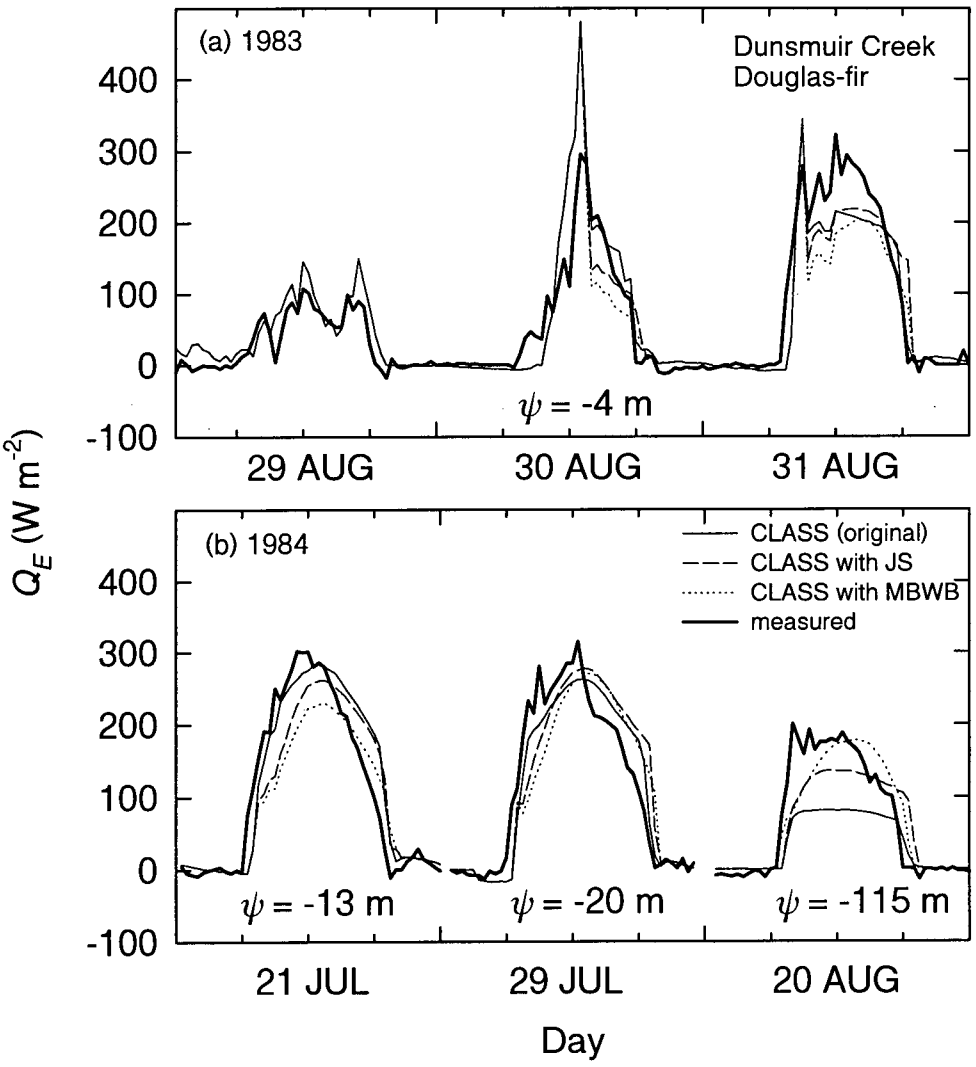

Fig. 3.10. Same as for Fig. 3.9, but for the Douglas-fir forest at Dunsmuir Creek on three consecutive days in 1983 (high ψ) (a) and 1984 (high to low ψ) (b).

The effectiveness of a canopy conductance parameterization, obtained using data measured in one forest, was tested by applying the parameterization to other forests of similar species composition and age. This was done by using the Dunsmuir Creek (Douglas-fir) parameterizations in CLASS to estimate Q_E at four other Douglas-fir forest sites (Browns River, Iron River 1, Iron River 2 and Haney). Tests were done for the four forests with high soil moisture conditions and for two of them (Iron River 1 and Iron River 2) with low soil moisture conditions. As the values of A of these forests were different, the effect of variation in A on g_c was taken into account by multiplying the estimated mean Douglas-fir stomatal conductance (g_s) by A. Mean g_s was obtained by dividing g_c of the Dunsmuir Creek Douglas-fir forest, obtained from Eq. (3.7), by its value of A. This assumes that the stomatal conductance characteristics for these five forests are the same. Working at the Iron River 2 site, Tan and Black (1976) showed that g_c (calculated with the PM equation using BREB measurements of Q_E) was closely approximated by the product of g_s (measured by porometer) and A. For a range of vegetation types and A, Kelliher et al. (1995) found that bulk surface conductance (which accounts for canopy and soil evaporation) was about 3 times g_s for conditions of plentiful soil water, adequate light, high relative humidity and moderate temperature. Fig. 3.11a compares the diurnal patterns of Q_E on typical days at the four forests calculated using CLASS with the original and the Dunsmuir Creek g_c parameterizations. The underestimation of Q_E during the daytime using the original CLASS parameterization was significantly improved using the JS and MBWB parameterizations for three of the forests

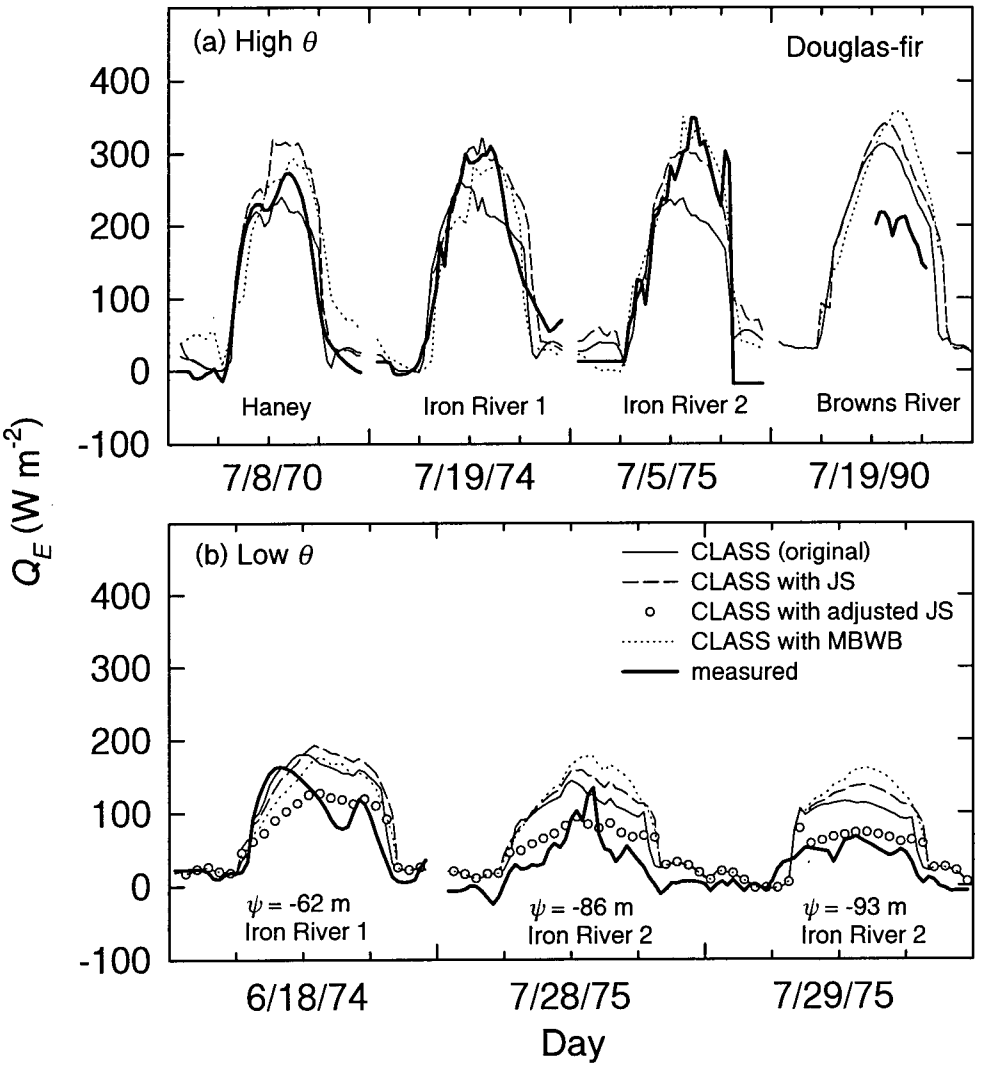

Fig. 3.11. Same as for Fig. 3.9, but for four other Douglas-fir forests with high ψ (a) and two of them with low ψ (b). Also shown is Q_E calculated by CLASS using the adjusted JS parameterization where $g_4(\psi)$ is replaced by that from the Iron River sites.

(Iron River 1 and 2, and Haney). The overestimation of Q_E using all three parameterizations at the Browns River forest is likely because the initial values of θ and ψ used were not representative due to the high stone content at the site (Lee and Black 1993). On the basis of the comparison involving the three forests, it appears that a g_c parameterization from one Douglas-fir site can be applied to others of similar age to provide reasonable estimates of Q_E under high soil moisture conditions. Three days from the two Iron River sites were selected to represent a range of low soil water potentials (-93 m < ψ < -62 m). All three parameterizations gave a significant overestimation of Q_E (Fig. 3.11b). To improve the performance of the JS parameterization, $g_4(\psi)$ was replaced in the JS parameterization (Eq. (3.7)) by $g_4(\psi)$ obtained from measurements made at the Iron River sites (see Fig. 3.3b). This adjusted JS parameterization gave better estimates than the other three parameterizations. For the MBWB parameterization, no adjustment of A_4 (ψ) was made because there were no measurements of canopy net assimilation rates at the two sites. These results suggest that under low soil moisture conditions, it appears to be much more difficult to apply a parameterization of g_c developed at one Douglas-fir forest to others.

3.8.2. Long-term simulations

In initial long-term tests, it was found that CLASS overestimated evaporation from the soil surface before and during the leaf emergence period (DOY 110 - 160). This was because Philip's formula significantly overestimated the relative humidity at the soil surface (Chapter 2 and Wu et al. 1999). Two alternative approaches were used: parameterization of (i) the relative humidity at the soil surface (the α approach) and (ii)

the soil resistance (the β approach) using average θ of the soil surface layer. To test the original CLASS, JS and MBWB parameterizations during the leaf emergence at the aspen site, the β approach was used because it gave better estimates of evaporation from the forest floor than the α approach.

Daily average values of Q_E above the aspen forest calculated by CLASS using three parameterizations were compared with eddy covariance measurements made during the 1994 growing season (Fig. 3.12). CLASS was initialized with the measured moisture and temperature at the beginning of the period. The JS and MBWB parameterizations gave better estimates of Q_E than the original CLASS parameterization during the full-leaf period (DOY 160 - 250) (Fig. 3.13). Over this period, the original CLASS and MBWB parameterizations underestimated Q_E on average by 12% and 9%, respectively, compared to a 3% overestimate by the JS parameterization (Table 3.4). On high radiation days, the original CLASS parameterization underestimated daily Q_E by about 26% (Fig. 3.13). The reason for the underestimation of Q_E during the period of leaf senescence (DOY 251 - 265) when using all three parameterizations is not clear, but is likely related to the infrequence of Λ measurements during this period when leaves were falling. The ratio of growing season evapotranspiration totals calculated using the JS, MBWB and original CLASS parameterizations to the measured value were 0.98, 0.87 and 0.84 (Table 3.4). These values reflect the effect of the higher conductance in the JS parameterization and show that over the long period the effects of differences in the conductance parameterizations still exist.

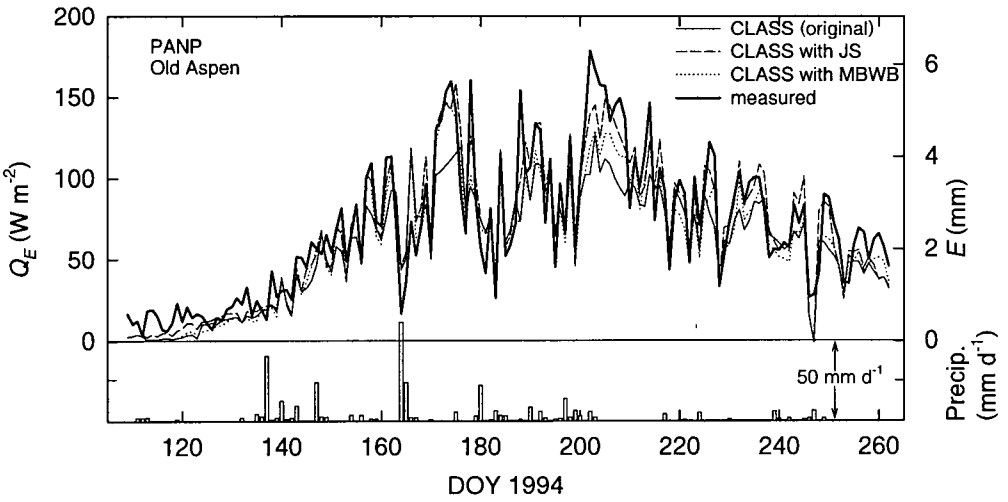

Fig. 3.12. Comparison of daily average Q_E calculated by CLASS using the original CLASS, JS and MBWB parameterizations with measured values for the aspen forest during the growing season (Apr 18-Sep 19) in 1994. Also shown is the daily precipitation.

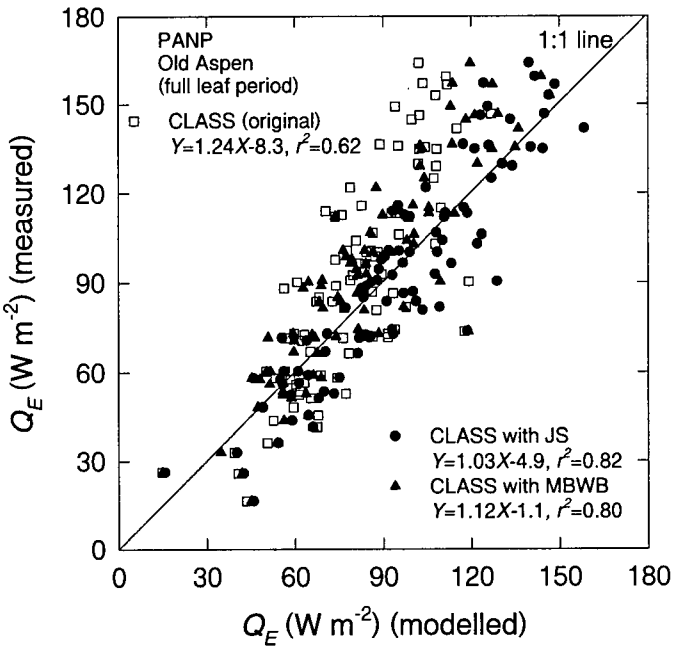

Fig. 3.13. Plot of measured daily average values of Q_E versus values calculated by CLASS with the three parameterizations in Fig. 3.13 for the aspen forest during the full leaf period (Jun 9- Sep 7) in 1994.

Table 3.4. CLASS calculated and measured evapotranspiration totals (mm) for the aspen forest at PANP and the Douglas-fir forest at Dunsmuir Creek

Period	Vegetation type	Soil moisture	CLASS	CLASS with JS	CLASS with MBWB	Measured
9 Jun - 7 Sep 1994	Aspen (full leaf period)	high	256.8 (0.88)[1]	299.7 (1.03)	264.0 (0.91)	291.8
18 Apr - 19 Sep 1994	Aspen (growing season)	high	317.1 (0.84)	367.9 (0.98)	327.7 (0.87)	375.3
24 - 31 Aug 1983	Douglas-fir	high	23.7 (1.22)	23.2 (1.20)	20.6 (1.06)	19.4
18 Jul - 25 Aug 1984	Douglas-fir	high to low	93.0 (0.89)	105.4 (1.01)	103.7 (0.99)	104.8

[1] Ratio of calculated to measured evapotranspiration.

Fig. 3.14 compares daily average Q_E calculated using CLASS and measured using the BREB method during the high soil moisture period in the 1983 growing season and the extended drying period in the 1984 growing season at the Dunsmuir Creek (Douglas-fir) site. CLASS was initialized with measured soil water content on DOY 235 in 1983 and DOY 200 in 1984. Calculated Q_E using the JS, MBWB and original CLASS parameterizations agreed reasonably well with the measurements except the latter underestimated Q_E during the end of the period in 1984 (after DOY 225) due to the predicted stomatal closure, which is evident in Fig. 3.10. The ratios of calculated to measured total evapotranspiration for the JS, MBWB and original CLASS parameterizations are 1.20, 1.06 and 1.22, respectively, for the 1983 period and 1.01, 0.99 and 0.89 for the 1984 period in Fig. 3.14 (Table 3.4). The corresponding r^2 values are 0.76, 0.79 and 0.64 for all days in Fig. 3.14, indicating better performance is achieved with the JS and MBWB parameterizations than the original CLASS parameterization over the wide range of soil water content.

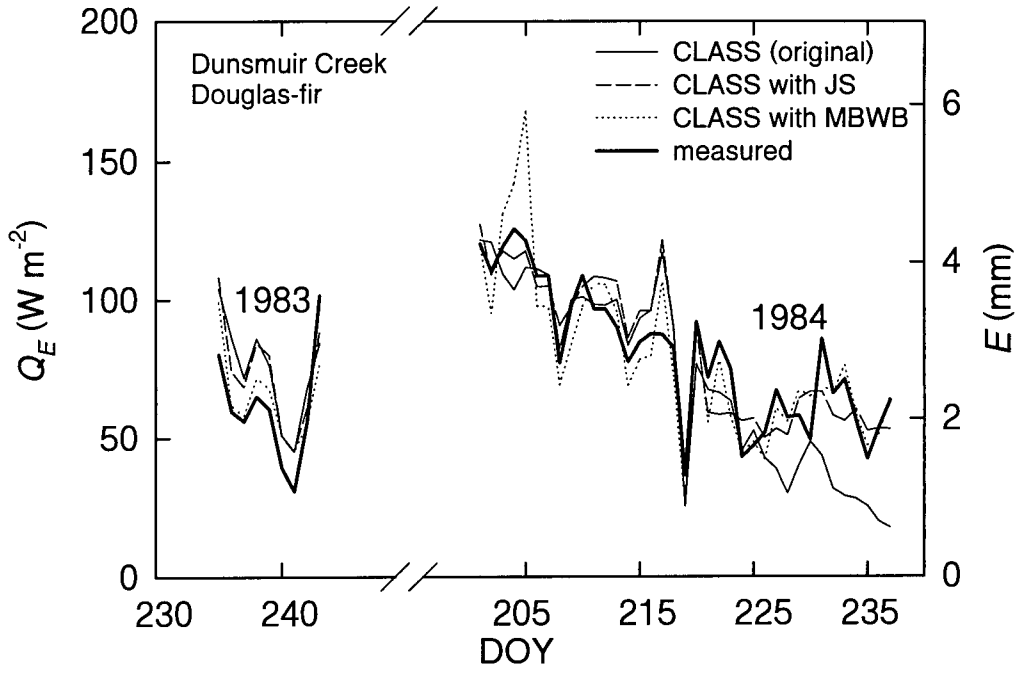

Fig. 3.14. Same as for Fig. 12 but for the Douglas-fir forest at Dunsmuir Creek during a short wet period (Aug 24-31) in 1983 and an extended drying period (Jul 18-Aug 25) in 1984.

3.9. Conclusions

Canopy conductance (g_c) is one of the main factors controlling the latent heat flux from forests because their canopies are closely coupled aerodynamically to the airstream above. This study evaluated several parameterizations of g_c of a conifer (Douglas-fir) and a deciduous (aspen) forest for application in CLASS.

In the case of the Douglas-fir forest, the original CLASS parameterization of g_c (based on the Jarvis-Stewart model) performed reasonably well for high soil moisture conditions, but underestimated g_c for low soil moisture conditions. More improvement

was achieved by optimizing the JS parameterization of g_c than by replacing it with the BWB or MBWB parameterizations. The latter were unable to characterize the daytime range of g_c as well as the JS parameterization.

In the case of the aspen forest with plentiful soil moisture, the original CLASS parameterization significantly underestimated g_c for high solar radiation conditions and slightly overestimated g_c for low solar radiation conditions. Improvements were made by modifying the relationships in the CLASS parameterization of g_c or using the MBWB parameterization. The latter, however, caused some depression in g_c at midday, a response to increasing vapour pressure deficit. Although this response occurs with many plant species, it has not yet been observed at the aspen site. The BWB parameterization was inferior to that of the MBWB.

The JS parameterization explained slightly more variance in g_c of both forests than the BWB and MBWB parameterizations probably because it contains more empirical parameters; however, the advantage of the BWB and MBWB parameterizations is that they are based on physiological processes and require fewer parameters. This parameterization requires a reliable estimate of the net assimilation rate of the canopy. For the aspen forest, this was modelled satisfactorily using a rectangular hyperbolic function of incoming solar radiation for each of three classes of Λ. The same model was used for the Douglas-fir forest except for two levels of soil moisture; however, it did not work as well as for the aspen forest. This was due to a lack of hourly soil CO_2 efflux measurements and the complex relationship between assimilation rate and light in this stand. The inadequacy of the model probably accounts for the poor performance of the BWB and MBWB parameterizations in the Douglas-fir forest.

Using the JS and MBWB parameterizations, CLASS gave better estimates of Q_E on half-hourly and daily bases than with the original CLASS parameterization. The original CLASS, JS and MBWB parameterizations underestimated evapotranspiration total by 12%, 3% and 9% over the full-leaf period at the aspen site in 1994 and by 11%, -1% and 1% over the extended drying period at the Douglas-fir site in 1984.

Based on measurements made during two high-soil-moisture years at the aspen site, g_c parameterizations using the first year's measurements successfully estimated Q_E over a short period of variable weather conditions during the second year. Conductance parameterizations developed at the Douglas-fir site successfully estimated Q_E at three of four other sites with similar-aged Douglas-fir forests under high soil moisture conditions. (The lack of success in the fourth forest was likely due to an inadequate characterization of the stone content in the root zone). When applied to the two sites which had low soil moisture conditions, they did not work satisfactorily because the response of conductance to soil moisture conditions was different between the sites. These results confirm the 'transferability' of g_c parameterizations in time (same site but different year) and space (other similar sites) when soil moisture is high, but suggest it may be more difficult when soil moisture is low. For deciduous forests, a reliable prediction model of the course of Λ during the growing season is necessary in using a g_c parameterization. This is particularly important during the leaf emergence and senescence periods and in the application of a g_c parameterization developed in one year to a subsequent year.

3.10. References

Avissar, R. and R. A. Pielke. 1991. The impact of plant stomatal control on mesoscale atmospheric circulations. *Agric. For. Meteorol.*, 54: 353-372.

Baldocchi, D. 1993. Scaling water and carbon dioxide exchange from leaves to a canopy: rules and tools. In: Ehleringer. J. R. and B. F. Christopher, (Eds), *Scaling Physiological Processes: Leaf to Globe,* Academic Press, Inc. California, pp. 77-115.

Baldocchi, D. 1997. Flux footprints within and over forest canopies. *Boundary-Layer Meteorol.*, 85: 273-292.

Ball, J. T., I. E. Woodrow and J. A. Berry. 1987. A model predicting stomatal conductance and its contribution to the control of photosynthesis under different environmental conditions. In: Progress in Photosynthesis Research (Ed. J. Biggens), Vol IV, Marlinus Nijhoff Publishers, Dordrecht, The Netherlands, pp. 221-224.

Black, T. A. and K. G. McNaughton. 1971. Psychrometric apparatus for Bowen ratio determination over forests. *Boundary-Layer Meteorol.*, 2: 246-254.

Black, T. A. 1979. Evapotranspiration from Douglas-fir stands exposed to soil water deficits. *Water Resources Research*, 15: 164-170.

Black, T. A. and F. M. Kelliher. 1989. Processes controlling understory evapotranspiration. *Phil. Trans. R. Soc. Lond.*, B324: 207-231.

Black, T. A., G. den Hartog, H. H. Neumann, P. D. Blanken, P. C. Yang, C. Russell, Z. Nesic, X. Lee, S. C. Chen, R. Staebler and M. D. Novak. 1996. Annual cycles of water vapour and carbon dioxide fluxes in and above a boreal aspen forest. *Global Change Biology*, 2: 219-229.

Blanken, P. D. 1997. Evaporation within and above a boreal aspen forest, *Ph.D. Thesis*, University of British Columbia, Vancouver, BC, Canada, 185 pp.

Blanken, P. D., T. A. Black, P.C. Yang, H. H. Neumann, Z. Nesic, R. Staebler, G. den Hartog, M. D. Novak and X. Lee. 1997. Energy balance and canopy conductance of a boreal aspen forest: partitioning overstory and understory components. *J. Geophys. Res.*, 102 D24, 28915-28927.

Blanken, P. D. and W.R. Rouse. 1996. Evidence of water conservation mechanisms in several subarctic wetland species. *Journal of Applied Ecology*, 33: 842-850.

Chen, J. M., P. D. Blanken, T. A. Black, M. Guilbeault and S. G. Chen. 1997. Radiation regime and canopy architecture in a boreal aspen forest. *Agric. For. Meteorol.*, 86: 107-125.

Chen, W. J., T. A. Black, P. C. Yang, A. G. Barr, H. H. Neumann, Z. nesic, M. D. Novak, J. Eley, R. J. Ketler and R. Cuenca. 1998. Effects of climatic variability on the annual carbon sequestration by a boreal aspen forest. *Global Change Biology*, (in press).

Collatz, G. J., Ball, J. T., Grivet, C. and J. A Berry. 1991. Physiological and environmental regulation of stomatal conductance, photosynthesis and transpiration: a model that includes a laminar boundary layer. *Agric. For. Meteorol.*, 54: 107-136.

Curtis, J. R. 1975. Evapotranspiration from a dry Douglas-fir forest. *M.Sc. Thesis*, University of British Columbia, Vancouver, BC, Canada, 47 pp.

Dickinson, R. E., A. Henderson-Sellers, P. J. Kennedy and M. F. Wilson. 1986. Biosphere-Atmosphere Transfer Scheme (BATS) for the NCAR Community Climate Model. National Centre for Atmospheric Research, Boulder, Colorado, NCAR/TN-275+STR, 69 pp.

Gash, J. H. C., W. J. Shuttleworth, C. R. Lloyd, J.-C. Andre, J.-P. Goutorbe and J. Gelpe. 1989. Micrometeorological measurements in Les Lands Forests during HAPEX-MOBILHY. *Agric. For. Meteorol.*, 46: 131-147.

Jarvis, P. G. 1976. The interpretation of the variation in leaf water potential and stomatal conductance found in canopies in the field. *Phil. Trans. R. Soc.*, Lond. B. 273: 593-610.

Jarvis, P. G. and K. G. McNaughton. 1986. Stomatal control of transpiration: scaling up from leaf to region. *Adv. Ecol. Res.*, 15: 1-49.

Jarvis, P. G. 1993. Prospects for bottom-up models. In: Ehleringer, J. R. and B. F. Christopher, (Eds), *Scaling Physiological Processes: Leaf to Globe,* Academic Press, Inc. California, 115-126.

Kaufmann, M. R. 1982. Evaluation of season, temperature, and water stress effects on stomata using a leaf conductance model. *Plant Physiol.*, 69: 1023-1026.

Kelliher, F. M., R. Leuning, M. R. Raupach, E.-D. Schulze. 1995. Maximun conductances for evaporation from global vegetation types. *Agric. For. Meteorol.*, 73: 1-16.

Lee, X. and T. A. Black. 1993. Atmospheric turbulence within and above a Douglas-fir stand. Part II: Eddy fluxes of sensible heat and water vapour. *Boundary-Layer Meteorol.*, 64: 368-389.

Lloyd, J. 1991. Modelling stomatal responses to environment. In: *Macadamia integrifolia. Aust. J. Plant Physiol.*, 18: 649-660.

Leuning, R. 1995. A critical appraisal of a combined stomatal-photosynthesis model for C_3 plants. *Plant, Cell and Environment*, 18: 339-355.

McCaughey, J. H. and A. Iacobelli. 1994.Modelling stomatal conductance in a northern deciduous forest. Chalk River, Ontario. *Canadian Journal of Forest Research*, 24, 904-910.

MaNaughton, K. G. and T. A. Black. 1973. A study of evapotranspiration from a Douglas fir forest using the energy balance approach. *Water Resources Research*, 9: 1579-1590.

Monteith, J. L. 1981. Evaporation and surface temperature. *Quart. J. R. Meteorol. Soc.*, 107: 1-27.

Monteith, J. L. 1995. A reinterpretation of stomatal responses to humidity: theoretical paper. *Plant, Cell & Environment*, 18: 357-364.

Mott, K. A. and D.F. Parkhurst. 1991. Stomatal responses to humidity in air and helox. *Plant, Cell & Environment*, 14: 509-515.

Owen, P. R. and W. R. Thompson. 1963. Heat transfer across rough surfaces. *Journal of Fluid Mechanics*, 15: 321-334.

Price, D. T. 1987. Some effects of variation in weather and soil water storage on evapotranspiration and net photosynthesis of a young Douglas-fir stand. *Ph.D. Thesis*, University of British Columbia, Vancouver, BC.

Price, D. T. and T. A. Black. 1989. Estimation of forest transpiration and CO_2 uptake using the Penman-Monteith equation and a physiological photosynthesis model. In: *Estimation of Areal Evapotranspiration, IAHS Publ.*, 177: 213-228.

Price, D. T. and T. A. Black. 1990. Effects of short-term variation in weather on diurnal canopy CO_2 flux and evapotranspiration of a juvenile Douglas-fir stand. *Agric. For. Meteorol.*, 50: 139-158.

Price, D. T. and T. A. Black. 1991. Effects of summertime changes in weather and root-zone soil water storage on canopy CO_2 flux and evapotranspiration of two juvenile Douglas-fir stands. *Agric. For. Meteorol.*, 53: 303-323.

Robert, J. 1983. Forest transpiration: A conservative hydrological process? *Journal of Hydrology*, 66: 133-141.

Ruimy, A., P. G. Jarvis, D. D. Baldocchi and B. Saugier. 1995. CO_2 fluxes over plant canopies and solar radiation: a review. *Advances in Ecological Research*, 26: 1-63.

Schuepp, P., M. Y. Leclerc, J. I. MacPherson and R. L. Desjardins. 1990. Footprint prediction of scalar fluxes from analytical solutions of the diffusion equation. *Boundary-Layer Meteorology*, 50: 355-373.

Schulze, E. D. and A. E. Hall. 1982. Stomatal responses, water loss and CO_2 assimilation of plants in contrasting environments. In: Lange, O.L., P.S. Nobel, C.B. Osmond and H. Zeigler, (Eds), *Physiological Plant Ecology II, Water Relations and Carbon Assimilation, Encyclopedia of Plant Physiology,* Vol. 12b. Springer-Verlag, New York, 181-230.

Sellers, P. J, Y. Mintz, Y. C. Sud and A. Dalcher. 1986. A simple biosphere model (SiB) for use within general circulation models. *J. Atmos. Sci.* 43: 505-531.

Sellers, P., Hall, F., Margolis, H., Kelly, R., Baldocchi, D. D., den Hartog, G., Cihlar, J., Ryan, M. G., Goodison, B., Crill, P., Ranson, K. J., Lettermaier, D. and Wickland, E. 1995. The boreal ecosystem-atmosphere study (BOREAS): An overview and early results from 1994 field year. *Bull. of the Amer. Meteorol. Soc.*, 76: 1549-1577.

Sellers, P. J., D. A. Randall, G. J. Collatz, J. A. Berry, C. B. Field, D. A. Dazlich, C. Zhang, G. D. Collelo and L. Bounoua. 1996. A revised land surface parameterization (SiB2) for atmospheric GCMs. Part I: Model Formulation. *Journal of Climate*, 9: 676-705.

Smith, E. A., G. A. Hodges, M. Bacrania, H. J. Cooper, M. A. Owens, R. Chappell and W. Kincannon. 1997. BOREAS net radiometer engineering study. Final report (NASA grant NAG5-2447). Dept. of Meteorol., Florida State University, FL.

Spittlehouse, D. L. and T. A. Black. 1979. Determination of forest evapotranpiration using Bowen ratio and eddy correlation measurements. *Journal of Applied Meteorol.*, 18: 647-653.

Stewart, J. B. 1988. Modelling surface conductance of pine forest. *Agric For. Meteorol.*, 43: 19-35.

Stewart, J. B. 1989. On the use of the Penman-Monteith equation for determining areal evapotranspiration. In *Estimation of Areal Evapotranspiration, IAHS Publ.*, 177: 13-12.

Tan, C. S. and T. A. Black. 1976. Factors affecting the canopy resistance of a Douglas-fir forest. *Boundary-Layer Meteorol.*, 10: 475-488.

Tan, C. S., T. A. Black and J. U. Nnyamah. 1977. Characteristics of stomatal diffusion resistance in a Douglas-fir forest exposed to soil water deficits. *Can. J. For. Res.*, 7: 595-604.

Verma, S. B. 1989. Aerodynamic resistances to transfers of heat, mass and momentum. In: *Estimation of Areal Evapotranspiration, IAHS Publ.*, 177: 13-20.

Verseghy, D. L. 1991. CLASS - A Canadian land surface scheme for GCMs, I. Soil model. *Int. J. Climatol.* 11: 111-133.

Verseghy, D. L., N. A. McFarlane, and M. Lazare. 1993. CLASS - a Canadian land surface scheme for GCMs, II. Vegetation model and coupled runs. *Int. J. Climatol.* 13: 347-370.

Webb, E. K., G. I. Pearman and R. Leuning. 1980. Correction of flux measurements for density effects due to heat and water vapor transfer. *Quart. J. R. Meteorol. Soc.*, 106: 85-100.

Wu, A., T. A. Black, D. L. Verseghy, M. D. Novak and W. G. Bailey. 1999. Testing the α and β methods of estimating evaporation from bare and vegetated surfaces in CLASS, *Atmosphere-Ocean* (accepted).

Yang, P. C. 1998. Carbon dioxide flux within and above a boreal aspen forest, *Ph.D. Thesis*, Univ. of British Columbia, Vancouver, BC, 229 pp.

CHAPTER 4

VALIDATION OF THE CANADIAN LAND SURFACE SCHEME WITH IMPROVED PARAMETERIZATIONS FOR A BOREAL ASPEN FOREST FOR YEARS 1994 TO 1998

4.1. Introduction

In Chapters 2 and 3, calculations of the energy balance components using the Canadian Land Surface Scheme (CLASS) with measured values of meteorological variables collected in the field as forcing atmospheric boundary conditions, i.e. "stand-alone" calculations, were made and compared with observations from two bare soils, an agricultural crop and six forests. Others have carried out similar tests of CLASS for a variety of surface types (Desborough et al. 1996; Mahfouf et al. 1996; Liang et al. 1998), as part of the Project for Intercomparison of Land-Surface Parameterization Schemes (PILPS) (Henderson-Sellers et al. 1993). One obvious problem identified from these tests was that CLASS overestimated evaporation from the soil surface when the soil was dry. In the tests conducted for vegetated surfaces, it was found that CLASS performed well for Douglas-fir forests but underestimated canopy transpiration for a boreal aspen forest under conditions of high solar radiation.

Two improved parameterizations were proposed in Chapters 2 and 3 to deal with the problems mentioned above: (1) a surface resistance term was used in the calculation of evaporation from the soil surface (the β method), whereas the original CLASS version computed the relative humidity at the soil surface thermodynamically using Philip's (1957) relationship, (2) the original CLASS parameterization of canopy conductance (hereafter referred to as the CLASS JS parameterization because it was developed from

the parameterizations given by Jarvis (1976) and Stewart (1988) was either modified to give a more realistic response to environmental variables or replaced by a more physiologically-based parameterization (hereafter referred to as the MBWB parameterization because it was a modified version of that given by Ball et al. (1987). Chapter 2 confirmed that modelled evaporation from the soil surface was significantly overestimated by Philip's relationship because of the difficulty of estimating the relative humidity at the soil surface in models with a thick soil surface layer (i.e. 5 - 10 cm). The β method gave much better estimates of evaporation from the soil than Philip's relationship. Chapter 3 showed that the CLASS JS parameterization underestimated aspen conductance for high solar radiation conditions and slightly overestimated it for low solar radiation conditions. Its performance was slightly inferior to the modified JS and MBWB parameterizations at the aspen site.

Although the modified JS parameterization worked slightly better than the MBWB parameterization during the growing season in 1994 and for a short summer period in 1996 (Chapter 3), it is still not clear which parameterization gives better performance over a long-term period at the aspen site. It is thus desirable to continue the validation with data collected from continuous long-term observations. This is particularly important for the validation of modelled soil hydraulic processes. The following modelled processes are compared with observations: snowmelt, infiltration, soil water content and subsurface drainage.

4.2. Experimental site and data

4.2.1. Experimental site

The experimental site has been described in Chapters 2 and 3. The following is a brief description relevant to this chapter. The site (53° 38"N 106° 12"S), located in the southern part of Prince Albert National Park (PANP) about 50 km northwest of Prince Albert, Saskatchewan, Canada. It was one of ten flux sites used in the Boreal Ecosystem-Atmosphere Study (BOREAS), a large-scale short-term investigation of carbon, water and energy exchange between the atmosphere and the boreal forest (Sellers et al. 1995). Since 1997, it had been one of the Canadian Boreal Ecosystem Research and Monitoring Sites (BERMS) and part of the Ameriflux Network. This network was set up in 1997 to coordinate the monitoring of CO_2 and H_2O vapour exchange above representative North American ecosystems and currently is part of an integrated terrestrial flux network (FluxNet) to accomplish this on a global scale.

The site consists of an extensive stand of aspen (*Populus tremuloides* Michx.) about 21 m tall and 70 years old in 1994. At that time, average tree diameter at the 1.5 m height was 17 cm and the stand density 830 stem ha^{-1}. The understory is mainly composed of hazelnut (*Corylus cornuta* Marsh.) about 2 m tall with occasional clumps of alder (*Alnus crispa* (Ait.) Pursch), sparse shrubs (e.g. prickly rose *Rosa acicularis* Lindl., wild rose *Rosa woodsii* Lindl.) and grasses. The soil is an Orthic Gray Luvisol with an 8-10 cm deep surface organic layer which has a bulk density of 160 kg m^{-3}. The mineral soil has a silty-clay texture and a bulk density of about 1300 kg m^{-3}. Tree roots penetrate to a depth of about 0.6 - 1.2 m. The terrain is generally level and fetch exceeds 3 km in all directions.

4.4.2. Validation data

Validation data include measured fluxes of the energy balance components, albedos, profiles of soil water content and snowmelt time and growing-season water balance. Net radiation, Q^* (W m^{-2}), was measured using net radiometers (model S-1, Swissteco Instruments, Oberriet, Switzerland and model CN-1, Middleton Instruments, Melbourne, Australia) in 1994 and 1996 and calculated from measurements using upward and downward facing pyrgeometers (Eppley model PIR) and upward and downward facing pyranometers (Kipp and Zonen CM11) in 1997 and 1998. Sensible and latent heat fluxes, Q_H and Q_E (W m^{-2}), were measured using the eddy-covariance method at 39 m above the ground in 1994 and from 20 April 1996 to the end of 1998 (Black et al. 1996; Blanken et al. 1997, Chen et al. 1998). The soil surface heat flux, G_0 (W m^{-2}), was calculated by adding the heat flux at the 3-cm depth measured using heat flux plates and the rate of heat storage in the layer of soil above the plates. All of the above observations are available as a time series of one-half hour averages. Soil water content, θ (m^3 m^{-3}), was measured using time domain reflectometry (TDR). In 1994, near-surface θ was measured using two TDR probes (each consisting of three stainless steel rods 3 mm in diameter and 30 cm long) positioned horizontally in the organic (8 cm depth) and mineral (15 cm) horizons. The probe in the organic horizon was calibrated using gravimetric measurements of soil moisture in the 3-6 cm layer. In addition, six TDR rods (Gabel Corp., Victoria, BC) with five segments (0-15, 15-30, 30-60, 60-90, 90-120 cm) were read manually using a Tektronix model 1502B/1502C cable length tester in 1994 (Blanken et al. 1997). From spring 1996 to the end of 1998, θ was measured using eight of the segmented TDR rods installed along a 50 m transect and two model 615 soil water

reflectometers (Campbell Scientific Inc., Logan, Utah) installed in two profiles (2.5, 7.5, 22.5, 45, 60-90 cm). The rods were monitored automatically using a system based on a CSI model 21X data logger. In 1998, the TDR rods and reflectometers were calibrated using θ measured gravimetrically to a depth of 60 cm (Rob Swanson 1998, personal communication). The leaf area index, Λ (m^2 m^{-2}), of the overstory and understory was measured optically using the LI-COR model LAI-2000 plant canopy analyzer (one used above and below the aspen canopy in 1994 at least at four locations, and one mounted above the aspen canopy and a second one used at six locations below in 1997 and 1998) (A. G. Barr and P. Pacholek 1998, personal communication). Because Λ was only measured on one day during the full-leaf period in the summer of 1996, the time series of Λ was calculated by multiplying the daily average fraction of the downward photosynthetic photon flux density above the forest transmitted through the aspen canopy by the ratio of Λ to the transmitted fraction on the day Λ was measured (Chen et al. 1998).

4.2.3. Meteorological conditions

The advantage of using this long-term dataset is that it provides a unique opportunity to validate CLASS over five consecutive years with varying climatic conditions. The mean air temperature in spring (March to May) varied from 0.5 to 8.0 °C, causing leaf emergence to vary between 5 to 40 days (see Fig. 4.2 later). This also had a significant effect on the growing season length. On the other hand, no significant variation in annual total precipitation was found for the four years, and their values were close to the 30-year normal of 400 mm at the Prince Albert airport (Fig. 4.1). The

cumulative measured evaporation for 1994, 1996, 1997 and 1998 accounted for 90%, 85%, 85% and 80% of the annual precipitation. Blanken (1997) showed that the change in the root zone water storage between the beginning and end of the 1994 growing season was approximately equal to the accumulated difference between precipitation (P) and evapotranspiration (E) over the growing season ($\int(P-E)dt$), i.e. surface runoff and drainage at 1.2-m depth were small (< 30 mm).

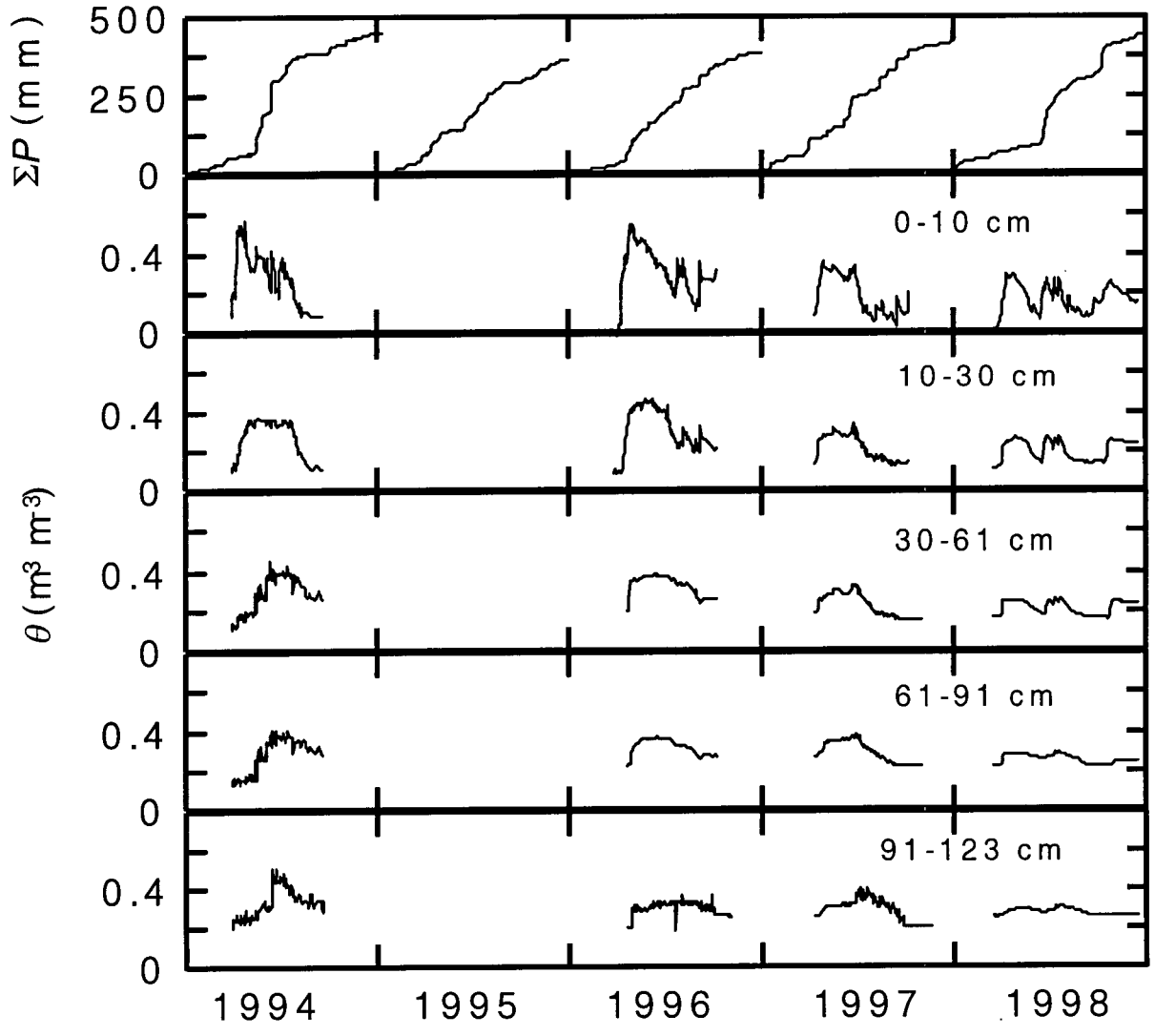

Fig. 4.1. Cumulative precipitation (P) and soil water content (θ) measured using time-domain reflectometry (TDR) for soil layers 0 - 10, 10 - 30, 30 - 61, 61 - 91 and 91 - 123 cm in 1994, 1996, 1997 and 1998 at the aspen site.

Fig. 4.1 shows the courses of θ at different depths in relation to the cumulative precipitation for 1994 to 1998. Although there was some spatial variability in θ along the transect, the results presented herein, which were obtained from a single TDR profile over the four years, were considered representative of the variation during each year as well as between years. Snowmelt and additional rainfall generally resulted in a rapid increase in θ in early spring. The rise in θ started earliest in 1998 because of the unusually warm early spring probably due to an effect of the strong El Niño year in 1997 and 1998. From the end of April to the middle of July, the variation in θ between years depended on rainfall. With the decrease in rainfall after July and a continuing evaporative demand, θ decreased gradually throughout the remainder of the growing season. High θ throughout the growing season of 1996 was probably because of a more even rainfall distribution than in other years. Generally aspen transpiration appeared not to be limited by θ, probably because at the depths (0.9 to 1.2 m) to which the aspen roots can penetrate, θ remained relatively high (Blanken et al. 1997). The only possible soil moisture stress occurred during the second week of May to the middle of June in 1998 when the total precipitation was only 4 mm and θ from the surface down to a depth of 60 cm was the lowest (0.10 - 0.15 m^3 m^{-3}) of the five growing seasons.

4.3. Parameterizations and validation procedures

4.3.1. CLASS parameterizations

Except when completely wet, the canopy foliage exerts some degree of physiological control upon the evaporation rate. Under these conditions, a canopy

conductance, g_c (m s^{-1}), is required in the evaporation formulation, and the canopy conductance concept is the essential part of most canopy models. The CLASS JS parameterization is given by (Verseghy et al. 1993)

$$g_c = \frac{g_{c,\max}\Lambda}{\Lambda_{\max} f_1(K_\downarrow) f_2(\Delta e) f_3(\psi) f_4(T_0)} \tag{4.1}$$

where $g_{c,\,max}$ is the maximum value of the canopy conductance, f_1, f_2, f_3 and f_4 are the functions accounting for the effects of solar radiation, $K_\downarrow$ (W m^{-2}), atmospheric saturation deficit, Δe (kPa), soil water potential, ψ (m), and canopy temperature, T_0 (°C), respectively. These are given by

$$\begin{aligned}
&g_{\mathrm{c,max}} = 20.0 \text{ mm s}^{-1} \\
&f_1(K_\downarrow) = \max(1.0, 500.0 / K_\downarrow - 1.5) \\
&f_2(\Delta e) = \max(1.0, \Delta e / 5.0) \\
&f_3(\psi) = \max(1.0, -\psi / 40.0) \\
&f_4(T_0) = \begin{cases} 1.0 & 40^\circ C > T_0 > 0^\circ C \\ 5.0 g_{c,\max}\Lambda / \Lambda_{\max} & T_0 \geq 40^\circ C \text{ or } T_0 \leq 0^\circ C \end{cases}
\end{aligned} \tag{4.2}$$

Surface soil wetness determines whether evaporation from the soil surface occurs at the potential rate or is limited by soil water supply. Many land surface models calculate evaporation by parameterizing the relative humidity (α) at the soil surface (the α method) or the surface resistance (r_{soil} (s m^{-1})) to water vapour transfer (the β method) (Chapter 2). In CLASS, α is determined using Philip's (1957) thermodynamic relationship

$$\alpha = \exp[g\psi_s / R_v T_s] \tag{4.3}$$

where g is the acceleration due to gravity (m s^{-2}), R_v (J kg^{-1} K^{-1}) is the gas constant for water vapour at the soil surface temperature T_s (K), and ψ_s is the soil matric potential at the soil surface. Evaporation from the soil surface is calculated as

$$Q_E = L_v \varrho_a (\alpha q_{sat}[T_s] - q_a) / r_a \tag{4.4}$$

where L_v is the latent heat of vaporization (J kg^{-1}), ϱ_a is the density of air (kg m^{-3}), q_a is the specific humidity of the air at a reference height (kg kg^{-1}), q_{sat} is the saturation value at T_s, and r_a is the aerodynamic resistance between the soil surface and the reference height (s m^{-1}).

4.3.2. Improved parameterizations for the aspen forest

The modified JS parameterization for the aspen forest was developed in Chapter 3, although the parameterization has been slightly modified to incorporate the effect of the decrease in θ early in the summer of 1998

$$g_c = g_{c,\max} g_1(\Lambda) g_2(Q_p) g_3(\Delta e) g_4(\theta) g_5(T_0) \tag{4.5}$$

where g_1, g_2, g_3, g_4, and g_5 are the functions accounting for the effects of Λ, incident photosynthetic photon flux density, Q_p (μmol m^{-2} s^{-1}), Δe, θ and T_0, respectively, and are given by

$$\begin{aligned}
&g_{c,\max} = 32.6\,\text{mm s}^{-1} \\
&g_1(\Lambda) = \Lambda / \Lambda_{\max} \\
&g_2(Q_p) = \frac{Q_p}{Q_p + 430} \\
&g_3(\Delta e) = \exp(-0.645 \Delta e) \\
&g_4(\theta) = \begin{cases} 1 - \exp[6.0(\theta - \theta_{sat})] & \theta \le \theta_c \\ 1 & \theta > \theta_c \end{cases} \\
&g_5(T_0) = 1.0
\end{aligned} \tag{4.6}$$

where θ_{sat} is the saturation soil water content or porosity, θ_c is the critical value of θ below which g_c is affected by soil water stress (θ_c was determined to be 0.20), $\Lambda_{\max}$ is the maximum value of Λ. Note g_4 is a very approximate function developed to account for

the early summer dry period in 1998 and $g_5(T_0)$ = 1.0 indicates that no temperature effect has been identified.

The MBWB parameterization was also described in Chapter 3 which was written as

$$g_c = m\frac{A_0}{\Delta e_0 c_0} + b \tag{4.7}$$

where each variable is defined at the canopy level and subscript '0' refers to the 'big leaf' surface. A_0 is the rate of net CO_2 assimilation (μmol m^{-2} s^{-1}), c_0 is the CO_2 mole fraction of the air (μmol mol^{-1}), Δe_0 is the vapour mol fraction difference between the big leaf surface and the atmosphere (mol mol^{-1}), and m (= 0.037) and b (= 143.0 mol m^{-2} s^{-1}) are the slope and intercept, respectively.

A canopy-level equation describing A_0 can be written as (Sellers et al. 1997a)

$$A_0 = V_{\max 0} A_1 A_2 \cdots A_5 \tag{4.8}$$

where $V_{\max 0}$ is the maximum photosynthetic capacity (μmol m^{-2} s^{-1}), the dimensionless parameters A_1 through A_5 describe the effects of Q_p, T_0, Δe_0 , ψ and c_0, respectively.

The effect of Q_p and Λ on A_0, i.e. $V_{\max 0} A_1$, found based on measurements made in 1994, can be expressed as (Chapter 3)

$$A_0 = \frac{0.0605 \times 6.379 Q_p \Lambda}{0.0605 Q_p + 6.379\Lambda} - 2.536 \tag{4.9}$$

Although they are small, the effects of air temperature, T_a (°C), and Δe_0 based on the same year measurements can be written as (Chen et al. 1998)

$$\begin{aligned} A_2 &= \frac{0.9612 \times 212.19 T_a}{0.9612 T_a + 212.19} - 0.8229 T_a - 0.1277 \\ A_3 &= \exp(-340.57\Delta e_0 + 0.4474) + 0.8951 \end{aligned} \tag{4.10}$$

Chen et al. (1998) found the model $A_0 = A_1 A_2 A_3$ explained about 70% of the variance in

measured daytime half-hourly A_0 in 1994 and 1996. No or little effect of θ on photosynthesis was found for 1994 (Chen et al. 1998) and from the second week of May to the middle of June in 1998 when the soil moisture was the lowest of the five growing seasons. Therefore, the effects of soil moisture stress and some other factors such as atmospheric CO_2 concentration were not considered here, as discussed in detail in Chapter 3.

In the calculation of evaporation from the soil, the β relationship was used to relate β, a dimensionless reciprocal of the sum of r_{soil} and r_a ($\beta = r_a/(r_a + r_{soil})$, to θ of a soil surface layer. When applied to CLASS with a 10-cm thick surface layer (Verseghy 1991), the β relationship is expressed as (Chapter 2)

$$\beta = 1/[1+1.2\times10^5(\theta_{sat}-\theta)^{11.0}] \tag{4.11}$$

and evaporation was calculated as

$$Q_E = L_v \varrho_a \beta (q_{sat}[T_s]-q_a)/r_a \tag{4.12}$$

4.3.3. Validation procedures

Five different tests were carried out (Table 4.1). Tests 1 and 2 were to examine how well the original version of CLASS performed and to determine the effect of removing any soil water limitation on g_c. Test 3 was to examine how the change in the winter albedo affected the simulation and how well the β method performed. Both modifications were made in a single test because their effects are in the different parts of the year. Tests 4 and 5 were to examine how well the modified JS and MBWB g_c parameterizations performed, respectively.

Table 4.1. Summary of the five tests

Test	Parameterization of g_c	Soil moisture used in the calculation of g_c	Soil evaporation formula	Winter albedo
1	CLASS JS Eq. (4.1&4.2)	ψ from CLASS	Philip's Eq. (4.3)	0.50
2	CLASS JS Eq. (4.1&4.2)	$\psi = -5.0$ m	Philip's Eq. (4.3)	0.50
3	CLASS JS Eq. (4.1&4.2)	$\psi = -5.0$ m	β method Eq. (4.11)	0.25
4	Modified JS Eq. (4.5&4.6)	$\theta = 0.25$ m^3 m^{-3} (equiv. to $\psi = -5.0$ m)* except for measured θ during May 1-June 15, 1998	β method Eq. (4.11)	0.25
5	MBWB Eq. (4.7-4.10)	Assume no soil moisture effect on g_c	β method Eq. (4.11)	0.25

* See the soil water retention relationship in Cuenca et al. (1997)

In each test, CLASS was run at a time step of 30 min for five years from 1 January 1994 to 1998 with one initialization at the beginning of this period. The input forcing data consisted of continuous half-hourly meteorological observations of air temperature, specific humidity, downward solar and longwave radiation, precipitation, air pressure and wind speed measured at 39 m above the ground. Values of Λ at each time step calculated by CLASS were not used but taken from an extrapolated half-hourly time series of Λ obtained using measured values. Initial conditions and soil and vegetation properties are listed in Table 4.2.

Seasonal variation in Λ generated by CLASS is controlled by the air temperature and the temperature of the top soil layer (Verseghy et al. 1993). However, examination of the relationship of Λ to environmental variables showed that air temperature was the main factor in determining when the aspen bud burst began (Chen et al. 1998). Comparison between Λ of the aspen forest calculated by CLASS with measured values showed that there were significant discrepancies during the periods of aspen and hazelnut leaf

emergence and senescence (Fig. 4.2). The measured yearly Λ_{max} also varied between years. Modelling leaf development is beyond the scope of this thesis. Alternative approaches to the estimation are available, e.g. use of satellite data (Sellers et al. 1997a).

Table 4.2. Initial conditions on 1 January 1994 and soil and vegetation properties

Parameter	Value
initial soil water content	0.130, 0.150 and 0.255 m^3 m^{-3} for layers 1, 2 and 3
initial soil temperature	-2.5, -2.0 and 0.5 °C for layers 1, 2 and 3
soil texture index	1.0 for sand (20%) and 4.4 for clay (20%)
soil drainage index	0.0 (1.0 for freely-draining soils, 0.0 for poorly draining soils)
soil colour index	4.0 (1.0 for dark soils, 12.0 for light soils)
initial snow mass*	56 mm (liquid water equivalent)
initial snow density*	158 kg m^{-3}
vegetation type	broadleaf tree
fractional vegetation cover	100%
leaf area index	0.0 (minimum) to 5.6 m^2 m^{-2} (maximum)
maximum above-ground canopy biomass	20 kg m^{-2}
rooting depth	0.6 m
roughness length	0.1h (h is the canopy height (21 m))
vegetation reflectivity	0.5 (visible), 0.29 (near-infrared)
winter albedo	0.5

* See measured snow parameters during the BOREAS winter field campaign in Chang et al. (1997)

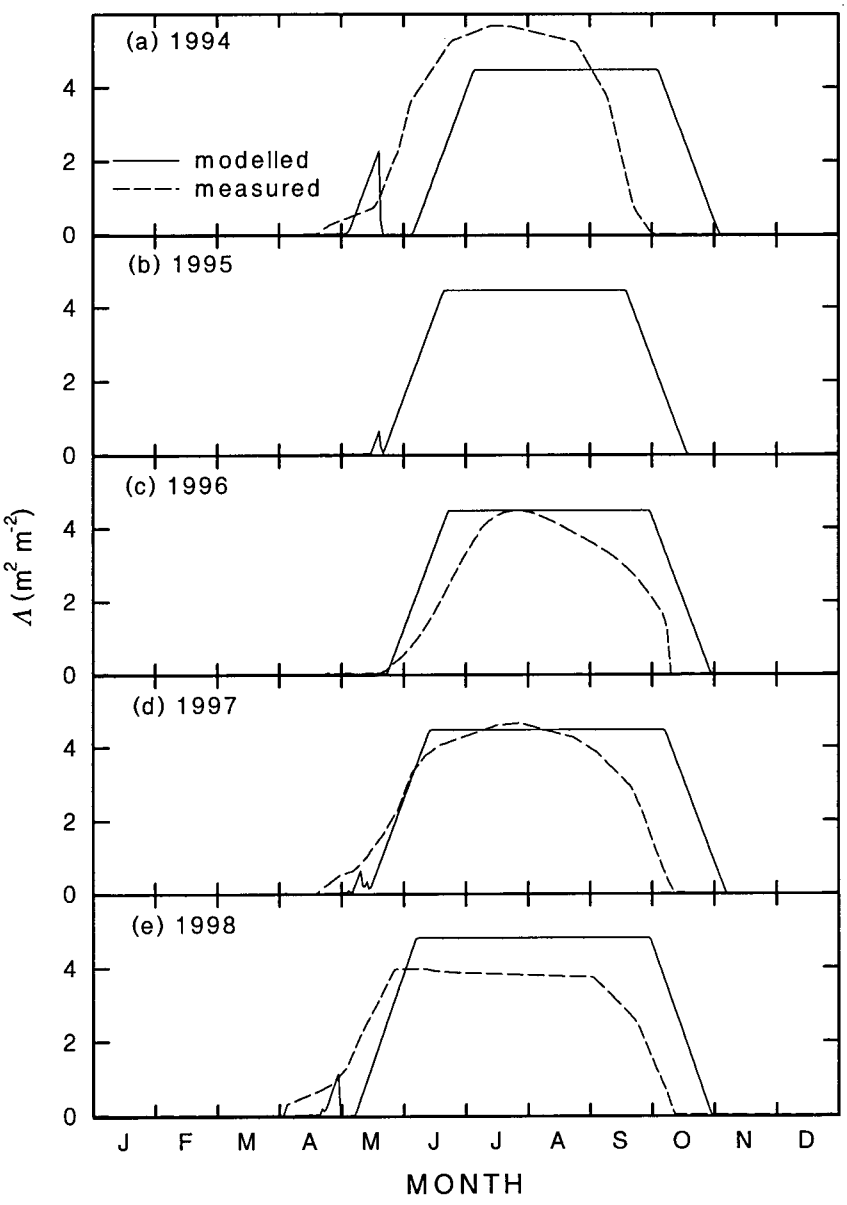

Fig. 4.2. Comparison between CLASS generated and measured Λ of the aspen forest from 1994 to 1998.

4.4. Validation results

4.4.1. Net radiation, albedo and snowmelt time

Fig. 4.3 compares the modelled daily average Q^* obtained from tests 2 and 3 with observations. Results obtained from other tests were not shown because the difference in Q^* between these tests was found to be mainly related to the change of the winter albedo. There was good agreement between the modelled and measured Q^* throughout each year except before the modelled snowmelt when modelled Q^* from test 2 was significantly underestimated, particularly in 1997 and 1998. Examination of the snowmelt time predicted by test 2 indicated it was about 25 days later than the observed snowmelt time (Table 4.3) (A. G. Barr, P. Pacholek and C. Hrynkiw 1998, personal communication). This was because the winter albedo of the forest used in test 2 was much higher than measured values (Fig. 4.4). There was only a small percentage of observed albedo higher than 0.3 during the winter. Other boreal forest types also have a considerably low winter albedo due to the efficient interception of shortwave radiation by the trees (Betts and Ball 1997). However, many land surface models still used a winter albedo of around 0.8 rather than a value of around 0.25 observed in the field (Sellers et al. 1997b). With the change of the winter albedo from 0.50 to 0.25 in test 3, the modelled Q^* before the leaf emergence was significantly increased (Fig. 4.3) and the modelled snowmelt time was closer to the actual values (Table 4.3). The decrease in the winter albedo also significantly reduced the overestimation of the surface runoff after snowmelt (this is likely because a decrease in the winter albedo causes a gradual rather than rapid snowmelt process) which led to much better agreement between modelled and measured θ (see Fig. 4.11 later).

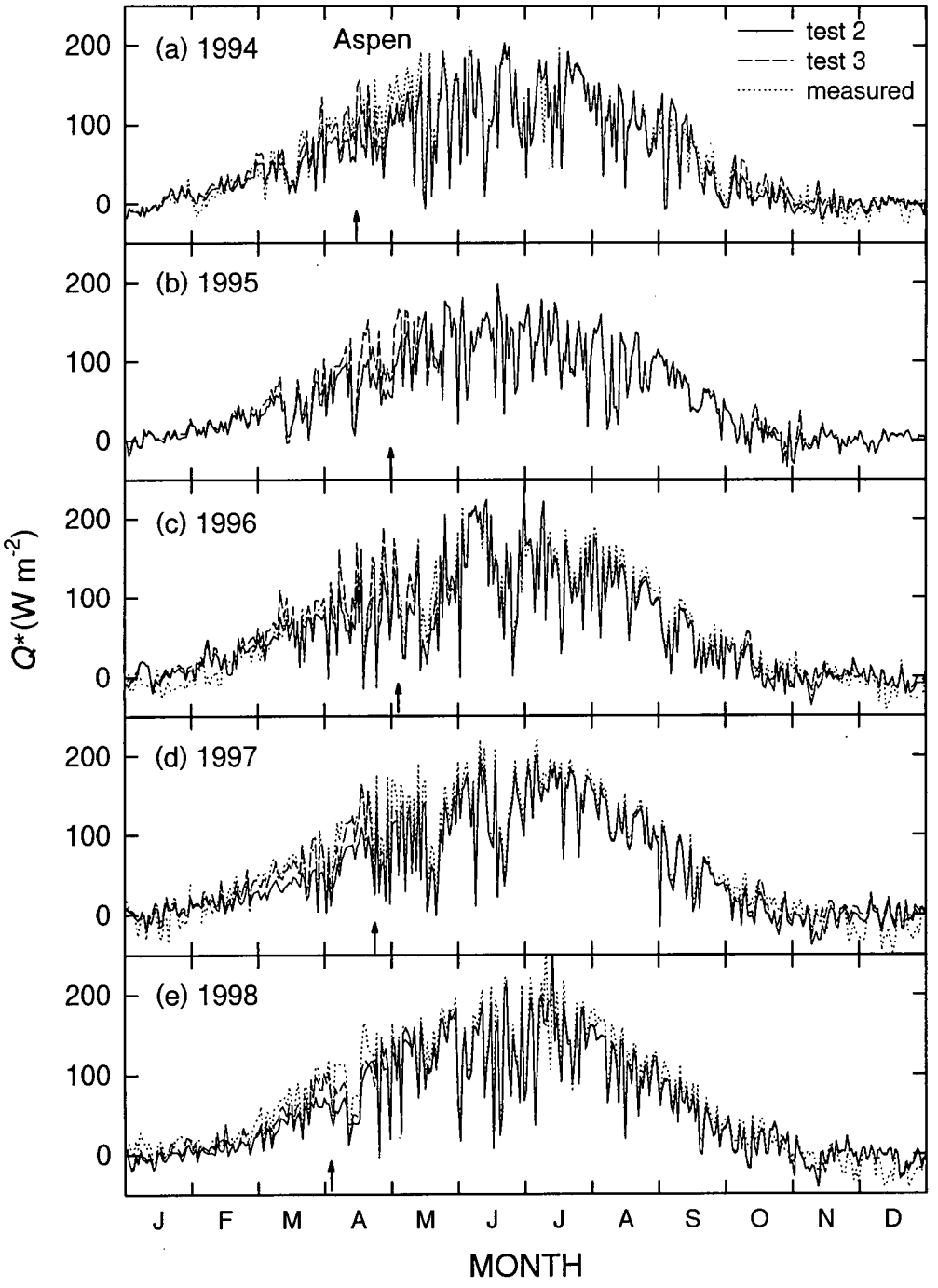

Fig. 4.3. Comparison between modelled and measured daily average Q^* from 1994 to 1998. The observed snowmelt time is also marked (arrow).

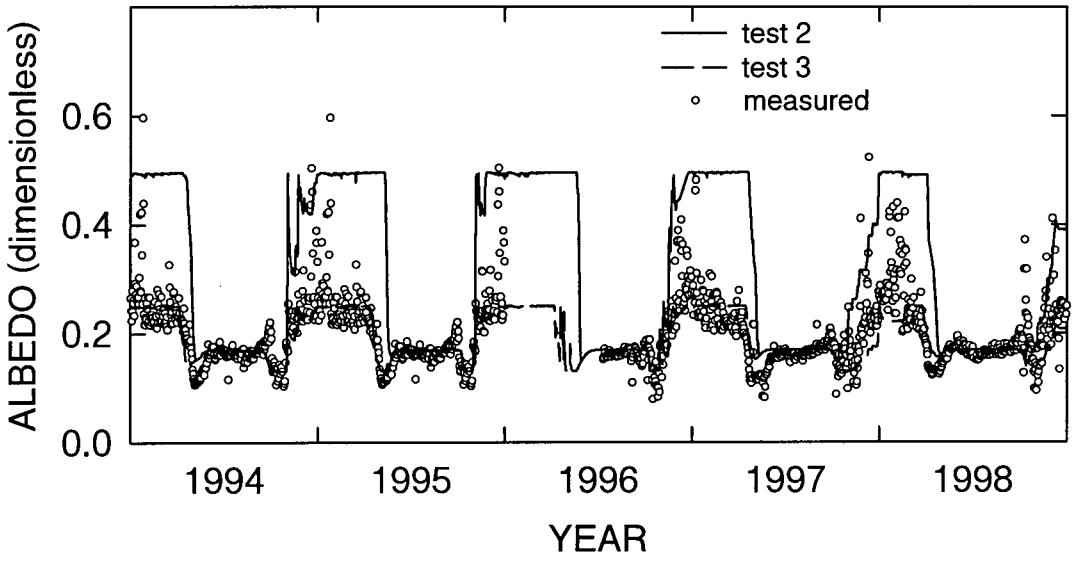

Fig. 4.4. Comparison of modelled and measured daily albedo.

Table 4.3. Comparison of modelled and measured snowmelt time. The time unit is the day of year (DOY)

Year	Test 2	Test 3	Measured
1994	130	120	105
1995	145	126	121
1996	150	132	125
1997	134	124	114
1998	120	114	94

4.4.2. Latent, sensible and soil surface heat fluxes

The comparison between modelled daily Q_E obtained from test 1 and measured values is shown in Fig. 4.5. The significant underestimation of Q_E late in the 1996 growing season, in the middle of the 1997 growing season and in the early part and middle of the 1998 growing season was because g_c was significantly underestimated. This was caused by low values of modelled θ (see Fig. 4.11 later). On the other hand, Q_E was overestimated during the leaf emergence and senescence periods because evaporation from the soil surface was overestimated.

The overestimation of Q_E during the leaf emergence and senescence periods was effectively corrected by using the β method, as shown in test 4 (Fig. 4.6). As the difference among tests 3 to 5 only depends on which parameterization of g_c is used in each test (Table 4.1), Fig. 4.6 only shows the comparison between tests 2 and 4 (the comparison of the different parameterizations of g_c will be made later in Fig. 4.8). It was evident that tests 2 and 4 performed much better than test 1 in the calculation of Q_E during the full-leaf period (middle of June to the end of August). Assuming that soil moisture did not limit the aspen g_c, a value of ψ = -5.0 m was used in tests 2 and 4 during the growing season (Table 4.1). This assumption appeared to work well for 1994, 1996 and in the late growing season in 1998. However, in the spring and early summer of 1998, a significant overestimation of Q_E occurred as a result of neglecting the effect of the soil moisture stress. Both rainfall and soil moisture during this period were the lowest for the corresponding period in the five years, while both air and soil temperatures were

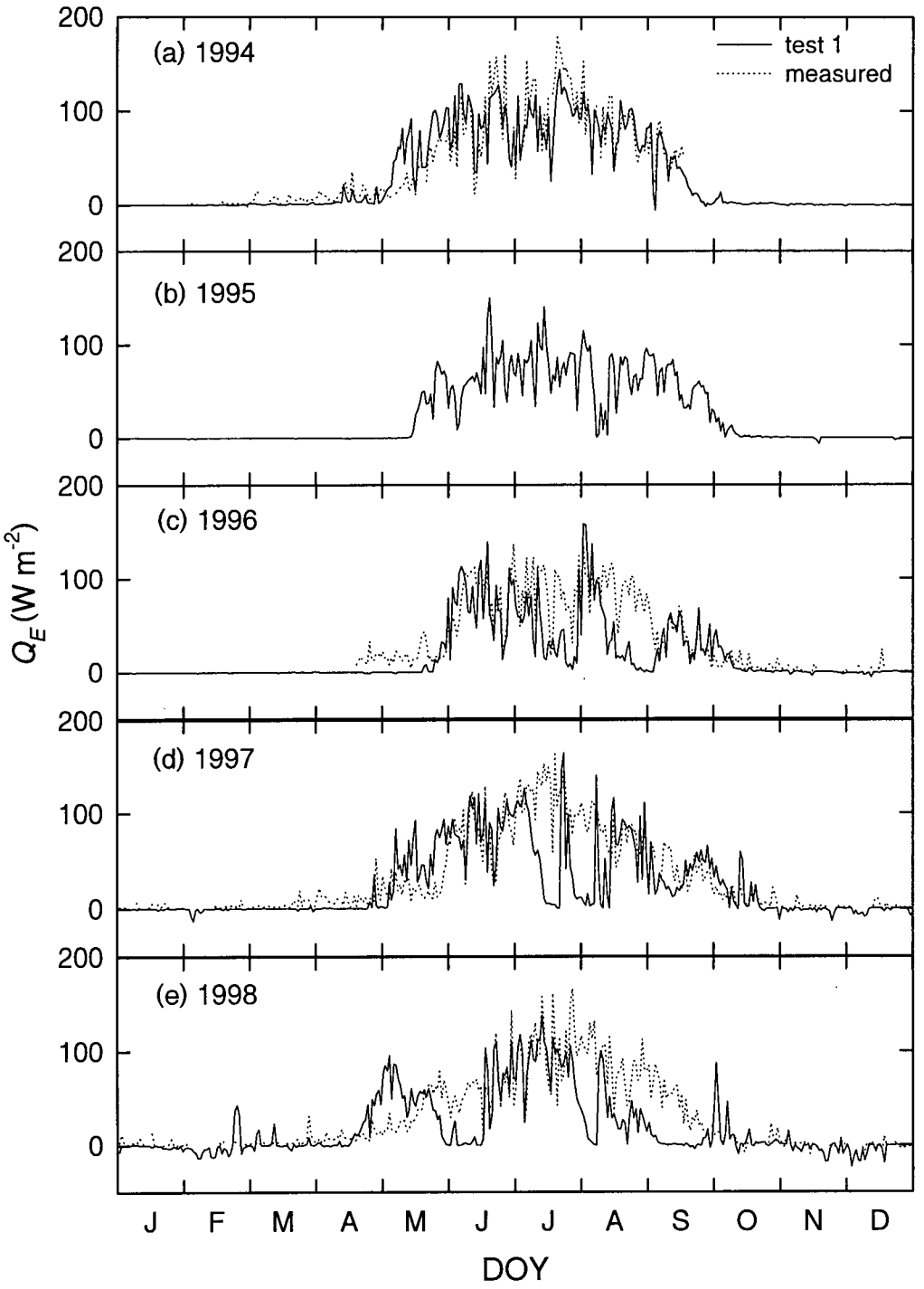

Fig. 4.5. Comparison of modelled daily average Q_E from test 1 with observations from 1994 to 1998.

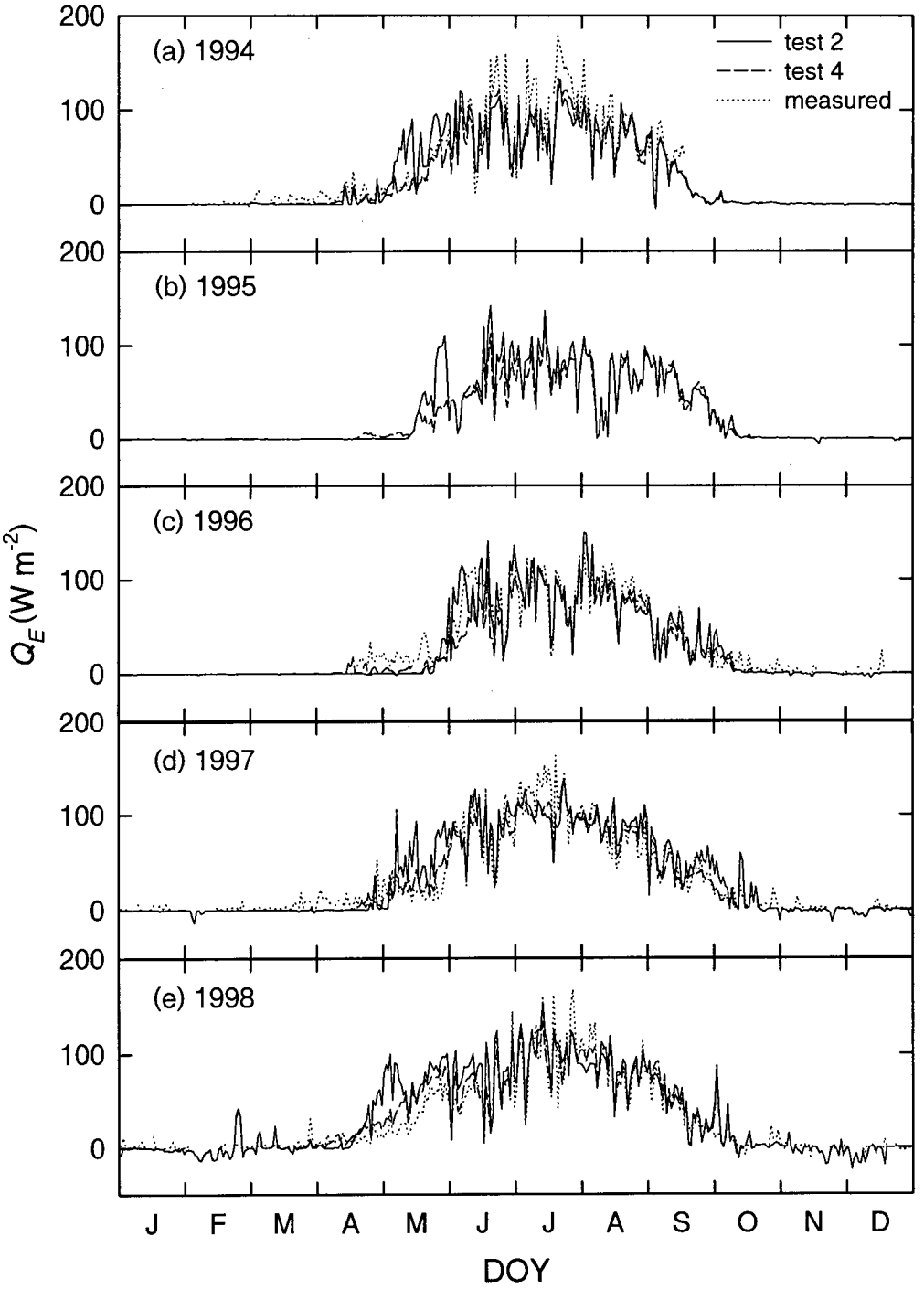

Fig. 4.6. Comparison of modelled daily average Q_E from tests 2 and 4 with observations from 1994 to 1998.

the highest. A simple treatment using $g_4(\theta)$ from Eq. (4.6) in test 4 gave reasonably good estimates of Q_E in 1998 (Fig. 4.6e). The reason that tests 2 and 4 could not generate high Q_E values during the full-leaf period of 1994 is not very clear. It was probably related to the calculation of evaporation from the intercepted precipitation by the canopy as rainfall was most frequent in this year. On the other hand, the ensemble averaging procedure used in the development of the modified JS parameterization probably averaged out some variation of g_c with Q_p or Δe (Chapter 3). Leaf age is also an important factor (Avissar and Pielke 1991) and its effect has not been included in the parameterization. The comparison between modelled and measured evapotranspiration totals are listed in Table 4.4.

Chapter 3 indicated that g_c calculated using the modified JS parameterization was higher than those from the CLASS JS parameterization under high solar radiation conditions. However, Fig. 4.6 shows that there was no significant difference between Q_E from tests 2 and 4 during the full-leaf period. Examination of the modelled evapotranspiration above the canopy and evaporation from the soil in 1994 indicated that this was mainly due to the difference in the calculation of evaporation from the soil surface (Fig. 4.7a). Although it was small in total, the evaporation from the soil during both the leaf-emergence and full-leaf periods was underestimated by the β method. It was likely because θ of the surface layer was underestimated due to the frequent rainfall and high porosity of the surface organic layer. The measured evaporation from the soil during the leaf-emergence period was based on measured net radiation at the forest floor (Chen et al. 1996). Results from a 15-day mid-summer lysimeter experiment indicated that soil

evaporation accounted for about 5% of forest evapotranspiration during the full-leaf period (Black et al. 1996).

Table 4.4. Comparison of modelled and measured evapotranspiration totals at the aspen site.

Year	Modelled evap. totals (mm)		Measured evap.	Precipitation
	test 2	test4	Totals (mm)	(mm)
1994	354	320	390	450
	(231)[1]	(234)	(283)	
1995	324	278	M	363
	(237)	(210)	M	
1996	323	272	330	385
	(245)	(226)	(246)	
1997	416	365	360	420
	(274)	(262)	(269)	
1998	426	382	350	440
	(271)	(261)	(266)	

[1] Evapotranspiration total during the full-leaf period (DOY 170 to 259). M denotes missing.

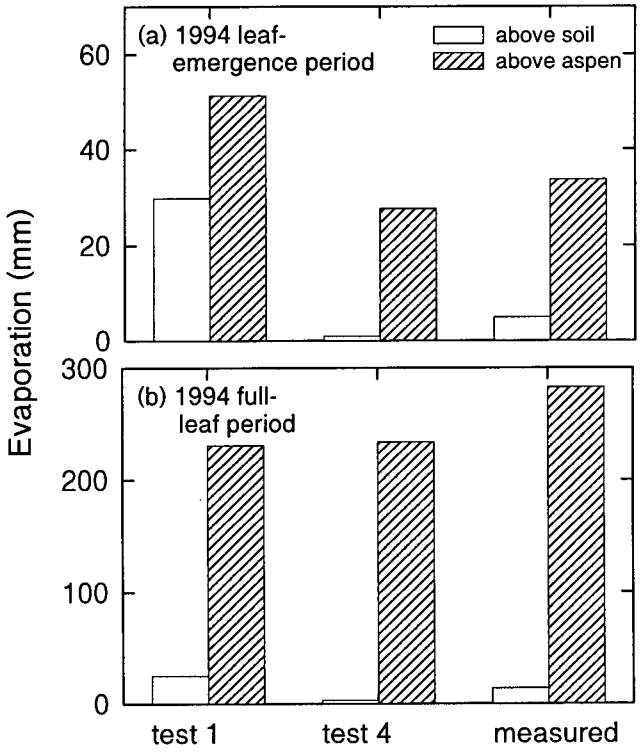

Fig. 4.7. Comparison of modelled evaporation totals from the soil and above the forest with observations in 1994. (a) leaf emergence period (DOY 121 to 150). (b) full-leaf period (DOY 170 to 259).

Fig. 4.8 compares the performance of the CLASS JS, modified JS and MBWB parameterizations (tests 3 to 5) in estimating daily average Q_E during the full-leaf period for years 1994 to 1998. No significant difference in the performance was found for each parameterization from year to year. As both the modified JS and MBWB parameterizations were derived using the 1994 data, they gave the highest r^2 in that year, compared to r^2 to the other years. Over the four years, the modified JS parameterization consistently performed better and gave higher g_c values than the MBWB and CLASS JS parameterizations. Both the root mean square error and the absolute value of the average deviation (d) error were the lowest for the modified JS parameterization. On average, the modified JS parameterization underestimated daily average Q_E by about 3%, compared to 10% and 16%, respectively, by the CLASS JS and MBWB parameterizations. It is unlikely that the reason that the MBWB parameterization did not give estimates of g_c as good as expected was due to errors in the calculation of the aspen canopy assimilation rate, since using the measured A_0 in the MBWB parameterization did not significantly improve the estimation of g_c. Comparison of measured g_c and values calculated using the MBWB and BWB parameterizations indicated that this was because the two parameterizations generated a depression in g_c during midday hours (Chapter 3). Although midday stomatal closure has been observed in some tree species (e.g. Tan and Black 1976, Blanken and Rouse 1996) and modelled by the BWB model (Collatz et al. 1991), it was not observed in 1994 (Blanken's, 1997, canopy conductance analysis) or in 1996 (the stomatal conductance measurements mentioned in Chapter 3). Blanken (1997) attributed the absence of midday stomatal closure to the lack of soil water stress and the high drought tolerance of aspen.

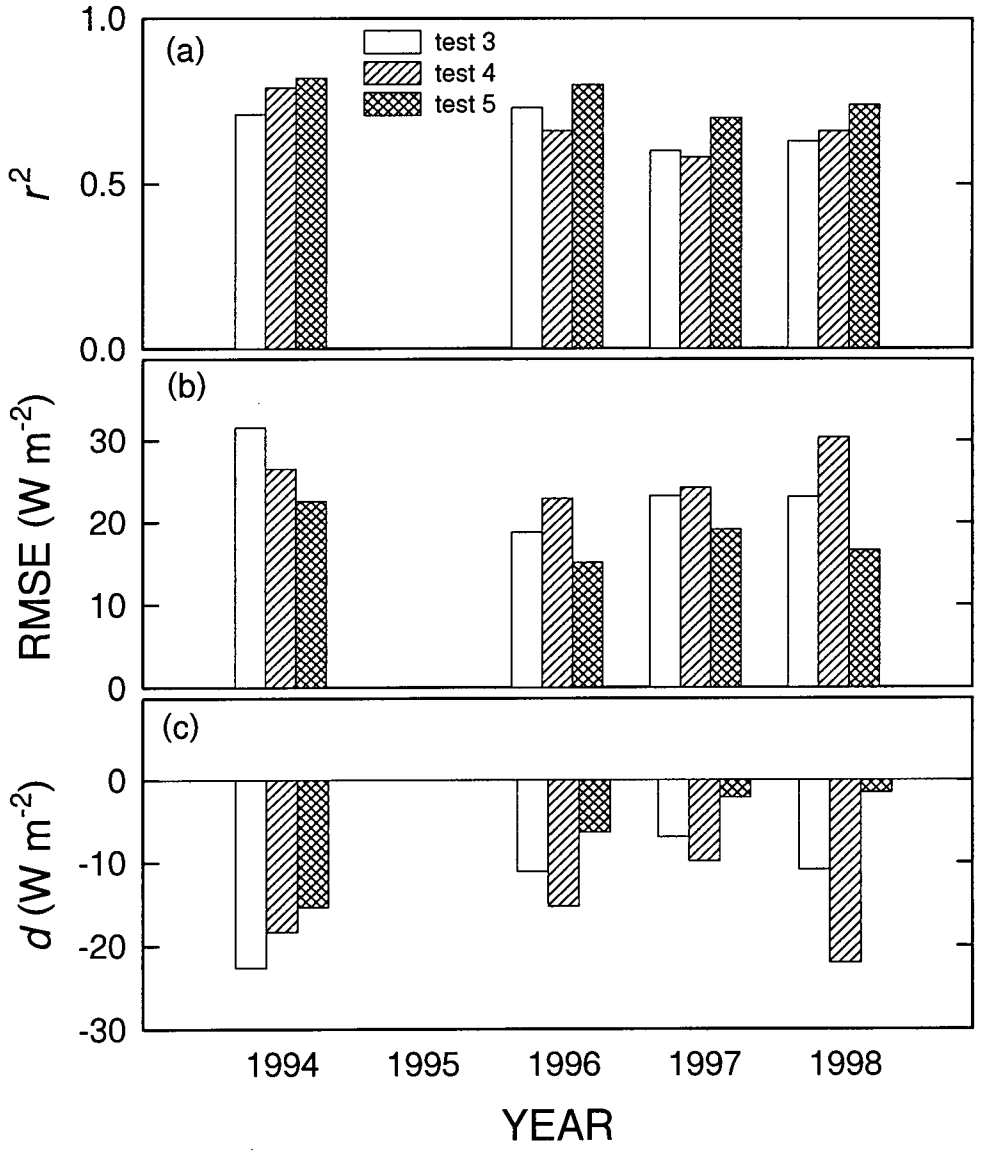

Fig. 4.8. The coefficient of determination (r^2), root mean square error (RMSE) and average deviation (d) in the comparison between measured and calculated daily average Q_E obtained from tests 3 to 5 during the full-leaf periods of 1994 and 1996 to 1998.

As Q_E was modelled reasonably well by the three parameterizations during the full-leaf period, no significant difference between Q_H calculated using the three parameterization was found because the available energy is mainly partitioned between Q_E and Q_H. Comparison between tests 2 and 4 also shows that using the β method does not contribute much to the improvement of Q_H before leaf emergence or after leaf senescence (Fig. 4.9). The significant overestimation of Q_H after snowmelt to the end of leaf emergence in 1994, 1997 and 1998 and during the senescence in 1997 was likely due to the presence of the high-porosity litter layer (comprised of undecomposed leaves and twigs) on the forest floor which acts as an effective mulch in sharply reducing evaporation from the forest floor. Fig. 4.10, as an example, shows that the day-to-day variability in the modelled daily G_0 is much larger than measured values in 1996 especially before leaf emergence. The lack of a surface organic layer in CLASS is believed to be the main reason that caused Q_H to be underestimated and G_0 overestimated.

4.4.3. Soil water content

The modelled course of θ for each soil layer obtained from tests 1, 2 and 4 is shown in Fig. 4.11. The results from tests 3 and 5 are not shown because they were quite similar to those from test 4. The very different treatment of the response of g_c to ψ in tests 1 and 2 only causes a slight change in θ for layer 3, indicating that the effect of the modelled ψ on g_c was small during most of the growing season in test 1. As the β method prevents excessive evaporation from the soil surface when the soil is dry, θ of layer 1 obtained from test 4 dropped more slowly than those from test 1. Examination of the

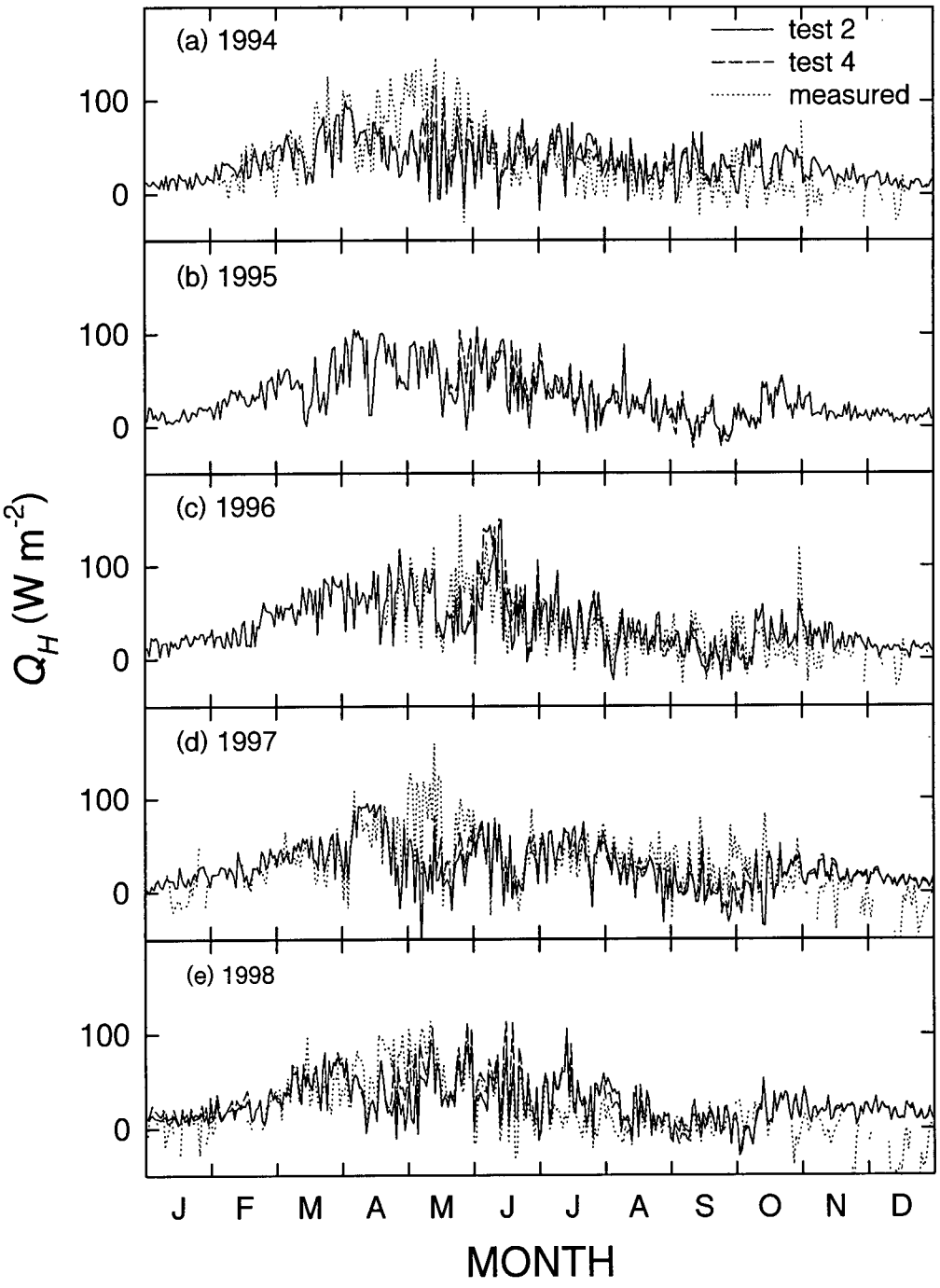

Fig. 4.9. Comparison of modelled daily average Q_H from tests 2 and 4 with observations from 1994 to 1998.

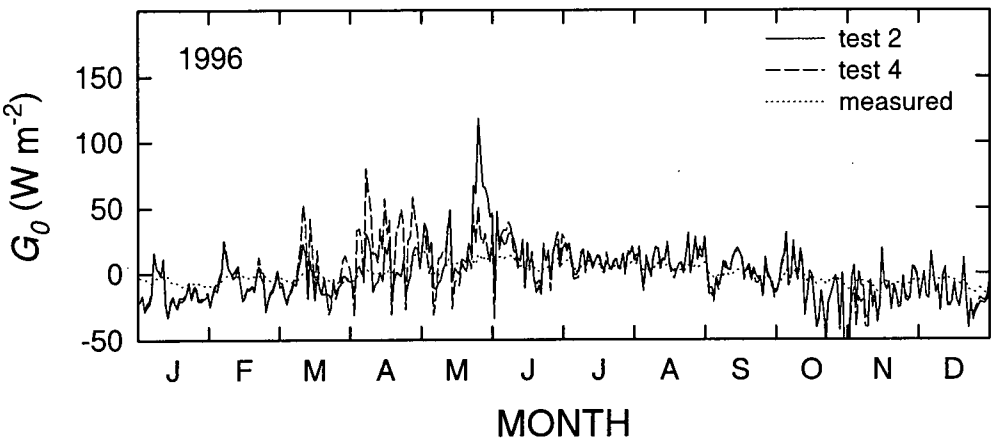

Fig. 4.10. Comparison of modelled daily average G_0 from tests 2 and 4 with observations in 1996.

simulation of the surface runoff after snowmelt showed that test 4 (with low winter albedo) generated much less surface runoff than test 1 (with high winter albedo). Consequently, θ of both layers 1 to 3 obtained from test 4 is significantly higher than those from test 1 as a result of a cumulative effect of using the β method and low winter albedo throughout all the years, especially for θ of layer 3. The earlier snowmelt in response to the lower winter albedo in test 4 caused θ of layers 1 to 3 to rise earlier than in test 1. Low modelled values of θ during the winter is due to the freezing of the soil water in layers 1 and 2 and partial freezing in layer 3 and the values shown here are for the liquid soil water content (Verseghy 1991). Although direct comparison between the modelled and measured θ was difficult because of the spatial variability of soil properties, a better correspondence was obtained from test 4 than those from test 1 (Fig. 4.11). There

was still a slight declining trend for θ of layer 3 from year to year in test 4, although observations showed no gradual depletion of soil water in the deep mineral soil. This was because the surface runoff after snowmelt was still overestimated (surface runoff was about 130 and 80 mm in tests 2 and 4, respectively, compared to a measured value of about 30 mm indicated by Blanken's water balance analysis), since the modelled drainage was found to be very small. Bonan (1994) and Pitman (1993) and some others have confirmed that the parameterization of the infiltration capacity greatly affects the calculation of Q_E and Q_H because it controls the supply of surface melt or ponded water on the soil surface. This parameterization is important because the surface organic layer at the aspen site has a high infiltration capacity. The effect of the calculation of infiltration on simulations will not be discussed in detail here. Since modelled ψ or θ did not affect the calculation of g_c in tests 2 to 5, the overestimation of the surface runoff did not have much effect on the calculation of Q_E and Q_H from the canopy. Its impact on the calculation of the evaporation from the soil surface during the spring months was small because the soil generally maintained a relatively high θ for layers 1 and 2 due to the frequent precipitation. These results emphasize the need for further improvement in dealing with soil water movement in CLASS for the aspen site.

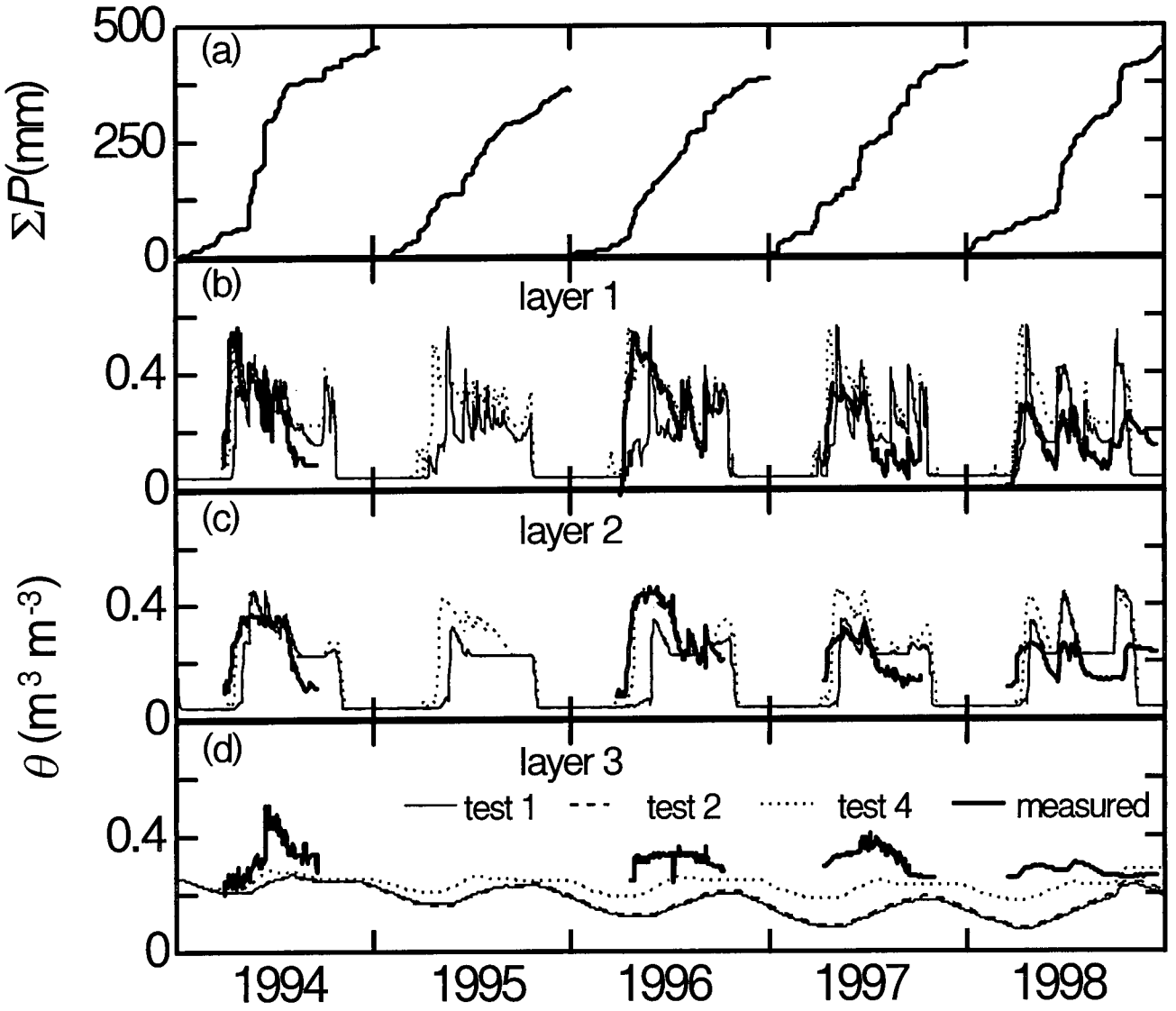

Fig. 4.11 Comparison of modelled (tests 1, 2 and 4) and measured volumetric water content, θ, over the five years. The three modelled soil layers are 0 - 10 cm, 10 - 35 cm, and 35 - 410 cm, respectively. The three measured soil layers are 0 - 10 cm, 10 - 35 cm, and 91 - 123 cm, respectively (see also Fig. 4.1). Also shown is the cumulative precipitation (ΣP).

4.5. Conclusions

The following conclusions can be drawn using the long-term (1994 to 1998) dataset: (1) the β method was effective in significantly improving the calculation of the latent heat fluxes during the leaf emergence and senescence periods, (2) reducing the winter albedo from 0.50 to the more realistic value of 0.25 significantly improved the calculation of winter net radiation, generated snowmelt times only 5-10 days later than observations and significantly reduced the overestimation of the surface runoff after snowmelt, (3) the combination of the β method and the change in the winter albedo resulted in much better agreement between modelled and measured soil water content, (4) generally no significant difference in the performance of the CLASS JS, modified JS and MBWB parameterizations was found from year to year, confirming the temporal transferability of the parameterization of canopy conductance, (5) further improvements to the canopy conductance characteristics will require a growing season with a shortage of precipitation from late June to early August to better account for the effect of the soil moisture stress and (6) the future development of land surface process models requires to pay a more attention to the parameterization of soil and snow hydrologic processes.

4.6. References

Avissar, R. and R. A. Pielke. 1991. The impact of plant stomatal control on mesoscale atmospheric circulations. *Agric. For. Meteorol.*, 54: 353-372.

Betts, A. K. and J. H. Ball. 1997. Albedo over the boreal forest. *J. Geophys. Res.*, 102 D24, 28901-28909.

Ball, J. T., I. E. Woodrow and J. A. Berry. 1987. A model predicting stomatal conductance and its contribution to the control of photosynthesis under different environmental conditions. In: Progress in Photosynthesis Research (Ed. J. Biggens). Vol IV, Marlinus Nijhoff Publishers, Dordrecht, The Netherlands, pp. 221-224.

Black, T. A., G. den Hartog, H. H. Neumann, P. D. Blanken, P. C. Yang, C. Russell, Z. Nesic, X. Lee, S. C. Chen, R. Staebler and M. D. Novak. 1996. Annual cycles of water vapour and carbon dioxide fluxes in and above a boreal aspen forest. *Global Change Biology*, 2: 219-229.

Blanken, P. D. 1997. Evaporation within and above a boreal aspen forest. Ph.D. Thesis, University of British Columbia, Vancouver, BC, Canada, 185 pp.

Blanken, P. D. and W. R. Rouse. 1996. Evidence of water conservation mechanisms in several subarctic wetland species. *Journal of Applied Ecology*, 33: 842-850.

Blanken, P. D., T. A. Black, P.C. Yang, H. H. Neumann, Z. Nesic, R. Staebler, G. den Hartog, M. D. Novak and X. Lee. 1997. Energy balance and canopy conductance of a boreal aspen forest: partitioning overstory and understory components. *J. Geophys. Res.*, 102 D24, 28915-28927.

Bonan, G. B. 1994. Comparison of two land surface process models using prescribed forcings. *J. Geophys. Res.*, 99 D12, 25803-25818.

Chang, A. T. C., J. L. Foster and D. K. Hall. 1997. Snow parameters derived from microwave measurements during the BOREAS winter field campaign. *J. Geophys. Res.*, 102 D24, 29663-29671.

Chen, W. J., T. A. Black, P. C. Yang, A. G. Barr, H. H. Neumann, Z. Nesic, M. D. Novak, J. Eley, R. J. Ketler and R. Cuenca. 1998. Effects of climatic variability on the annual carbon sequestration by a boreal aspen forest. *Global Change Biology* (in press).

Chen, J. M., P. D. Blanken, T. A. Black, M. Guilbeault and S. Chen. 1997. Radiation

regime and canopy architecture in a boreal aspen forest. *Agric. For. Meteorol.*, 86: 107-125.

Collatz, G. J., J. T. Ball, C. Grivet and J. A Berry. 1991. Physiological and environmental regulation of stomatal conductance, photosynthesis and transpiration: a model that includes a laminar boundary layer. *Agric. For. Meteorol.*, 54: 107-136.

Cuenca, R. H., D. E. Stangel and S. F. Kelly. 1997. Soil water balance in a boreal forest. *J. Geophys. Res.*, 102 D24, 29355-29365.

Desborough, C. E., A. J. Pitman and P. Irannejad. 1996. Analysis of the relationship between bare soil evaporation and soil moisture simulated by 13 land surface schemes for a simple non-vegetated site. *Global and Planetary Change*, 13: 47-56.

Henderson-Sellers, A., Z.-L. Yiang and R. E. Dickinson. 1993. The project for intercomparison of land-surface parameterization schemes. *Bull. Amer. Meteor. Soc.*, 74, 1335-1349.

Jarvis, P. G. 1976. The interpretation of the variation in leaf water potential and stomatal conductance found in canopies in the field. *Phil. Trans. R. Soc.*, Lond. B. 273: 593-610.

Liang, X. and co-authors. The Project for Intercomparison of Land-Surface Parameterization Schemes (PILPS) Phase 2c: Red-Arkansas river basin experiment. 2. Spatial and temporal analysis of energy fluxes. *Global and Planetary Change* (in press).

Mahfouf, J.-F., C. Ciret, A. Ducharne, P. Irranejad, J. Noilhan, Y. Shao, P. Thornton, Y. Xue and Z.-L. Yang. 1996. Analysis of transpiration results from RICE and PILPS workshop. *Global and Planetary Change*, 13: 73-88.

Philip, J. R. 1957. Evaporation and moisture and heat fields in the soil. *J. Meteorol.*, 14: 354-366.

Pitman, A. J., A. Henderson-Sellers, F. Abramopoulos, R. Avissar, G. Bonan, A. Boone, J. G. Cogley, R. E. Dickinson, M. Ek, D. Entekhabi, J. Famiglietti, J. R. Garratt, M. Frech, A. Hahmann, R. Koster, E. Kowalczyk, K. Laval, J. Lean, T. J. Lee, D. Letternmaier, X. Liang, J. -F. Mahfouf, L. Mahrt, C. Milly, K. Mitchell, N. de Noblet, J. Noilhan, H. Pan, R. Pielke, A. Robock, C. Rosenzweig, S. W. Running, A. Schlosser, R. Scott, M. Suarez, S. Thompson, D. L. Verseghy, P. Wetzel, E. Wood, Y. Xue, Z. -L. Yang and L. Zhang. 1993. Results from off-line Control Simulation Phase of Project for intercomparison of land-surface parameterization schemes (PILPS): GEWEX Tech. Note, *IGPO Publ.* Series 7, 47 pp.

Sellers, P., F. Hall, H. Margolis, R. Kelly, D. D. Baldocchi, G. den Hartog, J. Cihlar, M.

G. Ryan, B. Goodison, P. Crill, K. J. Ranson, D. Lettermaier and E. Wickland. 1995. The boreal ecosystem-atmosphere study (BOREAS): An overview and early results from 1994 field year. *Bull. of the Amer. Meteorol. Soc.*, 76: 1549-1577.

Sellers, P. J., R. E. Dickinson, D. A. Randall, A. K. Betts, F. G. Hall, J. A. Berry, G. J. Collatz, A. S. Denning, H. A. Mooney, C. A. Nobre, N. Sato, C. B. Field, A. Henderson-Sellers. 1997a. Modelling the exchanges of energy, water, and carbon between continents and atmosphere. *Science*, 275: 502-509.

Sellers, P. J., F. G. Hall, R. D. Kelly, A. T. Black, D. D. Baldocchi, J. Berry, M. G. Ryan, K. J. Ranson, P. M. Crill, D. P. Lettenmaier, H. Margolis, J. Cihlar, J. A. Newcomer, D. Fitzgerald, P. G. Jarvis, S. T. Gower, D. Halliwell, D. Williams, B. Goodison, D. E. Wickland and F. E. Guertin. 1997b. BOREAS in 1997: Experiment overview, scientific results, and future directions. *J. Geophys. Res.*, 102 D24, 28731-28769.

Stewart, J. B. 1988. Modelling surface conductance of pine forest. *Agric For. Meteorol.*, 43: 19-35.

Tan, C. S. and T. A. Black. 1976. Factors affecting the canopy resistance of a Douglas-fir forest. *Boundary-Layer Meteorol.*, 10: 475-488.

Verseghy, D. L. 1991. CLASS - A Canadian land surface scheme for GCMs, I. Soil model. *Int. J. Climatol.*, 11: 111-133.

Verseghy, D. L., N. A. McFarlane and M. Lazare. 1993. CLASS - a Canadian land surface scheme for GCMs, II. Vegetation model and coupled runs. *Int. J. Climatol.*, 13: 347-370.

CHAPTER 5

THE IMPORTANCE OF THE 'NEAR-FIELD' RESISTANCE IN THE CALCULATION OF SENSIBLE AND LATENT HEAT FLUXES ABOVE PLANT CANOPIES

5.1. Introduction

Most land surface schemes used in atmospheric general circulation models (GCMs) treat both the canopy and soil as a separated two-layer system (e.g. Biosphere-Atmospheric Transfer Scheme (BATS) (Dickinson et al. 1986), revised Simple Biosphere model (SiB2) (Sellers et al. 1996), Bare Essentials of Surface Transfer (BEST) (Pitman et al. 1991), Canadian Land Surface Scheme (CLASS) (Verseghy 1991, Verseghy et al. 1993), and the European Centre for Medium-Range Weather Forecasts (ECMWF) land surface scheme (Viterbo and Beljaars 1995). Foliage temperature and surface soil temperatures are calculated, based on the surface energy balance equation applied to the canopy layer and to the upper thin soil surface layer. Sensible and latent heat fluxes from the ground and canopy combine in the canopy air space to give the total fluxes passed to the atmosphere.

These fluxes are usually calculated using the gradient-diffusion relationship, i.e. K-theory (e.g. Waggoner and Reifsnyder 1968). In recent years, the applicability of K-theory within and just above plant canopies has been challenged by observations of countergradient flux (e.g. Denmead and Bradley 1985, Thurtell 1989). As eddy sizes within most plant canopies are of the same order as the canopy height, the validity of K-theory is questionable for the calculation of scalar exchange within canopies. Multi-layer vegetation models that use higher-order-closure approaches (e.g. Wilson 1989, Meyers

and Baldocchi 1988) or Lagrangian principles (e.g. Dolman and Wallace 1991, Katul et al. 1997) can simulate some of the features of turbulent transfer processes within canopies more accurately than *K*-theory. However, these models require detailed information on canopy structure and consume considerable amounts of computer time, making them unsuitable for GCMs.

A recent study by McNaughton and Van den Hurk (1995) showed that Raupach's (1989a, b) Lagrangian-based 'localized near-field' (LNF) theory can be used to construct a two-layer surface model consisting of a single canopy layer and a ground layer. By adding a 'lateral' resistance ('near-field' resistance) in the two-layer resistance network, the canopy is isolated from the vertical diffusion components. This allows the flux to be directed upwards even when the scalar concentration in the canopy is higher than that below the canopy. Sensitivity studies have shown that the near-field effect on the energy balance of crops is small (Van den Hurk and McNaughton 1995, Dolman and Wallace 1991). In contrast, by solving the "inverse problem" (Raupach 1989a), Katul et al. (1997) showed that the LNF theory gave better estimates of the CO_2 flux at the 9-m height in a 13-m tall loblolly pine forest than *K*-theory. Lee and Black (1994) found that this approach worked satisfactorily in calculating the total sensible heat flux from a Douglas-fir forest but emphasized the importance of better modelling of the heat exchange at the soil surface. Few studies, however, have evaluated the importance of accounting for the near-field effect in the calculation of scalar fluxes above forests using direct flux measurements. This study addresses this issue. Two forests with distinctly different canopy structure (i.e. different vertical distributions of scalar sources) were selected: the first was a Douglas-fir forest with virtually no understory (the same forest which was

used in Lee and Black's, 1994, study), while the second was a boreal aspen forest with a thick understory. Simulations were conducted in two different modes: (1) sensible heat fluxes above the two forests are calculated from measured air temperature profiles using the flux-gradient relationship to evaluate the effect of the inclusion of the near-field resistance on sensible heat flux calculations, and (2) energy balance components above the canopy and soil surface were calculated using CLASS to investigate the impact of the inclusion of the near-field resistance on these components. In the latter mode, the comparison was extended to a soybean crop.

5.2. Sites and measurements

The Douglas-fir site was briefly described in Chapter 3. The following is a detailed description of the site. The Douglas-fir (*Pseudotsuga menziesii* (Mirb.) Franco) site was located near Browns River about 10 km west of Courtenay on Vancouver Island (125°10' W, 49°42' N) at an elevation of 450 m (Lee 1992, Lee and Black 1993a, b). The stand, which was planted in 1962, and thinned and pruned below the 6-m height in 1988, was 16.7 m tall in 1990 and had a leaf area index (Λ) of 5.4. The forest floor was littered with dead branches and tree trunks, with very little understory vegetation (e.g. salal (*Gaultheria shallon* Pursh)). Measurements were conducted during a two-week rainless period in July and August 1990. The turbulent fluxes were measured with two eddy-covariance technique systems, with one mounted permanently at a height of 23.0 m and the other at various heights (2.0, 7.0, 10.0 and 16.7 m) in the stand. Air temperature and wind speed were measured continuously with 25 μm unshielded chromel-constantan thermocouples and sensitive cup anemometers, respectively, at heights of 0.9, 2.0, 4.6,

7.0, 10.0, 12.7, 16.7 and 23.0 m. Soil heat flux was measured with two pairs of soil heat flux plates placed at a depth of 3 cm and two nickel wire integrating thermometers to correct for the change in heat storage in the surface soil layer above the plates. Supporting measurements included soil water content, humidity, wind direction, and radiation above the stand and near the forest floor. The profile of the leaf area density of the stand was obtained from intensive destructive sampling on several trees of selected sizes.

The boreal aspen site has been described in Chapters 2 to 4. The following is a brief description relevant to this chapter. The site was in a 70-year-old (in 1994) extensive boreal aspen forest (*Populus tremuloides* Michx.) in the southern part of Prince Albert National Park about 50 km northwest of Prince Albert, Saskatchewan (Black et al. 1996, Blanken et al. 1997). The trees were 21 m tall and the understory was dominated by a uniform cover of hazelnut (*Corylus cornuta* Marsh) with a mean height of 2 m. Maximum leaf area indices were 2.3 and 3.3 for the aspen and hazelnut in 1994, respectively. Canopy closure was around 90% (Sellers et al. 1994). Crown space was limited to the upper 5-6 m beneath which was a branchless trunk space. Measurements were conducted from the winter of 1993 to end of the growing season of 1994, and from 1996 to present, as part of the Boreal Ecosystem-Atmosphere Study (BOREAS), a large-scale short-term investigation of carbon, water and energy exchange between the atmosphere and the boreal forest (Sellers et al. 1995). Since 1997, the site has been one of the Canadian Boreal Ecosystem Research and Monitoring Sites (BERMS) and part of the Ameriflux Network. The fluxes of latent and sensible heat from the forest were measured at the 39-m height above the ground using the eddy-covariance technique (Black et al. 1996, Blanken et al. 1997, 1998, Chen et al. 1998). The air temperature profile was

obtained from 25 μm unshielded chromel-constantan thermocouple measurements at the following heights: 0.1, 0.98, 2.2, 4.1, 6.4, 9.5, 12.6, 15.7, 18.8, 21.9, 25.0, 27.7, 31.4 and 39.2 m. The vapour pressure profile was obtained from measurements made using an infrared gas analyzer (model 6262, LI-COR Inc. Lincoln, NE) and stenoid-valve system, located in a hut at the base of the flux tower, which measured water vapour and CO_2 concentration of air drawn (25 L min^{-1} per level) down Dekoron tubing from the following heights: 0.8, 2.3, 9.9, 16.1, 19.2, 22.3, 25.4 and 34.6 m. Aspen and hazelnut leaf temperatures were measured in 1994 using infrared thermometers enclosed in a constant temperature container mounted at the 30-m (aspen) and 4-m heights (hazelnut) oriented downward at 45° to the normal. Additional measurements included net, solar and photosynthetic active radiation at 33 m above the ground. Soil heat flux was measured at a depth of 3 cm with heat flux plates. The 0 - 3 cm rate of heat storage was measured using two integrating thermometers. Supporting measurements included precipitation, soil water content and soil evaporation.

Soybean (*Glycine max* (L.) Harosoy 63) crop data were collected from a level, 2.6 hectare rectangular field over the growing season in 1974 at the Ontario Ministry of Agriculture and Food Horticultural Experiment Station located near Simcoe, Ontario (the same dataset as used in Chapter 2). The crop was planted on June 6 (DOY 157) and Λ reached unity on July 13 (DOY 194). Maximum Λ (2.93) was reached on August 20 (DOY 232), after which it decreased. The sensible and latent heat fluxes were measured using the Bowen ratio method during the daytime. Details of the instrumentation and measurement program have been described elsewhere (Bailey and Davies 1981a, b).

5.3. Theory

5.3.1. Outline of the localized near-field theory

In Lagrangian models, scalar movement depends solely on the statistics of the turbulence and not on diffusion over the local concentration gradient. The scalar concentration at a particular canopy level is determined by tracking an ensemble of 'marked fluid particles' carrying the scalar released from a given source density, which allows the effect of fluid particle history to be taken into account. With Raupach's (1989a, b) LNF theory, turbulence dispersion is decomposed into two different processes in the time limits when $t \geq T_L$ (far-field) and $t \leq T_L$ (near-field), where T_L is the Lagrangian integral time scale (s). The far-field component is described by pure diffusion, while the near-field component is a correction term because real scalar particles do not behave according to diffusion theory shortly after release (Taylor 1921). The mean concentration $C(z)$ can also be decomposed into far-field $C_f(z)$ and near-field $C_n(z)$ components, so that

$$C(z) = C_f(z) + C_n(z) \tag{5.1}$$

The far-field concentration $C_f(z)$ is the solution to the diffusion equation

$$\frac{\partial}{\partial z}\left(K(z)\frac{\partial C_f(z)}{\partial z}\right) = -S_c(z) \tag{5.2}$$

where $S_c(z)$ is the profile of a scalar source density (e.g. J m^{-3} s^{-1} for heat), and $K(z)$ is the eddy diffusivity (m^2 s^{-1}) profile given by

$$K(z) = \sigma_w^2(z) T_L(z) \tag{5.3}$$

where $\sigma_w(z)$ is the standard deviation of vertical velocity (m s^{-1}) at the height z (m) above

ground. Raupach (1988) suggested that σ_w (z) and T_L (z) can be approximated by the following linear profiles based on existing data

$$\frac{\sigma_w}{u_*} = \begin{cases} a_1 & z > h \\ a_0 + (a_1 - a_0)\dfrac{z}{h} & z \le h \end{cases} \tag{5.4}$$

$$\frac{T_L(z)u_*}{h} = \max\left\{c_0, \frac{k(z-d)}{a_1 h}\right\} \tag{5.5}$$

where h is the tree height (m), d is the zero plane displacement height (m), k is the von Karman constant, u_* is the friction velocity (m s^{-1}) and the constants are a_1 = 1.25, a_0 = 0.25 and c_0 = 0.3. Raupach (1988) showed that $K(z)$ obtained from Eqs (5.3) to (5.5) approaches the limit ku_* (z - d) predicted by Monin-Obukhov similarity theory well above the canopy. A value of $d = 0.7h$ was used for the Douglas-fir (Lee and Black 1993a) and a value of d = 13.2 m was determined for the aspen forest (Simpson et al. 1997). The profile of σ_w (z) recommended by Raupach (1988) is similar to the measured mean σ_w (z) profiles for both the Douglas-fir and aspen forests (Fig. 5.1). However, σ_w (z) measured at each height has a high standard deviation (shown in Fig. 5.1 for the aspen forest). Eq. (5.5) assumes that T_L is constant within the canopy. Experimental evidence appears to support the use of constant T_L in the canopy (Legg et al. 1986, Leclerc et al. 1988).

Raupach's (1989a, b) expression for the near-field concentration $C_n(z)$ is

$$C_n(z) = \int_0^h \frac{S_c(z')}{\sigma_w(z')}\left\{k_n\left[\frac{z-z'}{\sigma_w(z')T_L(z')}\right] + k_n\left[\frac{z+z'}{\sigma_w(z')T_L(z')}\right]\right\}dz' \tag{5.6}$$

where the function k_n (x) in Eq. (5.6) is a near-field kernel function given by

$$k_n \approx -0.3984\ln(1-e^{-x}) - 0.1562e^{-x} \tag{5.7}$$

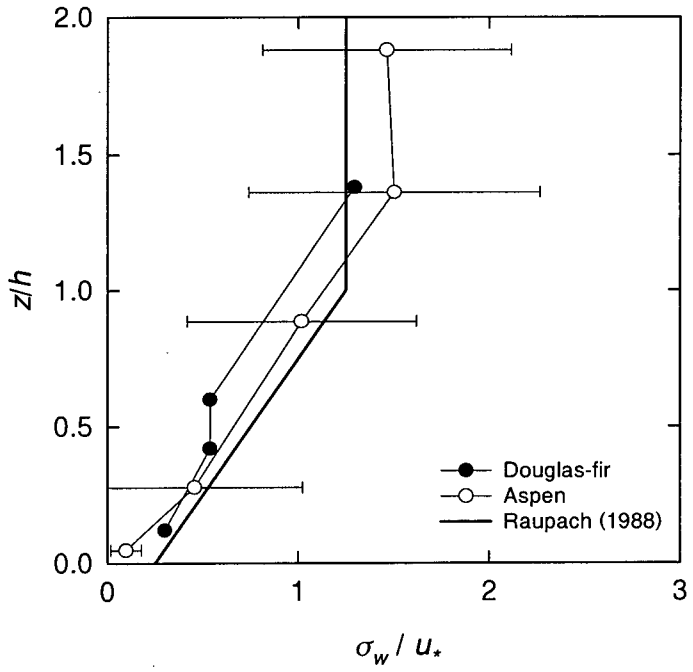

Fig. 5.1. Vertical profiles of σ_w / u_* measured in the Douglas-fir and aspen forests and recommended by Raupach (1988). Also shown is the standard deviation of σ_w / u_* for the aspen forest. u_* was measured at the 23-m and 39.5-m heights for the Douglas-fir and aspen forests, respectively. Data were collected during periods of July 19 to August 1, 1990 for the Douglas-fir forest and August 10 to September 19, 1994 for the aspen forest.

5.3.2. Parameterization of the near-field resistance r_n

The near-field effect can not be represented in terms of a resistance model due to its non-local origin. However, in a larger-scale application, it will be sufficient to use an average value of the near-field concentration $\overline{C}_n$ (Van den Hurk and McNaughton 1995). The inclusion of $\overline{C}_n$ in a two-layer resistance model would have the same effect on the total scalar flux as the inclusion of the true profile $C_n(z)$ has in a full multi-layer vegetation model. $\overline{C}_n$ is defined by

$$\overline{C}_n = \int_0^1 \phi(\zeta) C_n(\zeta) d\zeta \tag{5.8}$$

where ϕ (ζ) is a dimensionless source density distribution $\phi(\zeta) = S_c(\zeta) / \overline{S}_c$, with an integral of unity over the tree height, where $\overline{S}_c$ is the mean canopy overstory and understory source density over the tree height and ζ is the dimensionless height ($\zeta = z/h$). This average near-field concentration can be related to the total scalar flux originating from the canopy source ($h\overline{S}_c$) using a resistance formulation

$$r_n = \frac{\overline{C}_n}{h\overline{S}_c} \tag{5.9}$$

where the near-field resistance, r_n (s m^{-1}), represents the average concentration rise in the source layer per unit canopy flux due to the near-field effect, and could be placed in series with the boundary-layer resistance of the canopy layer in the two-layer surface model (Van den Hurk and McNaughton, 1995).

5.4. Results and Discussions

5.4.1. Estimation of r_n for the two forests

To estimate r_n using Eqs. (5.6) to (5.9), $\phi(z)$ must be specified and thus $C_n(z)$ and $\overline{C}_n$ can be determined. The profile of $\phi(z)$ depends on both the physiological and physical properties of the forest canopy (overstory and understory). Fig. 5.2a shows that the vertical distributions of Λ of the two forests are completely different. The profile of $\phi(z)$ for the Douglas-fir forest was well represented by a beta function as follows (Fig. 5.2b) (Lee, 1992)

$$\phi(z)=\begin{cases}10.3\left(\dfrac{z-5.5}{h-5.5}\right)^{0.80}\left(1-\dfrac{z-5.5}{h-5.5}\right)^{1.44} & 5.5\le z\le h\\ 0 & z<5.5 \text{ and } z>h\end{cases} \quad (5.10)$$

For the aspen stand, its source density profile consists of a 'high' and a 'low' part. One is for the overstory canopy and the other one is for the understory canopy. A common procedure to estimate $\phi(z)$ is to assume that it is proportional to the product of net radiation and Λ at level z (Van den Hurk and McNaughton, 1995). Since net radiation below the overstory at the 4-m height (i.e. above the understory) was 26% of that above the overstory (Blanken et al. 1997), the total source strengths for the overstory and understory were estimated to be 0.7 and 0.3, respectively. Using two beta distributions for the 'high' and 'low' sources, $\phi(z)$ can be expressed as (Fig. 5.2b)

$$\phi(z)=\begin{cases}12.0\left(\dfrac{z-15.0}{h-15.0}\right)^{0.65}\left(1.0-\dfrac{z-15.0}{h-15.0}\right)^{1.4} & 15.0\le z\le h \text{ (oversrory)}\\ 20.0\left(\dfrac{z-0.4}{h'-0.4}\right)^{0.7}\left(1.0-\dfrac{z-0.4}{h'-0.4}\right)^{1.3} & 0.4\le z\le h' \text{ (understory)}\\ 0.0 & z \text{ outside the above ranges}\end{cases} \quad (5.11)$$

where h and h' are the heights of the overstory (21 m) and understory (2 m), respectively.

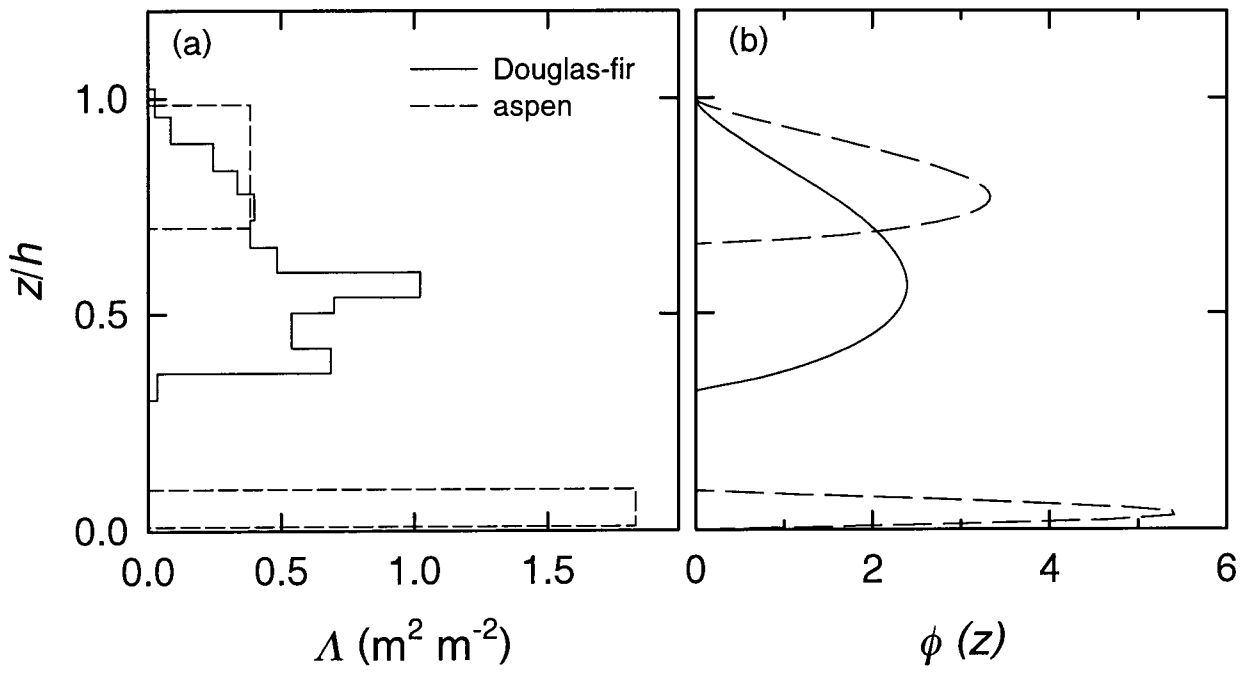

Fig. 5.2. Profiles of Λ (a) and canopy source density (b) for the Douglas-fir and aspen forests. See Eqs. (5.10) and (5.11) for analytical forms for $\phi(z)$.

Fig. 5.3 shows profiles of normalized C_n (z) for the two forests computed using Eq. (5.6) with $S_c(z) = \overline{S}_c \phi(z)$ and profiles of σ_w and T_L given by Eqs. (5.4) and (5.5), respectively. Although the total aspen overstory source strength is significantly stronger than that of the understory, the near-field effect for the understory, which extends to the ground, is actually stronger than that for the overstory. This is also shown from the temperature profile (Fig. 5.4) where the temperature gradient reversal within the understory is larger than that in the overstory.

Using measured half-hourly values of σ_w and u_* at the 39-m height for the aspen forest and at the 23-m height for the Douglas-fir forest, values of r_n were computed

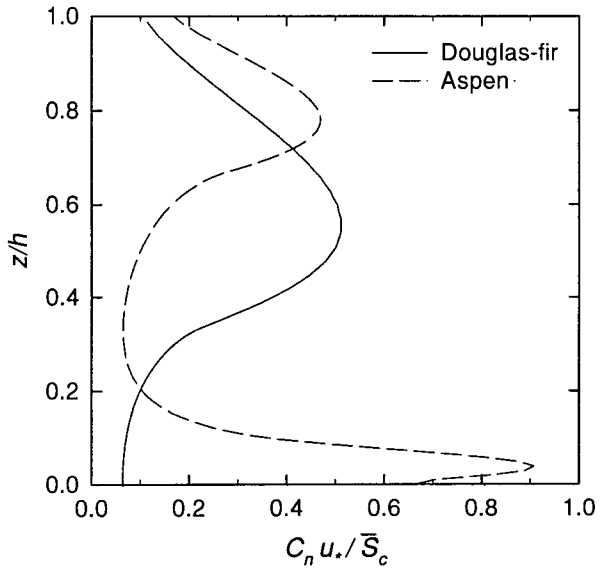

Fig. 5.3. Profiles of normalized near-field concentration ($C_n u_* / \overline{S}_c$) for the Douglas-fir and aspen forests.

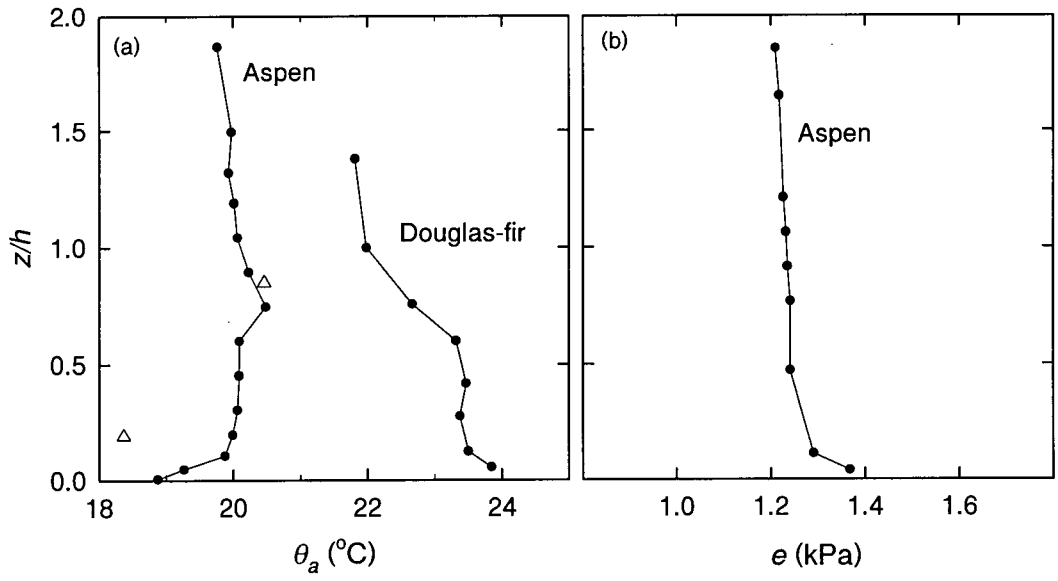

Fig. 5.4. Profiles of daytime potential temperature θ_a (°C) for the Douglas-fir and aspen forests (a) and a profile of daytime vapour pressure e (kPa) for the aspen forest (b). Values were obtained by averaging over the daytime (10:00 to 17:30 CST) from July 19 to August 1 in 1990 for the Douglas-fir forest and July 29 to August 27 in 1994 for the aspen forest. Also shown are mean values of leaf temperature obtained using infrared thermometers installed at 30 m (for aspen) and 4 m (for hazelnut) in the aspen forest (triangles).

using Eqs (5.6) to (5.9) and plotted against u_* and σ_w (Figs. 5.5 and 5.6). The correlation between r_n and σ_w was significantly lower than that between r_n and u_* probably due to the effect of stability. The value of the Douglas-fir r_n ($0.42/u_*$) was just within the range ($0.32/u_*$ to $0.42/u_*$) reported by Van den Hurk and McNaughton (1995) for most canopy structure types. The value for the aspen stand ($0.53/u_*$) was slightly higher than their values because in their calculations, results from two-level source density profiles were not included. This indicate that the near-field effect from the understory source contributed a significant increase in r_n

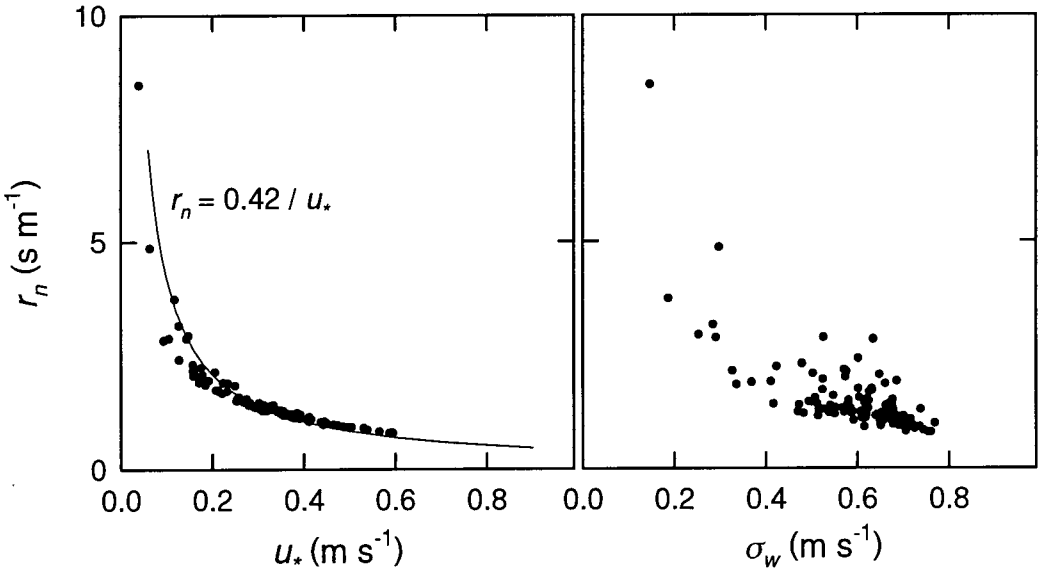

Fig. 5.5. Relationship between r_n and u_*, between r_n and σ_w for the Douglas-fir forest. The solid line represents $r_n = 0.42/u_*$.

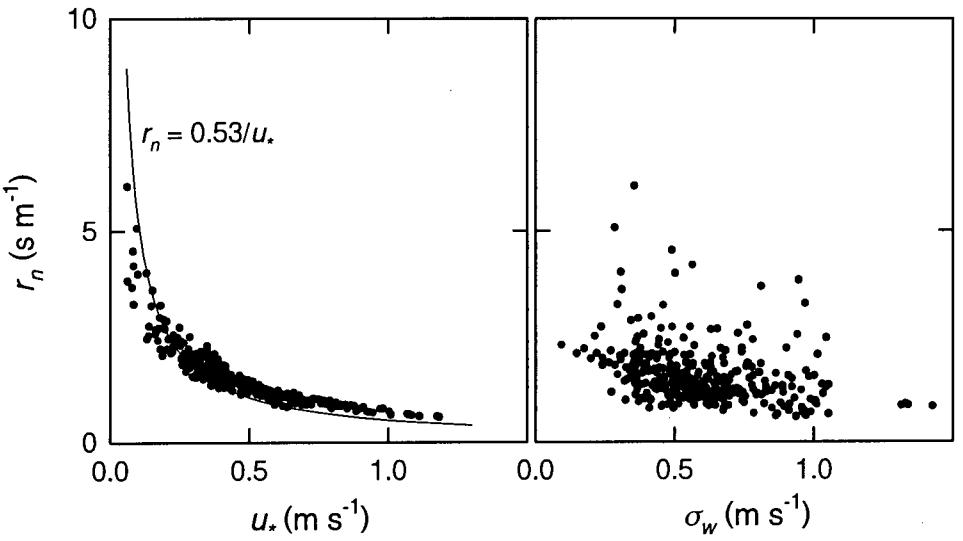

Fig. 5.6. Same as Fig. 5.5 but for the aspen forest.

5.4.2. The effect of r_n on the calculation of sensible heat flux

There was little sensible heat flux below the aspen overstory (Blanken et al. 1997) and the sensible heat flux from the forest floor was only 10-15% of above-forest values in the Douglas-fir forest (Lee and Black 1993b). By incorporating r_n into the flux-gradient relationship, as shown in the resistance network (Fig. 5.7) and neglecting the sensible heat flux from the forest floor, the sensible heat flux above the canopy, $Q_{H,g}$ (W m^{-2}), can be calculated using

$$Q_H = \varrho_a c_p \frac{T_{a,c} - T_a}{r_{f1} + r_n} \tag{5.12}$$

where ϱ_a is the density of air (kg m^{-3}), c_p is the specific heat of air at constant pressure (J kg^{-1} K^{-1}), $T_{a,c}$ is the air temperature of mean canopy flow (°C), T_a is the air temperature at the reference height (°C), and r_{f1} is the aerodynamic resistance (or far-field resistance) to

heat transfer between the canopy source height and the reference height (s m^{-1}). Values of $T_{a,c}$ were taken from measured air temperatures close to the displacement height as the best representative of the air temperature of mean canopy flow. Using Eqs. (5.3)-(5.5), r_{f1} was computed using

$$r_{f1} = \int_{h_c}^{z_R} dz / K(z) \qquad (5.13)$$

where z_R is the reference height (m), and h_c is the effective canopy source height (m). h_c corresponded closely with the displacement height which is often estimated as $0.7h$. Note that the maximum canopy air temperature occurred at this height (Fig. 5.4). Also shown in the figure is that the aspen leaf temperature measured with the infrared thermometer was very close to the air temperature measured at $z = 0.7h$, indicating the close coupling between the leaf surface and the air at h_c. The maximum air temperature observed at $z = 0.7h$ is unlikely due to measurement errors, since examination of the air temperature profile confirmed that the maximum disappeared in very windy conditions or at night (on calm nights, cold air shedding from radiatively cooled foliage caused mixing within the

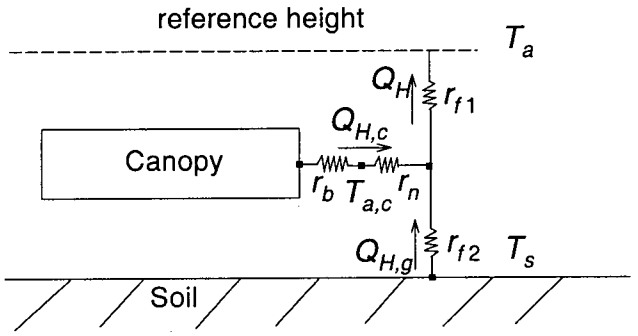

Fig. 5.7. Resistance network of a two-layer (canopy and soil) surface model, where r_{f1} and r_{f2} are the far-field resistances, r_n the near-field resistance, r_b the leaf boundary-layer resistance, and T_a, $T_{a,c}$ and T_s are temperatures at the reference height, effective canopy source height and the soil surface, respectively. The sensible heat fluxes from the canopy, ground and whole system are represented by $Q_{H,c}$, $Q_{H,g}$ and Q_H, respectively.

canopy (Yang 1998)). The significantly lower radiation temperature at $z = 0.2h$ was likely due to the shading of the hazelnut leaves by the aspen canopy (Sun and Mahrt 1995).

To show the importance of r_n relative to r_{f1} in the calculation of Q_H using Eq. (5.12), the ratio of r_n to r_{f1} is plotted against u_* (Fig. 5.8). When u_* is low (< 0.3 m s^{-1}), r_n can be as large as r_{f1}, indicating the importance of the near-field correction. This is different from the constant ratio of r_n to r_{f1} suggested by McNaughton and Van den Hurk (1995). The dependence of the ratio on u_* in Fig. 5.8 is more realistic because in their calculations σ_w was not obtained from measurements but was computed using Eq. (5.4) (i.e. σ_w is proportional to u_*). Three summer days were used to compare the daytime

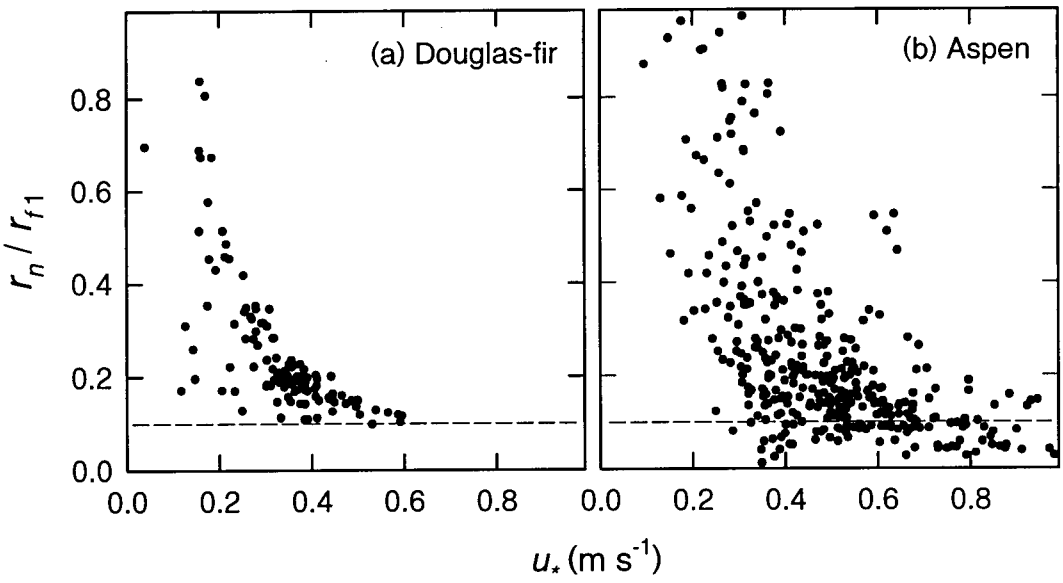

Fig. 5.8. Relationship between r_n / r_{f1} and u_* for the Douglas-fir (a) and aspen (b) forests. The value of r_n / r_{f1} from McNaughton and Van den Hurk (1995) is also shown (dashed lines).

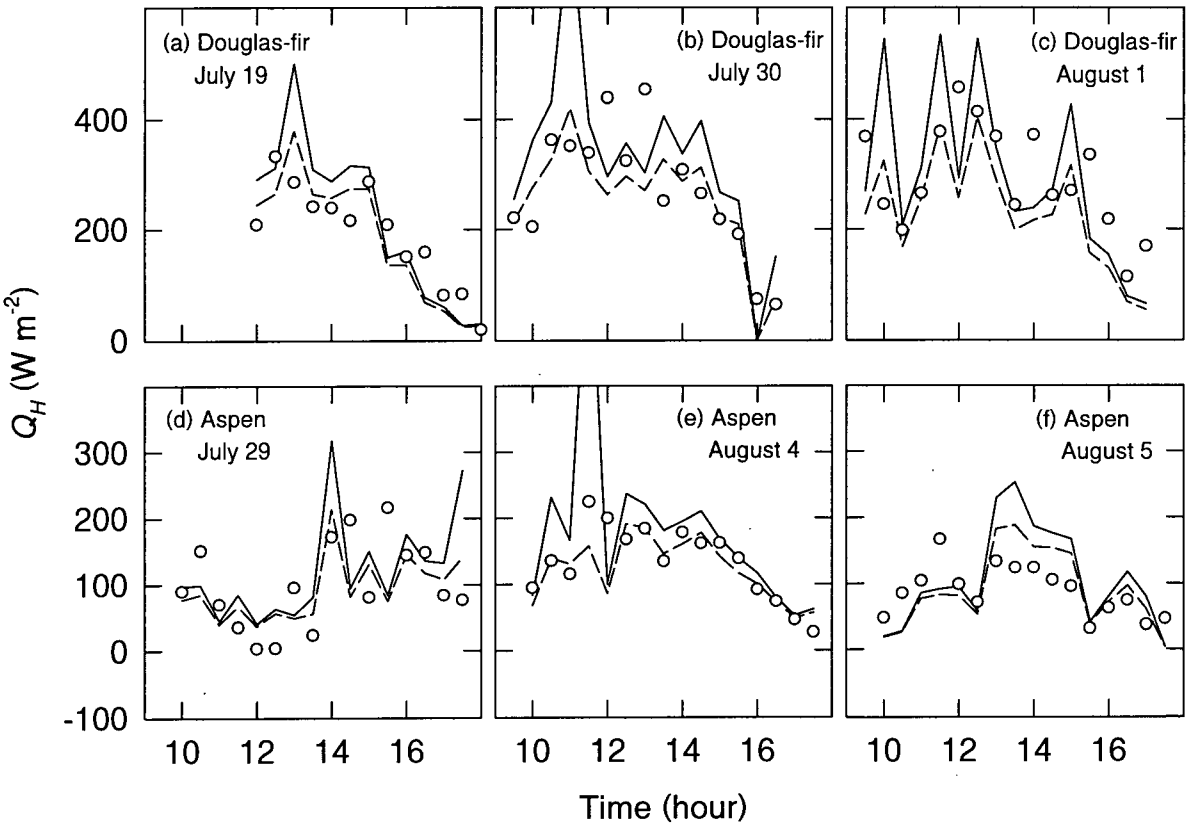

Fig. 5.9. Comparison of modelled Q_H without the use of r_n (solid line) and with the use of r_n (dash line) and measured values (symbol) on three selective days for the Douglas-fir and aspen forests. The reference heights at the Douglas-fir and aspen forests are 39.0 and 23.0 m, respectively.

courses of Q_H calculated using Eq. (5.12) with measurements for both forests (Fig. 5.9). Values of Q_H were also computed without the inclusion of r_n in Eq. (5.12). Fig. 5.9 shows that using the near-field correction significantly reduced unreasonably high values of Q_H often associated with low u_*. These results show that the inclusion of the near-field resistance gives better estimates of fluxes above the forest. Comparison of modelled and measured daytime mean values of Q_H also shows that better agreement was obtained by

including the near-field correction (Fig. 5.10). Table 5.1 lists the coefficient of determination (r^2), root mean square error (RMSE) and average deviation (d) over the entire test period for the Douglas-fir forest (July 19 to August 1 in 1990) and the aspen forest (July 29 to August 27 in 1994).

Table 5.1 Results of the coefficient of determination (r^2), root mean square error (RMSE) and average deviation (d)

Site	r^2		RMSE (W m^{-2})		d (W m^{-2})		Total half-hourly number
	no r_n	with r_n	no r_n	with r_n	no r_n	with r_n	
Douglas-fir	0.31	0.56	174.0	81.0	62.5	-10.5	118
Aspen	0.02	0.15	256.0	74.0	87.3	20.1	384

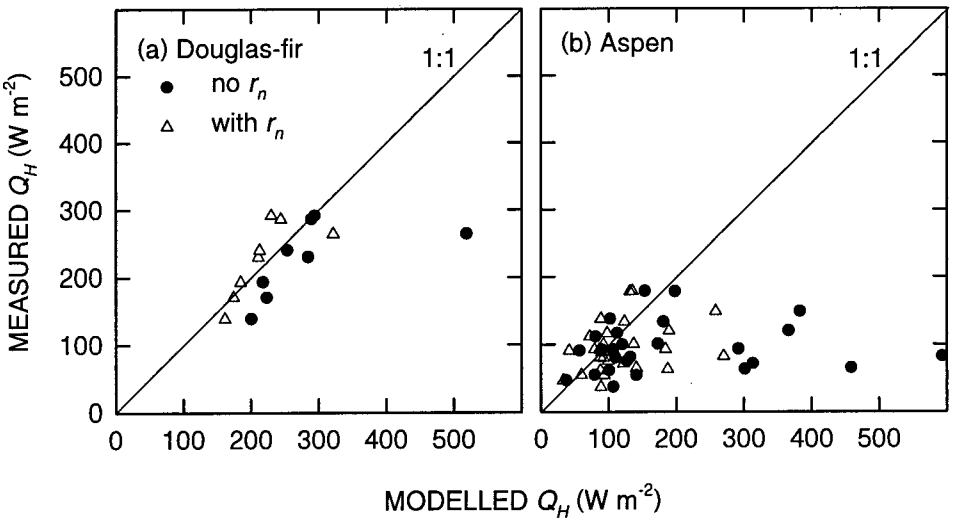

Fig. 5.10. Effect of including the near-field correction in the calculation of daytime means of Q_H for the Douglas-fir (a) and aspen (b) forests.

The latent heat flux was significantly underestimated (by more than 50%) using the flux-gradient relationship (Eq. (5.12)) with the measured temperature difference replaced by the measured vapour pressure difference. The reason for this discrepancy is

not very clear. Examination of the vapour pressure profile in the aspen forest indicated that there was very little near-field effect in contrast with the air temperature profile (Fig. 5.4b). This is unlikely due to measurement errors because measured values consistently decreased with the measurement height. It is possible because the canopy latent heat source distribution is much different from the canopy sensible heat source distribution.

5.4.3. The effect of r_n on the energy balance components calculated by CLASS

The effect of the inclusion of r_n in CLASS depends largely on the ratio of r_n to the aerodynamic resistance, r_a (s m^{-1}), given by $u/u_*^2 + B^{-1}/u_*$ (Verma 1989), where B^{-1} is the sublayer Stanton number. In Fig 5.11, the ratio is plotted against u_* for both Douglas-fir and aspen forests. In the calculation of r_a, measured values of u_* were used and the values of B^{-1} were assumed to be 2.0 (Brutsaert 1984) and 2.5 (Blanken et al. 1997) for the

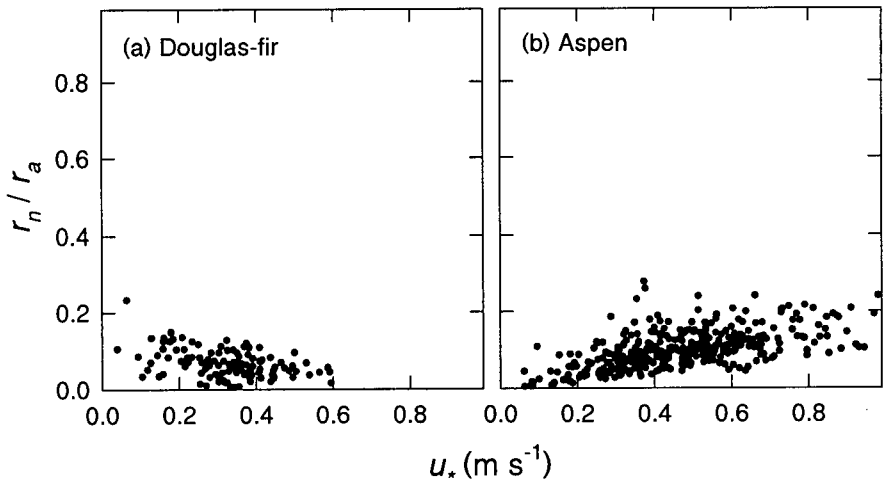

Fig. 5.11. Relationship between r_n / r_a and u_* for the Douglas-fir (a) and aspen (b) forests.

Douglas-fir and aspen stands, respectively. The ratio of r_n to r_a tended to decrease with u_* for the Douglas-fir forest and increase with u_* for the aspen forest. However, in contrast to r_n / r_{f1} (see Fig. 5.8), r_n / r_a was small (less than 0.2). This suggests that in land surface models like CLASS where fluxes from the canopy are computed using a canopy temperature, the effect of the near-field correction on flux calculations is likely to be small.

The effect of including r_n in CLASS was determined by calculating the difference between values of each energy balance component calculated using CLASS with and without r_n. This served as a test of model sensitivity to r_n and was done rather than making comparisons between the calculated and measured components because errors in canopy resistance and r_a are as large as r_n. Tests were carried out for the two forests and the soybean crop. The value of r_n for the soybean crop was assumed to be $0.36/u_*$, a mean value for most canopies given by Van den Hurk and McNaughton (1995). The difference was calculated, using Q_E as an example, from $\Delta Q_E = Q_E$ (without r_n) - Q_E (with r_n). Table 5.1 lists daytime average differences for each energy balance component for the three vegetation types. In contrast to the results obtained from the calculation of Q_H using the flux-gradient relationship in the previous section, adding r_n in CLASS did not cause significant differences in the energy balance components both above and below the canopy layer for the three vegetated surfaces. As discussed previously, this was due to the small value of r_n relative to the value of r_a. Although placing r_n in series with the r_a tends to reduce both sensible and latent heat fluxes from the canopy layer, the energy balance constraint for the canopy layer forces the canopy temperature to increase, which largely offsets the effect of r_n (Van den Hurk and McNaughton 1995). The values of ΔQ_H were

Table 5.1. Effects of including r_n in CLASS on the daytime average energy balance components (W m^{-2}) for three vegetation types. The difference in a component (e.g. ΔQ_E) was calculated by subtracting the value obtained without r_n in CLASS from the value with r_n included. Q_H and Q_E are the sensible and latent heat fluxes above the canopy, G_o is the soil heat flux, Q^*_g, $Q_{H,g}$ and $Q_{E,g}$ are the net radiation, sensible heat flux and latent heat flux at the soil surface.

Date	Vegetation type	ΔQ_H	ΔQ_E	ΔG_0	ΔQ^*_g	$\Delta Q_{H,g}$	$\Delta Q_{E,g}$
Jul 27/84	Douglas-fir	8.04	- 6.55	- 0.25	- 0.86	- 0.09	- 0.52
Jul 28/84		6.96	- 5.78	- 0.03	- 0.84	- 0.11	- 0.69
Jul 29/84		7.80	- 6.25	- 0.14	- 1.16	- 0.02	- 1.00
Jul 30/84		7.85	- 6.28	0.07	- 1.27	0.04	- 1.39
Jul 31/84		7.63	- 6.10	- 0.08	- 0.96	0.00	- 0.88
Aug 1/84		6.95	- 5.96	- 0.06	- 0.51	- 0.21	- 0.24
Aug 2/84		7.42	- 5.99	- 0.27	- 0.57	- 0.23	0.07
Aug 13/94	Aspen	5.13	- 3.57	- 0.31	- 0.71	- 0.23	- 0.17
Aug 14/94		3.99	- 2.83	- 0.06	- 0.56	- 0.14	- 0.36
Aug 15/94		3.56	- 2.62	0.17	- 0.51	- 0.09	- 0.60
Aug 16/94		0.20	- 0.05	- 0.02	- 0.06	- 0.02	- 0.03
Aug 17/94		3.91	- 2.93	- 0.21	- 0.51	- 0.18	- 0.12
Aug 18/94		2.70	- 2.03	- 0.01	- 0.35	- 0.15	0.19
Aug 4/74	Soybean crop	0.17	- 0.17	0.01	- 0.05	- 0.05	- 0.01
Aug 5/74		0.53	- 0.51	- 0.02	- 0.07	- 0.05	- 0.00
Aug 6/74		1.18	- 1.17	- 0.02	- 0.17	- 0.13	- 0.03
Aug 7/74		1.23	- 1.26	0.02	- 0.16	- 0.17	- 0.03

about 7.5 and 3.0 W m^{-2} for the Douglas-fir and aspen stands, respectively, compared to corresponding the values of 70 and 67 W m^{-2} obtained from the calculation using Eq. (5.12) with the measured air temperature difference. The effect of including r_n in the calculation of the energy balance components for the soybean crop was smaller than that for the two forests. Using a two-layer surface model of Shuttleworth and Wallace (1985), Van den Hurk and McNaughton (1995) found that the effect of the inclusion r_n in the model on the predicted evaporation from theoretical sparse and dense crops was less than 4% (which is less than any of errors that arise from direct measurements). Dolman and Wallace (1991) found that setting the near-field effect to zero in a multi-layer coupled

Lagrangian-energy-balance model changed the total evaporation from a sparse crop by less than 2%.

5.5. Conclusions

This study evaluated the effect of adding the near-field resistance r_n computed using Raupach's (1989a,b) Lagrangian localized near-field (LNF) theory in the calculation of sensible and latent heat fluxes above a Douglas-fir, an aspen forest and a soybean crop. The Douglas-fir forest had virtually no understory, while the aspen forest had a thick understory. Simulations were conducted in two different modes: (1) sensible heat fluxes above the canopy were calculated using the flux-gradient relationship with the measured air temperature difference between the effective canopy source height and the reference height, and (2) energy balance components above the canopy and at the soil surface were calculated using CLASS.

The value of r_n for the Douglas-fir forest ($0.42/u_*$) was close to values of r_n suggested by McNaughton and Van den Hurk (1995). The higher value for the aspen forest ($0.53/u_*$) was likely due to the occurrence of the understory source. Furthermore, the far-field resistance (r_{f1}) for the two forests was found to be less dependent on u_* than McNaughton and Van den Hurk (1995) suggested (in their study r_{f1} is assumed to be proportional to $1/u_*$). This caused the ratio of r_n to r_{f1} to increase with decreasing u_*, while McNaughton and Van den Hurk (1995) suggested a constant ratio. Without accounting for the near-field effect, the sensible heat flux above the two forests was significantly overestimated by using the flux-gradient relationship with measured air temperature differences between the effective canopy source height and the reference

height. Adding r_n in the flux-gradient relationship significantly improved the calculation of the sensible heat flux above both forests.

The sensitivity of the inclusion of r_n in CLASS was tested for both forests and a soybean crop. In contrast to the results above, it only had a small effect on the calculated energy balance components both above and below the canopies. This was because values of r_n were much smaller than values of the aerodynamic resistance because the latter includes the excess resistance (which accounts for the leaf boundary layer resistance to water vapour and heat transfer) which is much larger than r_{f1}. The present study shows that for practical purposes, K-theory remains an adequate description of turbulent transfer in CLASS and other large-scale models.

5.6. References

Bailey, W. G. and J. A. Davies. 1981a. Evaporation from soybeans. *Boundary-Layer Meteorol.*, 20: 417-428.

Bailey, W. G. and J. A. Davies. 1981b. The effect of uncertainty in aerodynamic resistance on evaporation estimates from the combination model. *Boundary-Layer Meteorol.*, 20: 187-199.

Black, T. A., G. den Hartog, H. H. Neumann, P. D. Blanken, P. C. Yang, C. Russell, Z. Nesic, X. Lee, S. C. Chen, R. Staebler and M. D. Novak. 1996. Annual cycles of water vapour and carbon dioxide fluxes in and above a boreal aspen forest. *Global Change Biology*, 2: 219-229.

Blanken, P. D., T. A. Black, P.C. Yang, H. H. Neumann, Z. Nesic, R. Staebler, G. den Hartog, M. D. Novak and X. Lee. 1997. Energy balance and canopy conductance of a boreal aspen forest: partitioning overstory and understory components. *J. Geophys. Res.*, 102 D24, 28915-28927.

Blanken, P. D., T. A. Black, H. H. Neumann, G. den Hartog, P. C. Yang, Z. Nesic, R. Staebler, W. Chen and M. D. Novak. 1998. Turbulent flux measurements above and below the overstory of a boreal aspen forest. *Boundary-Layer Meteorol.*, 89: 109-140.

Brutsaert, W. 1984. Evaporation into the Atmosphere. D. Reidel, Norwell, Mass.

Chen, W. J., T. A. Black, P. C. Yang, A. G. Barr, H. H. Neumann, Z. Nesic, M. D. Novak, J. Eley, R. J. Ketler and R. Cuenca. 1999. Effects of climatic variability on the annual carbon sequestration by a boreal aspen forest. *Global Change Biology* 5, 41-53.

Denmead, O. T. and E. F. Bradley. 1985. Flux-gradient relationships in a forest canopy. In: B.A. Hutchison and B.B. Hicks (Editors), *The Forest-Atmosphere Interaction*, Reidel, Dordrecht, 421-442.

Dickinson, R. E., A. Henderson-Sellers, P. J. Kennedy and M. F. Wilson. 1986. Biosphere-Atmosphere Transfer Scheme (BATS) for the NCAR Community Climate Model. National Centre for Atmospheric Research, Boulder, Colorado, NCAR/TN-275+STR, 69 pp.

Dolman, A. J. and J. S. Wallace. 1991. Lagrangian and K-theory approaches in modelling evaporation from sparse canopies. *Q. J. R. Meteorol. Soc.*, 117: 1325-1340.

Katul, G, R. Oren, D. Ellsworth, C. I. Hsieh and N. Phillips. 1997. A Lagrangian dispersion model for predicting CO_2 sources, sinks, and fluxes in a uniform loblolly pine (*Pinus taeda L.*) stand. *J. Geophys. Res.*, 102(D8): 9309-9321.

Leclerc, M. Y., G. W. Thurtell and G. E. Kidd. 1988. Measurements and Langevin simulations of mean tracer concentration fields downwind from a circular line source inside an alfalfa canopy. *Boundary-Layer Meteorol.*, 43: 287-308.

Lee, X. 1992. Atmospheric turbulence within and above a coniferous forest. *Ph.D. Thesis*, University of British Columbia, Vancouver, BC, Canada, 179 pp.

Lee, X. and T. A. Black. 1993a. Atmospheric turbulence within and above a Douglas-fir stand. Part I: Statistical properties of the velocity field, *Boundary-Layer Meteorol.*, 64: 149-174.

Lee, X. and T. A. Black. 1993b. Atmospheric turbulence within and above a Douglas-fir stand. Part II: Eddy fluxes of sensible heat and water vapour. *Boundary-Layer Meteorol.*, 64: 368-389.

Lee, X. and T. A. Black. 1994. Use of within-stand concentration profiles to determine atmosphere-forest exchange rates. 21st Conference on Agricultural and Forest Meteorology, San Diego, California, 148-151.

Legg, B. J., M. R. Raupach and P. A. Coppin. 1986. Experiment on scalar dispersion within a plant canopy. Part III: An elevated line source. *Boundary-Layer Meteorol.*, 35: 277-302.

McNaughton, K. G. and B. J. J. M. Van den Hurk. 1995. A Lagrangian revision of the resistors in the two-layer model for calculating the energy budget of a plant canopy. *Boundary-Layer Meteorol.*, 74: 261-288.

Meyers, T. P. and D. D. Baldocchi. 1988. A comparison of models for deriving dry deposition fluxes of O_3 and SO_2 to a forest canopy. *Tellus*, 40B, 270-284.

Pitman, A. J., Z.-L. Yang, J. G. Cogley and A. Henderson- Sellers. 1991. Description of bare essentials of surface transfer for the Bureau of Meteorology Research Centre AGCM. *Res. Rep.* 32, Bur. of Meteorol. Res. Cent., Melbourne, Victoria, Australia.

Raupach, M. R. 1988. Canopy transport processes. In: W. L. Steffen and O. T. Denmead (Editors), Flow and Transport in the Natural Environment: Advances and Applications. Springer-Verlag, Berlin, 95-127.

Raupach, M. R. 1989a. Applying Lagrangian fluid mechanics to infer scalar source distributions from concentration profiles in plant canopies. *Agric. For. Meteorol.*, 47: 85-108.

Raupach, M. R. 1989b. A practical Lagrangian method for relating scalar concentration to source distributions in vegetation canopies. *Q. J. R. Meteorol.*, 115: 609-632.

Sellers, P. J., et al. (Eds.). 1994. Experiment plan: Boreal Ecosystem-Atmosphere Study, version 3.0, NASA Goddard Space Flight Cent., Greenbelt, Md., 730 pp.

Sellers, P., F. Hall, H. Margolis, R. Kelly, D. D. Baldocchi, G. den Hartog, J. Cihlar, M. G. Ryan, B. Goodison, P. Crill, K. J. Ranson, D. Lettermaier and E. Wickland. 1995. The boreal ecosystem-atmosphere study (BOREAS): An overview and early results from 1994 field year. *Bull. of the Amer. Meteorol. Soc.*, 76: 1549-1577.

Sellers, P. J., D. A. Randall, G. J. Collatz, J. A. Berry, C. B. Field, D. A. Dazlich, C. Zhang, G. D. Collelo and L. Bounoua. 1996. A revised land surface parameterization (SiB2) for atmospheric GCMs. Part I: Model formulation. *Journal of Climate*, 9: 676-705.

Shuttleworth, W. J. and J. S. Wallace. 1985. Evaporation from sparse crops - an energy combination theory. *Q. J. R. Meteorol. Soc.*, 111: 839-855.

Simpson, I. J., G. C. Edwards, G. W. Thurtell, G. den Hartog, H. H. Neumann and R. M. Staebler. 1997. Micrometeorological measurements of methane and nitrous oxide exchange above a boreal aspen. *J. Geophys. Res.*, 102(D24): 29321-29329.

Sun, J. and L. Mahrt. 1995. Temperature variation: Application to BOREAS. *Boundary-layer Meteorol.*, 76: 291-301.

Taylor, G. I. 1921. Diffusion by continuous movements. *Proc. London Math. Soc.*, Ser. A., 20, 196-211.

Thurtell, G. W. 1989. Comments on using *K*-theory within and above the plant canopy to model diffusion processes. In: *Estimation of Areal Evapotranspiration, IAHS Publ.*, 177: 81-85.

Van den Hurk, B. J. J. M. and K. G. McNaughton. 1995. Implementation of near-field dispersion in a simple two-layer surface resistance model. *J. Hydrol.*, 166: 293-311.

Verma, S. B. 1989. Aerodynamic resistances to transfers of heat, mass and momentum. In: *Estimation of Areal Evapotranspiration, IAHS Publ.*, 177: 13-20.

Verseghy, D. L. 1991. CLASS - A Canadian land surface scheme for GCMs. I. Soil model. *Int. J. Climatol.*, 11: 111-133.

Verseghy, D. L., N. A. McFarlane and M. Lazare. 1993. CLASS - a Canadian land surface scheme for GCMs. II. Vegetation model and coupled runs. *Int. J. Climatol.*, 13: 347-370.

Viterbo, P. and A. C. M. Beljaars. 1995. An improved land surface parameterization scheme in the ECMWF model and its validation. *J. Climate*, 8: 2716-2748.

Waggoner, P. E. and W. E. Reifsnyder. 1968. Simulation of the temperature, humidity and evaporation profiles in a leaf canopy. *J. Appl. Meteorol.*, 7: 400-409.

Wilson, J. D. 1989. Turbulent transport within the plant canopy. In: *Estimation of Areal Evapotranspiration*, edited by T. A. Black, D. L. Spittlehouse, M. D. Novak and D. T. Price, LAHS Publ., 177, 43-80.

Yang, P. C. 1998. Carbon dioxide flux within and above a boreal aspen forest, *Ph.D. Thesis*, Univ. of British Columbia, Vancouver, BC, 229 pp.

CHAPTER 6

COMPARISON OF TWO-LAYER AND SINGLE-LAYER CANOPY MODELS OF EVAPORATION FROM A BOREAL ASPEN FOREST

6.1. Introduction

Multi-layer models of plant canopy evaporation have been developed in recent years to account for the vertical variation in leaf area index, radiation, wind speed and turbulence within the vegetation. Such models can better describe the exchange processes within the canopy, but are complex, require a large number of parameters and need considerable computation time. Furthermore, the improved accuracy of these models in calculating above-canopy fluxes compared to single-layer models is often not significant. This has led to the cautioning comment by Raupach and Finnigan (1988) that 'single-layer models of evaporation from plant canopies are incorrect but useful, whereas multi-layer models are correct but useless'. Dolman and Wallace (1991) showed that there was little difference between the evaporation rates above a sparse agricultural crop obtained using a multi-layer canopy evaporation model and two single-layer canopy models. This issue is particularly relevant in developing efficient but realistic canopy models for land surface schemes that are to be used in general circulation models.

In many forests where there is relatively little understory, single-layer canopy models would be expected to perform adequately. Some forests have a significant understory, e.g. young Douglas-fir forests on the east coast Vancouver Island which often have a thick salal (*Gaultheria shallon* Pursh) understory (Kelliher et al. 1986) and aspen-hazelnut forests in the mixedwood section of the southern boreal forests in central

Saskatchewan (Kabzems et al. 1986, Black et al. 1996). It would seem reasonable to expect that a two-layer model, which has the advantage of predicting understory evaporation, would be superiour to a single-layer model in these stands in the calculation of total canopy evaporation because understory available energy flux, and canopy and boundary-layer resistances are significantly different from those of the overstory.

With regard to the importance of the near-field effect in modelling forest evaporation, the analysis in Chapter 5 showed that the inclusion of Van den Hurk and McNaughton's (1995) near-field resistance had only a small effect in the single-layer canopy model in CLASS. The impact of the near-field effect, however, in a two-layer canopy model is not obvious. For these reasons, the objectives of this chapter are (1) to compare two two-layer canopy models, one using Raupach's (1989) Lagrangian localized near-field (LNF) theory and the other using K-theory to describe turbulent transport, and (2) to determine whether these models are superiour to a single-layer canopy model using K-theory in the calculation of total canopy evaporation. Model outputs will be compared with meteorological and eddy-covariance flux measurements made during the full-leaf period of 1994 in the old aspen forest described in Chapter 3.

6.2. Theory

Since there was little sensible ($Q_{H,g}$) and latent ($Q_{E,g}$) heat flux from the soil surface in the aspen forest during the full-leaf period (Black et al. 1996), $Q_{H,g}$ and $Q_{E,g}$ were neglected in the following analysis. This significantly simplified the three models and eliminated the effects of errors in the calculation of $Q_{H,g}$ and $Q_{E,g}$.

6.2.1. Single- and two-layer models based on *K*-theory

In the single-layer ('big leaf') canopy evaporation model used here (Fig. 6.1), the latent heat flux from the canopy, $Q_{E,c}$ (W m^{-2}), is given by the combination (or Penman-Monteith) equation

$$Q_{E,c} = \frac{sQ + \varrho_a c_p \Delta e_a / r_a}{s + \gamma(1 + r_c / r_a)} \tag{6.1}$$

where Q is the available energy flux (W m^{-2}), Δe_a is the ambient saturation (vapour pressure) deficit (kPa), ϱ_a is the air density (kg m^{-3}), c_p is the specific heat of air at constant pressure (J kg^{-1} K^{-1}), γ is the psychrometric constant (kPa K^{-1}), s is the slope of the saturation vapour pressure curve (kPa K^{-1}), and r_a and r_c are the aerodynamic and canopy resistances (s m^{-1}), respectively. The sensible heat flux from the canopy, $Q_{H,c}$ (W m^{-2}), is given by

$$Q_{H,c} = \frac{\gamma Q - \varrho_a c_p \Delta e_a / (r_a + r_c)}{\gamma + s r_a / (r_a + r_c)} \tag{6.2}$$

The two-layer canopy model is based on a multi-layer model developed by Chen (1984). In his model, Eqs. (6.1) and (6.2) were applied to each layer and these equations together with the relationships between flux densities and relevant driving variables between two adjacent layers consisted of a closed set of equations for all unknown variables. When applied to two canopy layers with no sensible and latent heat fluxes from the soil surface, these relationships were written as

$$Q_{H,1} + Q_{H,2} = \frac{\varrho_a c_p (T_{a,1} - T_a)}{r_{a,1}} \tag{6.3a}$$

$$Q_{H,2} = \frac{\varrho_a c_p (T_{a,2} - T_{a,1})}{r_{a,2}} \tag{6.3b}$$

$$Q_{E,1} + Q_{E,2} = \frac{\varrho_a c_p (e_{a,1} - e_a)}{\gamma r_{a,1}} \tag{6.4a}$$

$$Q_{E,2} = \frac{\varrho_a c_p (e_{a,2} - e_{a,1})}{\gamma r_{a,2}} \tag{6.4b}$$

where T_a is the air temperature at the reference height (°C), "1" and "2" represent layers 1 and 2, respectively, $T_{a,i}$ and $e_{a,i}$ (i = 1, 2) are the temperature (°C) and vapour pressure (kPa) of the air in layer i, $r_{a,1}$ and $r_{a,2}$ are the resistances (s m^{-1}) in the vertical direction due to turbulent exchange between layer 1 and the reference height and between layers 2 and 1, respectively (Fig. 6.1).

The saturation vapour pressure at the ambient air temperature, e^* (T_a) (kPa), can be expressed as

$$e^*(T_a) = e^*(T_p) + s(T_a - T_p) \tag{6.5}$$

where T_p is an arbitrary temperature close to T_a (within a few °C) and s is evaluated at (T_p + T_a)/2. With the above equation, the saturation deficit for layer i, Δe_i ($\Delta e_i = e^*(T_{a,i}) - e_{a,i}$) can be expressed as

$$\Delta e_i = sT_{a,i} - e_{a,i} + e^*(T_p) - sT_p \tag{6.6}$$

By taking the difference between Δe_i of the layers i-1 and i, the constant e^* (T_p) – sT_p in Eq. (6.6) is eliminated, so that

$$\Delta e_i - \Delta e_{i-1} = s(T_{a,i} - T_{a,i-1}) - (e_{a,i} - e_{a,i-1}) \tag{6.7}$$

By defining $J_i = Q_{H,i} - (\gamma/s)Q_{E,i}$ (McNaughton 1976, Chen 1984) and combining Eqs. (6.3) and (6.4) with Eq. (6.7), the following equations are derived

$$(J_1 + J_2) r_{a,1} = \frac{\varrho_a c_p}{s} (\Delta e_1 - \Delta e_a) \tag{6.8}$$

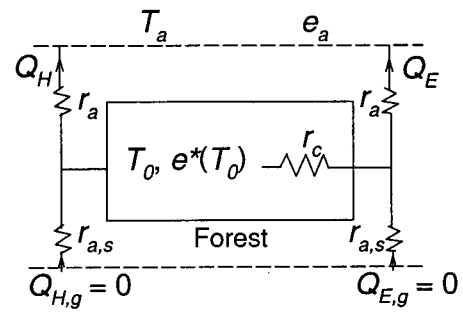

1. *K*-theory single-layer model

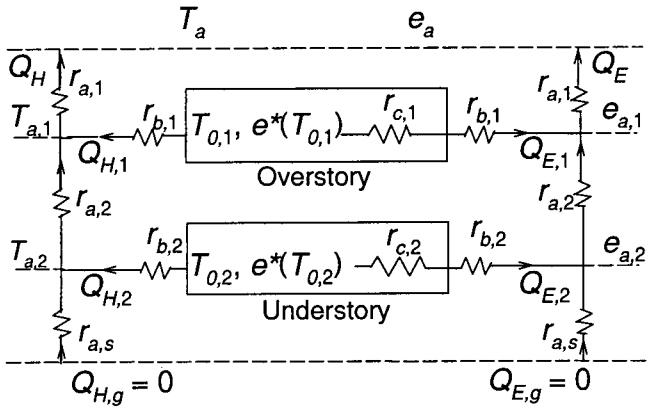

2. *K*-theory two-layer model

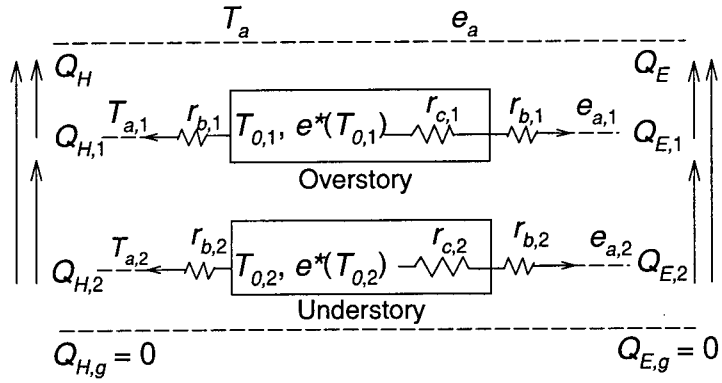

3. Langrangian two-layer model

Fig.6.1. Diagrams of the three canopy evaporation models. r_a in the single-layer model is the aerodynamic resistance which is the sum of the leaf boundary-layer resistance and the aerodynamic resistance between canopy mean air stream and the reference height. $r_{a,s}$ is the aerodynamic resistance between the soil surface and canopy mean air stream. T_0, $T_{0,1}$ and $T_{0,2}$ are the effective forest, overstory and understory canopy temperatures, respectively. The definition of the rest of the symbols can be found in the text.

$$J_2 r_{a,2} = \frac{Q_a c_p}{s}(\Delta e_2 - \Delta e_1) \tag{6.9}$$

Substitution of Eqs. (6.1) and (6.2) for layer i into the definition of J_i (above) gives the following equation

$$J_i r_i = -\frac{Q_a c_p}{s}\Delta e_i + \alpha r_{c,i} Q_i \tag{6.10}$$

where Q_i (W m^{-2}) is the available energy flux for layer i (i = 1, 2) and r_i and α are defined as

$$r_i = r_{b,i} + \alpha r_{c,i} \tag{6.11}$$

$$\alpha = \gamma / (\gamma + s) \tag{6.12}$$

Eqs. (6.8), (6.9) and (6.10) represent four independent equations with four unknowns: Δe_1, Δe_2, J_1 and J_2. Hence, this is a closed system. Substitution of the solved values of Δe_1 and Δe_2 into Eqs. (6.1) and (6.2) written for each canopy layer gives the respective fluxes.

6.2.2. A two-layer model based on the LNF theory

An outline of the LNF theory was given in Chapter 5. The Lagrangian model used here is the same as that developed by Dolman and Wallace (1991) except that it has only two canopy layers (Fig. 6.1), while their model has multilayers. In each layer, similar to the K-theory based two-layer model, the sensible and latent fluxes are calculated using Eqs. (6.1) and (6.2). The only difference between the Lagrangian and K-theory models is the method used for the calculation of Δe_1 and Δe_2.

According to Raupach (1989), the scalar concentrations in each layer can be expressed as

$$C_i - C_a = \sum_{j=1}^{n} m_{ij} S_{c,j} \Delta z_j \tag{6.13}$$

where C_i and C_a are the scalar concentrations in layer i and at the reference height, respectively (e.g. J m^{-3} for heat), Δz_j is the vertical depth in layer j, $S_{c,j}$ is the scalar source density in layer j, m_{ij} is the concentration in layer i, relative to the concentration at the reference height, produced by a source of unit strength in layer j ($S_{c,j}\Delta z_j = 1$), so that

$$m_{ij} = (C_i - C_a) / (S_{c,j} \Delta z_j) \tag{6.14}$$

The estimation of the concentration profile from each unit source is carried out using Eqs. (5.1) to (5.7) in Chapter 5 until all elements of the matrix m_{ij} are computed. Similar to Eq. (6.7), $\Delta e_i - \Delta e_a$ can be written as

$$\Delta e_i - \Delta e_a = s(T_i - T_a) - (e_i - e_a) \tag{6.15}$$

Referring to Eq. (6.13), it can be shown that (Dolman and Wallace 1991)

$$\Delta e_i - \Delta e_a = \left[s / (\varrho_a c_p) \right] \sum_{j=1}^{n} m_{ij} J_j \tag{6.16}$$

Using the definition of J_i and substituting Eqs. (6.1) and (6.2) for layer i into Eq. (6.16), it follows that

$$b_i = \sum_{j=1}^{n} a_{ij} \Delta e_j \tag{6.17}$$

where the column vector $\boldsymbol{B}$ is given as

$$b_i = \Delta e_a + (s / \varrho_a c_p) \sum_{j=1}^{n} \frac{Q_j m_{ij}}{1 + r_{b,j} / \alpha r_{c,j}} \tag{6.18}$$

The elements of the coefficient matrix $\boldsymbol{A}$ are defined as

$$a_{ij} = \begin{cases} m_{ij} / (r_{b,j} + \alpha r_{c,j}) & i \neq j \\ 1 + m_{ij} / (r_{b,j} + \alpha r_{c,j}) & i = j \end{cases} \qquad (6.19)$$

These equations can be solved with standard matrix procedures for a system of linear equations. When applied to a two-layer canopy model, values of Δe_1 and Δe_2 are obtained.

6.3. Parameterizations used in the models

The three models (the *K*-theory single-layer model, the *K*-theory two-layer model and the Lagrangian two-layer model) were applied to the aspen forest during the full-leaf period in 1994. A detailed description of the experimental site can be found in Chapter 3. The parameterization of canopy conductance of the aspen forest was also described in Chapter 3. The parameterizations of canopy conductance of the aspen overstory and aspen understory were given by Blanken et al. (1997) and Blanken (1997). The partitioning of the available energy flux between the overstory and understory was based on net radiation measurements made using a tram that moved back and forth along two 65-m long cables suspended above 4 m above the ground (Black et al. 1996, Chen et al. 1997). The values of $r_{a,1}$ and $r_{a,2}$ were determined by integrating the reciprocal of eddy diffusivity $K(z)$ from the aspen effective source height h_c (see Chapter 5) to the upper flux measurement height (39 m) and from the hazelnut understory height (2 m) to the lower flux measurement height (4 m), respectively (see Eq. (5.13) in Chapter 5). Values of $r_{b,1}$ and $r_{b,2}$ were computed following McNaughton and Van den Hurk (1995). Table 6.1 lists all parameters used in the three models.

Table 6.1. Parameters used in the three models: g_c, $g_{c,1}$ and $g_{c,2}$ are canopy conductances (canopy conductance is the reciprocal of canopy resistance) of the aspen forest, aspen overstory and aspen understory, respectively (mm s^{-1}), Q_p is the above-canopy photosynthetically active radiation flux (μmol m^{-2} s^{-1}), Λ is the leaf area index (one-sided basis) of the aspen overstory (m^2 m^{-2}), B^{-1} is the dimensionless sublayer Stanton number (Owen and Thompson 1963, Verma 1989), u and u_* are the measured wind speed and friction velocity at the 39-m height, respectively (m s^{-1}), l_1 and l_2 are the aspen and hazelnut leaf dimensions, respectively (m) and β is an index of turbulence development (2.5 is for fully-developed outdoor turbulence).

Parameter	Value	
g_c	$32.6\frac{Q_p}{Q_p+430}\exp(-0.645\Delta e)$ (single-layer model)	
$g_{c,1}$	$19.0\exp(-0.530\Delta e_1)$	$1400 \le Q_p$
	$20.7\exp(-0.773\Delta e_1)$	$800 < Q_p < 1400$
	$11.9\exp(-0.922\Delta e_1)$	$200 \le Q_p \le 800$
$g_{c,2}$	$22.7\exp(-1.96\Delta e_2)$	$1400 \le Q_p$
	$18.6\exp(-2.00\Delta e_2)$	$800 < Q_p < 1400$
	$9.70\exp(-2.54\Delta e_2)$	$200 \le Q_p \le 800$
Q	$0.95Q^*$ (single-layer model)	
Q_1	$(1.0-0.47\exp(-0.3\Lambda))Q^*$	
Q_2	$(0.47\exp(-0.3\Lambda)-0.05)Q^*$	
r_a	$u/u_*^2 + B^{-1}/u_*$ (single-layer model)	
$r_{a,1}$	$2.4/u_*$	
$r_{a,2}$	$1.9/u_*$	
$r_{b,1}$	$150\beta(l_1/u)$	
$r_{b,2}$	$150\beta(l_2/u)$	
$m_{11}, m_{12}, m_{21}, m_{22}$	25.0, 1.7, 3.2, 109.0	

6.4. Results

6.4.1. Sensitivity tests

For single-layer canopies, the sensitivity of evaporation to changes in the available energy flux or saturation deficit can be determined from the McNaughton and Jarvis (1983) decoupling factor ($\Omega = (1 + s/\gamma)/(1 + s/\gamma + r_c/r_a)$). The fractional change in evaporation from the canopy (dE/E) resulting from a fractional change in canopy resistance (dr_c/r_c) is given by $dE/E = (1 - \Omega)dr_c/r_c$ (Jarvis and McNaughton 1986). If $r_c/r_a << 1$, then Ω is close to 1, indicating strong decoupling, so that a change in r_c has little effect on evaporation and evaporation is almost entirely dependent on available energy. Conversely, if $r_c/r_a >> 1$, then Ω is close to 0, indicating strong coupling, so that a fractional change in r_c can be expected to cause an almost proportional change in evaporation from the canopy and evaporation is almost entirely dependent on saturation deficit. For forests, the value of Ω is found to be low, typically less than 0.5 (a value of 0.36 was found for the aspen forest (Blanken 1997), indicating considerable control of evaporation by r_c.

Dolman and Wallace (1991) did an analysis of the sensitivity of total evaporation obtained using their multi-layer Lagrangian model to several parameters and they found that the sensitivity was very low except to stomatal resistance in which case a 25% change caused a 15% change in total evaporation. In the case of the two-layer models discussed here, the sensitivity of the calculations of $Q_{E,1}$ and $Q_{E,2}$ to Q_1, Q_2, $r_{c,1}$, $r_{c,2}$, $r_{b,1}$ and $r_{b,2}$ was investigated. Fig. 6.2 shows the percentage changes in the latent heat flux

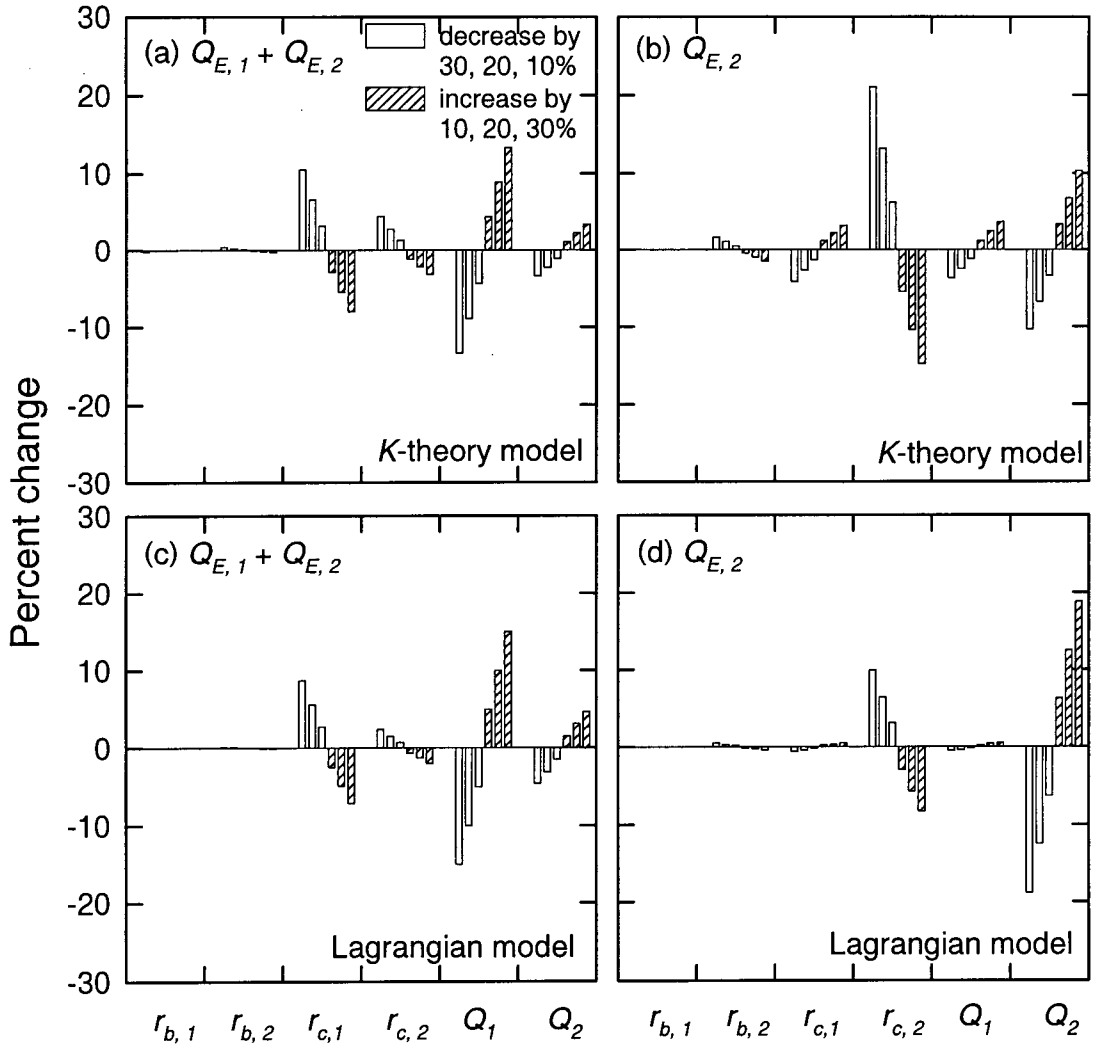

Fig. 6.2. Simulation of the effect on the latent heat flux of decreasing the values of each individual parameter by 30%, 20% and 10% (empty bars), and increasing them by 10%, 20% and 30% (shaded bars) used in the two two-layer models. (a) and (b) Latent heat flux above and below the aspen overstory calculated by the *K*-theory model. (c) and (d) As for Fig. 6.2a and 6.2b but for the Lagrangian model.

above and below the overstory obtained using the two model resulting from changes in the individual variables. The percentage change (Δ) due to the change in a single variable was calculated as Δ = [(CHNG – CONT)/CONT]×100% where CONT is the modelled control value and CHNG is the value computed after a 10%, 20%, and 30% change in a single variable (Pitman 1994). Typical control conditions during midday hours for the aspen forest used in these calculations were set as Δe_a = 1.0 kPa, $r_{b,1}$ = 20 s m^{-1}, $r_{b,2}$ = 30 s m^{-1}, $r_{c,1}$ = 80 s m^{-1}, $r_{c,2}$ = 200 s m^{-1}, Q_1 = 350 W m^{-2} and Q_2 = 100 W m^{-2}. Fig. (6.2) shows that in the simulation of the total latent heat flux, $Q_{E,1} + Q_{E,2}$, the two models are more sensitive to Q_1 and $r_{c,1}$ than Q_2 and $r_{c,2}$, while $r_{b,1}$ and $r_{b,2}$ have negligible effect on $Q_{E,1}$ and $Q_{E,2}$, respectively. Increase in $r_{c,1}$ by 30% led to a decrease in the total latent heat flux obtained using the K-theory and Lagrangian model by 8% and 7%, respectively. The calculation of $Q_{E,2}$ was only controlled by $r_{c,2}$ and Q_2. However, $Q_{E,2}$ modelled using K-theory was more sensitive to $r_{c,2}$ than when modelled using the Lagrangian model.

6.4.2. Performance of the models

The performance of the three models was tested using the same six consecutive days used in Chapter 3 (August 13 to 18, 1994). The first three days were cloudless with a wide range of Δe, August 16 was overcast, while August 17 and 18 were partly cloudy. Temperature profiles during this period indicated that there was a strong inversion in the lower part of the aspen overstory and within the hazelnut understory (Fig. 6.3). The inversion in the lower part of the aspen overstory was evident by the fact that both air temperatures measured at the 16.1- and 19.2-m heights were higher than those measured above and below these two heights (for some reason, the air temperature measured at the

19.2-m height on August 15 showed very little increase). The inversion in the understory, however, was usually stronger than that in the lower part of the overstory and the sensible heat flux (Q_H) at the 4-m height during this period was usually upwards, i.e. occurrence of counter-gradient flow (see Fig.6.5).

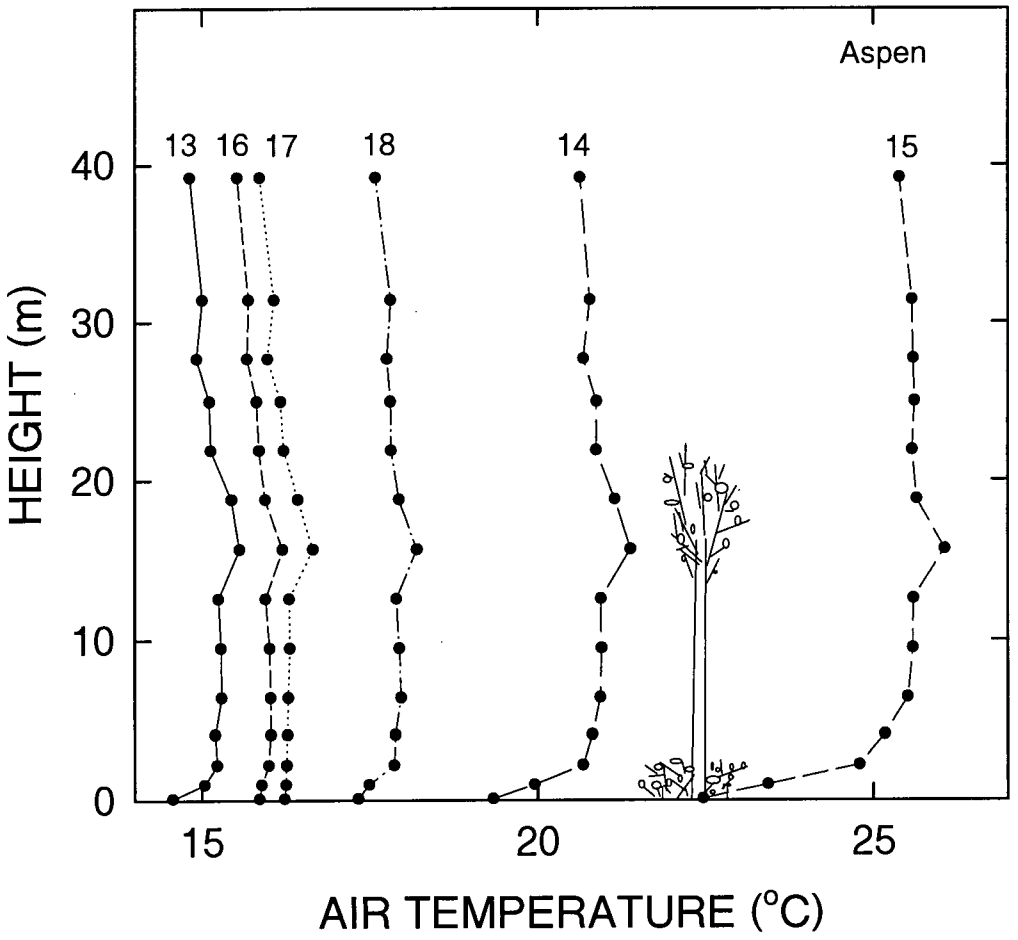

Fig. 6.3. Profiles of the daytime (10:00 -17:30 CST) average air temperature observed in the aspen forest from August 13 to 18, 1994. The numbers next to each profile are the date.

Fig. 6.4 compares the values of Δe_1 and Δe_2 computed using the two two-layer models with those measured at the 16.1-m (where the maximum air temperature occurred) and 4-m heights during the six-day period, respectively. In the case of Δe_1, there was a close correspondence between the values obtained using the two models. The Lagrangian model gave slightly higher values during the midday hours on the first three cloud-free days than the K-theory model. The observed near-field effect, i.e. the "bump", was not indicated by a systematic difference between K-theory model and the Lagrangian model. In the case of Δe_2, there was also a close correspondence between the values obtained using the two models except during the midday hours on August 15 when values from the Lagrangian model were significantly higher than those from the K-theory model (the temperature inversions on August 15 were the strongest of the six days (Fig. 6.3)). Furthermore, the model values were often significantly higher than measured values. Some of the overestimation may be the result of errors in determining $r_{c,2}$ because of its large temporal variability (Blanken 1997) which was also evident in porometer measurements made in 1996. For both Δe_1 and Δe_2, the close correspondence between values from K-theory and the Lagrangian models indicates the strong control by the available energy and canopy resistance (Fig. 6.2) and consequently a relatively small near-field effect. This suggests that the difference between evaporation from the canopy estimated using K-theory model and the Lagrangian model is likely very small (see below).

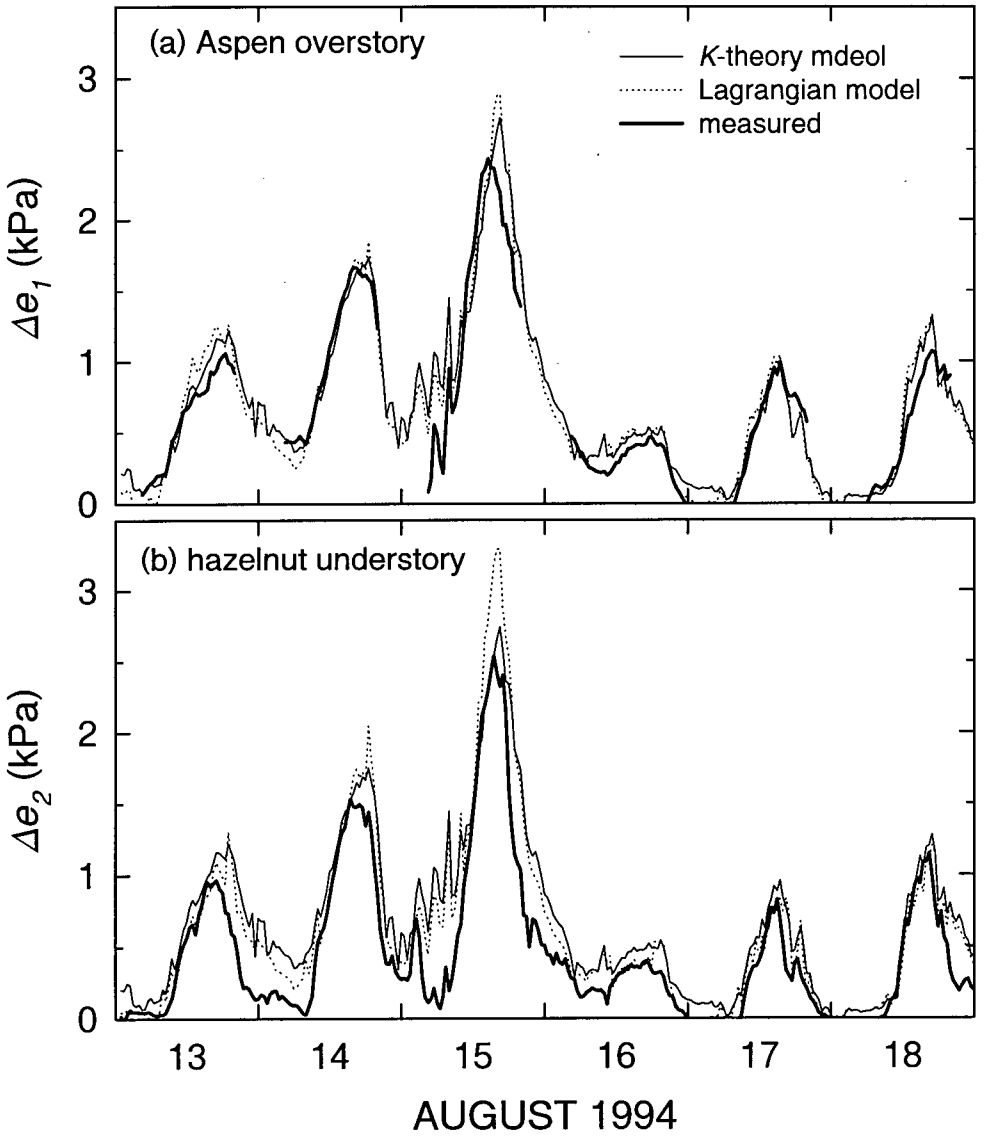

Fig. 6.4. Comparison of half-hourly values of Δe_1 (a) and Δe_2 (b) calculated using the two two-layer models with the measured values for the aspen forest from August 13 to 18, 1994. Measured values were obtained at the 16.1-m height for the overstory and the 4-m height for the understory, respectively.

Courses of modelled Q_E and Q_H above the aspen and hazelnut canopies obtained from the two two-layer models are compared with those from the single-layer model and measured values for the aspen forest during the same six-day period (Figs. 6.5 and 6.6). Since values of Δe_1 and Δe_2 calculated by the K-theory two-layer model were close to those obtained using the Lagrangian two-layer model, the modelled Q_E and Q_H by the two models were also very close. The six-day cumulative evaporation totals obtained by the single-layer model, and the K-theory and Lagrangian two-layer models overestimated the measured value by 10%, 13% and 13%, respectively. A simulation by CLASS, which also treats the plant canopy as a single layer, overestimated the cumulative evaporation total over the same six-day period by 8% when the forest canopy conductance parameterization was used (see Chapter 3). This indicates that simple, single-layer models often perform better than multi-layer models. Both figures show that the two-layer models gave reasonably good estimates of sensible and latent heat fluxes above the hazelnut understory except on August 15 when large discrepancies occurred. This was likely because $r_{c,2}$ (hazelnut canopy resistance) was significantly overestimated when Δe was extremely high (values on August 15 were the highest for 1994). Comparison of modelled and measured daytime average values of Q_E above the forest from July 29 to August 27 in 1994 also indicates that the single-layer model performed better than the two-layer models (Fig. 6.7). Values of r^2 and the root mean square error were 0.74 and 35.1 W m^{-2} for the single-layer model, 0.57 and 45.8 W m^{-2} for K-theory two-layer model and 0.62 and 43.3 W m^{-2} for the Lagrangian two-layer model. As indicated above, the close agreement between the results from the two-layer models indicates strong stomatal/energy control of evaporation in the simulation for the aspen forest.

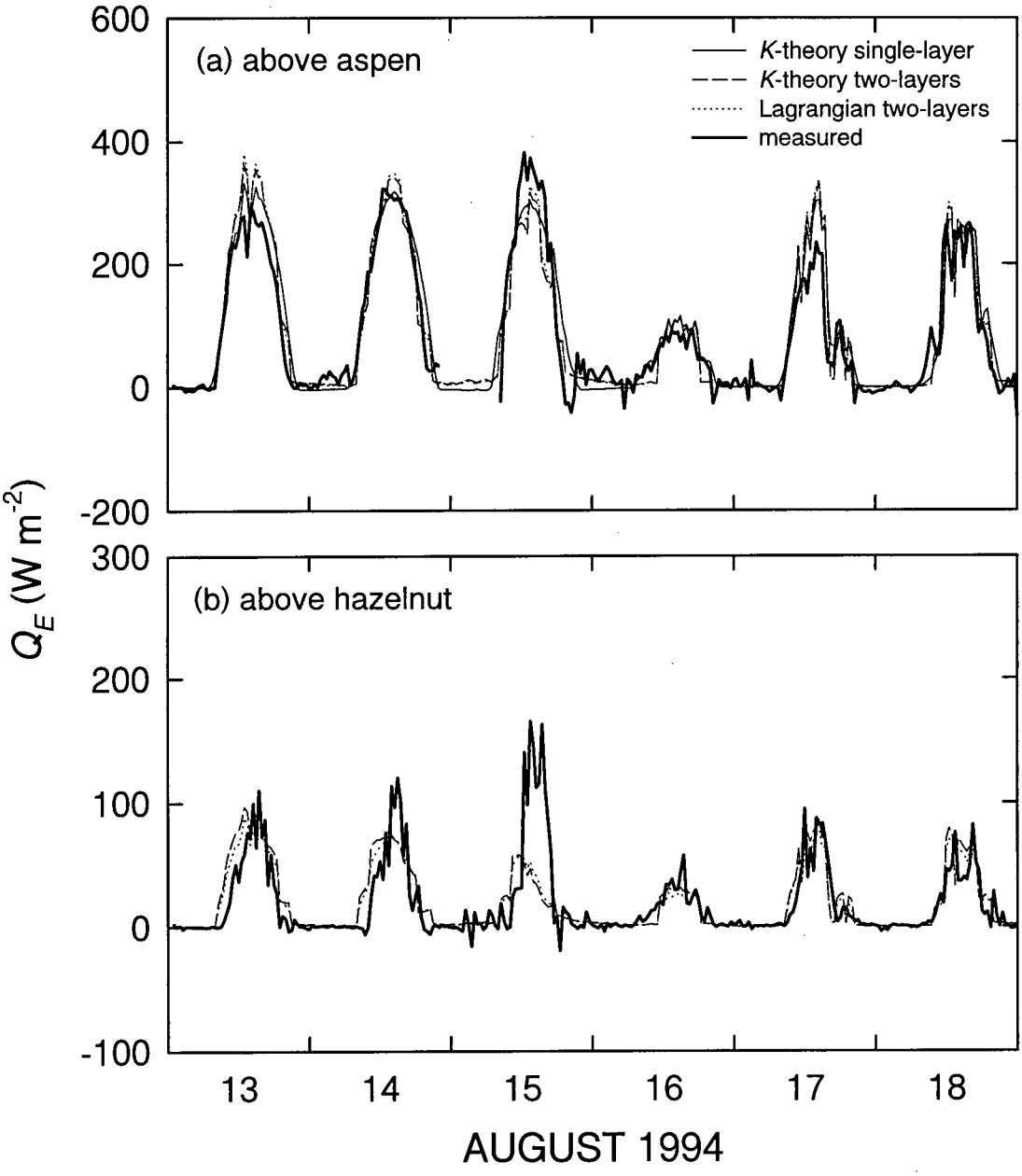

Fig. 6.5. Comparison of half-hourly values of the latent heat flux (Q_E) above the overstory (a) and understory (b) calculated using the two-layer models with the measured values at the 39- and 4-m heights, respectively, during the six-day period in Fig. 6.4.

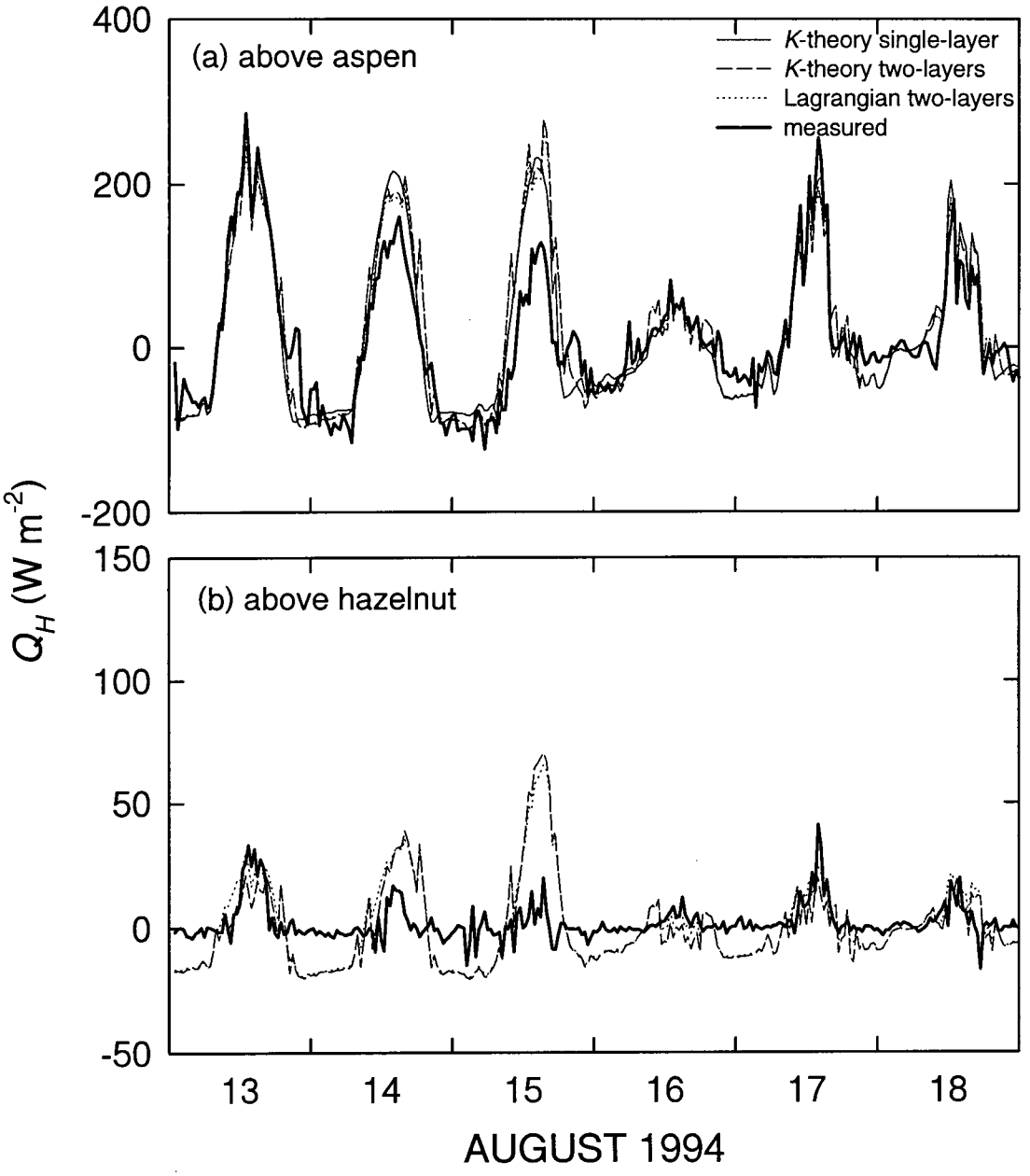

Fig. 6.6. Same as Fig. 6.5 but for the sensible heat flux (Q_H).

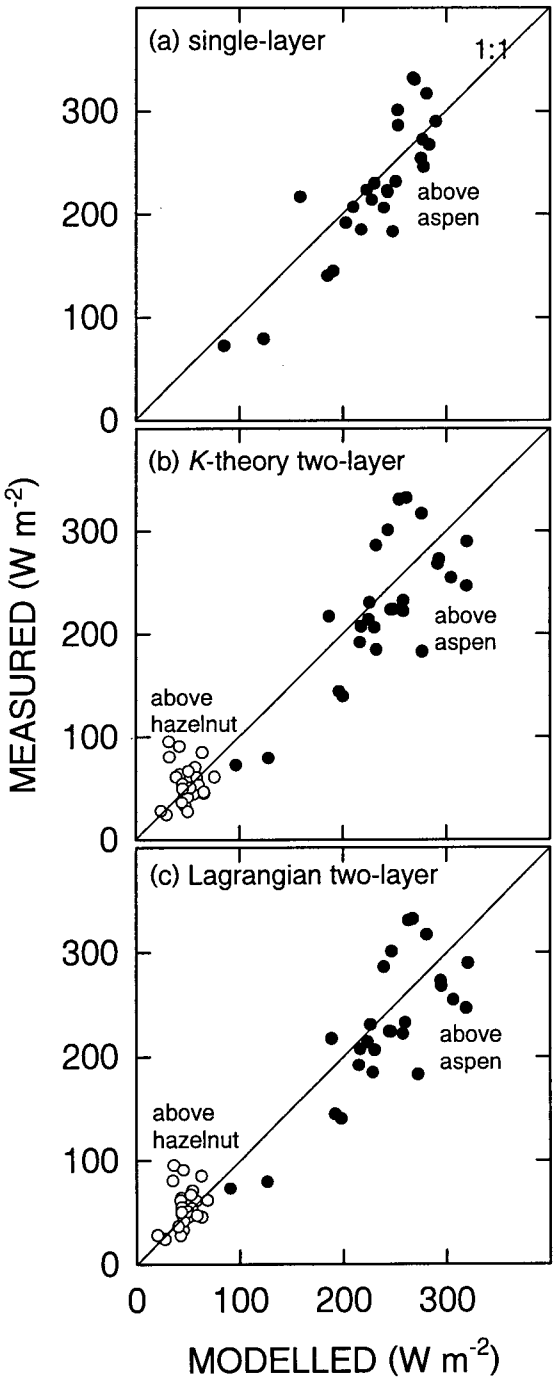

Fig. 6.7. Comparison of daytime means of the latent heat flux calculated using the single-layer model (a), the *K*-theory two-layer model (b) and the Lagrangian two-layer model (c) with measurements from July 29 to August 27, 1994.

6.5. Summary and conclusions

Three models (a K-theory single-layer, a K-theory two-layer and a Lagrangian two-layer) were compared in the calculation of evaporation from a boreal aspen forest. Two layers were used in the latter two models to account for the distinct overstory and understory canopies in this forest and to enable the partitioning of evaporation between overstory and understory. Generally good agreement was obtained between the evaporation rates above and below the overstory simulated using both two-layer models and values measured using the eddy-covariance technique. However, there was little difference between the evaporation rates obtained using the two models. In estimating the total evaporation from the forest, however, the single-layer model performed significantly better than the two-layer models.

These results confirm the conclusion of Van den Hurk and McNaughton (1995) and Dolman and Wallace (1991) that the difference between simulations obtained using K-theory and the Lagrangian evaporation models is small. This is because evaporation from strongly-coupled forest canopies, i.e. low Ω, is mainly controlled by stomatal conductance. This is consistent with the finding in Chapter 5 that adding the near-field resistance in CLASS had little effect on the latent heat flux calculations.

Although more parameters were included in the two-layer models than in the single-layer model, the single-layer model performed better than the two-layer models. This is likely due to the larger uncertainty in the canopy resistance of the aspen overstory ($r_{c,1}$) and hazelnut understory ($r_{c,2}$) than in the canopy resistance of the whole forest (r_c). The large uncertainty in $r_{c,1}$ and $r_{c,2}$ results from errors in partitioning evaporation between the overstory and understory canopies obtained using the eddy-covariance

measurements. These errors are primarily due to (1) the occasional occurrence of low wind speeds above the understory which cause underestimation of understory evaporation and (2) the large difference between the flux foot prints of the understory and overstory eddy-covariance sensors (the understory foot print is about a third of the above-forest foot print (Blanken 1997)). Parameterizing forest r_c avoids these uncertainties and probably gives better estimates of r_c because (1) the understory evaporation was only about 20% of the forest evaporation and (2) $r_{c,1}$ and $r_{c,2}$ were highly correlated. This is an illustration of the point made by Raupach and Finnigan (1988) that a large number of parameters required in multi-layer models (with associated errors) makes them less practical than single-layer models.

6.6. References

Black, T. A., G. den Hartog, H. H. Neumann, P. D. Blanken, P. C. Yang, C. Russell, Z. Nesic, X. Lee, S. C. Chen, R. Staebler and M. D. Novak. 1996. Annual cycles of water vapour and carbon dioxide fluxes in and above a boreal aspen forest. *Global Change Biology*, 2: 219-229.

Blanken, P. D., T. A. Black, P.C. Yang, H. H. Neumann, Z. Nesic, R. Staebler, G. den Hartog, M. D. Novak and X. Lee. 1997. Energy balance and canopy conductance of a boreal aspen forest: partitioning overstory and understory components. *J. Geophys. Res.*, 102 D24, 28915-28927.

Blanken, P. D. 1997. Evaporation within and above a boreal aspen forest, Ph.D. Thesis, University of British Columbia, Vancouver, BC, Canada, 185 pp.

Chen, J. 1984. Uncoupled multi-layer model for the transfer of sensible and latent heat flux densities from vegetation. *Boundary Layer Meteorol.*, 28: 213-226.

Chen, J. M., P. D. Blanken, T. A. Black, M. Guilbeault and S. Chen. 1997. Radiation regime and canopy architecture in a boreal aspen forest. *Agric. For. Meteorol.*, 86: 107-125.

Dolman, A. J. and J. S. Wallace. 1991. Lagrangian and K-theory approaches in modelling evaporation from sparse canopies. *Q. J. R. Meteorol. Soc.*, 117: 1325-1340.

Jarvis, P. G. and K. G. McNaughton. 1986. Stomatal control of transpiration: scaling up from leaf to region. *Adv. Ecol. Res.*, 15: 1-49.

Kabzems, A., A.L. Kosowan and W.C. Harris. 1986. Mixed wood section in an ecological perspective. Tech. Bull. No. 8. Sask. Parks and Renewable Resources, Saskatoon, Sask., 122 pp.

Kelliher, F.M., T.A. Black and D.T. Price. 1986. Estimating the effects of understory removal from a Douglas-fir forest using a two-layer canopy evapotranspiration model. *Water Resources Research*, 22: 1891-1899.

McNaughton, K. G. 1976. Evaporation and advection. II: Evaporation downwind of a boundary separating regions having different surface resistances and available energies. *Q. J. R. Meteorol. Soc.*, 102: 193-202.

McNaughton, K. G. and P. G. Jarvis. 1983. Predicting effects of vegetation changes on transpiration and evaporation. In: T. T. Kozlowski (Editor), *Water Deficits and Plant*

Growth, Academic, Orlando, Vol. 7, 1-47.

McNaughton, K. G. and B. J. J. M. Van den Hurk. 1995. A Lagrangian revision of the resistors in the two-layer model for calculating the energy budget of a plant canopy. *Boundary Layer Meteorol.*, 74: 261-288.

Owen, P. R. and W. R. Thompson. 1963. Heat transfer across rough surfaces. *Journal of Fluid Mechanics*, 15: 321-334.

Pitman, A. J. 1994. Assessing the sensitivity of a land-surface scheme to the parameter values using a single column model. *J. Climate*, 7: 1856-1869.

Raupach, M. R. and J. J. Finnigan. 1988. Single layer models of evaporation from plant communities are incorrect, but useful, whereas multi-layer models are correct but useless: discussion. *Aust. J. Plant Physiol.* 15: 705-716.

Raupach, M. R. 1989. A practical Lagrangian method for relating scalar concentration to source distributions in vegetation canopies. *Q. J. R. Meteorol.*, 115: 609-632.

Van den Hurk, B. J. J. M. and K. G. McNaughton. 1995. Implementation of near-field dispersion in a simple two-layer surface resistance model. *J. Hydrol.*, 166: 293-311.

Verma, S. B. 1989. Aerodynamic resistances to transfers of heat, mass and momentum. In: *Estimation of Areal Evapotranspiration, IAHS Publ.*, 177: 13-20.

CHAPTER 7

SUMMARY AND CONCLUSIONS

The Canadian Land Surface Scheme (CLASS) was evaluated in stand-alone format (off-line) to compare (i) modelled fluxes of radiation, heat, and water vapour with those measured above six west coast Douglas-fir forests, a boreal aspen forest, two agricultural crops and two bare soils, and (ii) modelled values of soil water content with those measured at a bare soil site over a 66-day summer period and at the aspen site over a five-year period. Improved parameterizations for calculating evaporation from the soil surface and canopy conductance (g_c) of the Douglas-fir and aspen forests were described to give better flux estimates. Furthermore, in view of the occurrence of counter-gradient flows and intermittent turbulence within the plant canopies which are neglected in current surface schemes, the effectiveness of the Lagrangian near-field resistance and a two-layer Lagrangian canopy evaporation model were tested. The latter was compared with single-layer and two-layer K-theory based models. The most important findings are summarized as follows:

(1) Evaporation from the soil surface was significantly overestimated by Philip's relationship when the soil surface was dry because the relative humidity at the soil surface (α) was overestimated. This was because Philip's relationship worked poorly with a thick surface soil layer as in CLASS. Inspection of relationships of α and β, a dimensionless soil water diffusion resistance, to surface soil water content (θ) for a

bare loam/silt-loam soil at Agassiz showed that they were sensitive to surface layer thickness and became better defined with greater layer thickness. When incorporated into CLASS, both relationships gave much better estimates of evaporation than Philip's relationship. Furthermore, the β relationship performed better than the α relationship.

(2) In long-term simulations of evaporation from the Agassiz bare soil, the effectiveness of the β relationship depended on how well θ of the soil surface layer was modelled. When forced to use measured θ, CLASS gave excellent estimates of evaporation with the β relationship, compared with a significant overestimation with Philip's relationship during drying periods. The effectiveness of the β relationship was also tested using data from a crop and two forests with different soil types and from another bare silt loam soil with a different surface layer thickness. It gave better estimates of evaporation from these surfaces than Philip's relationship.

(3) For the Douglas-fir forest at Dunsmuir Creek in 1983/84, the original CLASS parameterization of g_c, (based on the Jarvis-Stewart (JS) model) performed reasonably well for high soil moisture conditions, but underestimated g_c for low soil moisture conditions. For the aspen forest in 1994, the parameterization significantly underestimated g_c for conditions of high solar irradiance and slightly overestimated g_c for conditions of low solar irradiance. A new JS parameterization, the more physiologically-based Ball-Woodrow-Berry (BWB) parameterization and a modified BWB (MBWB) parameterization were evaluated for the two forests. More

improvement was achieved by using the new JS parameterization than the BWB and MBWB parameterizations. The latter two parameterizations were unable to characterize the daytime range of g_c as well as the JS parameterization.

(4) The successful application of the BWB and MBWB parameterizations required a reliable estimate of the net assimilation rate of the canopy. For the aspen forest, this was modelled satisfactorily using a rectangular hyperbolic function of incident photosynthetically active radiation (PAR) for each of three ranges (high, medium and low) of leaf area index (LAI). The same model was used for the Douglas-fir forest except for two levels of soil moisture. However, it did not work as well as for the aspen forest due to a lack of reliable estimates of soil CO_2 efflux and the complex relationship between assimilation rate and PAR in this forest.

(5) For the aspen forest, the new JS and MBWB parameterizations derived using 1994 data were applied to a five year period from 1994 to 1998, which generally had adequate root-zone soil moisture during the growing season except during the spring of 1998 when rainfall was low. Better agreement between CLASS modelled and measured latent heat fluxes was obtained using the new JS parameterization than the original CLASS and MBWB parameterizations. In the case of the Douglas-fir forest, the new JS and MBWB parameterizations performed better than the original CLASS parameterization. Both parameterizations, obtained using data from the Douglas-fir forest, were also applied to four other similar-aged Douglas-fir forests but with different values of LAI. They generally gave better estimates of evapotranspiration

than the original CLASS parameterization under high soil moisture conditions. In the case of low soil moisture conditions, which occurred in two of the forests, they did not work satisfactorily because the responses of conductance to soil moisture conditions at the two sites were different. This emphasizes the need for soil moisture measurements to adequate depths to account for changes in water uptake with respect to depth as the soil dries.

(6) The five-year test of CLASS for the aspen forest showed that significant improvement in the calculation of evaporation from the soil surface was achieved by using the β relationship during leaf emergence and senescence periods. The winter albedo used in CLASS (0.5) was too high which caused a significant delay in snowmelt and an underestimation of net radiation before snowmelt. Adjusting the winter albedo to a more realistic value of 0.25 (based on measurements) for the aspen site significantly improved the calculation of snowmelt time and the net radiation before modelled snowmelt. More importantly, the decrease in the winter albedo significantly reduced the overestimation of the surface runoff after snowmelt which led to better agreement between modelled and measured θ.

(7) McNaughton and van den Hurk's (1995) near-field resistance (r_n) was estimated using the Lagrangian localized near-field theory of Raupach (1989) for two forests: one with a thick understory (aspen) and the other with little understory (Douglas-fir). The value of r_n for the aspen forest was well approximated by $0.53/u_*$ (u_* is the friction velocity), compared to $0.42/ u_*$ for the Douglas-fir forest. The ratio of r_n to the far-

field resistance ($r_{f\,1}$) increased with decreasing u_*, compared to a constant ratio suggested by McNaughton and van den Hurk (1995). The ratio of r_n to the aerodynamic resistance (r_a) was much smaller (less than 0.2) than the ratio of r_n to r_{f1}. Including r_n in the flux-gradient relationship, which used the measured air temperature difference between the effective canopy source height and the reference height, significantly improved the calculation of the sensible heat fluxes from the two forests. However, since the ratio of r_n to r_a was small, the inclusion of r_n in CLASS only had a small effect on the calculated sensible and latent heat fluxes both above and below the canopy layer of both forests and an agricultural crop. It therefore suggests that, as found by others, for practical purposes *K*-theory remains an adequate approximation of turbulent transport in large-scale models.

(8) Three models (a *K*-theory single-layer model, a *K*-theory two-layer model and a Lagrangian two-layer model) were compared in the calculation of evaporation from the aspen forest. Two layers were used in the latter two models to account for the distinct overstory and understory canopies in this forest and to enable the partitioning of evaporation between overstory and understory. There was little difference between the evaporation rates obtained using the two two-layer models. Both models estimated the evaporation from the understory reasonably well. In estimating the total evaporation from the forest, however, the single-layer model performed significantly better than the two-layer models. These results (i) confirm that the difference between simulations obtained using *K*-theory and the Lagrangian evaporation models is small because evaporation from strongly-coupled forest canopies is mainly controlled by

stomatal conductance and (ii) illustrate the point made by Raupach and Finnigan (1988) that a large number of parameters required in multi-layer models (with associated errors) makes them less practical than single-layer models.

In conclusion, the β relationship obtained using data from a bare loam/silt-loam soil was found to be effective in improving the calculation of evaporation from other forest and agricultural soil surfaces. Until more experimental data are available to refine the coefficients used in the β relationship for different mineral and organic soils, it is recommended that this relationship be used in CLASS to approximate evaporation from other soil surfaces. Although this study has resulted in significant improvements to the parameterization of g_c, the original CLASS parameterization performed surprisingly well as was shown in PILPS, the Project for Intercomparison of Land-surface Parameterization Schemes (Chen et al. 1997). This illustrates the point made by Roberts (1983) and Kelliher et al. (1995) that there is a surprising conservatism in canopy conductance of natural vegetation types. The different responses of g_c to low θ in the two Douglas-fir forests are probably due to differences in the vertical distribution of water extraction by roots. This points to the importance of measuring soil moisture deep enough to take account of responses of g_c to changes in θ. Finally, this research shows that for land surface schemes like CLASS, a single-layer K-theory based canopy model appears to be adequate, even for forests with a substantial understory.

REFERENCES

Chen, T. H., A. Henderson-Sellers, P. C. D. Milly, A. J. Pitman, A. C. M. Beljaars, J. Polcher, F. Abramopoulos, A. Boone, S. Chang, F. Chen, Y. Dai, C. E. Desborough, R. E. Dickinson, L. Dumenil, M. Ek, J. R. Garratt, N. Gedney, Y. M. Gusev, J. Kim, R. Koster, E. A. Kowalczyk, K. Laval, J. Lean, D. Lettenmaier, X. Liang, J. -F. Mahfouf, H.-T. Mengelkamp, K. Mitchell, O. N. Nasonova, J. Noilhan, A. Robock, C. Rosenzweig, J. Schaake, C. A. Schlosser, J.-P. Schulz, Y. Shao, A. B. Shmakin, D. L. Verseghy, P. Wetzel, E. F. Wood, Y. Xue, Z. -L. Yang and Q. Zeng. 1997. Cabauw experimental results from the Project for Intercomparison of Land-Surface Parameterization Schemes. *J. Climate*, 10: 1194-1215

Kelliher, F. M., R. Leuning, M. R. Raupach and E.-D. Schulze. 1995. Maximum conductances for evaporation from global vegetation types. *Agric. For. Meteorol.*, 73: 1-16.

McNaughton, K. G. and B. J. J. M. Van den Hurk. 1995. A Lagrangian revision of the resistors in the two-layer model for calculating the energy budget of a plant canopy. *Boundary layer Meteorol.*, 74: 261-288.

Raupach, M. R. and J. J. Finnigan. 1988. Single layer models of evaporation from plant communities are incorrect, but useful, whereas multi-layer models are correct but useless: discussion. *Aust. J. Plant Physiol.* 15: 705-716.

Raupach, M. R. 1989. A practical Lagrangian method for relating scalar concentration to source distributions in vegetation canopies. *Q. J. R. Meteorol.*, 115: 609-632.

Roberts, J. 1983. Forest transpiration: a conservative hydrological process? *J. Hydrology*, 66: 133-141.

APPENDIX A

OUTLINE OF THE CANADIAN LAND SURFACE SCHEME

The formulation of the Canadian land surface scheme (CLASS) was documented in detail in Verseghy (1991) and Verseghy et al. (1993).

A.1. Outline of the CLASS Soil Model

The modelled soil column in CLASS is divided into three layers, which have depths of 0.10, 0.25, and 3.75m, respectively. The temperature and soil water content for each layer and at the soil surface are computed at each time step. Snow cover, if present, is modelled as a separate "soil" layer, with appropriate thermal and hydraulic properties based on the calculated depth and density of the snow pack. Heat and moisture transfers at the soil surface and between layers are calculated based on physical theory. The surface infiltration rate depends on the rainfall rate, the presence of water detained on the surface and the soil moisture profile.

CLASS has eight prognostic physical state variables for the soil model: surface temperature T_s, average soil temperatures $T_{i,g}$ (i = 1, 2 and 3) for the three layers, average soil moistures θ_i (i =1, 2, 3) and interception water/snow store W on soil surface. The governing equations are

$$Q_g^* + Q_{H,g} + Q_{E,g} = G_0 \tag{A.1}$$

$$T_{1,g}(t+1) = T_{1,g}(t) + \left[G(0,t) - G(z_1,t)\right]\frac{\Delta t}{C_1 \Delta z_1} \pm S_1 \tag{A.2}$$

$$T_{2,g}(t+1) = T_{2,g}(t) + \left[G(z_1,t) - G(z_2,t)\right]\frac{\Delta t}{C_2 \Delta z_2} \pm S_2 \quad \text{(A.3)}$$

$$T_{3,g}(t+1) = T_{3,g}(t) + G(z_2,t)\frac{\Delta t}{C_3 \Delta z_3} \pm S_3 \quad \text{(A.4)}$$

$$\theta_1(t+1) = \theta_1(t) + \left[F(0,t) - F(z_1,t)\right]\frac{\Delta t}{\Delta z_1} \quad \text{(A.5)}$$

$$\theta_2(t+1) = \theta_2(t) + \left[F(z_1,t) - F(z_2,t)\right]\frac{\Delta t}{\Delta z_2} \quad \text{(A.6)}$$

$$\theta_3(t+1) = \theta_3(t) + \left[F(z_2,t) - F(z_3,t)\right]\frac{\Delta t}{\Delta z_3} \quad \text{(A.7)}$$

$$W(t+1) = W(t) + r - I - E_i \quad \text{(A.8)}$$

where Q^*_g is the net radiation above soil surface, $Q_{H,\,g}$ and $Q_{E,\,g}$ are the sensible and latent heat fluxes from soil surface, respectively, G_0 and $G(z_i, t)$ are the soil heat flux at the surface and at the depth of z_i, respectively, Δz_i is the soil layer depth, C_i is the volumetric heat capacity of the soil, S_i is a correction term for freezing or thawing, $T_{i,\,g}$ and θ_i are the average soil temperature and volumetric soil moisture for layer i, $F(z_i,\ t)$ is the liquid water flow rate at depth of z_i, W is the water or snow-ice stored on the ground, r and I are the precipitation and infiltration rates, respectively, and E_i is the evaporation rate from ponded water present on the surface.

The surface heat flux G_0 is expressed in a linear combination of the soil temperatures:

$$G_0 = a_1 T_{1,g} + a_2 T_{2,g} + a_3 T_{3,g} + a_4 T_s + a_5 \quad \text{(A.9)}$$

where the a terms represent constants, determined depending on the soil physical and thermal properties.

$Q_{H,g}$ and $Q_{E,g}$ are given by the bulk transfer formulae:

$$Q_{H,g} = \varrho_a c_p u C_D [T_a - T_s] \tag{A.10}$$

$$Q_{E,g} = L_v \varrho_a u C_D [q_a - q_s] \tag{A.11}$$

where ϱ_a, c_p, T_a, and q_a represent the density, specific heat, temperature, and specific humidity of air in the surface layer, respectively, u is the wind speed, L_v is the latent heat of vaporization, and C_D is a drag coefficient. The surface specific humidity q_s can be expressed as

$$q_s = h_s \times q_{sat}[T_s] \tag{A.12}$$

where q_{sat} represents the saturated specific humidity at temperature T_s, and h, the relative humidity of air of the surface soil pore, is given by

$$h_s = \exp\left[\frac{-g\psi_s}{R_v T_s}\right] \tag{A.13}$$

where g is the acceleration due to gravity, ψ_s is the soil water tension at the surface determined by Eq. (A. 16) with $\theta_1(0)$ determined by extrapolating $\theta_1(z)$ to the soil surface, and R_v is the gas constant for water vapour.

Under conditions of no precipitation, $F(0)$ is given by the surface evaporation rate. The other $F(z_i)$ terms are calculated using the Darcian equation

$$F(z_i) = k(z_i)\left[\frac{d\psi}{dz} + 1\right]_{z=z_i} \tag{A.14}$$

where $k(z)$ represents the hydraulic conductivity at depth z. $k(z)$ and $\psi(z)$ are related to $\theta(z)$ and a soil texture parameter 'b' by power relations given by Clapp and Hornberger (1978):

$$k(z_i) = k_{sat}\left[\frac{\theta_1(z_1)}{\theta_p}\right]^{(2b+3)} \tag{A.15}$$

and

$$\psi(z_i) = \psi_{sat}\left[\frac{\theta_1(z_1)}{\theta_p}\right]^{-b} \tag{A.16}$$

where k_{sat} and ψ_{sat} represent the saturated hydraulic conductivity and effective saturated soil water tension, respectively, and θ_p is the pore volume fraction. CLASS uses derived relationships between b, θ_p, k_{sat}, ψ_{sat}, and soil texture by Cosby et al. (1984).

By substituting Eqs (A. 9) to (A. 11) into Eq. (A. 1), the resultant expression is a function only of T_s, certain meteorological variables supplied by input, and a set of known soil properties. The surface temperature T_s can thus be solved iteratively and substituted back into Eqs (A. 9) to (A. 11) to determine the energy balance terms for next step.

A.2. Outline of CLASS Vegetation Model

CLASS currently treated the vegetation cover as a single layer thermally separated from the ground. Four broad vegetation groups were recognized within the canopy-covered subareas of each grid square: needleleaf trees, broadleaf trees, crops and grass. The physical characteristics of the 'composite' canopy such as leaf area index, roughness length etc. were calculated by bulk averaging over the component vegetation types present on each grid cell. Canopy evapotranspiration rates depend on the presence of intercepted water on the canopy, and on the bulk stomatal resistance which varies with soil moisture, incoming solar radiation, atmospheric vapour pressure deficit, canopy temperature and leaf area index. Radiative and turbulent fluxes to the atmosphere from the canopy were calculated separately over each subarea. The former is on the basis of

calculated albedos and surface temperatures of the different surface components, and the latter is on the basis of Monin-Obukhov similarity theory with stability corrections based on the bulk Richardson numbers over the subareas.

CLASS has two prognostic physical state variables for the canopy layer: canopy temperature T_0, which also is calculated by iterative solution of the energy balance equation, and interception water/snow store W on vegetation surfaces. The governing equations are

$$Q_c^* + Q_{H,c} - Q_{H,g} + Q_{E,c} + S_h = \frac{C_c}{\Delta t}\left[T_0(t) - T_0(t-1)\right] \tag{A.17}$$

$$W_c(t+1) = W_c(t) + \hat{\chi} r \Delta t - E_{i,c} \tag{A.18}$$

where Q^*_c is the absorbed net radiation for the canopy layer, $Q_{H,\,c}$ and $Q_{H,\,g}$ are the sensible heat fluxes from the canopy and from the soil surface under the canopy, respectively, $Q_{E,\,c}$ is the latent heat flux from the canopy, S_h is the heat for freezing or thawing of moisture stored on the canopy, C_c is the effective canopy heat capacity, T_c is the canopy temperature, W is the water or snow-ice stored on the canopy, E_i is the evaporation rate from interception store, $\hat{\chi}$ is the canopy sky view factor, r is the precipitation rate.

The energy fluxes are given by the bulk transfer formulae:

$$Q_{H,c} = \varrho_a c_p (T_a - T_0)/r_a \tag{A.19}$$

$$Q_{E,c} = L_v \varrho_a \left[q_a - q_{sat}(T_0)\right]/(r_a + r_c) \tag{A.20}$$

$$Q_{H,g} = 1.9\times10^{-3} \varrho_a c_p \left[T_0 - T_s\right]\left[T'_s - T'_{a,0}\right]^{1/3} \tag{A.21}$$

where T_a is the air temperature, q_a and q_{sat} are the specific humidity and saturation specific humidity, respectively, T'_s and $T'_{a,0}$ are the virtual temperature of the ground and

air within the canopy, respectively, ϱ_a is the air density, c_p is the specific heat, L_v is the latent heat of vaporization of water, r_a is the aerodynamic resistance between canopy air space and reference height, r_c is the bulk stomatal resistance of canopy layer. r_a is calculated from the surface drag coefficient C_D and the wind speed u above the canopy as

$$r_a = [C_D u]^{-1} \tag{A.22}$$

where C_D is calculated based on Monin-Obukhov similarity theory with stability correction based on the bulk Richardson numbers over the subareas (Verseghy et al., 1993). If the canopy is dry (otherwise, r_c = 0.0 s m^{-1}), the canopy resistance r_c is described by the empirical model, similar to those by Jarvis (1976) and Stewart (1988):

$$r_c = r_{c,\min}[\Lambda_{\max} / \Lambda] f_1(K_\downarrow) f_2(\Delta e) f_3(\psi) f_4(T_a) \tag{A.23}$$

$$f_1(K_\downarrow) = \max(1.0, 500 / K_\downarrow - 1.5) \qquad (K_\downarrow \text{ in W m}^{-2}) \tag{A.24}$$

$$f_2(\Delta e) = \max(1.0, \Delta e / 0.5) \qquad (\Delta e \text{ in kPa}) \tag{A.25}$$

$$f_3(\psi) = \max(1.0, \psi / 40) \qquad (\psi \text{ in m}) \tag{A.26}$$

$$f_4(T_a) = \begin{cases} 1.0 & 40^\circ C > T_a > 0^\circ C \\ 5000\Lambda / (r_{c,\min}\Lambda_{\max}) & T_a \geq 40^\circ C \text{ or } T_a \leq 0^\circ C \end{cases} \tag{A.27}$$

where ψ is the minimum value of soil water tension in the soil layers contained within the rooting zone.

Finally, the radiative, sensible and latent heat fluxes of the canopy covered land surface, as seen by the overlying atmosphere, can be written as

$$K^\uparrow = \hat{\alpha}_c K_\downarrow \tag{A.28}$$

$$L^\uparrow = (1 - \hat{\chi})\sigma T_0^4 + \hat{\chi}\sigma T_s^4 \tag{A.29}$$

$$Q_H = -Q_{H,c} \tag{A.30}$$

$$Q_E = -Q_{E,c} - Q_{E,g/s} \tag{A.31}$$

where K and L are the shortwave and longwave radiation fluxes, respectively, $\hat{\alpha}_c$ is the canopy albedo, $Q_{E,\,g/s}$ is the evaporation from the ground surface under the canopy

$$Q_{E,g/s} = 1.9\times10^{-3} L_v \varrho_a \left[q_{a,c} - q_s\right]\left[T'_s - T'_{a,0}\right]^{1/3} \tag{A.32}$$

References

Clapp, R. B. and G. M. Hornberger. 1978. Empirical equations for some soil hydraulic properties. *Water Resour. Res.*, 14: 601-604.

Cosby, B. J., G. M. Hornberger, R. B. Clapp and T. R. Ginn. 1984. A statistical exploration of the relationship of soil moisture characteristics to the physical properties of soils. *Water Resour. Res.*, 20: 682-690.

Jarvis, P. G. 1976. The interpretation of the variation in leaf water potential and stomatal conductance found in canopies in the field. *Phil. Trans. R. Soc.*, Lond. B. 273: 593-610.

Stewart, J. B. 1988. Modelling surface conductance of pine forest. *Agric For. Meteorol.*, 43: 19-35.

Verseghy, D. L. 1991. CLASS - A Canadian land surface scheme for GCMs, I. Soil model. *Int. J. Climatol.*, 11: 111-133.

Verseghy, D. L.; N. A. McFarlane and M. Lazare. 1993. CLASS - a Canadian land surface scheme for GCMs, II. Vegetation model and coupled runs. *Int. J. Climatol.*, 13: 347-370.

APPENDIX B

COMPARISON OF EXTINCTION COEFFICIENTS, AERODYNAMIC RESISTANCE AND CANOPY TEMPERATURE IN DOUGLAS-FIR AND ASPEN FORESTS CALCULATED USING THE CANADIAN LAND SURFACE SCHEME WITH THOSE OBTAINED FROM MEASUREMENTS

B.1. Extinction Coefficients

The needle leaf extinction coefficients for the global and visible radiation used in CLASS were found to be significantly underestimated (Fig. B.1) based on the radiation measurements under a Douglas-fir overstory at Woss, BC, using a tram system (Black et

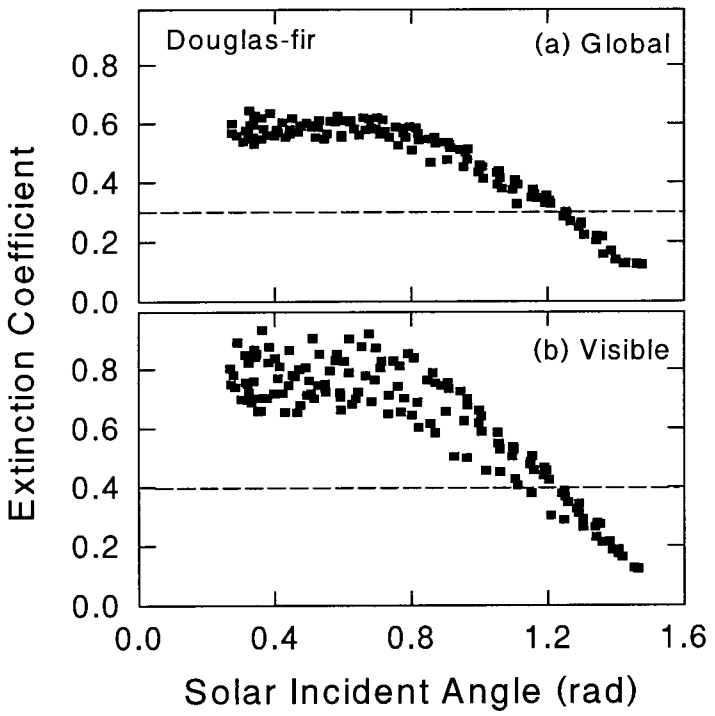

Fig. B.1. Comparison of the measured extinction coefficients in the global (a) and visible (b) ranges for the Douglas-fir forest at Woss, British Columbia, with those from CLASS (dashed straight lines).

al. 1991). Note that the extinction coefficients are strongly dependent on the solar incident angle, indicating leaf angular distribution of a Douglas-fir canopy is very much different from the case of a random distribution which would have a horizontal line. For a boreal aspen forest in Prince Albert National Park, Saskatchewan, the measured extinction coefficients for the global and visible radiation decreased with the increase of the plant area index (PAI = $\Lambda + a_w$ where Λ is the leaf area index and a_w is the wood area index equal to 0.62 for the aspen forest) based on the radiation measurements below the aspen overstory using a tram platform moving along a horizontal distance of 60-m (Blanken, 1997) (Fig. B.2). During the full leaf period, the CLASS extinction coefficients are close to those from measured values. High values at low PAI are believed to be related to the effect of the wood part of the aspen canopy.

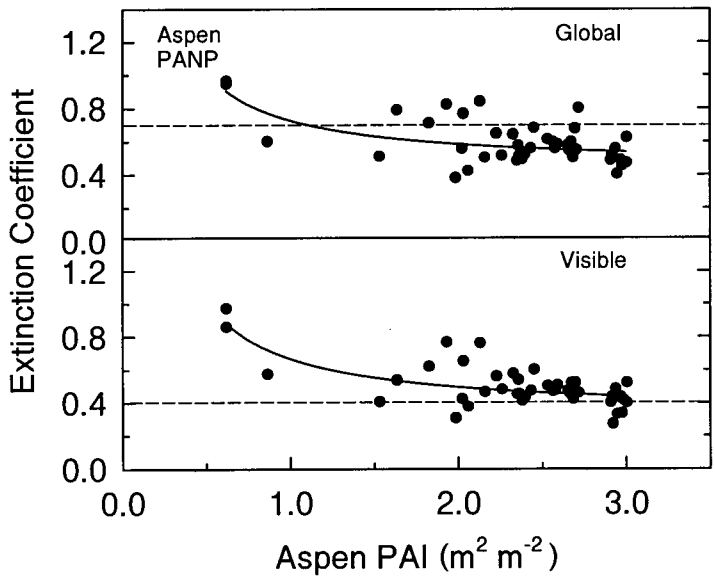

Fig. B. 2. Same as Fig. B.1 but for the aspen forest at Prince Albert, Saskatchewan.

The underestimation of the extinction coefficients can cause an underestimation of the absorbed net radiation for the canopy, and therefore lead to an underestimation of the modelled canopy temperature and the sensible heat flux from the canopy because both are computed from the energy balance equation. However, the final impact on the energy balance components depends on how well the canopy and aerodynamic resistances are estimated (Chapter 3).

B.2. Aerodynamic resistance

The aerodynamic resistance, r_a (s m^{-1}), was estimated using $u/u_*^2 + B^{-1}/u_*$, where u (m s^{-1}) is the wind speed, u_* (m s^{-1}) is the friction velocity (both measured), and B^{-1} is the dimensionless sublayer Stanton number (Owen and Thompson 1963, Verma 1989), which was set equal to 2.5 for the aspen forest (Blanken et al. 1997) and 2.0 for the Douglas-fir forest (Chapter 3). Fig. B.3 shows an example of comparison between r_a calculated by CLASS and those calculated from the measured wind velocity and friction velocity for the aspen forest on August 14, 1994. The selected day was cloudfree with weed speed at 39-m height typically around between 2 and 3 m s^{-1}. Values of daytime r_a from CLASS were about 2 to 3 times smaller than those estimated here. During the nighttime, however, values of CLASS r_a were much larger than the estimated values which caused the canopy temperature to be significantly underestimated (see Fig. B.4). Similar results were also found for the Douglas-fir forests at Dunsmuir Creek, Haney and Courtenay. The decrease in r_a would increase the modelled sensible heat flux. However, the effect of r_a on the calculation of the sensible and latent heat fluxes from the canopy during the daytime is small because r_a is generally much smaller than the canopy

resistance. For the Douglas-fir forests, however, it was found that the effect of low r_a and low extinction coefficients was largely offset by each other during the daytime.

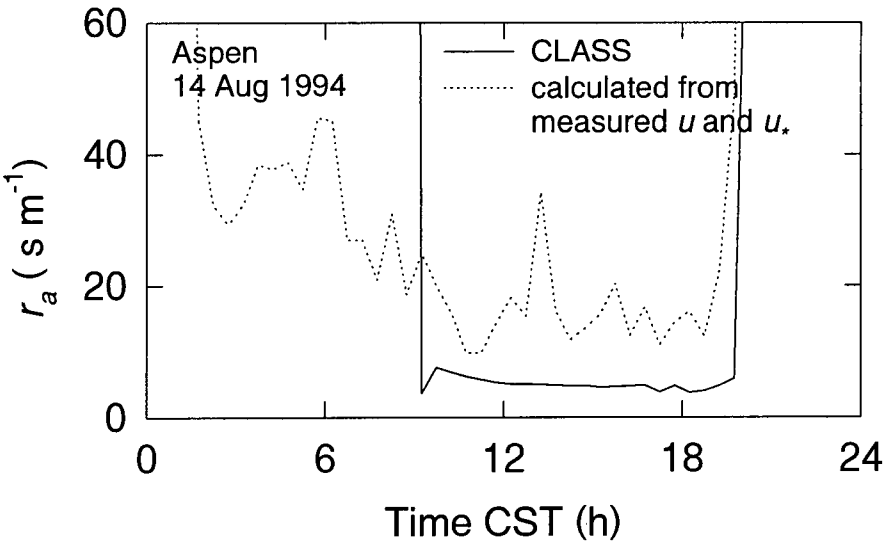

Fig. B.3. Comparison of the aerodynamic resistance from CLASS with those estimated based on the measurements of the wind speed and friction velocity for the aspen forest.

B.3. Canopy temperature

The simulated canopy temperature by CLASS is compared with leaf temperature measured using infrared thermometers and air temperature T_a measured at the 19-m height (note the aspen stand has an even-height of 21 m) above the ground for the aspen forest during the selected five-day period in 1994 used in Chapter 3 (Fig. B.4). The first three days were cloud-free with a wide range of saturation deficit. August 16 and 17 were overcast and partly cloudy, respectively. The good agreement between the measured leaf temperature and air temperature demonstrated the close coupling between the leaf surface

and the air surrounding the leaves. Blanken (1997) found that there was also close agreement between saturation deficit at the 'big leaf' surface and the ambient air. The simulated canopy temperatures agreed well with measured values during the daytime. However, there was a significant underestimation of canopy temperature during the

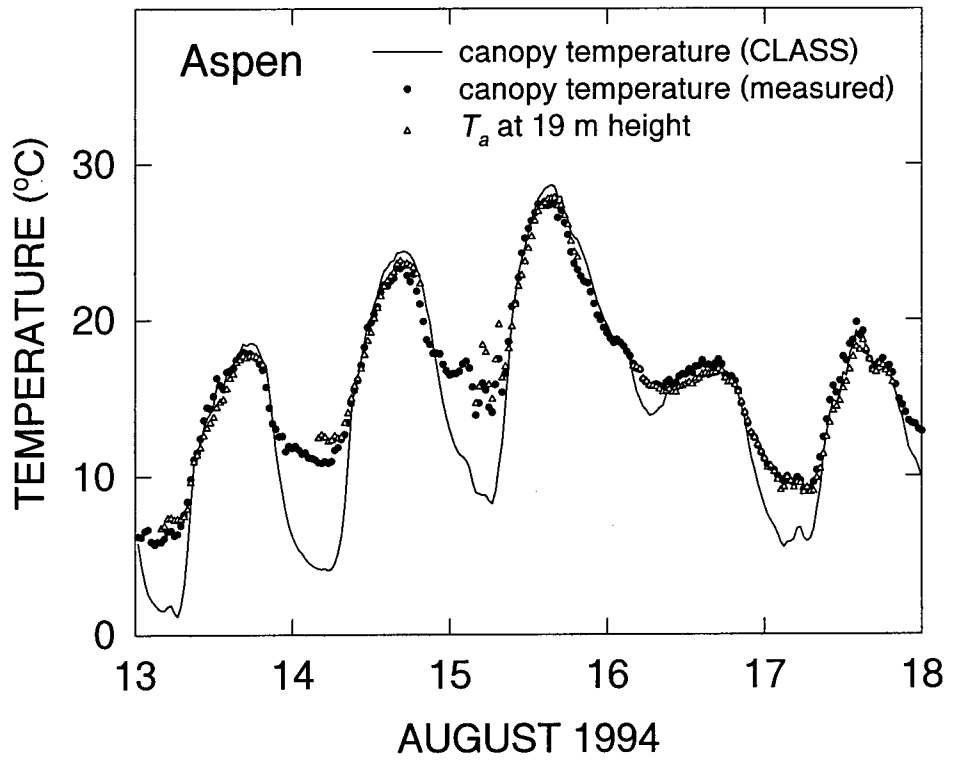

Fig. B.4. Comparison of hour-hourly simulated canopy temperature by CLASS with the leaf temperature measured using infrared thermometers for the aspen forest from August 13 to 17, 1994. Also shown is the air temperature (T_a) measured at 19-m height.

nighttime. This was because r_a at night was significantly overestimated (Fig. B.3). Examination of the nighttime r_a calculated using CLASS indicated that this was because the bulk Richardson number was significantly overestimated.

B.4. Conclusions

The extinction coefficients used in CLASS, which vary with vegetation type, agreed well with the measured values for a boreal aspen forest, but they were significantly lower than the measured values observed for a Douglas-fir forest. Values of the aerodynamic resistance calculated by CLASS were found to be underestimated during the daytime, but significantly overestimated during the nighttime. The latter was found to be caused by the overestimation of the bulk Richardson number. Canopy temperature was simulated well during the daytime, but underestimated during the nighttime due to the overestimation of the aerodynamic resistance.

References

Black, T. A., G. den Hartog, H. H. Neumann, P. D. Blanken, P. C. Yang, C. Russell, Z. Nesic, X. Lee, S. C. Chen, R. Staebler and M. D. Novak. 1996. Annual cycles of water vapour and carbon dioxide fluxes in and above a boreal aspen forest. *Global Change Biology*, 2: 219-229.

Black, T. A., J. M. Chen, X. Lee and R. M. Sagar. 1991. Characteristics of shortwave and longwave irradiances under a Douglas-fir forest stand. *Can. J. For. Res.*, 21(7):1020-1028.

Blanken, P. D. 1997. Evaporation within and above a boreal aspen forest. *Ph.D. Thesis*, University of British Columbia, Vancouver, BC, Canada. 185 pp.

Blanken, P. D., T. A. Black, P.C. Yang, H. H. Neumann, Z. Nesic, R. Staebler, G. den Hartog, M. D. Novak and X. Lee. 1997. Energy balance and canopy conductance of a boreal aspen forest: partitioning overstory and understory components. *J. Geophys. Res.*, 102 D24, 28915-28927.

Owen, P. R. and W. R. Thompson. 1963. Heat transfer across rough surfaces. *Journal of Fluid Mechanics*, 15: 321-334.

Verma, S. B. 1989. Aerodynamic resistances to transfers of heat, mass and momentum. In: *Estimation of Areal Evapotranspiration, IAHS Publ.*, 177: 13-20.

Verseghy, D. L., N. A. McFarlane, and M. Lazare. 1993. CLASS - a Canadian land surface scheme for GCMs, II. Vegetation model and coupled runs. *Int. J. Climatol.*, 13: 347-370.

APPENDIX C

TESTING THE PERFORMANCE OF THE CANADIAN LAND SURFACE SCHEME IN THE CALCULATION OF THE ENERGY BALANCE COMPONENTS FOR A WET ALFALFA CROP

The data were collected between July to September in 1992 from an alfalfa crop at Elora Research Station, Ontario, by the University of Guelph (K. King 1996, personal communication). During the observational period, the crop had an average height of 15 cm on July 11 and 40 cm on July 21. It was cut to a height of 15 cm on August 14. It then reached at a height of 30 cm on September 10. The maximum leaf area index was about 3.0. The sensible and latent heat fluxes were measured using the energy balance/Bowen ratio method.

Fig. C.1 compares the modelled and measured half-hourly energy balance components for the alfalfa crop at Elora on 6 September 1992. The soil moisture was high (the value of soil water content near the surface was 0.30 m^3 m^{-3}). The modelled net radiation, Q^* (W m^{-2}), was considerably close to measured values because measured Q^* was used as the longwave radiation forcing variable. Most of Q^* was partitioned between the latent heat flux, Q_E (W m^{-2}), and the soil heat flux, G_0 (W m^{-2}), due to high alfalfa canopy conductance (van Bavel, 1967, Hatterdorf et al., 1990) and the low leaf area index at this site. The modelled energy balance components by CLASS agreed reasonably well with measured values, except that modelled G_0 led measured G_0 earlier by about 3 hours, and modelled Q_E lagged measured Q_E. These discrepancies were believed to be related to the anomaly in the calculation of the diurnal course of the alfalfa canopy conductance, i.e.

the canopy conductance was likely underestimated during the morning but overestimated during the afternoon.

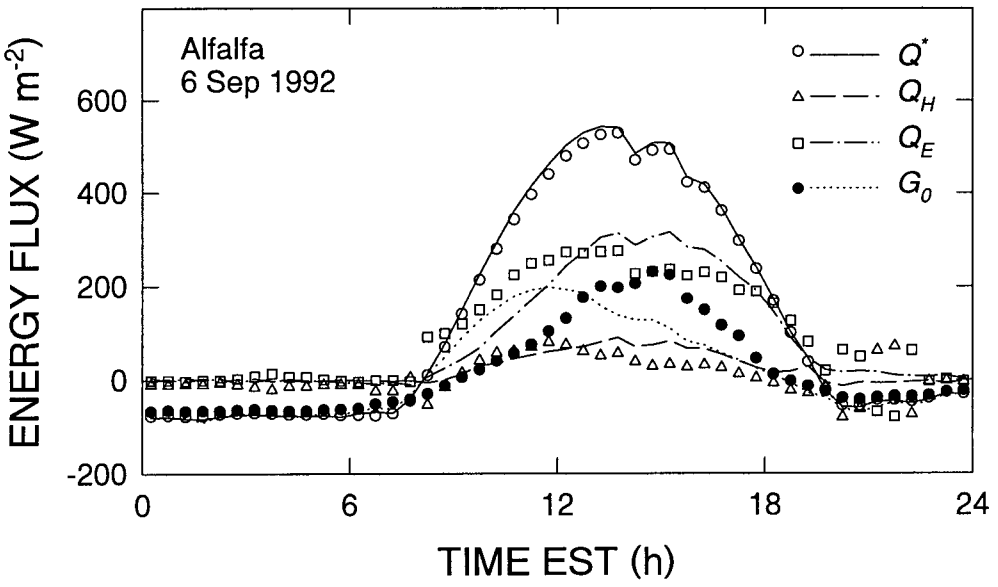

Fig. C.1. Simulated (lines) and observed (symbols) half-hourly energy balance terms for the alfalfa crop at Elora on September 6, 1992.

The long-term comparison is shown in Fig. C.2. There was consierable precipitation throughout the entire growing season, and therefore, the soil water content was generally quite high. The modelled 24-h average Q_E was systematically underestimated and Q_H overestimated. One possible reason was that as discussed above, the alfalfa canopy conductance was underestimated. For example, the minimum canopy resistance (reciprocal of the conductance) for alfalfa was found to be 15 s m^{-1} by Abdul-Jabban et al. (1985) and 30 to 41 s m^{-1} by Hattendorf et al. (1990), compared to a value of

50 s m^{-1} used in CLASS (Verseghy et al. 1993).

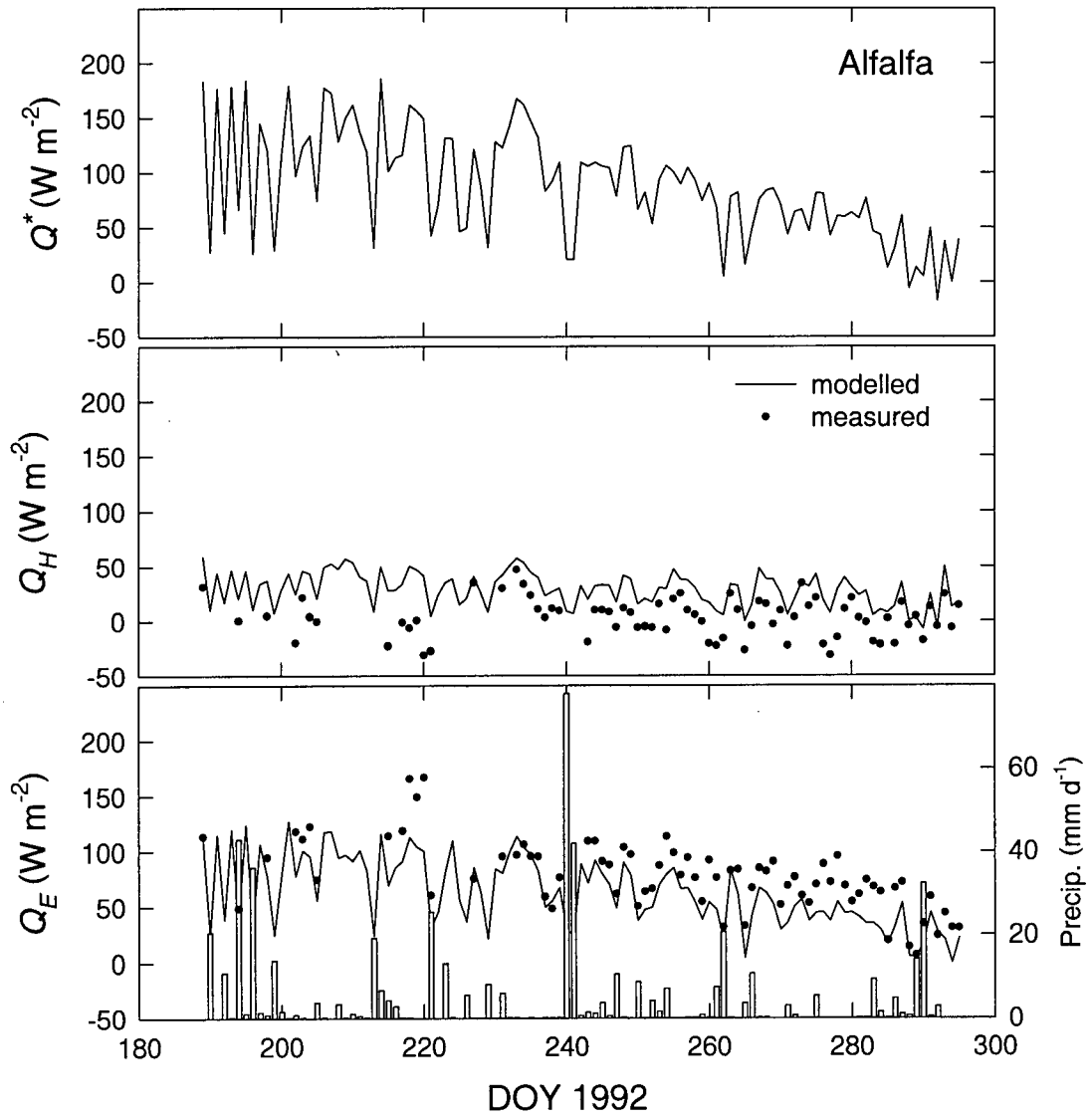

Fig. C.2. Simulated and observed daily energy balance terms for the alfalfa crop at Elora.

References

Abdul-Jabbar, A. S., D. G. Lugg, T. W. Sammis and L. W. Gay. 1985. Relationships between crop water stress index and alfalfa yield and evapotranspiration. *Trans. ASAE*, 28:454-461.

Hatterdorf, M. J., D. W. Evans and R. N. Peaden. 1990. Canopy temperature and stomatal conductance of water-stressed dormant and nondormant alfalfa types. *Agronomy Journal*, 82:873-877.

van Bavel, C. H. M. 1967. Changes in canopy resistance to water loss from alfalfa induced by soil water depletion. *Agric For. Meteorol.*, 4:165-176.

Verseghy, D. L., N. A. McFarlane, and M. Lazare. 1993. CLASS - a Canadian land surface scheme for GCMs, II. Vegetation model and coupled runs. *Int. J. Climatol.*, 13: 347-370.

APPENDIX D

POROMETER MEASUREMENTS OF STOMATAL CONDUCTANCE IN A BOREAL ASPEN FOREST

Stomatal conductance (g_s) measurements were made using a hand-held porometer (model 1600, LI-COR, Inc., Lincoln, NE) at the Old Aspen site during a 3-week (July 12 to August 8) Summer Intensive Field Campaign in 1996. These measurements were made for aspen (*Populus tremuloides* Michx.) overstory (see Fig. 3.1a) and hazelnut (*Corylus cornuta* Marsh.), alder (*Alnus crispa* (Ait.) Pursch) and wild sarsaparilla (*Aralia nudicaulis* L.) understory leaves. Values of g_s were plotted against ambient saturation deficit, Δe (kPa) (Fig. D.1 and D.2).

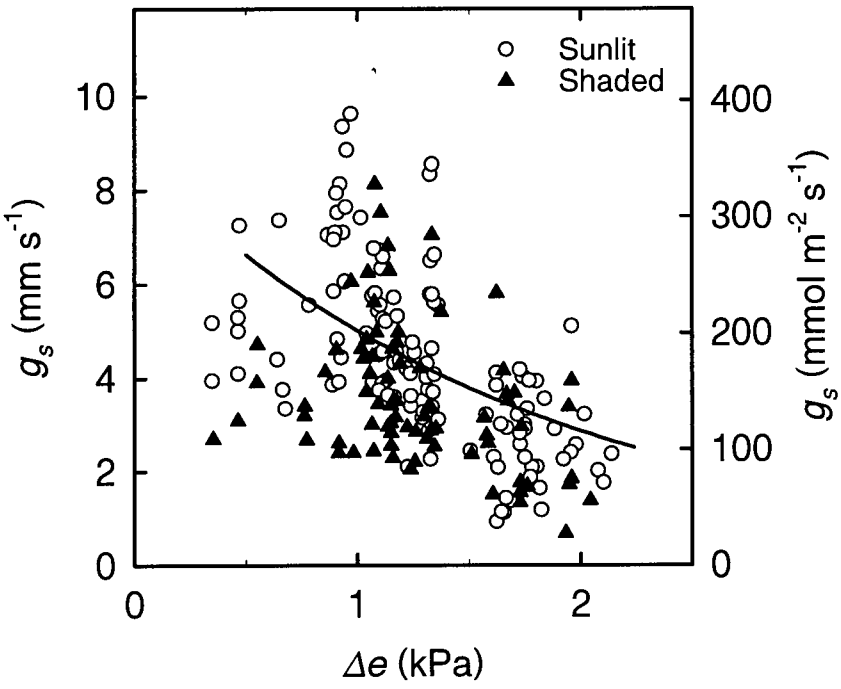

Fig. D.1. Hazelnut stomatal conductance (g_s) measured by porometer versus ambient vapour pressure deficit (Δe) on most days from 12 July to 9 August 1996 at the Old Aspen site.

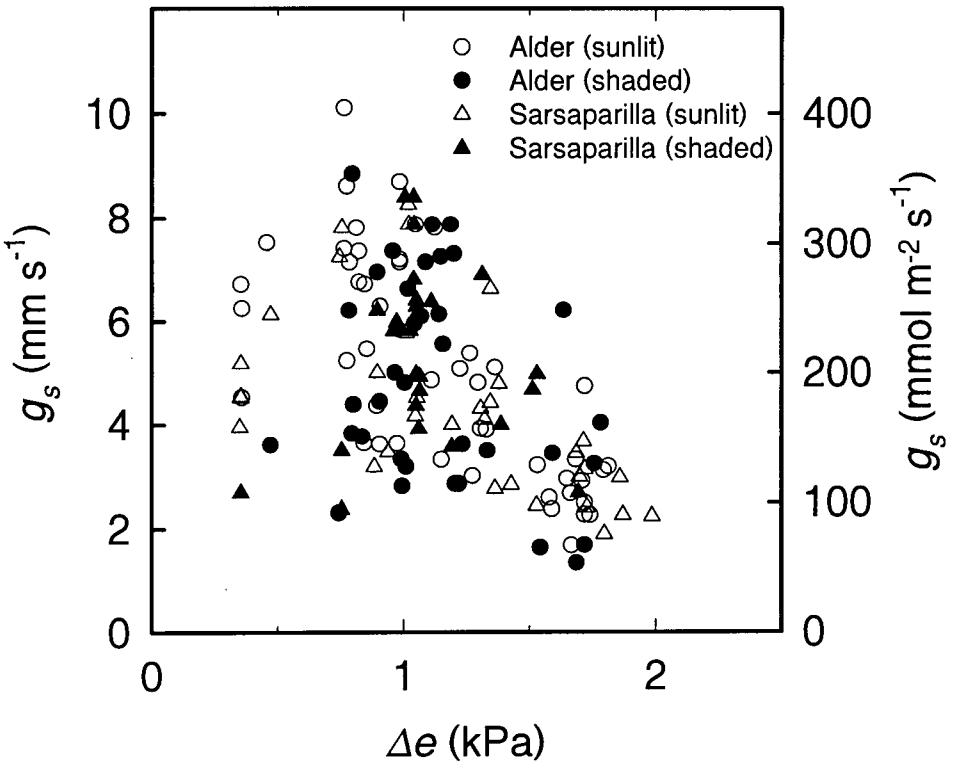

Fig. D.2. Alder and sarsaparilla g_s measured by porometer versus Δe on most days from 12 July to 9 August 1996 at the Old Aspen site.